Glykierung mittels Methylglyoxal verändert Glykosylierung und erhöht das invasive Potential von Tumoren des Nervensystems

Habilitationsschrift

zur Erlangung des akademischen Grades

Dr. med. habil.

für das Fachgebiet experimentelle Neurochirurgie

kumulative Schrift vorgelegt

der Medizinischen Fakultät

der Martin-Luther-Universität Halle-Wittenberg

von Dr. med. Maximilian Scheer

Gutachter: Prof. Dr. Nils Ole Schmidt

Prof. Dr. Roland Goldbrunner

Lehrprobe: 23.10.2024

Verteidigung: 12.11.2024

Referat

Nahezu alle Tumoren zeigen eine Veränderung des Stoffwechsels im Sinne einer aeroben Glykolyse. Dieses Phänomen wird auch als Warburg Effekt bezeichnet und führt zu einer Akkumulation von hochreaktiven Nebenprodukten der Glykolyse, wie z.B. Methylglyoxal (MGO). MGO wiederum gilt als einer der potentesten Präkursuren für die Glykierung. Durch die Modifikation der Stoffwechselvorgänge kommt es auch zu einer Änderung der Glykosylierung an der Zelloberfläche. Beide genannten Vorgänge gelten als „*Hallmarks of Cancer*“. Sowohl Glykierung als auch Glykosylierung zählen zu den posttranslationalen Modifikationen. Während diese Prozesse bei anderen Tumorerkrankungen gut erforscht sind und sich beispielsweise Reaktionsprodukte als Tumormarker etabliert haben, ist dies bei Tumoren des Nervensystems bisher nur unzureichend erforscht. Ziel der Arbeit war es den Einfluss von MGO auf verschiedene Tumoren des Nervensystems zu untersuchen. In dem drei verwendeten Modell unter Nutzung von Meningeom-, Neuroblastom- und Glioblastom-Zellen zeigte sich ein konzentrationsabhängiger Effekt sowohl hinsichtlich Zellviabilität als auch bezüglich der Induktion von Glykierung. In Abhängigkeit vom Zelltypen kam es zu einer Modifikation von Zelladhäsion sowie -migration. Zudem kam es durch Glykierung zu einer Steigerung der Invasivität in einigen der verwendeten Tumorzelllinien. Diese Beobachtungen korrelierten mit einer veränderten Expression von extrazellulären Matrixproteinen, wie einer vermehrten Expression von E-Cadherin. Neben der nicht-enzymatischen Glykierung, wurde durch eine MGO-Behandlung auch der enzymatische Prozess der Glykosylierung modifiziert und eine vermehrte Polysialylierung auf den Tumorzellen detektiert. In der Analyse des Expressionsverhaltens der Sialyltransferasen zeigte sich ein zelltypabhängiger Effekt, wobei hier teilweise gegensätzliche Muster, je nach Malignität der untersuchten Zelllinie zu beobachten waren. Die Ergebnisse unterstreichen die vermutete Rolle einiger Autoren von MGO als Tumorpromotor. Zudem ergeben sich erste Hinweise, dass MGO eine Rolle bei der Veränderung des Oberflächenprofils durch Glykosylierung spielt. Dieser Prozess ist relevant für das Umgehen einer Immunantwort durch die Tumorzelle (*Immune Escape).*

Scheer, Maximilian: Die Rolle von Glykierung und Glykosylierung bei Tumoren des Nervensystems, Halle (Saale), Univ., Med. Fak., Habil., 127 Seiten, 2024

Inhalt

Abkürzungsverzeichnis

AGE	*Advanced Glycation Endproducts*
AGE-R	AGE-*Receptor*
ATP	Adenosintriphosphat
Bzw.	beziehungsweise
C	Celsius
CA	Carbohydrat-Antigen
cDNA	*complementary DNA*
CD	*Cluster of differentiation*
CEA	Carcinoembryonales Antigen
CEL	Carboxyethyllysin
CIM	*Cell Invasion and Migration*
CML	Carboxymethyllysin
DNA	*Deoxyribonucleic acid*
EMT	Epithelial-mesenchymale Transition
Gal	Galaktosid
GalNAc	N-Acetylgalaktosamin
GNE	UDP-N-Acetylglucosamin-2-Epimerase/N-Acetyl Mannosamin-Kinase
Hba1c	Hämoglobin A1c
HDL	*High Density Lipoprotein*
HEK	*Human Embryonic Kidney*
HPLC	*High Performance Liquid Chromatography*
LDL	*Low Density Lipoprotein*
LD 50	mittlere letale Dosis
MAPK	Mitogen-aktivierte Protein-Kinase
MET	Mesenchymal-epitheliale Transition
MGO	Methylglyoxal
mM	Millimolar
MMP	Matrix-Metalloproteasen
Mol	Molar
mRNA	*messenger RNA*
MTT	(3-(4,5-Dimethylthiazol-2-yl)-2,5-diphenyltetrazoliumbromid)

NCAM	*Neural cell adhesion molecule*
Neu5C	N-Acetyl-Neuraminsäure
NF-κB	*Nuclear Factor kappa-light-chain-enhancer of activated B-cells*
NK-Zelle	Natürliche Killerzelle
PSA	Prostataspezifisches Antigen
PolySia	Polysialylierung
qPCR	*quantitative polymerase chain reaction*
RAGE	*Receptor for Advanced Glycation Endproducts*
RNA	*Ribonucleic acid*
RTCA	*Real-Time Cell Analyzer*
SDS	*Sodium Dodecyl Sulfate*
SIA	Sialinsäure
siRNA	*small interfering RNA*
ST	Sialyltransferase
sRAGE	*solube RAGE*
Stab	Stabilin
TGF-ß	*Transforming Growth Factor Beta*
TNF α	Tumornekrosefaktor Alpha
WHO	*World Health Organization*
XTT	(Natrium-2,3-bis-(2-methoxy-4-nitro-5-sulfophenyl)-5-[(phenylamino) carbonyl]-2H-Tetrazolium)
z.B.	zum Beispiel
µM	Mikromolar

1. Einleitung und Zielstellung

1.1. Posttranslationale Modifikationen

Als posttranslationale Modifikationen werden Veränderungen von Proteinen nach der Translation bezeichnet, wobei durch diese Modifikationen Proteinkonfirmation oder Bindungsaffinität beeinflusst werden (Voet 2006). Die Reaktionen sind teilweise intrinsisch und teilweise durch Umweltfaktoren bedingt. Momentan sind ca. 300 posttranslationale Modifikationen bekannt. Die Phosphorylierung oder Methylierung seien hier als bekannte Vertreter dieser Gruppe genannt (Lee et al. 2023). Zu diesen Modifikationen gehören auch Reaktionen von Kohlenhydratgruppen mit Proteinen. Man kann hier zwischen Glykierung und Glykosylierung unterscheiden (Olzscha 2019).

1.2. Glykierung

Mit dem Begriff Glykierung wird die Reaktion von hauptsächlich Proteinen, aber auch Lipiden oder Nukleinsäuren mit Carbonylen bezeichnet (Thornalley 2005). Ausgangsstoffe für diese nicht-enzymatische Reaktion sind ein reduzierender Zucker und eine freie, reaktive Aminogruppe. Über eine Kondensation entsteht zunächst eine Schiff'sche Base und durch weitere Umlagerungsschritte ein Amadori Produkt (Singh et al. 2001). Die Endformen aus den Reaktionen von Proteinen und Kohlenhydraten werden als *Advanced Glycation Endproducts* (AGEs) bezeichnet (Abbildung 1) (Brownlee 1995). Man kann bei der Glykierung eine exogene und eine endogene Form unterscheiden, die im Folgenden genauer spezifiziert werden sollen (Lima und Baynes 2013).

1.2.1. Exogene Glykierung

Bei dieser Form der Glykierung reagieren Proteine mit Kohlenhydraten außerhalb des Körpers. Dieser auch als Maillard-Reaktion bezeichnete Prozess läuft vermehrt bei Temperaturen von über 120°C ab. In der Lebensmittelindustrie spielt diese Reaktion eine wichtige Rolle, um einerseits Produkten die gewünschte Farbe zu geben und andererseits den Geschmack dadurch zu modifizieren bzw. zu verstärken (Prestes Fallavena et al. 2022). Kaffee, Brot, Pommes Frites aber auch Steaks erhalten wesentliche Teile ihres Geschmacks durch diese Reaktion. Reduzierende Zucker und Aminosäuren reagieren dabei zu AGEs (Poulsen et al. 2013). Diese Reaktion läuft ebenfalls bei der Bildung von Acrylamid ab,

welches als wahrscheinlich kanzerogen eingestuft wurde (International Agency for Research on Cancer 1994). Da heutzutage der Anteil technisch verarbeiteter Lebensmittel immer mehr zunimmt, steigt auch die Menge an zugeführten AGEs (Fotheringham et al. 2022; Uribarri et al. 2010).

Bei häufigem Verzehr von erhitzten Lebensmitteln kann es zur Akkumulation der AGEs kommen, da diese nur bis zu bestimmten Konzentrationen abgebaut und ausgeschieden werden können. Durch Anhäufung dieser Verbindungen im Körper steigt der oxidative Stress und es kann zu DNA-Schäden kommen (Taniguchi und Murata 2021; Poulsen et al. 2013).

Neben dem Verzehr von Lebensmitteln ist Rauchen ebenfalls als Quelle für die externe Zufuhr von AGEs zu nennen. Tabakblätter werden zu diesem Zweck in Anwesenheit von Zucker getrocknet, wobei wiederum AGEs entstehen. Die gebildeten Reaktionsprodukte werden beim Rauchen in die Lunge inhaliert und erreichen so das Körperinnere (Hoonhorst et al. 2016).

1.2.2 Endogene Glykierung

Auch im menschlichen Organismus finden Glykierungsvorgänge statt. Diese Reaktionen laufen im Blutkreislauf oder zytosolisch unter Beteiligung von Glukose, Fruktose sowie Ribose ab. Dabei entstehen stark reaktive Dicarbonylverbindungen, wie zum Beispiel Glyoxal oder Methylglyoxal (MGO) (Zhang et al. 2009; Kim et al. 2017). Dauerhaft erhöhte Blutglukosewerte, wie sie beim Diabetes mellitus vorkommen können, begünstigen die Entstehung von AGEs, welche eine zentrale Rolle bei der Pathophysiologie diabetischer Komplikationen spielen (Fishman et al. 2018; Khalid et al. 2022). Das glykierte Hämoglobin A1c (HbA1c) stellt eines der ersten entdeckten glykierten Proteine dar. Aufgrund der Lebensdauer der Erythrozyten von 8 bis 12 Wochen kann der HbA1c-Wert neben der Diagnostik auch als Marker für Langzeitblutzuckerwerte beim Diabetes mellitus genutzt werden (John et al. 2007).

1.2.3. Advanced Glycation Endproducts

Wie oben beschrieben, können die Glykierungsprodukte aus der Reaktion aus Proteinen und Kohlenhydraten sowohl exogen als auch endogen entstehen. Die Endprodukte dieser Reaktionen werden als AGEs bezeichnet und spielen eine entscheidende Rolle bei Alterungsprozessen und der Entstehung von diversen Krankheitsbildern (Kang et al. 2022; Schalkwijk et al. 2023). AGEs können diverse Effekte hervorrufen, wobei diese rezeptorabhängig als auch rezeptorunabhängig vermittelt werden können (Ott et al. 2014). Auf diese Möglichkeiten soll in den nächsten Abschnitten eingegangen werden. Bekannte Vertreter der AGE-Modifikationen sind Carboxyethyllysin (CEL) und Carboxymethyllysin (CML). CML ist aktuell der meistgenutzte Marker für die Entstehung von AGEs (Perrone et al. 2020).

AGEs werden auch beim physiologischen Prozess des Alterns gebildet. Untersuchungen konnten zeigen, dass bei Diabetikern aufgrund erhöhter Blutglukosewerte AGEs in höheren Konzentrationen nachweisbar sind und es bei den PatientInnen eher zu Folgeerscheinungen im Sinne eines beschleunigten Alterungsprozesses kommt (Abbildung 1) (Singh et al. 2001).

Rezeptorunabhängige AGE-vermittelte Effekte

Durch Ablagerung von AGEs in den Gefäßwänden kommt es zu einer Beschleunigung der Atherosklerose. AGEs begünstigen dabei die Oxidation von *Low Density Lipoprotein* (LDL), welche von Makrophagen aufgenommen werden. Es kommt in der Folge zur Ausbildung von sogenannten Schaumzellen. Dieser Vorgang wird auch als *Lipoprotein-induced-atherosclerosis*-Hypothese bezeichnet (Steinberg et al. 1989). Durch die resultierende Entzündungsreaktion kann sich eine Fibrose ausbilden und so die Atherosklerose weiter vorantreiben (Singh et al. 2022). Durch hohe Level an AGEs wird ebenfalls das *High Density Lipoprotein* (HDL) glykiert und so leichter oxidiert, wodurch es seinen protektiven Effekt verliert (Stirban et al. 2014). Bei den typischen diabetischen Folgeerscheinungen der Gefäße wird zwischen mikro- und makrovaskulären Komplikationen unterschieden. Zu den mikrovaskulären Komplikationen gehören die Retinopathie, Neuropathie sowie Nephropathie. Erkrankungsbilder wie die periphere arterielle Verschlusskrankheit, die koronare Herzkrankheit bis hin zum Herzinfarkt oder der Schlaganfall durch eine

Stenosierung der *Arteria carotis interna* werden zu den makrovaskulären Komplikationen gezählt (Abbildung 1) (Yamagishi und Imaizumi 2005).

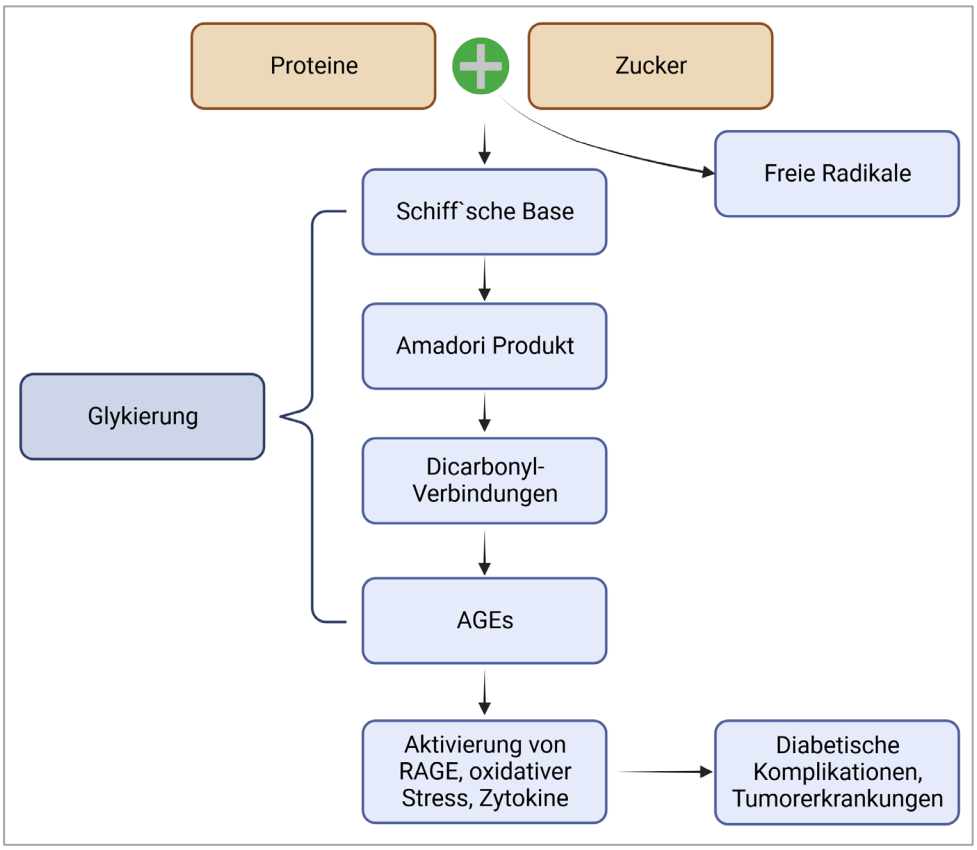

Abbildung 1: Schematische Darstellung der Glykierungsreaktion und Bildung der *Advanced Glycation Endproducts* (AGE) (modifiziert nach Kang et al. 2022)

AGEs sind ebenfalls bei der Pathogenese neurodegenerativer Erkrankungen von Bedeutung (Schalkwijk et al. 2023). Durch erhöhte AGE-Konzentrationen kann es zur Akkumulation von ß-Amyloid kommen, was in kausalem Zusammenhang mit der Entstehung des Morbus Alzheimer steht (Srikanth et al. 2011). Auch bei weiteren neurodegenerativen Krankheiten wie dem Morbus Parkinson, der Amyotrophen Lateralsklerose sowie Chorea Huntington spielt die Aggregation von ß-Amyloid eine entscheidende Rolle (Lim et al. 2019; Ross und Poirier 2004).

Alterungsprozesse der Haut werden ebenfalls durch Akkumulation von AGEs mitverursacht. Durch Glykierung von Kollagenen kommt es zur Ausbildung von komplexen Quervernetzungen, die vom Körper nicht mehr gespalten werden können. Matrix-Metalloproteasen (MMP), welche für den Abbau der Kollagene verantwortlich sind, können diese modifizierten Varianten nicht mehr abbauen. Durch Störung beim *Remodelling* bzw.

des physiologischen Umbauprozesses verlieren die Kollagene an Elastizität, mit der Folge eines beschleunigten Alterungsprozesses (Hofmann et al. 2013; Danby 2010).

Ähnlich ist bei den Kollagenen im Knochengewebe. Durch Glykierung und AGE-Bildung kommt es zur Ausbildung von Quervernetzungen zwischen Kollagenen und anderen Proteinen. Die mechanischen Eigenschaften des Knochens sind dadurch gestört und der Knochenumbau wird zudem behindert. Als Folge kann es zur Ausbildung einer Osteoporose kommen (Wang und Vashishth 2023).

Auch beim Gestationsdiabetes kann es durch erhöhte Blutglukosewerte zur vermehrten Bildung von AGEs kommen. In der Folge bildet sich ein pro-inflammatorisches Milieu und es kommt zu einer Steigerung der Komplikationsrate in der Schwangerschaft sowohl bei der Mutter als auch beim Ungeborenen (Sisay et al. 2020).

1.2.4. Rezeptoren für AGEs

AGEs können über membranständige Rezeptoren diverse Signalwege aktivieren. Zu diesen Rezeptoren gehört die Familie der AGE-Rezeptoren (AGE-R1, -R2, und -R3), welche überwiegend von Makrophagen, Endothelzellen, T-Lymphozyten sowie neuronalen Zellen exprimiert werden. Zu den Funktionen dieser Rezeptoren gehören unter anderem Zellwachstum, Adhäsion sowie Differenzierung (Stirban et al. 2014; Ott et al. 2014). Andererseits gibt es eine Gruppe von Scavenger-Rezeptoren, darunter z.B. Stabilin-1 und Stabilin-2 (Stab1 und Stab2) (Twarda-Clapa et al. 2022). Die Scavenger-Rezeptoren werden größtenteils auf Endothelzellen, Makrophagen sowie in der Leber exprimiert. Ihre Hauptaufgabe haben sie im Fettstoffwechsel, wie z.B. bei der endozytotischen Aufnahme von HDL bzw. LDL sowie der Degradation von AGEs (Ott et al. 2014). Der meistuntersuchte Rezeptor ist allerdings der *Receptor for Advanced Glycation Endproducts (RAGE)* (Twarda-Clapa et al. 2022).

Receptor for Advanced Glycation Endproducts (RAGE)

RAGE ist ein Transmembranprotein und gehört zur Immunglobulin-Superfamilie. Dieser Rezeptor besitzt drei extrazelluläre Domänen zur Bindung von Liganden, eine Transmembrandomäne zur Verankerung in der Zellmembran sowie eine zytosolische

Domäne, welche für die Signaltransduktion verantwortlich ist (Twarda-Clapa et al. 2022). Im Gegensatz zu den Scavenger-Rezeptoren erfolgt bei Aktivierung von RAGE keine Endozytose des Liganden (Twarda-Clapa et al. 2022).

Während der Embryonalzeit lässt sich eine starke Expression von RAGE nachweisen, bei welcher er in das Neuritenwachstum involviert ist. Verglichen mit dieser Expression ist sie beim Erwachsenen nur noch schwach ausgeprägt, wobei jedoch eine Überexpression bei vielen chronisch-entzündlichen sowie Tumor-Erkrankungen zu beobachten ist (Stirban et al. 2014; Ott et al. 2014). Viele Zellen des Immunsystems, wie z.B. Makrophagen oder dendritschen Zellen, exprimieren RAGE an der Zelloberfläche. Eine Aktivierung des Rezeptors bedingt eine pro-inflammatorische Kaskade mit einer Aktivierung von NF-κB, dem *Nuclear Factor kappa-light-chain-enhancer of activated B-cells* sowie einer Ausschüttung von Zytokinen, welches ein entzündliches Milieu schafft (Ott et al. 2014).

Bisher sind über 20 verschiedene Isoformen von RAGE bekannt, welche durch alternatives *Splicing* oder membranassosziierte Proteasen entstehen können (Jules et al. 2013). Als Varianten seien hier der *N-truncted RAGE*, der *dominant-negative RAGE* sowie der *soluble RAGE* (sRAGE) genannt (Jules et al. 2013). Da bei der *N-truncted* Variante Domäne auf der Extrazellulär fehlt, ist eine Bindung von Liganden nicht möglich. Am *dominant-negativ RAGE* können zwar Liganden binden, jedoch fehlt die zytoplasmatische Domäne, sodass keine Signaltransduktion stattfindet. Die lösliche Form des *RAGE (sRAGE)* besteht nur aus der extrazellulären Domäne (Lee und Park 2013). Aufgrund der fehlenden Transmembrandomäne kann *sRAGE* im Extrazellularraum an Liganden binden. Durch diese Bindung werden die Liganden neutralisiert, da keine Interaktion mit anderen RAGE-Varianten möglich ist (Lee und Park 2013). Im Gegensatz zu vielen anderen Rezeptoren erfolgt bei RAGE durch Stimulation eine positive Rückkopplung und dadurch eine vermehrte Expression (Ott et al. 2014).

Clearance

Auf Gewebeebene geschieht der Abbau von AGEs durch zelluläre proteolytische Systeme, die AGEs endozytieren und sie über rezeptorvermittelte und nicht rezeptorvermittelte Wege in Peptide abbauen, die dann wieder in den Blutkreislauf freigesetzt werden (Vlassara 2001).

Auf systemischer Ebene wird angenommen, dass der Abbau über die Leber sowie die Niere erfolgt (Nagai et al. 2007; Smedsrød et al. 1997; Miyata et al. 1998). Tiermodelle deuten darauf hin, dass AGEs von den Glomeruli der Niere gefiltert, von proximalen Tubuluszellen rückresorbiert und weiterverarbeitet werden. Anschließend erfolgt die Ausscheidung über den Urin (Fotheringham et al. 2022). Die Clearance hängt somit von der Nierenfunktion ab. Allerdings kann es an der Bowman-Membran der Niere zu Ablagerungen von AGEs kommen, welche einen fibrotischen Umbau bewirken können und so die Nierenfunktion im Sinne einer Nephropathie einschränken (Miyata et al. 1998; Fotheringham et al. 2022). Aufgrund ihrer Größe können komplexere AGE-Modifikationen nicht über die Bowman-Membran filtriert werden. Hierfür ist zunächst die Spaltung in kleinere Peptide notwendig (Miyata et al. 1998). Die Endothelzellen sowie Kupffer-Zellen der Leber spielen bei dieser Zersetzung eine entscheidende Rolle (Smedsrød et al. 1997; Fotheringham et al. 2022).

1.3. Glykosylierung

Die Reaktionspartner bei der Glykosylierung sind, ähnlich wie bei der Glykierung, Kohlenhydrate und Proteine bzw. Lipide. Der Unterschied besteht darin, dass bei diesem Prozess Enzyme die Reaktion katalysieren. Es handelt sich um eine der häufigsten posttranslationalen Modifikationen und betrifft etwa die Hälfte aller Proteine (Brooks 2006). Durch Glykosylierung kann beispielsweise die Proteinkonfirmation sowie die Affinität für Bindungspartner beeinflusst werden. Man kann zwischen zwei Formen, der N- und O-Glykosylierung, unterscheiden. Bei der N-Glykosylierung werden Glykane an Asparagin gebunden. Die Bindungspartner der Glykane bei der O-Glykosylierung sind meist Threonin oder Serin (Brooks 2006). Glykosylierte Moleküle sind entscheidend für Interaktion an der Zelloberfläche, wo sie auch als Glykokalix bezeichnet werden (Tarbell und Cancel 2016). Ein Hauptvertreter der beteiligten Enzyme bei der der Glykosylierung sind Sialyltransferasen (ST), auf welche im nächsten Abschnitt genauer eingegangen wird (Harduin-Lepers et al. 2001).

1.3.1. Sialyltransferasen

Eine besondere Rolle in der Saccharidzusammensetzung von Glykanen nehmen die Sialinsäuren ein, welche entweder als terminale Zucker oder in Form von langen Ketten

vorliegen. Die Enzyme, die die Übertragung von Sialinsäuren auf Protein- oder Lipid-gebundenen Glykane katalysieren, nennt man ST (Harduin-Lepers et al. 2001; Rosenstock und Kaufmann 2021).

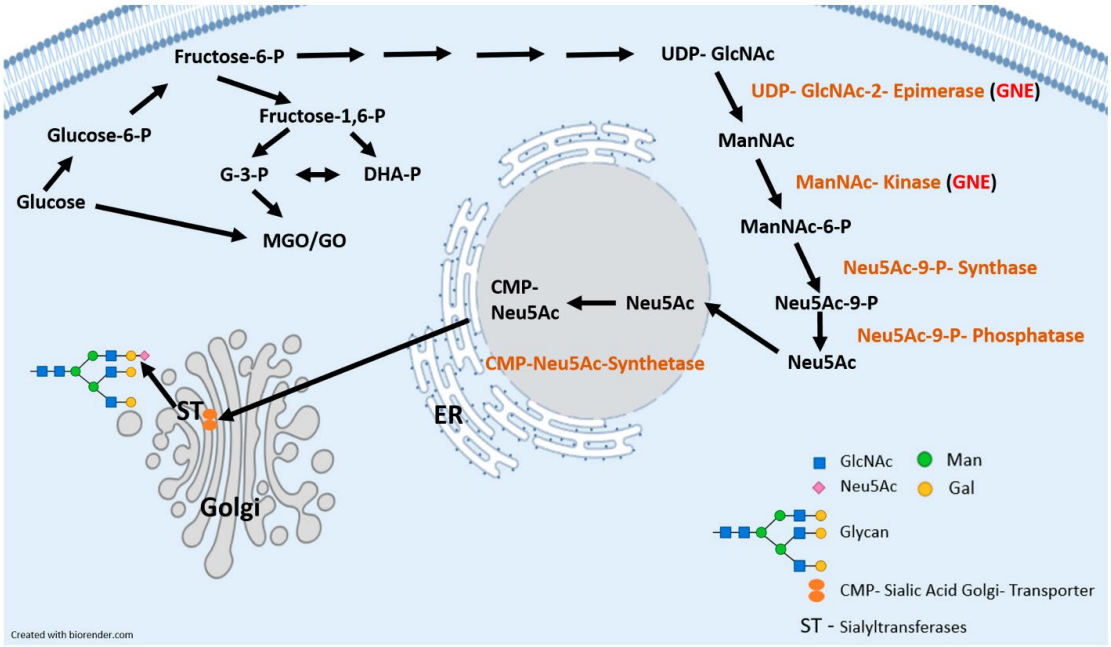

Abbildung 2. Schematische Übersicht Bildung zur Sialinsäure-Bionsynthese und Sialylierung; G-3-P = Glyceraldehyd-3-Phosphat; DHA-P = Dihydroxyacetonphosphat; MGO = Methylglyoxal; GO = Glyoxal; GlcNAc = N-Acetylglucosamin; Man = Mannose; Gal = Galaktose; Neu5Ac = N-Acetyl-Neuraminsäure; GNE = UDP-N-Acetylglucosamin-2-Epimerase/N-Acetyl-Mannosamin-Kinase; ER = Endoplasmatisches Retikulum (Selke et al. 2021a)

Als wichtigste Sialinsäure der Säugetiere gilt dabei die N-Acetyl-Neuraminsäure (Neu5Ac) (Comb und Roseman 1960). Die im Zytosol gelegene bifunktionelle UDP-N-Acetylglucosamin-2-Epimerase/N-Acetyl Mannosamin-Kinase (GNE) gilt als Schlüsselenzym der Sialinsäure-Biosynthese (Kontou et al. 2008; Stäsche et al. 1997). Anschließend folgen weitere Schritte der Sialinsäure-Biosynthese im Zytosol sowie Zellkern, bevor die Sialylierung beispielsweise der Glykanstrukturen von Proteinen im Golgi-Apparat stattfindet (Abbildung 2). Beim Menschen sind 20 ST bekannt, die Cytidinmonophosphat-aktivierte Sialinsäuren als Substrat verwenden (Datta 2009). Diese STs werden nach den von ihnen synthetisierten Kohlenhydrat-Bindungen in 4 Familien unterteilt: β-Galaktosid-α-2,3-Sialyltransferasen (ST3Gal1-6), β-Galaktosid- α-2,6-Sialyltransferasen (ST6Gal1-2), N-Acetyl-Galaktosamin (GalNAc)-α-2,6-Sialyltransferasen (ST6GalNAc1-6) und α-2,8-Sialyltransferasen (ST8SIA1-6). Die Mitglieder der ST3Gal-Familie übertragen Sialinsäuren auf terminale Galaktosereste über α-2,3-Bindungen, während die beiden bekannten Mitglieder der ST6Gal-Familie dies über α-2,6-Verknüpfungen tun. Die sechs Mitglieder der

ST6GalNAc-Familie übertragen Sialinsäuren von auf GalNAc-Reste über α-2,6-Verknüpfungen. Die Vertreter der ST8SIA-Familie übertragen Sialinsäuren auf andere terminale Sialinsäure-Reste über α-2,8-Verknüpfungen (Harduin-Lepers et al. 2001).

Die Polysialylierung ist eine besondere Form bei der Sialylierung, wobei zwischen 8 und 100 Sialinsäuren linear verknüpft werden. Die Synthese erfolgt hauptsächlich durch die ST8SIA2 sowie ST8SIA4 (Seifert et al. 2012). Auf die Bedeutung wird im folgenden Abschnitt weiter eingegangen.

1.3.3. Polysialinsäure (PolySia)

Polysialinsäure (PolySia) ist nur auf wenigen Zellen im menschlichen Körper vorhanden. Das neuronale Zell-Adhäsionsmolekül (*Neural cell adhesion molecule* = NCAM) gilt als der wichtigste Träger für PolySia im Menschen. NCAM-exprimierende Zellen sind nahezu exklusiv auf das zentrale Nervensystem beschränkt (Hildebrandt et al. 2010; Seifert et al. 2012). PolySia spielt eine wichtige Rolle bei der Entwicklung des zentralen Nervensystems und ist in der Embryonalphase hoch exprimiert (Hildebrandt et al. 2010; Schnaar et al. 2014). Allerdings kommt es auch durch hohe Blutglukosekonzentrationen bei PatientInnen mit Diabetes mellitus sowie in vielen Tumorerkrankungen zu einer gesteigerten PolySia (Brownlee 1995; Sato und Kitajima 2021). Es konnte gezeigt werden, dass PolySia eine Rolle bei der Tumorgenese sowie dessen Progression spielen (Veillon et al. 2018; Thiesler et al. 2022).

1.4. Posttranslationale Modifikationen bei Tumoren

Die meisten Tumoren nutzen zur Energiegewinnung eine veränderte Glykolyse, welche aerob abläuft. Dieses Phänomen wird auch als Warburg-Effekt bezeichnet und gilt als einer der „*Hallmarks of Cancer*“ (Hanahan und Weinberg 2011). Da zur Energiegewinnung bei der aeroben Glykolyse weniger Adenosintriphosphat (ATP) als bei der oxidativen Phosphorylierung gesunder Zellen generiert wird, muss diese vermehrt ablaufen. Dadurch kommt es zu einer Akkumulation hochreaktiver Zwischenprodukte, wie z.B. dem Dicarbonyl MGO (Leone et al. 2021). Diese reaktiven Zwischenprodukte führen wiederum zu einer vermehrten Bildung von AGEs (Kroemer und Pouyssegur 2008).

Erhöhte Konzentrationen von AGEs im Tumorgewebe sind bei vielen Entitäten mit einer schlechten Prognose assoziiert, da sie mit einer gesteigerten Migration und Invasion verbunden sind (Sharaf et al. 2015; Matou-Nasri et al. 2017). In der Expression veränderte extrazelluläre Matrixproteine sind oft in diesen Prozess involviert. Als Beispiel seien hier die Cadherine genannt. Eine Überexpression von N-Cadherin bei gleichzeitiger Repression von E-Cadherin gilt als kennzeichnend für die Epithelial-mesenchymale Transition (EMT). Dieser Prozess führt zu einem Verlust der Zellpolarität sowie Zellbindung und ermöglicht die Migration von Zellen. Er wird für die Metastasierung von Tumoren als entscheidend angesehen (Dongre und Weinberg 2019; Liao und Yang 2017). Einige Studien konnten darlegen, dass AGEs auch auf diesen Prozess Einfluss haben (Bai et al. 2015; Liang 2020; Selke et al. 2021b; Raghavan et al. 2016).

Das Risiko für einige Tumorentitäten scheint mit einer gesteigerten Glykierung zu korrelieren. So konnte gezeigt werden, dass hohe AGE-Konzentrationen im Blut, sei es durch eine ungesunde Ernährung oder als Folge eines Diabetes mellitus, mit erhöhtem Risiko für das Mammakarzinom, Prostatakarzinom oder Mundbogenkarzinom einhergehen (Twarda-Clapa et al. 2022). Weiterhin sind AGEs in der Lage über eine Aktivierung von RAGE ein pro-inflammatorisches Milieu zu schaffen und so die Tumorentstehung zu begünstigen (Chuah et al. 2013; Bierhaus et al. 2005; Gebhardt et al. 2008). Diverse Studien konnten nachweisen, dass RAGE durch Steigerung der Proliferation, Hemmung apoptischer Signalwege sowie Aktivierung anti-apoptischer Signalwege die Tumorprogression fördert (Twarda-Clapa et al. 2022; Sparvero et al. 2009; Zhao et al. 2014; Logsdon et al. 2007). Durch die positive Rückkopplung und reaktive Überexpression von RAGE kann dieser auch andere Liganden binden, wodurch die Effekte weiter verstärkt werden (Zhao et al. 2014; Logsdon et al. 2007; Twarda-Clapa et al. 2022). Der Nachweis der Überexpression von RAGE ist bei vielen Tumorerkrankungen mit einer schlechteren Prognose verbunden ist (Da Wang et al. 2015; Waghela et al. 2021).

Bei den meisten Tumoren kommt es nicht zu einer Alteration im Bereich der Glykierung, sondern auch zu einer veränderten Glykosylierung (Dobie und Skropeta 2021; Hanahan und Weinberg 2011). Tumor-assoziierte Glykane und Glykoproteine haben sich bei einigen Karzinomen als Tumormarker etabliert und werden dort als Verlaufsparameter genutzt. Bekannte Vertreter sind z.B. CA19-9 (*Cancer Antigen*) bei Pankreaskarzinomen, CA125 bei Ovarialkarzinomen, CEA (Carcinoembryonales Antigen) bei kolorektalen Karzinomen oder

PSA (Prostataspezifischen Antigen) beim Prostatakarzinom (Reiter et al. 2015; Silsirivanit 2019).

Einer der Hauptvertreter, der bei der Glykosylierung beteiligten Enzyme, sind die ST. Bei einigen Tumorerkrankungen, wie dem Mammakarzinom, Ovarialkarzinom oder Rektumkarzinom konnte nachgewiesen, dass eine Überexpression bestimmter ST mit einer gesteigerten Invasion bzw. Resistenzbildung gegenüber der Chemotherapie oder Bestrahlung einhergeht (Wu et al. 2018; Smithson et al. 2022; Hait et al. 2022).

Eines der Reaktionsprodukte von ST stellen Ganglioside dar. Diese befinden sich überwiegend auf der Zellmembran von Nervenzellen (Breiden und Sandhoff 2018). Es konnte allerdings auch gezeigt werden, dass das Gangliosid GM3 in vielen Tumorerkrankungen überexprimiert wird. Beim Bronchialkarzinom oder bei Melanomen ist dies der Fall. Eine Überexpression von GM3 kann die Zelladhäsion sowie die Proliferation beeinflussen (Zheng et al. 2019; Hakomori und Handa 2015).

Durch eine Veränderung der Sialylierung an der Zelloberfläche sind Tumorzellen außerdem in der Lage, die Zell-Zell-Interaktion zu beeinflussen. Zellen des Immunsystem, wie Natürliche Killer-Zellen (NK-Zellen), Makrophagen oder T-Zellen sind teilweise nicht in der Lage, die Tumorzellen zu erkennen (Nardy et al. 2016). Dieser Prozess wird auch als *Immune Escape* bezeichnet (Huang et al. 2022a; Jarahian et al. 2021).

Posttranslationale Modifikationen bei Tumoren des Nervensystems

Während sich einige Glykoproteine bzw. Glykane als Marker bei vielen Karzinomen etabliert haben und Effekte der Glykierung dort relativ gut erforscht sind, ist hinsichtlich Glykierung und Glykosylierung bei Tumoren des Nervensystems wenig bekannt. Es gibt lediglich einige Arbeiten beim Glioblastom, welche sich mit dieser Thematik beschäftigen. Hier konnte beispielsweise dargelegt werden, dass ein hohes Maß an PolySia an der Zelloberfläche mit einem kürzerem progressionsfreien sowie Gesamtüberleben bei den PatientInnen verbunden waren (Amoureux et al. 2010). In einer weiteren Studie konnte nachgewiesen werden, dass Glioblastom-Zelllinien auf ihrer Zelloberfläche verstärkt O-Glykosylierung aufweisen, wodurch die Immunantwort im Sinne des *Immune Escape* moduliert wird (Dusoswa et al. 2020). Die Effekte der Glykierung sind bei Tumoren des

Nervensystems nur unzureichend erforscht. Außerdem konnten bisher keine Glykane oder Glykoproteine als Marker identifiziert oder etabliert werden. Die *World Health Organization* (WHO) teilt Tumore des zentralen Nervensystems in die Grade 1 bis 4 ein. Gutartige Tumore ohne infiltratives Wachstum werden als Grad 1 eingestuft und sind mit einer Operation in der Regel kurativ zu behandeln. Als Grad 4 werden äußerst bösartige Tumoren eingestuft, welche mit einer drastischen Reduktion der Überlebenszeit einhergehen (Louis et al. 2021).

1.5. Die Rolle von Methylglyoxal

Initial ging man davon aus, dass hohe Glukose-Spiegel hauptsächlich für die Bildung von AGEs im Körper verantwortlich sind. Allerdings hat sich gezeigt, dass Glukose nicht sehr reaktiv ist. Tatsächlich ist MGO der potenteste Präkursor für die AGE-Bildung im Körper und reagiert rasch mit Aminosäuren von Proteinen, Lipiden und Nukleinsäuren (Schalkwijk und Stehouwer 2020; Khalid et al. 2022). Als hochreaktives Zwischenprodukt der Glykolyse kommt MGO in allen lebenden Zellen vor. MGO ist ein α-Ketoaldehyd und entsteht bei der Degradation von Glycerinaldehyd-3-phosphat oder auch bei der nicht-enzymatischen Fragmentierung von Zuckern (van der Bruggen et al. 2021; Chang und Wu 2006). Im menschlichen Körper ist MGO in deutlich geringeren Konzentrationen als Glukose nachweisbar und besitzt nur eine kurze Halbwertszeit, da es rasch an Proteine gebunden oder über das Glyoxalase-System abgebaut wird (Schalkwijk und Stehouwer 2020). Im Vergleich zu Glukose ist MGO jedoch circa 50.000-mal reaktiver und kann so rasch Proteinmodifikationen hervorrufen (Schalkwijk und Stehouwer 2020). Schätzungsweise 0,1-0,4 % der Glukose werden bei der Glykolyse zu MGO umgewandelt (Kuhla et al. 2005).

MGO ist in der Lage DNA-Schäden und Protein-Quervernetzungen durch Glykierung hervorzurufen. Viele Studien haben den Zusammenhang zwischen MGO, der AGE-Bildung, oxidativem Stress und pathologischen Folgeerscheinungen wie Diabetes mellitus, arterieller Hypertonie, beschleunigten Alterungsprozessen sowie neurodegenerativen Erkrankungen aufgezeigt (Yang et al. 2022; Schalkwijk und Stehouwer 2020).

Neben direkten strukturellen Veränderungen verursacht dieser Prozess zusätzlich zelluläre Effekte durch die Interaktion der gebildeten AGEs mit spezifischen Rezeptoren, wie z.B. RAGE, dessen Aktivierung zu oxidativem Stress und Inflammation führt (Schalkwijk und Stehouwer 2020).

MGO ist jedoch auch in der Lage die Aktivität von Transkriptionsfaktoren direkt zu beeinflussen. Untersuchungen in Saccharomyces konnten zeigen, dass eine Behandlung mit MGO die Aktivität von Transkriptionsfaktoren, wie Yap1, direkt erhöhen kann (Maeta et al. 2004). Im gleichen Modell konnte ebenfalls nachgewiesen werden, dass MGO den Mitogen-aktivierte Protein-Kinase (MAPK)-Weg aktiviert. Außerdem kann MGO den intrazellulären Calcium-Einstrom erhöhen und so den *Calcineurin-mediated Pathway* aktivieren (Maeta et al. 2005). In einem Modell mit ß-Zellen des Pankreas konnte gezeigt werden, dass eine Behandlung mit MGO die Insulin-Ausschüttung hemmt (Fiory et al. 2011). Weitere Autoren konnten in einem Ratten-Modell nachweisen, dass eine MGO-Behandlung mit einer deutlich erhöhten Insulinresistenz verbunden war (Fiory et al. 2011; Campbell et al. 2010; Guo et al. 2009)

Im menschlichen Liquor kommt MGO in Konzentrationen von 10-20 µmol vor (Kuhla et al. 2005). Es wird angenommen, dass MGO ähnliche Level im unteren mikromolaren Bereich innerhalb der Zellen erreicht (Rabbani und Thornalley 2012; Chang und Wu 2006; Chen et al. 2004). Da das Hirn einen hohen Glukose-Stoffwechsel aufweist, sind Zellen hier vergleichsweise viel MGO ausgesetzt (Allaman et al. 2015). Mögliche Folgeerscheinungen dauerhaft erhöhter MGO-Spiegel im Liquor sind eine Hirnatrophie sowie eine Verschlechterung der kognitiven Fähigkeiten (Lai et al. 2022). MGO kann je nach Konzentration auch zytotoxische Effekte besitzen (Kim et al. 2010). Daher weisen Astrozyten als Regulationsmechanismus eine stärkere Expression der Glyoxalase auf. Interessanterweise konnte gezeigt werden, dass das Glyoxalase-System bei neurodegenerativen Erkrankungen weniger stark exprimiert ist (Allaman et al. 2015).

Diverse Studien untersuchten den Einfluss von MGO bei Tumorerkrankungen. Beispielsweise fand sich eine erhöhte Migration sowie Invasion im Schilddrüsenkarzinom, welche durch MGO bedingt war (Antognelli et al. 2019; Antognelli et al. 2021b). Weiterhin ließ sich eine gesteigerte Proliferationsrate beim kolorektalen Karzinom im Maus-Modell durch MGO-Zufuhr beobachten (Lin et al. 2018). Auch bei Mammakarzinom-Zellen war unter MGO-Behandlung eine erhöhte Wachstums- sowie Metastasierungsrate in vivo ersichtlich (Nokin et al. 2016). Viele Autoren sehen MGO aufgrund dieser Effekte als Tumorpromotor an (Antognelli et al. 2019; Antognelli et al. 2021b; Lin et al. 2018; Bellier et al. 2019).

Einige Studien konnten zeigen, dass die Glykosylierung neben der Expression der entsprechenden Enzyme sowie dem Vorhandensein der Sialinsäuren als Substrat, stark vom Glukose-Angebot abhängt (Cheng et al. 2015; Wang et al. 2022; Nairn et al. 2008). Dass auch eine Behandlung mit MGO eine Induktion von Glykosylierung bewirkt, konnten bisher nur eigene Vorarbeiten zeigen (Scheer et al. 2020; Selke et al. 2021a; Schildhauer et al. 2023b).

1.6. Therapeutische Ansätze

Es gibt Ansätze, die Akkumulation von AGEs durch eine entsprechende Diät zu verhindern. Durch Reduktion der Zufuhr von Kohlenhydraten in Form von Monosacchariden konnten bei PatientInnen mit Diabetes mellitus rückläufige Werte für oxidativen Stress, Entzündung und Insulinresistenz konstatiert werden (Lim et al. 2019; Uribarri et al. 2003). Ebenso sank das Level an AGEs im Blut (Vlassara et al. 2002; Uribarri et al. 2003).

Im Bereich der Lebensmittelproduktion besteht die einfachste und kosteneffektivste Methode die Menge an AGEs zu senken, indem die Zubereitungstemperatur erniedrigt und die Luftfeuchtigkeit erhöht wird (Uribarri et al. 2010). Medikamentöse Therapie-Möglichkeiten bieten spezielle AGE-Inhibitoren, wie z.B. Pyridoxamine. In einem Tiermodell konnte hierdurch die Steifigkeit der Aorta durch signifikant reduziert werden (Wu et al. 2011). Eine weitere Möglichkeit bieten sogenannte AGE-*Cross-link breaker*, wie z.B. Phenacyl-Thiazolium. In einem Modell mit humaner Spongiosa konnte die Fragilität, welche durch die nicht-enzymatische Glykierung induziert wurde, durch die Behandlung mit einem *Cross-link breaker* deutlich reduziert werden (Bradke und Vashishth 2014).

Für einige Tumorerkrankungen gibt es ebenfalls erste präklinische Therapieansätze. Durch eine Inhibition von RAGE oder ST gelang in einigen Studien eine erneute Sensitivierung für die Strahlentherapie oder der Switch zu einem weniger aggressiven Tumor (Perez et al. 2021; Fu et al. 2021; Miró et al. 2022; Valiente et al. 2023). Da aufgrund des veränderten Metabolismus mit verstärkter MGO-Bildung auch das Glyoxalase-System in vielen Tumorzellen stärker exprimiert wird, gibt es auch Therapieansätze mit Glyoxalase-Inhibitoren, wodurch bei einigen Tumor-Modellen ebenfalls Resistenzen überwunden werden könnten (Antognelli et al. 2021a; Rabbani et al. 2018).

1.7. Zielstellung

In dieser kumulativen Habilitationsschrift wurden folgende Themenkomplexe bezüglich des Einflusses von MGO in drei Modellen mit Tumorzellen des Nervensystems untersucht. Dabei wurde auf folgende Aspekte eingegangen:

- Es wurde zunächst analysiert, welchen Einfluss eine Behandlung mit MGO in verschiedenen Konzentrationen auf die Zellmorphologie sowie Viabilität in den Modellen von Neuroblastomzellen, Meningeomzellen sowie Glioblastomzellen hat.
- Anhand der oben genannten drei Modelle wurde untersucht, ob durch MGO eine Glykierung induziert werden kann und ob die Konzentration von MGO diesen Vorgang beeinflusst.
- In dem Modell mit Neuroblastomzellen wurde analysiert, ob durch eine Behandlung mit MGO Änderungen im Grad der Glykosylierung zu beobachten sind.
- Es wurde im Zellkulturmodell benignen sowie malignen Meningeom-Zellen untersucht, ob eine Behandlung mit MGO einen Einfluss auf die Expression von Sialyltransferasen hat und ob auch Reaktionsprodukte dieser Enzyme, wie das Gangliosid GM3, eine veränderte Expression aufweisen.
- Anhang der Modelle von Meningeom-Zellen sowie Glioblastom-Zellen wurde die Expression von extrazellulären Matrixproteinen, wie z.B. Cadherine, mit und ohne MGO-Behandlung gegenübergestellt und analysiert.
- Mit Hilfe des *Real-Time Cell-Analysis*-Gerätes wurde in den oben genannten drei Modellsystem der Einfluss von MGO auf die Zelladhäsion, auf die chemotaktische Zellmigration sowie auf das Invasionsverhalten geprüft und ausgewertet.

2. Diskussion

Als Diskussionsbasis der Abschnitte 2.1. bis 2.9. liegen eigene Originalarbeiten zu Grunde, welche sich im Anhang befinden und die ausgewiesenen Abbildungen beinhalten.

2.1 Einfluss auf Zellviabilität und Morphologie

Anlage:

Scheer M, Bork K, Simon F, Nagasundaram M, Horstkorte R, Gnanapragassam VS (2020) Glycation Leads to Increased Polysialylation and Promotes the Metastatic Potential of Neuroblastoma Cells. Cells 9(4).

Selke P, Rosenstock P, Bork K, Strauss C, Horstkorte R, **Scheer M** (2021) Glycation of benign meningioma cells leads to increased invasion. Biol Chem.

Schildhauer P, Selke P, Scheller C, Strauss C, Horstkorte R, Leisz S, **Scheer M** (2023) Glycation Leads to Increased Invasion of Glioblastoma Cells. Cells 12(9):1219.

MGO wird von einigen Autoren als Tumorpromotor angesehen, welcher Proliferation und Invasion der Tumorzellen steigern kann (Antognelli et al. 2019; Nokin et al. 2016). Wiederum konnten andere Studien eher gegenteilige Effekte mit einer gesteigerten Apoptose und Reduktion von Proliferation sowie Invasion nachweisen (Kim et al. 2010; Guo et al. 2016). Daher war der erste Schritt, den Einfluss verschiedener Konzentrationen von MGO in den verwendeten Modellen mit Neuroblastom-, Meningeom- sowie Glioblastomzellen auf die Zellviabilität zu untersuchen (Schildhauer et al. 2023a; Scheer et al. 2020; Selke et al. 2021b). Für die vorgelegten Originalarbeiten wurden dabei die humane Neuroblastom-Zelllinie *Kelly*, die benigne Meningeom-Zelllinie *BEN-MEN1*, die maligne Meningeom-Zelllinie *IOMM-Lee* sowie die Gliom-Zelllinien LN229, U251, U343 und humane Astrozyten als Referenz genutzt. Bezüglich der Zellviabilität wurden der MTT (3-(4,5-Dimethylthiazol-2-yl) -2,5-diphenyltetrazoliumbromid)- bzw. XTT (Natrium-2,3-bis-(2-methoxy-4-nitro-5-sulfophenyl) -5-[(phenylamino)carbonyl]-2H-Tetrazolium)-Test genutzt. Beide basieren auf der Umwandlung des Tetrazolium-Salzes durch Dehydrogenase-Enzyme zu einem stark gefärbten Formazan-Farbstoff. Die durch den Farbstoff bedingte Absorption bei einer bestimmten Wellenlänge kann quantifiziert werden und so dieser Test als Maß für den Anteil vitaler Zellen herangezogen werden.

In dem Modell mit Neuroblastom-Zellen erfolgte die Behandlung mit MGO über 48 Stunden mit Konzentrationen von 5 bis 1000 µM. Eine signifikante Reduktion der Viabilität war ab einer Konzentration von bei 250 µM im MTT-Test ersichtlich (Scheer et al. 2020).

Das Modell mit Meningeom-Zellen des WHO-Grades 1 sowie 3 wurden Konzentrationen zwischen 0,1 mM sowie 1,0 mM untersucht. Im MTT-Test zeigte sich in beiden Zelllinien eine signifikante Reduktion der Zellviabilität bei 1,0 mM (Abbildung 3). Die Inkubation erfolgte im Vergleich zur Studie mit Neuroblastom-Zellen für 24 Stunden (Selke et al. 2021b).

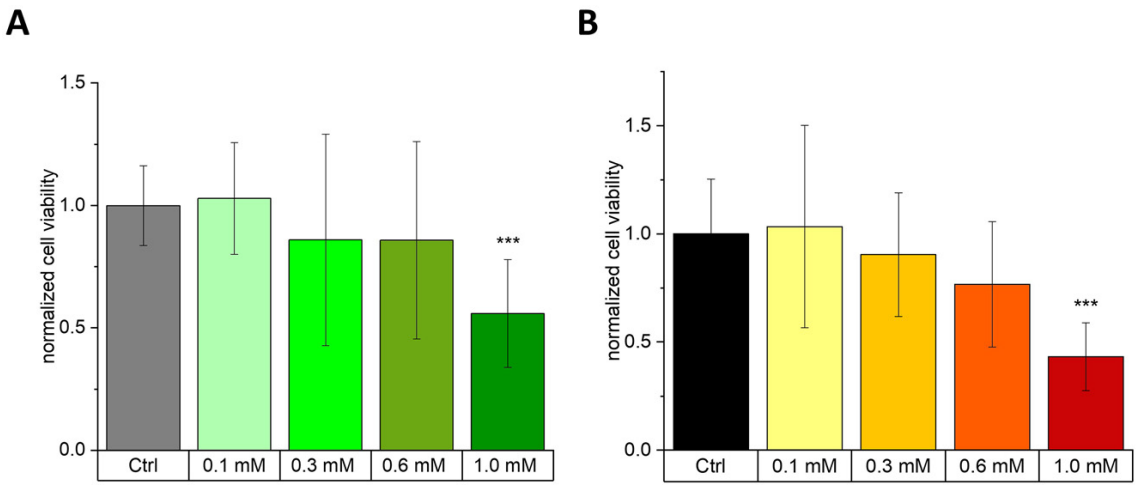

Abbildung 3: Zellviabilität von Meningeom-Zelllinien nach 24-stündiger MGO-Behandlung. Die Viabilität wurde mit einem MTT-Test für BEN-MEN-1 (WHO-Grad 1, **A**) und IOMM-Lee-Zellen (WHO-Grad 3, **B**) analysiert. Die Zellen wurden in Abwesenheit (Kontrolle, Ctrl) oder in Anwesenheit von MGO (0,1; 0,3; 0,6 und 1,0 mM) ausgesät. Beide Zelllinien zeigten eine abnehmende Stoffwechselaktivität mit steigender MGO-Konzentration. Die statistische Analyse wurde mit einem t-Test durchgeführt. Die Diagramme stellen die Mittelwerte und Standardabweichung von sieben unabhängigen biologischen Replikaten dar (***$p < 0{,}005$)

Zusätzlich wurde in der vorliegenden Originalarbeit auch der Einfluss auf die Zellmorphologie mittels Mikroskopie analysiert. Bei steigender Konzentration von MGO war eine Änderung mit eher rundlicher Form und mit weniger Zellausläufern ersichtlich. Die Effekte waren ab einer Konzentration von 0,6 mM augenscheinlich (Selke et al. 2021b).

Ein ähnlicher Ansatz erfolgte im Modell Glioblastom-Zellen. Auch hier wurden die Zellen für 24 Stunden mit MGO-Konzentrationen von 0,1 bis 1 mM behandelt und der Farbumschlag mittels XTT-Test analysiert. Eine signifikante Reduktion der Viabilität kam hier bereits 0,3 mM zur Darstellung. Interessanterweise zeigten humane Astrozyten, welche als gesunde Vergleichsgruppe dienten, eine höhere Toleranz mit einer signifikanten Reduktion der Viabilität ab 0,6 mM. Auch in diesem Modell zeigte sich ein Einfluss der MGO-Konzentration auf die Morphologie. So war hier, neben einer Reduktion der Zellzahl bei höheren Konzentrationen, auch eine Änderung hinzu einem eher sphärischen Aussehen im Vergleich zur unbehandelten Kontrolle ersichtlich (Schildhauer et al. 2023a).

Gleichartige Veränderungen im Bereich der Morphologie können durch äußere Stressoren und im Rahmen der Apoptose auftreten (Elmore 2007). Andere Autoren konnten dies auch nach Behandlung mit MGO nachweisen (Kalapos und Groot 1992; Nomura et al. 2020). Die Beobachtungen der morphologischen Änderungen bei höheren Konzentrationen von MGO korrelieren daher gut mit den Viabilitäts-Messungen in den hier zugrundeliegenden Arbeiten.

Die Daten in der Literatur zum Einfluss von MGO auf Zellviabilität und Proliferation variieren stark je nach Art der Anwendung und verwendeten Zell-Modell. Beispielsweise resultierte die Inkubation von HEK (*Human Embryonic Kidney*)-Zellen mit 0,1 – 0,3 mM MGO über einen Zeitraum von 24 Stunden in einer Steigerung Apoptose-Rate (Wang und Chang 2010). Bei der Gliom-Zelllinie U87 stimulierten niedrige Konzentrationen bis 0,3 mM MGO das Tumorwachstum, während höhere Dosen über 0,5 mM das Wachstum inhibierten (Nokin et al. 2017; Paul-Samojedny et al. 2016). Dosierung von über 0,5 mM waren in einer weiteren Studie mit RT4 Zellen sowie U87 Gliom-Zellen mit einer erhöhten Apoptose verbunden (Lee et al. 2009). Durch Verlängerung der Inkubationsdauer auf 72 Stunden führten bereits deutlich geringere Konzentration von 25 µM zu einer Reduktion der Proliferation in den Glioblastom-Zelllinien T98G sowie U87 (Paul-Samojedny et al. 2016). Andererseits konnten Lin et al. in einem Maus-Modell mit kolorektalem Karzinom durch intraperitoneale Zufuhr von 50 mg MGO je Kilogramm Körpergewicht die Proliferation der Tumorzellen signifikant steigern (Lin et al. 2018). Analoge Ergebnisse zeigten sich in einem Modell mit der Mammakarzinom-Zelllinie MDA-MB-231, bei der eine Behandlung mit 0,1 mM MGO zu einer Steigerung der Proliferation führte (Sharaf et al. 2015). Einige Autoren untersuchten mögliche Ursachen für protumorgene Eigenschaften durch eine Behandlung mit MGO. Oya-Ito et al. Konnten zeigen, dass MGO zu einer Glykierung des *Heat Schock Proteins 27* führt, welches das Zellüberleben fördert und anti-apoptotisch wirkt. (Oya-Ito et al. 2011). Die Abhängigkeit der Wirkung vom Zelltyp konnte in einer weiteren Studie aufgezeigt werden, in welcher die mittlere letale Dosis (LD 50) einer 24-stündigen MGO-Behandlung bei Neuronen und Astrozyten untersucht wurde. Es ergaben sich Werte von 3,3 mM für Astrozyten und 0,5 mM MGO für Neurone (Bélanger et al. 2011). Die eigenen Daten bestätigten insgesamt die aus der Literatur. Je nach Konzentration kann MGO die Proliferation fördern, aber auch zytotoxisch wirken.

2.2. Induktion von Glykierung

Anlage:

Scheer M, Bork K, Simon F, Nagasundaram M, Horstkorte R, Gnanapragassam VS (2020) Glycation Leads to Increased Polysialylation and Promotes the Metastatic Potential of Neuroblastoma Cells. Cells 9(4).

Selke P, Rosenstock P, Bork K, Strauss C, Horstkorte R, **Scheer M** (2021) Glycation of benign meningioma cells leads to increased invasion. Biol Chem.

Schildhauer P, Selke P, Scheller C, Strauss C, Horstkorte R, Leisz S, **Scheer M** (2023) Glycation Leads to Increased Invasion of Glioblastoma Cells. Cells 12(9):1219.

Ein Ziel dieser kumulativen Arbeit war es, den Effekt von Glykierung auf Tumoren des Nervensystems zu untersuchen. Diesbezüglich gilt MGO als der potenteste Präkursor für die Bildung von AGEs, den Endprodukten der Glykierungsreaktion (Bellier et al. 2019; Lai et al. 2022). Ob MGO Glykierung auch in den Modellen mit Neurobastom-, Meningeom- sowie Glioblastomzellen induzieren konnte und ob dies von der Konzentration abhängig war, wird im folgenden Abschnitt dargelegt. Die Daten der vorliegenden Originalarbeiten zur Glykierung wurden mittels *Western Blot*-Verfahren und anschließender *Sodium Dodecyl Sulfate* (SDS)-Gelelektrophorese generiert. Der Antikörper für Carboxymethyllysin (CML) hat sich als Nachweis der Glykierungsreaktion etabliert und kam auch hier zu Anwendung (Delgado-Andrade 2016; Jaisson und Gillery 2021; Takeuchi et al. 1999).

Im ersten Modell mit Neuroblastom-Zellen erfolgte die Behandlung mit 0,1 mM MGO über einen Zeitraum von 48 Stunden. Das Signal für CML konnte dadurch verfünffacht werden (Scheer et al. 2020). Eine vermehrte AGE-Bildung geht aufgrund einer positiven Rückkopplung häufig mit einer gesteigerten RAGE-Expression einher (Lee et al. 2021; Oliveira et al. 2022). In diesem Modell war dies ab 0,3 mM im Western Blot ersichtlich. Da es bei dieser Konzentration zu einer Beeinträchtigung der Viabilität kam, wurden die Daten in der Originalarbeit nicht gezeigt. In dem zweiten Modell mit Meningeom-Zellen kam es zu einem konzentrationsabhängigen Effekt hinsichtlich des CML-Signals. Eine signifikante Steigerung des Signals war sowohl in der WHO-Grad 1-Zelllinie als auch in der WHO-Grad 3-Zelllinie ab 0,3 mM nachweisbar (Selke et al. 2021b). In beiden Zelllinien kam es durch die Modifikation der Glykierung als zu einer vermehrten RAGE- Expression (Daten nicht gezeigt) (Selke et al. 2021b).

Bei den Versuchen mit Glioblastom-Zellen und den humanen Astrozyten zeigte sich ebenfalls ein konzentrationsabhängiger Effekt hinsichtlich des CML-Signals nach MGO-

Behandlung. Jedoch variierte der Effekt zwischen den Zelllinien. Eine signifikante Steigerung des Signals war bei LN229-Zellen ab 0,3 mM nachweisbar, bei U251-Zellen ab 1,0 mM, bei U343-Zellen und humanen Astrozyten ab 0,6 mM (Schildhauer et al. 2023a).

Die Art der Anwendung von MGO zur Induktion von Glykierung ist in der Literatur sehr variabel. Die Glykierung erfolgt dabei, analog zu den eigenen Arbeiten, teilweise direkt durch Zugabe des Reagenzes zur Zellkultur, teilweise indirekt durch Nutzung von glykiertem Serum-Albumin (Nam et al. 2021; Nokin et al. 2016; Sharaf et al. 2015). Einige Autoren nutzten im Tiermodell auch die orale Zufuhr von MGO oder eine intraperitoneale Applikation bei einem Kolonkarzinom-Modell (Zunkel et al. 2020; Lin et al. 2018). Die Anwendung von MGO führte jedoch immer zu einer gesteigerten Glykierung (Nokin et al. 2017; Nam et al. 2021; Lin et al. 2018). Baig et al. zeigten in ihrer Studie, dass bei Myoblasten-Zellen des Typs C2C12 eine Behandlung mit MGO mit Konzentration zwischen 0,1 mM bis 0,4 mM über den Zeitraum von 4 Tagen sowohl zu einer vermehrten Glykierung als auch zu einer Steigerung der RAGE-Expression führt (Baig et al. 2017). Neben einem konzentrationsabhängigen zytotoxischen Effekt von MGO war bei Untersuchungen unter Nutzung von *Saccharomyces cerevisiae* auch ein Einfluss des Behandlungszeitraumes ersichtlich. Interessanterweise war der Effekt nach 4 Stunden stärker als nach 24 Stunden (Tupe et al. 2019). Eine weitere Studie konnte in humanen Stroma-Zellen des Knochenmarks eine signifikante Steigerung der Glykierung durch eine Behandlung mit MGO nachweisen. Zur Anwendung kam eine Konzentration von 0,8 mM über einen Zeitraum von 96 Stunden, wobei höhere Konzentrationen einen toxischen Effekt zeigten (Waqas et al. 2022).

Medeiros et al. nutzten ein Maus-Modell zum akuten Lungenversagen, bei dem eine intranasale MGO-Zufuhr mit einer erhöhten Expression von RAGE im Lungengewebe (bronchoalveoläre Lavage) einherging. Dies war verbunden einem signifikanten Anstieg reaktiver Sauerstoffspezies. Der Effekt konnte durch gleichzeitige Gabe des oralen Antidiabetikums Metformin normalisiert werden (Medeiros et al. 2021). Eine Steigerung der RAGE-Expression war ebenso in einem Maus-Modell nach oraler Zufuhr von MGO in Urothel-Zellen zu verzeichnen (Oliveira et al. 2022). In einem vergleichbaren Modell war durch diese Art der Anwendung auch eine vermehrte RAGE-Expression im Hippocampus der Tiere nachweisbar (Pucci et al. 2021). Ähnliche Ergebnisse zeigten sich in Mesangiumzellen nach Behandlung mit MGO, bei welchen eine vermehrte RAGE-Expression mit Steigerung

pro-inflammotorischer Proteine wie des Tumornekrosefaktors Alpha (TNF α) nachweisbar waren. Durch RAGE-Knockout ließ dieser Effekt komplett umkehren (Lee et al. 2021).

2.3. Induktion von Glykosylierung

Anlage:

Scheer M, Bork K, Simon F, Nagasundaram M, Horstkorte R, Gnanapragassam VS (2020) Glycation Leads to Increased Polysialylation and Promotes the Metastatic Potential of Neuroblastoma Cells. Cells 9(4).

Neben der nicht-enzymatischen Glykierung sollte auch die enzymatische Glykosylierung in der kumulativen Arbeit berücksichtigt werden, welche bei vielen Tumoren als prognostischer Marker gilt (Thiesler et al. 2022). In der vorliegenden Originalarbeit wurden Neuroblastom-Zellen zunächst mit 100 µM MGO für 48 Stunden inkubiert. Die Messung der Sialinsäure-Menge erfolgte via *High Performance Liquid Chromatography* (HPLC). Außerdem erfolgte der Nachweis der Polysialylierung unter Zuhilfenahme eines PolySia-Antikörpers mittels *Western Blot*-Verfahren. Auch das Molekül NCAM wurde in dieser Arbeit mittels *Western Blot* analysiert.

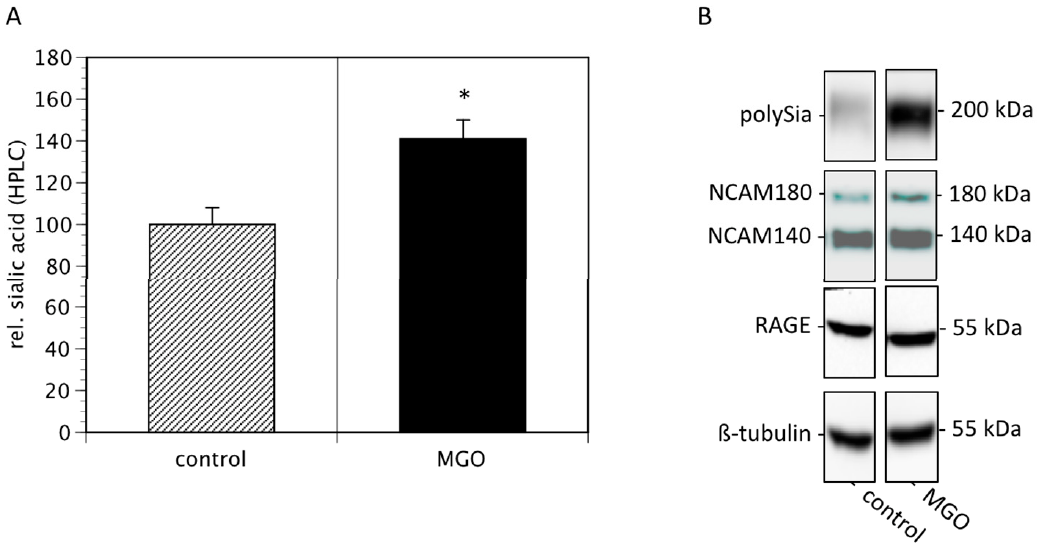

Abbildung 4: Neuroblastom-Zellen wurden in Abwesenheit (Kontrolle) oder Anwesenheit von 100 µM MGO für 48 h inkubiert. (A) Darstellung der HPLC-Analyse nach vorheriger Spaltung und Markierung der Sialinsäuren. Die Diagramme stellen die Mittelwerte und Standardabweichung von drei unabhängigen biologischen Replikaten dar (* $p < 0,05$). (B) Darstellung der Western Blots. Der Nachweis der Polysialylierung erfolgte mit monoklonalem 735-Antikörper. Die NCAM-Expression wurde mit dem monoklonalen 123C3-Antikörper analysiert. Zur Kontrolle wurden ß-Tubulin-Färbungen verwendet.

In der HPLC-Analyse zeigte sich durch MGO-Behandlung eine Steigerung der relativen Sialinsäure-Menge um nahezu 50% (Abbildung 4A). Hinsichtlich der Polysialylierung war

eine drastische Steigerung PolySia-Signal im *Western Blot* nach MGO-Behandlung zu verzeichnen. Das Signal für NCAM, als einer der wichtigsten Träger für PolySia im Menschen gilt, zeigte wiederum keine Änderung durch eine MGO-Behandlung (Hildebrandt et al. 2010). Wie im Abschnitt zuvor erwähnt, zeigte RAGE bei dieser Konzentration noch keine Änderung. Die Bestimmung von ß-Tubulin diente als Kontrolle (Scheer et al. 2020).

Ebenfalls in einem Modell mit Neuroblastom-Zellen (Typ IMR32) war durch eine Modifikation der PolySia eine Regredienz der Migration zu beobachten. PolySia wurde hier durch Zugabe von Sialinsäure-Vorstufen induziert (Seifert et al. 2012). Als bisher einzige Arbeitsgruppe haben wir nachgewiesen, dass eine Behandlung mit MGO ebenfalls Einfluss auf die Glykosylierung hat.

Das Enzym GNE gilt als Schlüsselenzym der Sialinsäure-Produktion. Hagenhaus et al. konnten in Ihrer Arbeit zeigen, dass MGO die Aktivität dieses Enzyms beeinflussen kann. In den verwendeten Myoblasten des Typs C2C12 war nach MGO-Behandlung eine Reduktion der Aktivität auf circa 13% des Ausgangswertes zu verzeichnen (Hagenhaus et al. 2023). Eine weitere Studie konnte zeigen, dass ein spezifischer GNE-Knockout in Muskelzellen mit drastischer Reduktion der Sialylierung einherging (Harazi et al. 2023). Aufgrund der gestiegenen Sialinsäure-Menge in der vorgelegten Originalarbeit, wäre eher ein gegensätzlicher Effekt in diesem Zusammenhang zu vermuten.

PolySia, welche durch Vertreter der ST8SIA-Familie verknüpft werden, sind in vielen Tumorarten überexprimiert. Beispiele hierfür sind das nicht-kleinzellige Bronchialkarzinom, Lymphome, das Pankreaskarzinom oder das Mammakarzinom. Zumeist ist hier NCAM Träger für PolySia (Sato und Kitajima 2021). Weiterhin gilt PolySia bei einigen Tumoren, wie dem Glioblastom, als negativer prognostischer Marker (Amoureux et al. 2010).

Neben PolySia ist eine Modifikation der Sialylierung bei vielen Tumorarten nachweisbar. Diese haben sich in einigen Fällen als Marker für den Therapieerfolg etabliert. Erwähnt seien hier Vertreter wie PSA, CEA oder CA 19-9 (Reiter et al. 2015; Silsirivanit 2019).

Durch eine Modifikation der Sialylierung sind auch Reaktionsprodukte wie Ganglioside an der Zelloberfläche modifiziert. Beispielweise konnte eine Überexpression des Gangliosids GM3 auf Melanomzellen oder Mammakarzinomzellen nachgewiesen werden (Munkley 2022). Die Sialylierung ist mitverantwortlich für den Tumorprogress und die Metastasierung,

dadurch dass sie Prozesse wie Adhäsion und Invasion beeinflusst sowie Zelltod-Signalwege hemmt (Häuselmann und Borsig 2014; Dobie und Skropeta 2021). Außerdem können Zellen des Immunsystems durch die Modifikation der membranständigen Glykoproteine Tumorzellen nicht mehr erkennen. Dadurch sind diese in der Lage einer Immunantwort zu umgehen *(Immune Escape)* (Dusoswa et al. 2020). Eine Steigerung des PolySia-Signals in der vorgelegten Arbeit unterstreicht daher den aggressiveren Phänotyp der Neuroblastom-Zellen nach MGO-Behandlung.

2.4. Expression von Sialyltransferasen

Anlage:

Selke P, Bork K, Zhang T, Wuhrer M, Strauss C, Horstkorte R, **Scheer M** (2021) Glycation Interferes with the Expression of Sialyltransferases in Meningiomas. Cells 10(12).

Die Sialylierung an der Zelloberfläche ist einerseits abhängig von der Sialinsäure-Produktion, wie im Abschnitt zuvor angedeutet. Andererseits ist sie von der enzymatischen Verknüpfung an der Zielstruktur durch ST abhängig (Harduin-Lepers et al. 2001). Dies wurde in der vorliegenden Originalarbeit im Modell mit Meningeom-Zelllinien des WHO-Grades 1 sowie 3 analysiert. Die Ergebnisse basieren auf der Messung mittels sondenbasierter quantitativer Polymerasenkettenreaktion (qPCR) nach vorheriger RNA-Extraktion und Transkription in komplementärer Desoxyribonukelinsäure (*complementary* DNA = cDNA). Gegenübergestellt wurde die Expression der unbehandelten Kontrolle sowie nach einer Inkubation mit 0,3 mM MGO über einen Zeitraum von 24 Stunden. Beim Vergleich der unbehandelten Kontrollen der benignen sowie maligne Zellen zeigten sich Unterschiede in dem Signal einiger Sialyltransferasen. Beispielsweise war die ST8SIA2 in der Grad 1 Zelllinie stark exprimiert und nur schwach in der malignen Zelllinie. Gleiches gilt für die ST8SIA6, welche ebenfalls in der benignen Linie deutlich stärker exprimiert war. Die ST6GAL2 war in der malignen Linie nicht exprimiert, während sie in der benignen Zelllinie im Intermediär-Bereich exprimiert wurde. Durch die Glykierung kam es in der benignen Linie eher zu einer Steigerung der Expression eines Großteils der ST, wie z.B. bei ST3GAL1-2, ST6GAL1-2 oder ST8SIA1. In der malignen Zelllinie zeigten sich gegenteilige Effekte mit einer reduzierten Expression dieser ST (Selke et al. 2021a).

Der Expressionsgrad der ST in verschiedenen Tumoren war Gegenstand einiger Arbeiten in der Literatur. Die ST3GAL1 war im Ovarkarzinom überexprimiert und zudem in die EMT involviert, wobei der *Transforming Growth Factor Beta* (TGF-ß) - Signalweg aktiviert wurde. Dadurch kam es zu einer Steigerung der Migration sowie Proliferation der Tumorzellen (Wu et al. 2018). In der eigenen Arbeit war diese ST in der benignen Zelllinie ebenfalls stärker exprimiert und zeigte eine Korrelation mit einer Steigerung der Invasion (s. Abschnitt 2.9) (Selke et al. 2021a).

Auch die Expression von ST3GAL2 zeigte ein ähnliches Verhalten nach MGO-Behandlung (Selke et al. 2021a). Hohe Level an ST3GAL2 waren bei Patientinnen mit Ovar- und Mammakarzinom mit einer schlechten Prognose assoziiert (Aloia et al. 2015). Der Expressionsgrad der ST3GAL2 sowie die Gesamtmenge der Sialinsäuren zeigten bei PatientInnen mit einer chronisch myeloischen Leukämie eine Korrelation zum Tumorstadium und konnten so als Verlaufs-Marker genutzt werden. Eine Überexpression dieser ST war darüber hinaus mit einer Resistenz gegenüber dem Tyrosinkinase-Inhibitor Imatinib vergesellschaftet (Patel et al. 2022). Auf der anderen Seite gelang es Deschuyter et al. durch einen gezielten *Knock-out* von ST3GAL2 Proliferation, Migration und Invasion in-vitro sowie in-vivo bei kolorektalem Karzinom zu verringern (Deschuyter et al. 2022). In Zellen des Mundbodenkarzinom zeigte sich hingegen eine Herunterregulation von ST3GAL2 im Vergleich zum Normalgewebe (Mehta et al. 2020).

Neben Vertretern der ST3GAL-Reihe zeigte sich auch eine vermehrte Expression von ST6GAL1 in der benignen Zelllinie nach MGO-Behandlung in der vorliegenden Originalarbeit (Selke et al. 2021a). In der Literatur finden sich einige Quellen, welche ähnliche Ergebnisse beschreiben. Hait et al. zeigten, dass eine Überexpression von ST6GAL1 in Zellen des Mammakarzinoms mit einer gesteigerten Proliferation und Invasivität verbunden war (Hait et al. 2022). Im Rektumkarzinom war eine Überexpression von ST6GAL1 mit einer Resistenz gegenüber Chemotherapie sowie Radiatio assoziiert (Smithson et al. 2022).

Durch die MGO-Behandlung war in der vorgelegten Originalarbeit weiterhin auch eine vermehrte Expression von ST6GAL2 nachweisbar (Selke et al. 2021a). Xu et al. konnten zeigen, dass eine Überexpression mit einem aggressiveren Verhalten sowie einer schlechteren Prognose beim follikulären Schilddrüsenkarzinom verbunden war (Xu et al. 2020). Andererseits schien eine Herunterregulation von ST6GAL2 im Mammakarzinom mit einem verlängerten Überleben und geringer Invasivität verbunden zu sein. Eine starke

Expression dieser ST fand sich überwiegend in Patientinnen mit fortgeschrittenem Tumorstadium (Cheng et al. 2020). Insgesamt scheinen die Beobachtung der eigenen Arbeit mit Steigerung der Expression einzelner ST in der benignen Zelllinie durch MGO-Behandlung bei gleichzeitiger Steigerung der Invasivität sich mit den Daten der Literatur zu decken.

2.5. Gangliosid GM3 Expression

Anlage:

Selke P, Bork K, Zhang T, Wuhrer M, Strauss C, Horstkorte R, **Scheer M** (2021) Glycation Interferes with the Expression of Sialyltransferases in Meningiomas. Cells 10(12).

Ganglioside stellen eines der Reaktionsprodukte der ST dar (Breiden und Sandhoff 2018). Typischerweise kommt es durch Modifikation der Expression von ST auch zu einer Veränderung der Sialylierung sowie Kumulation von Glykanen an der Zelloberfläche (Munkley 2022).

Aufgrund der Modifikation von ST3GAL5 in der vorliegenden Originalarbeit, erfolgte ebenfalls die Messung der Konzentration eines typischen Reaktionsproduktes, nämlich des Gangliosids GM3. Die Ergebnisse basieren auf der Messung durch Nano-Flüssigchromatographie mit porösem graphiertem Kohlenstoff, gekoppelt mit einem Tandem-Massenspektrometer. Korrelierend zur verringerten Expression von ST3GAL5 in der benignen Zelllinie nach MGO-Behandlung war auch das Signal von GM3 reduziert (Selke et al. 2021a). Wie im Abschnitt zuvor beschrieben, erfolgte die Inkubation mit 0,3 mM MGO über einen Zeitraum von 24 Stunden.

GM3 ist bei vielen Karzinomen, wie z.B. dem Melanom oder dem Bronchialkarzinom überexprimiert (Zheng et al. 2019). Weitere Studien konnten zeigen, dass GM3 zudem die Zelladhäsion sowie das Tumorwachstum beeinflusst (Hakomori und Handa 2015). In einer klinischen Studie zeigte sich, dass die GM3-Konzentration im Serum als Biomarker für das Vorhandensein sowie das Tumorstadium bei Patientinnen mit einem Mammakarzinom geeignet war (Li et al. 2019). Ein gezieltes *Silencing* von GM3 durch *small interfering RNA* (siRNA) war in Zellen des Mammakarzinoms mit einer reduzierten Migrations- und Invasionsrate sowie einer Reduktion der Proliferation verbunden (Gu et al. 2008). Die verringerte Expression von GM3 nach MGO-Behandlung bei gleichzeitiger Steigerung der

Invasivität in der vorgelegten Originalarbeit steht daher in Kontrast zu den hier aufgeführten Quellen.

2.6. Expression von extrazellulären Matrixproteinen und Transkriptionsfaktoren

Anlage:

Selke P, Rosenstock P, Bork K, Strauss C, Horstkorte R, **Scheer M** (2021) Glycation of benign meningioma cells leads to increased invasion. Biol Chem.

Schildhauer P, Selke P, Scheller C, Strauss C, Horstkorte R, Leisz S, **Scheer M** (2023) Glycation Leads to Increased Invasion of Glioblastoma Cells. Cells 12(9):1219.

Als extrazelluläre Matrix wird der gesamte Gewebeanteil im Interzellularraum bezeichnet. Dies können Fasern wie Kollagene oder retikuläre Fasern, Adhäsionsmoleküle oder Proteoglykane sein. Diese sind essenziell für Zell-Zell-Interaktionen und die Gewebearchitektur. Zudem spielen Sie eine Rolle bei gerichteter Zielbewegung und Polarität der Zellen (Ayad 1998).

In den vorliegenden Originalarbeiten wurde die Expression von E- und N-Cadherinen in Meningeom- sowie Glioblastom-Zellen mittels *Western Blot*-Verfahren untersucht (Selke et al. 2021b; Schildhauer et al. 2023a). In der benignen Meningeom-Zelllinie kam es durch Behandlung mit 0,3 mM MGO über einen Zeitraum von 24 Stunden zu einer Steigerung der E-Cadherin-Expression bei gleichzeitiger Reduktion der N-Cadherin-Expression. Im Vergleich zeigte die maligne Meningeom-Zelllinie weder eine Änderung der E-Cadherin- noch der N-Cadherin-Expression. Im unbehandelten Zustand zeigten die malignen Zellen ein deutlich stärkeres Signal für E-Cadherin, wohingegen die N-Cadherin-Expression der unbehandelten Kontrollen in der benignen Zelllinie stärker war (Selke et al. 2021b).

Ähnliche Ergebnisse zeigten sich im zweiten verwendeten Modell mit Glioblastomzellen. Hier erfolgte eine Inkubation mit MGO mit Konzentrationen zwischen 0,3 bis 1,0 mM über einen Zeitraum von 24 Stunden, wobei sich ein konzentrationsabhängiger Effekt zeigte. Auch hier fand sich ein stärkeres Signal für E-Cadherin bei den Zelllinien U343 und U251 bei gleichzeitig reduziertem Signal von N-Cadherin in U343-Zellen. In der Zelllinie LN 229 führte MGO zu keiner Änderung der E-Cadherin-Expression und zu einer diskreten, nicht signifikanten Reduktion der N-Cadherin-Expression. Als Referenz wurden humane Astrozyten verwendet, welche keine E-Cadherin-Expression aufwiesen und eine drastische

Reduktion der N-Cadherin-Expression durch MGO-Behandlung zur Darstellung kam (Schildhauer et al. 2023a).

Eine Veränderung der Cadherin-Expression kann die Zellpolarität, das Adhäsionsvermögen sowie die Invasivität von Zellen beeinflussen. Typischerweise kommt es dabei zu einer gegenläufigen Regulation dieser Glykoproteine, wobei eine Hochregulation von N-Cadherin auch mit dem Prozess der EMT und eine Hochregulation von E-Cadherin mit dem Prozess der Mesenchymal-epithelialen Transition (MET) einhergeht (Liao und Yang 2017).

Bei Meningeomen ist eine geringe Expression von E-Cadherin überwiegend bei invasiven und höhergradigen Tumoren nachweisbar (Utsuki et al. 2005; Wallesch et al. 2017). Ein kompletter Verlust von E-Cadherin fand sich bei dem seltenen Fall eines metastasierten, malignes Meningeoms (Lisowski et al. 2023). Im Einklang mit fanden Zhou et al. eine hohe Expression von E-Cadherin im Tumormaterial von PatientInnen mit einem WHO-Grad 1 Meningeom. Dies korrelierte stark mit einem weniger invasiven Verhalten (Zhou et al. 2010). Dem gegenüber ließen sich hohe N-Cadherin-Werte bei malignen Meningeomen nachweisen und waren mit einem verstärkten perifokalen Ödem in der Bildgebung assoziiert (Rutkowski et al. 2018). In der vorliegenden Originalarbeit fand sich, im Kontrast zu den aufgeführten Quellen, eine starke Expression von E-Cadherin in der malignen Zelllinie sowie eine verstärkte Expression durch Glykierung in der benignen Zelllinie, was mit einer gesteigerten Invasion verbunden war. Hinsichtlich der Modifikation der Cadherine durch Glykierung finden sich keine Daten in der Literatur.

Einfluss der E-Cadherin-Expression beim Glioblastom ergeben sich kontroverse Angaben in der Literatur. Die Gruppe um Lewis-Tuffin et al. zeigte, dass E-Cadherin nur selten von Glioblastom-Zellen exprimiert wurde. Im Falle einer E-Cadherin-Expression war dies mit einer verstärkten Invasion im Tiermodell verbunden (Lewis-Tuffin et al. 2010). In anderen Studien war hingegen eine erhöhte E-Cadherin-Expression mit einer verringerten Invasion verbunden (Zhao et al. 2019). Yu et al. demonstrierten, dass eine stärkere Invasion sowie Migration mit einer vermehrten Expression von N-Cadherin und verringerten Expression von E-Cadherin verbunden war (Yu et al. 2016). Eine erhöhte Expression von N-Cadherin war in Glioblastom-Zellen ebenfalls mit einer Radioresistenz assoziiert (Osuka et al. 2021).

Der Einfluss der Glykierung auf die Cadherin-Expression konnte in weiteren Studien dargelegt werden. Im kolorektalen Karzinom war eine Glykierung mit einer Reduktion der

Expression von E-Cadherin verbunden. Zudem kam es dadurch zu einer Steigerung der Invasion und Proliferation (Liang 2020). Bei humanen peritonealen Mesothelzellen konnte durch Inkubation mit Glukose-Abbauprodukte, darunter auch MGO, eine EMT mit Reduktion von E-Cadherin induziert werden. Zudem kam es durch die Glykierung zu einer Überexpression von TGF-ß (Liang 2020; Oh et al. 2010). Durch eine MGO-bedingte Glykierung war in Myofibroblasten eine Steigerung des Gesamt-Cadherins zu beobachten, was mit einer verringerten Adhäsion sowie verstärkten Migration verbunden war (Yuen et al. 2010).

In der vorgestellten Originalarbeit wurde in Glioblastomzellen der Einfluss der MGO-Behandlung auf die Expression weiterer Proteine der extrazellulären Matrix Expression sowie einiger Transkriptionsfaktoren mittels *messenger RNA* (mRNA)-basierten qPCR analysiert. Untersucht wurde der Effekt nach einer Inkubation mit 0,3 mM MGO über einen Zeitraum von 24 Stunden (Schildhauer et al. 2023a). Eingegangen wird hier auf die Ergebnisse mit den stärksten Effekten. Interessanterweise waren teils starke, zelltypspezifische Effekte zu beobachten. In den Linien U251 sowie U343 kam es durch MGO-Behandlung zu einer vermehrten Expression des Transmembran Glykoproteins CD44 (CD = *Cluster of differentiation*). Dieser Effekt zeigte sich auch bei Referenz mit humanen Astrozyten, jedoch nicht bei den LN229. CD44 zeigte eine starke Expression bei vielen Tumoren und eine Überexpression war mit einer schlechten Prognose assoziiert (Chen et al. 2018). Auch bei Gliomen konnte gezeigt werden, dass der Grad der Expression von CD44 mit der Prognose korreliert (Du et al. 2022). Zusätzlich wurde in Schnittkulturen demonstriert, dass die Abwesenheit von CD44 mit einer deutlichen verringerten Invasivität in Glioblastom-Zellen verbunden war (Ivanova et al. 2022). Dass Glykierung die Expression von CD44 induzieren kann, konnte Kishikawa et al. im Modell mit humanen Monozyten zeigen (Kishikawa et al. 2006). Die Behandlung mit MGO konnte auch in Muskelzellen die CD44-Expression stimulieren. Untersucht wurde das Sekretom von murinen Muskelzellen nach entsprechender Vorbehandlung (Bai et al. 2020).

Das Proteoglykan Brevican ist ein weiterer typischer Vertreter der extrazellulären Matrix. In der angehängten Originalarbeit kam es durch MGO-Behandlung zu einer Steigerung in den Zelllinien LN229 sowie U251 (Schildhauer et al. 2023a). Brevican wird von vielen Gliomen überexprimiert (Giamanco und Matthews 2020). Es konnte ferner gezeigt werden, dass Expression von Brevican mit einem fortgeschrittenen Tumorstadium korreliert (Dwyer et al.

2014). Durch einen gezielten *Knockout* von Brevican in der Zelllinie U251 wurde sowohl die Invasivität als auch die Proliferation gehemmt (Lu et al. 2012). Der Einfluss von MGO bzw. Glykierung auf die Expression von Brevican ist in der wissenschaftlichen Literatur bisher nicht beschrieben worden.

In den Zelllinien LN229 sowie U251 zeigte sich in der vorliegenden Originalarbeit nach MGO-Behandlung eine Expressionssteigerung von Tenascin C, welches ein weiteres Glykoprotein der extrazellulären Matrix darstellt (Schildhauer et al. 2023a). Tenascin C ist relevant für die Morphogenese oder die Signalweiterleitung und wird im Rahmen der Wundheilung verstärkt exprimiert (Midwood et al. 2016). Aber auch bei chronisch-entzündlichen Erkrankungen oder Tumoren kommt es zu einer Überexpression (Midwood et al. 2016). In Gliomen korrelierte der Expressionsgrad von Tenascin C mit dem Grad der Invasivität (Xia et al. 2016). Auch Rupp et al. konnten zeigen, dass eine starke Expression von Tenascin C beim Glioblastom mit einer schlechteren Prognose einherging und zudem eine wichtige Rolle bei Tumorangiogenese spielte (Rupp et al. 2016). Eine Modulation der Expression von Tenascin C durch Glykierung oder MGO wurde durch andere Autoren bisher nicht untersucht.

Die MGO-Behandlung führte in der Zelllinie LN229 außerdem zu einer Steigerung der Expression von Versican, Thrombospondin sowie der Zinkfingerproteine SNAI1 und 2 (Schildhauer et al. 2023a). Versican gehört zur Klasse der Proteoglykane und ist wichtig für Prozesse wie Migration, Adhäsion und Proliferation. Eine Überexpression in Gliomen war mit einer Förderung der Tumorproliferation assoziiert (Hu et al. 2015). Onken et al. konnten in ihrer Studie den protumorösen Einfluss von Versican auf Migration sowie Proliferation in Glioblastomzellen aufzeigen (Onken et al. 2014).

Thrombospondin zählt zu den Glykoproteinen und kann Prozesse wie Angiogenese, Migration sowie Proliferation beeinflussen (Qi et al. 2021). Untersuchungen bei Gliomen zeigten, dass Thrombospondin im Tumorgewebe verglichen mit dem Normalgewebe deutlich höher exprimiert war. Eine Überexpression dieses Glykoproteins korrelierte weiterhin mit einer gesteigerten Proliferation sowie Migration in malignen Gliomen (Huang et al. 2022b). In einer Kohorte von PatientInnen mit Hirntumoren zeigte sich, dass die Blutserum-Werte von Thrombospondin mit dem Grad der Malignität des vorliegenden Hirntumors vergesellschaftete waren. Die Werte lagen bei malignen Gliomen deutlich höher

als bei niedriggradigen Gliomen oder Meningeomen (Kemerdere et al. 2021). Daher nutzten einige Autoren Thrombospondin bereits als Biomarker, um das Therapieansprechen zu monitoren (Qi et al. 2021). Andere Autoren haben den Einfluss von Glykierung oder MGO auf die Expression der beiden zuletzt genannten Vertreter der extrazellulären Matrix bisher nicht untersucht.

Die Transkriptionsfaktoren *Snail* (SNAI 1) und *Slug* (SNAI 2) sind Zinkfingerproteine, welche die Motilität von Zellen beeinflussen und sind beispielsweise im Rahmen der Wundheilung stärker exprimiert. Sie bedingten in Tumorzellen aber auch den Switch zu einem mesenchymalen Typen im Rahmen der EMT (Ganesan et al. 2016). Bei Gliomen waren sie in die Migration sowie Invasion involviert (Wang et al. 2021; Yuan et al. 2019; Zhong et al. 2020). In der vorliegenden Originalarbeit waren diese Zinkfingerproteine nach MGO-Behandlung in LN229 ebenfalls erhöht. Der Einfluss von MGO bzw. Glykierung auf SNAI-Proteine war bisher noch nicht Gegenstand in der Literatur.

Die Expression des Zytokins TGF-ß unter dem Einfluss von MGO wurde in der vorliegenden Originalarbeit ebenfalls analysiert. In den Zelllinien LN229 sowie U251 war eine Steigerung der Expression durch Glykierung zu beobachten (Schildhauer et al. 2023a). Es ist bekannt, dass TGF-ß in die Prozesse Proliferation sowie Invasion involviert ist (Kaminska et al. 2013). Eine Aktivierung von TGF-ß führte in Gliomzellen zur Verhinderung des proteasomalen Abbaus der Tumorzellen und konnte zudem Invasion sowie Migration fördern (Chao et al. 2020; Yan et al. 2022). Eine weitere Studie zeigte, dass TGF-ß durch eine Hochregulation von Claudin 4 maßgeblich für die Invasivität von Glioblastomzellen verantwortlich war (Yan et al. 2022). Sutariya et al. konnten in ihrer Arbeit zeigen, dass Hyperglykämie sowie AGEs zu einer vermehrten Expression von TGF-ß führten und eine diabetische Stoffwechsellage verschiedene Dysplasien fördern konnte (Sutariya et al. 2016).

Für die Motilität von Zellen sind Enzyme wichtig, welche die umgebende Matrix umbauen können. Typische Vertreter sind MMP, welche für den physiologischen Umbaus der ECM, aber auch für pathologische Prozesse wie der Metastasierung entscheidend sind (Almeida et al. 2022). In der vorliegenden Originalarbeit zeigte sich nach MGO-Behandlung eine Reduktion der MMP2 in der Zelllinie U251 sowie eine gesteigerte Expression in den Zelllinien LN229 sowie U343 (Schildhauer et al. 2023a). In anderen Arbeiten konnte nachgewiesen werden, dass hohe Level von MMP2 im Glioblastom mit einer schlechteren Prognose der

PatientInnen assoziiert waren (Zhou et al. 2019). Guan et al. zeigten, dass eine Hochregulation von MMP2 mit einer gesteigerten Invasion von Gliomzellen einherging (Guan et al. 2012). Wiederum war durch eine gezielte Suppression von MMP2 mittels *siRNA* eine Induktion der Apoptose in Gliomzellen zu beobachten (Kesanakurti et al. 2011). Die veränderte Expression der extrazellulären Matrixproteine sowie Transkriptionsfaktoren in dieser Arbeit nach MGO-Behandlung korreliert insgesamt gut mit der Modulation der Invasivität (s. Abschnitt 2.9.).

2.7. Einfluss auf Adhäsion

Anlage:

Scheer M, Bork K, Simon F, Nagasundaram M, Horstkorte R, Gnanapragassam VS (2020) Glycation Leads to Increased Polysialylation and Promotes the Metastatic Potential of Neuroblastoma Cells. Cells 9(4).

Selke P, Rosenstock P, Bork K, Strauss C, Horstkorte R, **Scheer M** (2021) Glycation of benign meningioma cells leads to increased invasion. Biol Chem.

Schildhauer P, Selke P, Scheller C, Strauss C, Horstkorte R, Leisz S, **Scheer M** (2023) Glycation Leads to Increased Invasion of Glioblastoma Cells. Cells 12(9):1219.

Veränderungen im Bereich der Zelladhäsion sind für physiologische Prozesse von Relevanz, können aber auch ein Kennzeichen für eine maligne Entartung sein. Erst durch eine Modifikation der Adhäsion werden Vorgänge wie Migration oder auch eine Metastasierung ermöglicht (Läubli und Borsig 2019). Ein Faktor für die Zelladhäsion ist die Interaktion mit der Basallamina, wie sie beispielsweise auch bei der Blut-Hirn-Schranke vorkommt (Hawkins und Davis 2005). Typische Bestandteile dieser Basallamina sind Moleküle wie Kollagen IV, Fibronektin, Vitronektin oder Laminin. Durch akute und chronische Erkrankung kann es zu Veränderung im Bereich der Basallamina kommen (Thomsen et al. 2017).

Die Ergebnisse der vorgestellten Originalarbeiten zur Adhäsion, Migration sowie Invasion beruhen auf Versuchen mit dem *Real-Time Cell Analyzer* (RTCA). Das Gerät basiert auf goldbeschichteten Elektroden, welche die Änderung der Impedanz über die Zeit messen. Somit lassen sich Aussagen zu Adhäsion und Proliferation der Zellen machen. Für die Messung der Adhäsion wurden *E-Plates* genutzt. Je nach Versuchsaufbau ist dies aber auch für Prozesse wie Migration und Invasion möglich (Stefanowicz-Hajduk und Ochocka 2020).

Im Modell mit Neuroblastomzellen erfolgte die Untersuchung der Adhäsion auf mit Laminin, Vitronektin und Fibronektin beschichteten Platten. Gemessen wurde die Adhäsion alle 5 Minuten über einen Zeitraum von 4 Stunden. Durch eine Behandlung mit 0,1 mM MGO über

einen Zeitraum von 48 Stunden kam es zu einer Reduktion der Adhäsion auf allen verwendeten Substraten. Beim Vergleich der unbehandelten Kontrollen zeigte sich die stärkste Adhäsion auf Laminin, gefolgt von Vitronektin (Scheer et al. 2020).

Im Modell mit benignen sowie malignen Meningeomzellen wurde die Adhäsion auf Kollagen IV sowie Fibronektin untersucht. Die Messpunkte wurden mit einem Intervall von 5 Minuten über einen Zeitraum von 4 Stunden definiert. Es wurde einerseits untersucht, welche Effekte hinsichtlich der Adhäsion durch Glykierung der Zellen zu beobachten sind, andererseits wurden auch die Effekte der Glykierung der Substrate durch MGO untersucht. Es zeigte sich, dass die MGO-Behandlung keinen Einfluss auf das Adhäsionsverhalten beider Zelllinien hat. Die stärkste Adhäsion war auf Fibronektin zu beobachten (Abbildung 5) (Selke et al. 2021b).

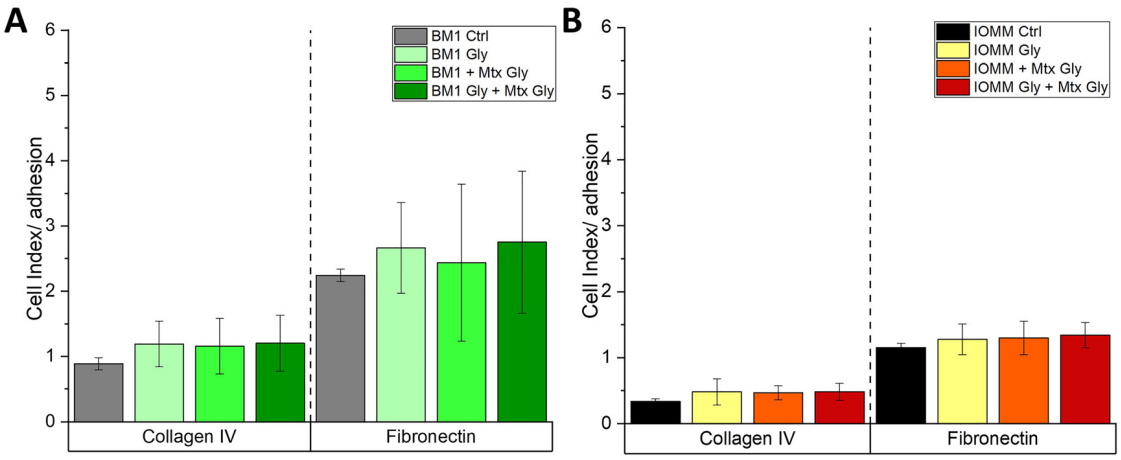

Abbildung 5: Adhäsion von Meningeom-Zellen bei MGO-Behandlung. BEN-MEN-1 (BM1) (A) und IOMM-Lee (IOMM) (B) Zellen wurden in Abwesenheit (Ctrl) oder Anwesenheit von 0,3 mM MGO auf Kollagen IV (links) oder Fibronektin (rechts) ausgesät. Die Diagramme zeigen die Adhäsion mit oder ohne Behandlung mit unbehandelten oder behandelten Zellen nach 2 Stunden. Die grauen und schwarzen Balken in (A) und (B) stellen die als Kontrolle dar. Die Diagramme stellen die Mittelwerte und Standardabweichung von vier unabhängigen biologischen Replikaten dar; (Mtx = Matrix; Gly = MGO-Behandlung).

Der Effekt der MGO-Behandlung wurde ebenfalls in verschiedenen Glioblastomzellen untersucht. Die Zellen wurden zuvor für 24 Stunden mit 0,3 bzw. 0,6 mM MGO vorbehandelt und die Substrate Kollagen IV sowie Fibronektin genutzt. Die Messung erfolgte alle 15 Minuten über einen Zeitraum von 24 Stunden. Die Glykierung zeigte in keiner der Zelllinien einen Einfluss auf die Adhäsion. Es kamen jedoch Unterschiede zwischen den Zelllinien zur Darstellung. Die Adhäsion der Zelllinie LN229 war am stärksten auf Fibronektin ausgeprägt. Dies galt auch für die humanen Astrozyten. Bei der Linie U251 war die Adhäsion am stärksten auf der unbehandelten Platte nachweisbar (Schildhauer et al. 2023a).

Eine Affektion der Adhäsion durch eine MGO-Behandlung ließ sich ebenso in PC12-Zellen nachweisen. Neben der Induktion einer Glykierung kam es zu einer Reduktion der Zelladhäsion auf Kollagen IV sowie Laminin (Bennmann et al. 2014). Ähnliche Ergebnisse zeigten sich durch eine MGO-basierte Glykierung in einem Wundheilungsmodell, bei der es zu einer Reduktion der Adhäsion kam (Alqahtani et al. 2021). Eine MGO-Behandlung führte auch in Zellen des Leberkarzinoms zu einer Reduktion der Adhäsion (Loarca et al. 2013). Es finden sich weitere Studien in der Literatur, welche aufzeigen, dass AGEs die Adhäsion in verschiedenen Zellsystem beeinflussen konnten (Li et al. 2012; Touré et al. 2008; Cheng et al. 2013). Als Bestandteil der extrazellulären Matrix können Kollagene das Adhäsionsverhalten beeinflussen. Bansode et al. demonstrierten, dass eine Glykierung durch Ribose die longitudinale Anordnung Kollagen-Fibrillen verändert und so die Adhäsion moduliert hat (Bansode et al. 2020).

Noch häufiger als der Einfluss der Glykierung auf die Adhäsion wurde jedoch der Einfluss von Glykosylierung untersucht. Glykosylierte Lektine auf Tumorzellen konnten Prozesse wie Adhäsion und Migration negativ beeinflussen und förderten so den Tumorprogress (Häuselmann und Borsig 2014). Im Pankreaskarzinom wurde gezeigt, dass die Glykosylierung das Adhäsionsverhalten über Modulation der Integrine sowie E-Cadherin-Expression beeinflusst hat. In der gleichen Studie wurden ebenfalls transfizierte Zellen mit einer Überexpression von ST3GAL2 untersucht. Dies resultierte in einer gesteigerten Expression von CA 19-9 und war zusätzlich mit einer verringerten Adhäsion sowie gesteigerten Expression von E-Cadherin verbunden (Bassagañas et al. 2014). Die Daten der eigenen Originalarbeiten sind inhomogen. Der Einfluss von MGO auf das Adhäsionsverhalten scheint stark von den Zelltypen abzuhängen.

2.8. Einfluss auf Migration

Anlage:

Scheer M, Bork K, Simon F, Nagasundaram M, Horstkorte R, Gnanapragassam VS (2020) Glycation Leads to Increased Polysialylation and Promotes the Metastatic Potential of Neuroblastoma Cells. Cells 9(4).

Selke P, Rosenstock P, Bork K, Strauss C, Horstkorte R, **Scheer M** (2021) Glycation of benign meningioma cells leads to increased invasion. Biol Chem.

Schildhauer P, Selke P, Scheller C, Strauss C, Horstkorte R, Leisz S, **Scheer M** (2023) Glycation Leads to Increased Invasion of Glioblastoma Cells. Cells 12(9):1219.

Die Migration von Zellen ist essentiell für physiologische Prozesse wie die Wundheilung, ebenso bedeutungsvoll ist sie für die Zellen des Immunsystems oder auch im Rahmen der Embryonalentwicklung. Sie spielt aber auch eine Rolle bei der Entartung von Zellen und ermöglich so beispielsweise die Metastasierung (Trepat et al. 2012)

Analog zu den Untersuchungen der Adhäsion wurde die Migration in den gleichen Zellsystemen unter dem Einfluss von MGO untersucht. Dies erfolgte mittels RTCA-Gerätes unter Zuhilfenahme von *Cell Invasion and Migration (CIM)-Plates,* welche eine obere und untere Kammer besitzen. Diese Kammern sind durch eine poröse Membran getrennt, wobei in der unteren Kammer die goldbeschichteten Elektroden die Impedanz-Änderung über die Zeit messen. Die chemotaktische Zellmigration basiert auf einem Konzentrationsgefälle des Serums von oberer zur unteren Kammer (Selvik et al. 2014). In der ersten Originalarbeit zeigte sich bei Neuroblastomzellen nach einer Inkubation mit 0,1 mM über 24 Stunden eine drastische Steigerung der Migration. Die Messung erfolgte alle 15 Minuten über einen Zeitraum von 24 Stunden (Scheer et al. 2020). In dem Modell mit benignen sowie malignen Meningeomzellen kam es durch Behandlung der Zellen mit 0,3 mM MGO über 24 Stunden zu keiner Veränderung hinsichtlich der chemotaktischen Zellmigration. Auch hier waren die Messpunkte alle 15 Minuten über einen Zeitraum von 24 Stunden (Selke et al. 2021b). Ähnliche Ergebnisse wurden unter Verwendung verschiedener Glioblastom-Zelllinien durch Inkubation der Zellen mit 0,3 mM sowie 0,6 mM über 24 Stunden erzielt, bei denen es zu keiner Änderung des Migrationsverhaltens kam (Abbildung 6). Analog zu den vorherigen Arbeiten wurden die Messpunkte auf alle 15 Minuten definiert und der Messzeitraum betrug nun 48 Stunden (Schildhauer et al. 2023a).

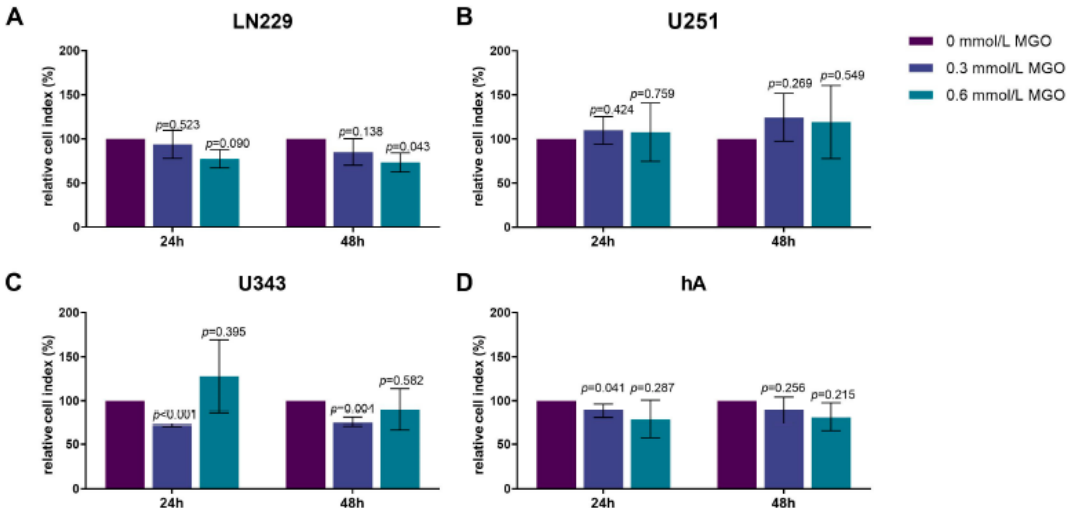

Abbildung 6: Chemotaktische Zell-Migration von Gliom-Zelllinien und humanen Astrozyten nach MGO-Behandlung. Diagramme zeigen die Chemotaxis von LN229 (A), U251 (B), U343 (C) und hA (D) nach 24 h und 48 h, normalisiert auf Kontrollzellen, nach Behandlung mit 0,3 oder 0,6 mM MGO. Die statistische Analyse erfolgte mittels Student's t-test. Die Diagramme stellen die Mittelwerte und Standardabweichung von drei unabhängigen biologischen Replikaten dar.

In der Literatur ist der Einfluss von MGO auf das Migrationsverhalten in diverses Karzinom bereits gut dokumentiert. Eine MGO-Behandlung führte bei Zellen des hepatozellulären Karzinoms zu einer Reduktion der Migration, jedoch ohne die Zellviabilität zu beeinflussen (Loarca et al. 2013). Bei der gleichen Tumorentität führte eine Inhibierung von der Glyoxalase 1, welche für den Abbau von MGO mitverantwortlich ist, zu einem Anstieg der MGO-Konzentration. Diese war verbunden mit einer Reduktion der Migration sowie einem besseren Ansprechen auf den Multikinase-Inhibitor Sorafenib (Michel et al. 2019). In anderen Karzinomen zeigten sich gegensätzliche Effekte. Zellen des anaplastischen Schilddrüsenkarzinoms wiesen hohe Level an MGO auf, welche mit einem hohen Maß an oxidativem Stress sowie einer erhöhten Migration im Vergleich zum papillären Schilddrüsenkarzinom korrelierte. Die Effekte ließen sich in der Studie durch die Anwendung eines MGO-Fängers umkehren (Antognelli et al. 2021b). Nokin et al. demonstrierten in ihrer Studie an Zellen des Mammakarzinoms, dass MGO pro-migratorische Signalwege aktiviert, wie beispielsweise die MAPK (Nokin et al. 2019). Eine weitere Studie demonstrierte, dass MGO das Migrationsverhalten von Zellen des Mammakarzinoms steigerte (Sharaf et al. 2015). Weiterhin konnte in einem ähnlichen Modell gezeigt werden, dass die Glukosekonzentration mit dem Level der gebildeten AGEs sowie der Migrationsrate im Mammakarzinom korrelierte. Durch die Anwendung eines Cross-*link breakers* ließ sich die

Migrationsrate wieder reduzieren (Rowe et al. 2022). Pan et al. konnten außerdem zeigen, dass bei einer Kohorte von Patientinnen mit Mammakarzinomen das Level von AGEs im Blutserum mit dem Metastasierungsstatus korrelierte. Parallel erfolgte in der gleichen Arbeit der Einsatz von Zellkulturen, wodurch Glykierung der Zellen eine gesteigerte Migration sowie Überexpression von RAGE zu beobachten war (Pan et al. 2022). Insgesamt deckt sich das gesteigerte Migrationsverhalten in zwei der vorgelegten Originalarbeiten mit den Daten der Literatur, wobei der Zelltyp von Bedeutung scheint.

2.9. Einfluss auf Invasion

Anlage:

Scheer M, Bork K, Simon F, Nagasundaram M, Horstkorte R, Gnanapragassam VS (2020) Glycation Leads to Increased Polysialylation and Promotes the Metastatic Potential of Neuroblastoma Cells. Cells 9(4).

Selke P, Rosenstock P, Bork K, Strauss C, Horstkorte R, **Scheer M** (2021) Glycation of benign meningioma cells leads to increased invasion. Biol Chem.

Schildhauer P, Selke P, Scheller C, Strauss C, Horstkorte R, Leisz S, **Scheer M** (2023) Glycation Leads to Increased Invasion of Glioblastoma Cells. Cells 12(9):1219.

Im folgenden Abschnitt soll auf die Resultate zu den Untersuchungen des Invasionsverhalten der drei verwendeten Zell-Systeme eingegangen werden. Die Invasivität von entarteten Zellen ist einer der wichtigsten Parameter für die Malignität von Tumoren. Für den Prozess der Invasion kommt es zu einem Zusammenspiel von einer Modifikation der Adhäsion, einer gesteigerten Zellmigration sowie Produktion von proteolytischen Faktoren, wie z.B. MMP (Vollmann-Zwerenz et al. 2020). Tumorzellen sind so in der Lage, die umgebende extrazelluläre Matrix zu durchbrechen, andere Gewebe zu infiltrieren und können so Metastasen ausbilden (Krakhmal et al. 2015). Im Falle von Hirntumoren hängt die Malignität maßgeblich von der Invasivität ab, welche die operative Behandlung erschwert und die Prognose drastisch reduziert. Eine Metastasierung kommt hier nur in Einzelfällen vor (Vollmann-Zwerenz et al. 2020).

Bei den vorgelegten Originalarbeiten wurde zur Untersuchung der Invasion ein ähnlicher Versuchsaufbau wie bei Migration mit CIM-Plates verwendet. Grundlage ist erneut ein Konzentrationsgefälle von serumfreiem Medium in der oberen Kammer zu serumhaltigem Medium in der unteren Kammer. Die Platten wurden nun zusätzlich mit einer Basalmembran-Matrix inkubiert. Im Modell mit Neuroblastomzellen zeigte sich durch eine

MGO-Behandlung eine drastische Steigerung der Invasion um den Faktor 6. Es erfolgte eine Vorbehandlung mit 0,1 mM MGO über einen Zeitraum von 48 Stunden. Die Messung wurde mit einem Intervall von 15 Minuten über insgesamt 24 Stunden durchgeführt. In der zweiten vorgelegten Originalarbeit kam es durch Glykierung der benignen Meningeom-Zellen zu einer signifikanten Steigerung des Invasionsverhalten im Vergleich zur unbehandelten Kontrolle um den Faktor 3.

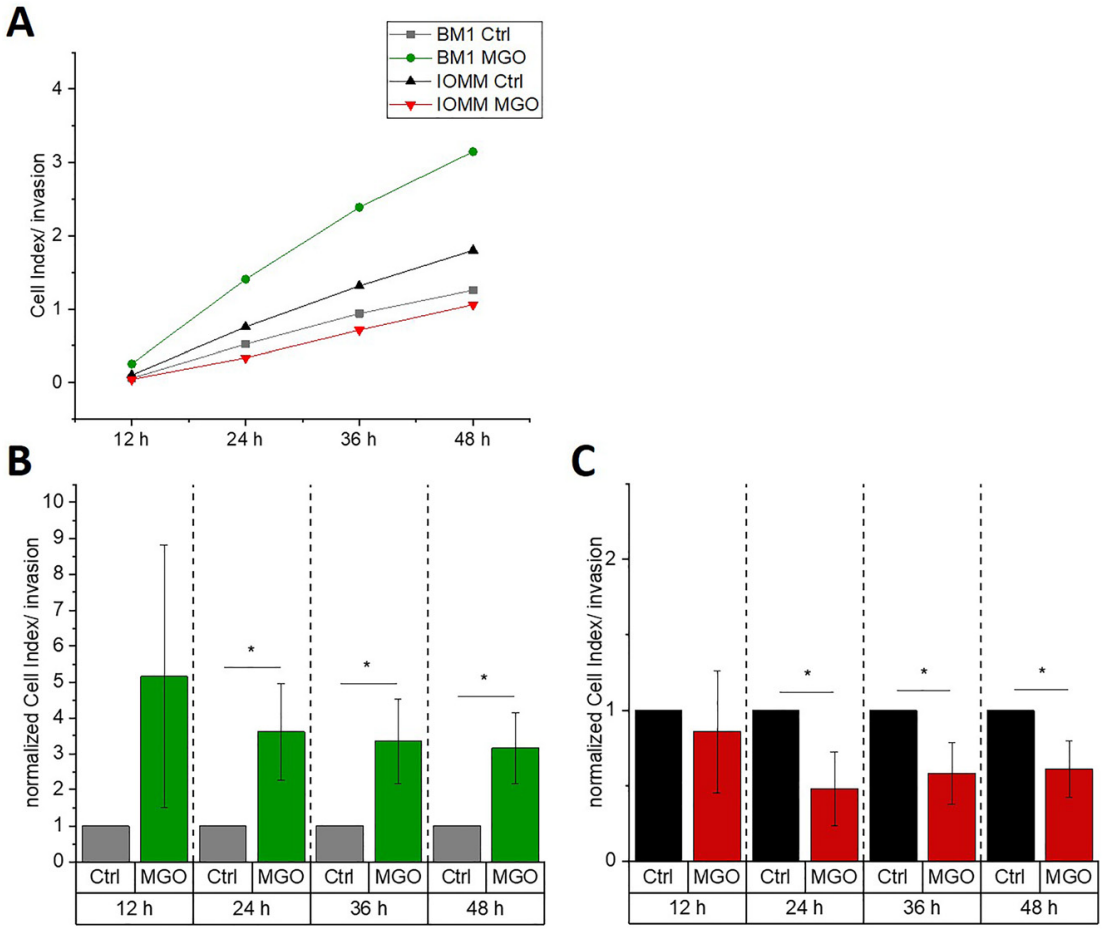

Abbildung 7: Invasion von Meningeomzellen. BEN-MEN-1 (A, B) und IOMM-Lee (A, C) wurden 48 Stunden lang in Abwesenheit (Ctrl) oder Anwesenheit von 0,3 mM MGO kultiviert. Die Diagramme zeigen die Invasion (dargestellt als Zellindizes) mit Behandlung (MGO) oder ohne Behandlung (Ctrl) für 12 h, 24 h (BEN-MEN-1: p = 0,012; IOMM-Lee: p = 0,0347), 36 h (BEN-MEN-1: p = 0,0112; IOMM-Lee: p = 0,0377) und 48 h (BEN-MEN-1: p = 0,0324; IOMM-Lee: p = 0,0374). In den Diagrammen (B) und (C) sind normalisierte Zellindizes für beide Zelllinien im Vergleich zu den Kontrollen dargestellt. Die statistische Analyse wurde mit dem t-Test durchgeführt. Fehlerbalken stellen SD dar. (n = 4; *p < 0,05).

Die Behandlung mit MGO erfolgte über einen Zeitraum von 24 Stunden mit einer Konzentration von 0,3 mM. Die Messintervalle waren alle 15 Minuten mit einem Messzeitraum von 48 Stunden. Interessanterweise war bei den malignen Meningeomzellen ein gegenteiliger Effekt mit einer Reduktion der Invasivität zu beobachten. Beim Vergleich

der beiden Zelllinien, war die Invasivität der benignen und glykierten Zelllinie stärker als in der unbehandelten, malignen Zelllinie (Abbildung 7) (Selke et al. 2021b).

Im letzten Modell mit Verwendung verschiedener Glioblastomzellen erfolgte die Inkubation mit 0,3 bzw. 0,6 mM MGO über einen Zeitraum von 24 Stunden. Das Messintervall wurde auf 15 Minuten über einen Zeitraum von 48 Stunden definiert. In allen Glioblastom-Zelllinien (LN229, U251, U343) war eine Steigerung der Invasivität durch Glykierung ersichtlich, wobei sich Unterschiede zwischen den Zelllinien zeigte. Die Effekte waren bei LN229 sowie U343 bei 0,6 mM MGO stärker ausgeprägt; wohingegen der Effekt bei U251 stärker bei 0,3 mM MGO war. Als Referenz wurden humane Astrozyten verwendet, bei denen es durch MGO-Behandlung zu einer Reduktion der gemessenen Invasivität kam (Schildhauer et al. 2023a).

In der Literatur finden sich einige Arbeiten, welche vergleichbare Ergebnisse bei anderen Tumorentitäten generieren konnten. Antognelli et al. zeigten, dass MGO beim anaplastischen Schilddrüsenkarzinom zu einer signifikanten Steigerung des Invasionsverhalten führte. Die Effekte waren durch Aktivierung der Glyoxalase 1, welche mitverantwortlich für den Abbau von MGO ist, wieder reversibel (Antognelli et al. 2019). Eine induzierte diabetische Stoffwechsellage führte in einem Maus-Modell mit Pankreaskarzinom zu erhöhten AGE- sowie MGO-Spiegeln. Dies war verbunden mit einer gesteigerten Invasivität in der histologischen Aufarbeitung (Menini et al. 2020).

Zum Einfluss der Glykierung beim Mammakarzinom finden sich mehrere Quellen. Eine MGO-Behandlung war in Zelllinien des Mammakarzinoms mit einer Steigerung der Invasion durch eine Basalmembran-Matrix verbunden (Sharaf et al. 2015). Suh et al. nutzten ein 3D Kollagen-Matrix-Modell, bei dem eine gesteigerte Invasivität bei Mammakarzinomzellen durch Glykierung der Kollagen-Matrix zu beobachten war (Suh et al. 2019). Eine weitere Studie mit Organoiden vom Mammakarzinom zeigte, dass die Glykierung zu einer Zunahme des Durchmessers der Kollagenfasern führte, welche mit einer Steigerung der Invasion verbunden war. Die glykierten Tumorzellen sonderten zudem Enzyme wie Loxl3 ab, welche zusätzlich die Invasion förderten (Koorman et al. 2022).

Bei der Untersuchung von Patienten-Proben mit kolorektalen Karzinomen bzw. deren Vorstufen, korrelierten die MGO-Level im Gewebe mit dem Grad der Malignität. Sie waren in niedriggradigen Dysplasien im Vergleich zu hochgradigen Dysplasien deutlich geringer

und am stärksten beim invasiven Karzinom ausgeprägt. Interessanterweise waren die MGO-Level im peritumoralem Gewebe dabei nochmals höher (Chou et al. 2021). In einem Modell mit Kolonkarzinomzellen führte eine Behandlung mit AGEs zu einer Steigerung der Invasion. Dies war verbunden mit einer verringerten Expression von E-Cadherin, als Zeichen einer EMT (Liang 2020).

Andererseits finden sich einige wenige Arbeiten, welche gegenteilige Effekte hinsichtlich der Invasivität nach MGO-Behandlung beobachtet haben. In der Studie von Guo et al. war eine MGO-Behandlung von Mammakarzinomzellen mit einer reduzierten Invasivität verbunden, wobei ebenfalls eine gesteigerte Apoptose-Rate beschrieben wurde. Die verwendeten MGO-Konzentrationen lagen über denen anderer Autoren (Guo et al. 2016). In einem Modell mit Leberkarzinom-Zelllinien führte eine Behandlung mit MGO gleichfalls zu einer verringerten Migration sowie Invasion. Der Effekt war hier abhängig vom Expressionsstatus des Tumorsuppressors P53 (Loarca et al. 2013). Die Art der Inkubation als auch der Zelltyp scheinen entscheidend für den Einfluss auf das Invasionsverhalten der Zellen zu sein, was sich so auch in den eigenen Arbeiten bestätigt hat.

3. Zusammenfassung

Bei nahezu allen Tumoren findet sich eine veränderte, sogenannte aerobe Glykolyse, welche zur Energieproduktion genutzt wird. Dieses Phänomen wird auch als Warburg-Effekt bezeichnet und führt zur Akkumulation von hochreaktiven Nebenprodukten der Glykolyse, wie Methylglyoxal (MGO). MGO gilt als einer der potentesten Präkursoren der Glykierung, als eine Form der posttranslationalen Modifikationen.

Ein weiteres Merkmal vieler Tumoren ist die veränderte Glykosylierung an der Zelloberfläche, wodurch Tumore in der Lage sind, eine Immunantwort zu umgehen (*Immune Escape*). Bei vielen Tumorerkrankungen haben sich glykosylierte Oberflächenmoleküle als Biomarker etabliert. Sowohl die veränderte Glykolyse, welche eine vermehrte Glykierung bedingt, als auch die Modifikation der Glykosylierung gelten als "*Hallmarks of Cancer"*.

In der vorliegenden kumulativen Schrift wurde der Einfluss von MGO auf drei verschiedene Tumoren des Nervensystems untersucht. Neben einer konzentrationsabhängigen Zytotoxizität konnte eine konzentrationsabhängige Induktion von Glykierung nachgewiesen werden. Als bisher einzige Arbeitsgruppe gelang der Nachweis, dass MGO auch zu einer Induktion der Glykosylierung führt. So führte die Behandlung mit MGO zu einer Steigerung der Polysialylierung sowie der relativen Menge an Sialinsäuren in Neuroblastomzellen. Außerdem fand sich eine Modifikation der ST bei Meningeom-Zellen, wobei hier gegensätzlich Effekte zwischen benigner und maligner Zelllinie zur Darstellung kamen. In der WHO-Grad 1 Zelllinie war ein Großteil der ST hochreguliert.

Zusätzlich wurde das Verhalten der Tumorzellen unter MGO-Einfluss hinsichtlich Adhäsion, Migration sowie Invasion untersucht. Die Ergebnisse zeigte eine Abhängigkeit vom Zelltypen. So führte die Glykierung zu einer Reduktion der Adhäsion bei Neuroblastom-Zellen. Eine Steigerung des Migrationsverhaltens war bei Glioblastom- sowie Neuroblastomzellen zu beobachten. Bei allen Modellen ließ sich eine Steigerung der Invasivität nachweisen. Passend zu einer Modifikation von Migration sowie Invasion waren Veränderungen der Expression von extrazellulären Matrixproteinen. Beispielsweise führte MGO zu einer Steigerung der E-Cadherin Expression bei gleichzeitiger Reduktion von N-Cadherin in benignen Meningeomzellen sowie zwei Glioblastom-Zelllinien.

Insgesamt wird durch die vorliegende Arbeit die von einigen Autoren vermutete Rolle von MGO als Tumorpromotor unterstrichen.

4. Literaturverzeichnis

Allaman, Igor; Bélanger, Mireille; Magistretti, Pierre J. (2015): Methylglyoxal, the dark side of glycolysis. In: *Frontiers in neuroscience* 9, S. 23. DOI: 10.3389/fnins.2015.00023.

Almeida, Luiz G. N. de; Thode, Hayley; Eslambolchi, Yekta; Chopra, Sameeksha; Young, Daniel; Gill, Sean et al. (2022): Matrix Metalloproteinases: From Molecular Mechanisms to Physiology, Pathophysiology, and Pharmacology. In: *Pharmacological reviews* 74 (3), S. 712–768. DOI: 10.1124/pharmrev.121.000349.

Aloia, Andrea; Petrova, Evgeniya; Tomiuk, Stefan; Bissels, Ute; Déas, Olivier; Saini, Massimo et al. (2015): The sialyl-glycolipid stage-specific embryonic antigen 4 marks a subpopulation of chemotherapy-resistant breast cancer cells with mesenchymal features. In: *Breast cancer research : BCR* 17 (1), S. 146. DOI: 10.1186/s13058-015-0652-6.

Alqahtani, Ali S.; Li, Kong M.; Razmovski-Naumovski, Valentina; Kam, Antony; Alam, Perwez; Li, George Q. (2021): Attenuation of methylglyoxal-induced glycation and cellular dysfunction in wound healing by Centella cordifolia. In: *Saudi journal of biological sciences* 28 (1), S. 813–824. DOI: 10.1016/j.sjbs.2020.11.016.

Amoureux, Marie-Claude; Coulibaly, Béma; Chinot, Olivier; Loundou, Anderson; Metellus, Philippe; Rougon, Geneviève; Figarella-Branger, Dominique (2010): Polysialic acid neural cell adhesion molecule (PSA-NCAM) is an adverse prognosis factor in glioblastoma, and regulates olig2 expression in glioma cell lines. In: *BMC cancer* 10, S. 91. DOI: 10.1186/1471-2407-10-91.

Antognelli, Cinzia; Mandarano, Martina; Prosperi, Enrico; Sidoni, Angelo; Talesa, Vincenzo Nicola (2021a): Glyoxalase-1-Dependent Methylglyoxal Depletion Sustains PD-L1 Expression in Metastatic Prostate Cancer Cells: A Novel Mechanism in Cancer Immunosurveillance Escape and a Potential Novel Target to Overcome PD-L1 Blockade Resistance. In: *Cancers* 13 (12), S. 2965. DOI: 10.3390/cancers13122965.

Antognelli, Cinzia; Marinucci, Lorella; Frosini, Roberta; Macchioni, Lara; Talesa, Vincenzo Nicola (2021b): Metastatic Prostate Cancer Cells Secrete Methylglyoxal-Derived MG-H1 to Reprogram Human Osteoblasts into a Dedifferentiated, Malignant-like Phenotype: A Possible Novel Player in Prostate Cancer Bone Metastases. In: *International journal of molecular sciences* 22 (19). DOI: 10.3390/ijms221910191.

Antognelli, Cinzia; Moretti, Sonia; Frosini, Roberta; Puxeddu, Efisio; Sidoni, Angelo; Talesa, Vincenzo N. (2019): Methylglyoxal Acts as a Tumor-Promoting Factor in Anaplastic Thyroid Cancer. In: *Cells* 8 (6). DOI: 10.3390/cells8060547.

Ayad, Shirley (1998): The extracellular matrix factsbook. 2nd ed. San Diego: Academic Press (Factsbook series). Online verfügbar unter https://ebookcentral.proquest.com/lib/kxp/detail.action?docID=405521.

Bai, Shakuntala; Chaurasiya, Arvindkumar H.; Banarjee, Reema; Walke, Prachi B.; Rashid, Faraz; Unnikrishnan, Ambika G.; Kulkarni, Mahesh J. (2020): CD44, a Predominant Protein in Methylglyoxal-Induced Secretome of Muscle Cells, is Elevated in Diabetic Plasma. In: *ACS omega* 5 (39), S. 25016–25028. DOI: 10.1021/acsomega.0c01318.

Bai, Yi-Hua; Wang, Jia-Ping; Yang, Min; Zeng, Yi; Jiang, Hong-Ying (2015): SiRNA-HMGA2 weakened AGEs-induced epithelial-to-mesenchymal transition in tubular epithelial cells. In: *Biochemical and biophysical research communications* 457 (4), S. 730–735. DOI: 10.1016/j.bbrc.2015.01.063.

Baig, Mohammad Hassan; Jan, Arif Tasleem; Rabbani, Gulam; Ahmad, Khurshid; Ashraf, Jalaluddin M.; Kim, Taeyeon et al. (2017): Methylglyoxal and Advanced Glycation End products: Insight of the regulatory machinery affecting the myogenic program and of its modulation by natural compounds. In: *Scientific reports* 7 (1), S. 5916. DOI: 10.1038/s41598-017-06067-5.

Bansode, Sneha; Bashtanova, Uliana; Li, Rui; Clark, Jonathan; Müller, Karin H.; Puszkarska, Anna et al. (2020): Glycation changes molecular organization and charge distribution in type I collagen fibrils. In: *Scientific reports* 10. DOI: 10.1038/s41598-020-60250-9.

Bassagañas, Sònia; Carvalho, Sandra; Dias, Ana M.; Pérez-Garay, Marta; Ortiz, M. Rosa; Figueras, Joan et al. (2014): Pancreatic cancer cell glycosylation regulates cell adhesion and invasion through the modulation of α2β1 integrin and E-cadherin function. In: *PloS one* 9 (5), e98595. DOI: 10.1371/journal.pone.0098595.

Bélanger, Mireille; Yang, Jiangyan; Petit, Jean-Marie; Laroche, Thierry; Magistretti, Pierre J.; Allaman, Igor (2011): Role of the glyoxalase system in astrocyte-mediated neuroprotection. In: *The Journal of neuroscience : the official journal of the Society for Neuroscience* 31 (50), S. 18338–18352. DOI: 10.1523/JNEUROSCI.1249-11.2011.

Bellier, Justine; Nokin, Marie-Julie; Lardé, Eva; Karoyan, Philippe; Peulen, Olivier; Castronovo, Vincent; Bellahcène, Akeila (2019): Methylglyoxal, a potent inducer of AGEs, connects between diabetes and cancer. In: *Diabetes research and clinical practice* 148, S. 200–211. DOI: 10.1016/j.diabres.2019.01.002.

Bennmann, Dorit; Horstkorte, Rüdiger; Hofmann, Britt; Jacobs, Kathleen; Navarrete-Santos, Alexander; Simm, Andreas et al. (2014): Advanced glycation endproducts interfere with adhesion and neurite outgrowth. In: *PloS one* 9 (11), e112115. DOI: 10.1371/journal.pone.0112115.

Bierhaus, Angelika; Humpert, Per M.; Morcos, Michael; Wendt, Thoralf; Chavakis, Triantafyllos; Arnold, Bernd et al. (2005): Understanding RAGE, the receptor for advanced glycation end products. In: *Journal of molecular medicine (Berlin, Germany)* 83 (11), S. 876–886. DOI: 10.1007/s00109-005-0688-7.

Bradke, Brian S.; Vashishth, Deepak (2014): N-phenacylthiazolium bromide reduces bone fragility induced by nonenzymatic glycation. In: *PloS one* 9 (7), e103199. DOI: 10.1371/journal.pone.0103199.

Breiden, Bernadette; Sandhoff, Konrad (2018): Ganglioside Metabolism and Its Inherited Diseases. In: *Methods in molecular biology (Clifton, N.J.)* 1804, S. 97–141. DOI: 10.1007/978-1-4939-8552-4_5.

Brooks, Susan A. (2006): Protein glycosylation in diverse cell systems: implications for modification and analysis of recombinant proteins. In: *Expert review of proteomics* 3 (3), S. 345–359. DOI: 10.1586/14789450.3.3.345.

Brownlee, M. (1995): Advanced protein glycosylation in diabetes and aging. In: *Annual review of medicine* 46, S. 223–234. DOI: 10.1146/annurev.med.46.1.223.

Campbell, A. K.; Matthews, S. B.; Vassel, N.; Cox, C. D.; Naseem, R.; Chaichi, J. et al. (2010): Bacterial metabolic 'toxins': a new mechanism for lactose and food intolerance, and irritable bowel syndrome. In: *Toxicology* 278 (3), S. 268–276. DOI: 10.1016/j.tox.2010.09.001.

Chang, Tuanjie; Wu, Lingyun (2006): Methylglyoxal, oxidative stress, and hypertension. In: *Canadian journal of physiology and pharmacology* 84 (12), S. 1229–1238. DOI: 10.1139/y06-077.

Chao, Min; Liu, Nan; Sun, Zhichuan; Jiang, Yongli; Jiang, Tongtong; Xv, Meng et al. (2020): TGF-β Signaling Promotes Glioma Progression Through Stabilizing Sox9. In: *Frontiers in immunology* 11, S. 592080. DOI: 10.3389/fimmu.2020.592080.

Chen, Chen; Zhao, Shujie; Karnad, Anand; Freeman, James W. (2018): The biology and role of CD44 in cancer progression: therapeutic implications. In: *Journal of hematology & oncology* 11 (1), S. 64. DOI: 10.1186/s13045-018-0605-5.

Chen, Feng; Wollmer, M. Axel; Hoerndli, Frederic; Münch, Gerald; Kuhla, Björn; Rogaev, Evgeny I. et al. (2004): Role for glyoxalase I in Alzheimer's disease. In: *Proceedings of the National Academy of Sciences of the United States of America* 101 (20), S. 7687–7692. DOI: 10.1073/pnas.0402338101.

Cheng, Cailian; Zheng, Zhenda; Shi, Chenggang; Liu, Xun; Ye, Zengchun; Lou, Tanqi (2013): Advanced glycation end-products reduce podocyte adhesion by activating the renin-angiotensin system and increasing integrin-linked kinase. In: *Experimental and therapeutic medicine* 6 (6), S. 1494–1498. DOI: 10.3892/etm.2013.1312.

Cheng, Chunming; Ru, Peng; Geng, Feng; Liu, Junfeng; Yoo, Ji Young; Wu, Xiaoning et al. (2015): Glucose-Mediated N-glycosylation of SCAP Is Essential for SREBP-1 Activation and Tumor Growth. In: *Cancer cell* 28 (5), S. 569–581. DOI: 10.1016/j.ccell.2015.09.021.

Cheng, Junchi; Wang, Rong; Zhong, Guansheng; Chen, Xi; Cheng, Yun; Li, Wei; Yang, Yunshan (2020): ST6GAL2 Downregulation Inhibits Cell Adhesion and Invasion and is Associated with Improved Patient Survival in Breast Cancer. In: *OncoTargets and therapy* 13, S. 903–914. DOI: 10.2147/OTT.S230847.

Chou, Chu-Kuang; Yang, Po-Chun; Tsai, Pei-Yun; Yang, Hsin-Yi; Tsai, Kun-Feng; Chen, Tsung-Hsien et al. (2021): Methylglyoxal Levels in Human Colorectal Precancer and Cancer: Analysis of Tumor and Peritumor Tissue. In: *Life (Basel, Switzerland)* 11 (12). DOI: 10.3390/life11121319.

Chuah, Yaw Kuang; Basir, Rusliza; Talib, Herni; Tie, Tung Hing; Nordin, Norshariza (2013): Receptor for advanced glycation end products and its involvement in inflammatory diseases. In: *International journal of inflammation* 2013, S. 403460. DOI: 10.1155/2013/403460.

Comb, Donald G.; Roseman, Saul (1960): The Sialic Acids. In: *The Journal of biological chemistry* 235 (9), S. 2529–2537. DOI: 10.1016/S0021-9258(19)76908-7.

Da Wang; Li, Tingting; Ye, Gengtai; Shen, Zhiyong; Hu, Yanfeng; Mou, Tingyu et al. (2015): Overexpression of the Receptor for Advanced Glycation Endproducts (RAGE) is associated with poor prognosis in gastric cancer. In: *PloS one* 10 (4), e0122697. DOI: 10.1371/journal.pone.0122697.

Danby, F. William (2010): Nutrition and aging skin: sugar and glycation. In: *Clinics in dermatology* 28 (4), S. 409–411. DOI: 10.1016/j.clindermatol.2010.03.018.

Datta, Arun K. (2009): Comparative sequence analysis in the sialyltransferase protein family: analysis of motifs. In: *Current drug targets* 10 (6), S. 483–498. DOI: 10.2174/138945009788488422.

Delgado-Andrade, Cristina (2016): Carboxymethyl-lysine: thirty years of investigation in the field of AGE formation. In: *Food & function* 7 (1), S. 46–57. DOI: 10.1039/c5fo00918a.

Deschuyter, Marlène; Leger, David Yannick; Verboom, Anne; Chaunavel, Alain; Maftah, Abderrahman; Petit, Jean-Michel (2022): ST3GAL2 knock-down decreases tumoral character of colorectal cancer cells in vitro and in vivo. In: *American Journal of Cancer Research* 12 (1), S. 280–302.

Dobie, Christopher; Skropeta, Danielle (2021): Insights into the role of sialylation in cancer progression and metastasis. In: *British journal of cancer* 124 (1), S. 76–90. DOI: 10.1038/s41416-020-01126-7.

Dongre, Anushka; Weinberg, Robert A. (2019): New insights into the mechanisms of epithelial-mesenchymal transition and implications for cancer. In: *Nature reviews. Molecular cell biology* 20 (2), S. 69–84. DOI: 10.1038/s41580-018-0080-4.

Du, Zhanxin; Wang, Yaqing; Liang, Jiaqi; Gao, Shaowei; Cai, Xiaoying; Yu, Yu et al. (2022): Association of glioma CD44 expression with glial dynamics in the tumour microenvironment and patient prognosis. In: *Computational and structural biotechnology journal* 20, S. 5203–5217. DOI: 10.1016/j.csbj.2022.09.003.

Dusoswa, Sophie A.; Verhoeff, Jan; Abels, Erik; Méndez-Huergo, Santiago P.; Croci, Diego O.; Kuijper, Lisan H. et al. (2020): Glioblastomas exploit truncated O-linked glycans for local and distant immune modulation via the macrophage galactose-type lectin. In: *Proceedings of the National Academy of Sciences of the United States of America* 117 (7), S. 3693–3703. DOI: 10.1073/pnas.1907921117.

Dwyer, Chrissa A.; Bi, Wenya Linda; Viapiano, Mariano S.; Matthews, Russell T. (2014): Brevican knockdown reduces late-stage glioma tumor aggressiveness. In: *Journal of neuro-oncology* 120 (1), S. 63–72. DOI: 10.1007/s11060-014-1541-z.

Elmore, Susan (2007): Apoptosis: A Review of Programmed Cell Death. In: *Toxicol Pathol* 35 (4), S. 495–516. DOI: 10.1080/01926230701320337.

Fiory, F.; Lombardi, A.; Miele, C.; Giudicelli, J.; Beguinot, F.; van Obberghen, E. (2011): Methylglyoxal impairs insulin signalling and insulin action on glucose-induced insulin secretion in the pancreatic beta cell line INS-1E. In: *Diabetologia* 54 (11), S. 2941–2952. DOI: 10.1007/s00125-011-2280-8.

Fishman, Sarah Louise; Sonmez, Halis; Basman, Craig; Singh, Varinder; Poretsky, Leonid (2018): The role of advanced glycation end-products in the development of coronary artery disease in patients with and without diabetes mellitus: a review. In: *Molecular medicine (Cambridge, Mass.)* 24 (1), S. 59. DOI: 10.1186/s10020-018-0060-3.

Fotheringham, Amelia K.; Gallo, Linda A.; Borg, Danielle J.; Forbes, Josephine M. (2022): Advanced Glycation End Products (AGEs) and Chronic Kidney Disease: Does the Modern Diet AGE the Kidney? In: *Nutrients* 14 (13). DOI: 10.3390/nu14132675.

Fu, Chih-Wei; Tsai, Han-En; Chen, Wei-Sheng; Chang, Tzu-Ting; Chen, Chia-Ling; Hsiao, Pei-Wen; Li, Wen-Shan (2021): Sialyltransferase Inhibitors Suppress Breast Cancer Metastasis. In: *Journal of medicinal chemistry* 64 (1), S. 527–542. DOI: 10.1021/acs.jmedchem.0c01477.

Ganesan, Ramya; Mallets, Elizabeth; Gomez-Cambronero, Julian (2016): The transcription factors Slug (SNAI2) and Snail (SNAI1) regulate phospholipase D (PLD) promoter in opposite ways towards cancer cell invasion. In: *Molecular oncology* 10 (5), S. 663–676. DOI: 10.1016/j.molonc.2015.12.006.

Gebhardt, Christoffer; Riehl, Astrid; Durchdewald, Moritz; Németh, Julia; Fürstenberger, Gerhard; Müller-Decker, Karin et al. (2008): RAGE signaling sustains inflammation and promotes tumor development. In: *The Journal of experimental medicine* 205 (2), S. 275–285. DOI: 10.1084/jem.20070679.

Giamanco, Kristin A.; Matthews, Russell T. (2020): The Role of BEHAB/Brevican in the Tumor Microenvironment: Mediating Glioma Cell Invasion and Motility. In: *Advances in experimental medicine and biology* 1272, S. 117–132. DOI: 10.1007/978-3-030-48457-6_7.

Gu, Yuchao; Zhang, Junhua; Mi, Wenyi; Yang, Jing; Han, Feng; Lu, Xinzhi; Yu, Wengong (2008): Silencing of GM3 synthase suppresses lung metastasis of murine breast cancer cells. In: *Breast cancer research : BCR* 10 (1), R1. DOI: 10.1186/bcr1841.

Guan, Hongyu; Cai, Junchao; Zhang, Nu; Wu, Jueheng; Yuan, Jie; Li, Jun; Li, Mengfeng (2012): Sp1 is upregulated in human glioma, promotes MMP-2-mediated cell invasion and predicts poor clinical outcome. In: *International journal of cancer* 130 (3), S. 593–601. DOI: 10.1002/ijc.26049.

Guo, Qi; Mori, Takefumi; Jiang, Yue; Hu, Chunyan; Osaki, Yusuke; Yoneki, Yoshimi et al. (2009): Methylglyoxal contributes to the development of insulin resistance and salt sensitivity in Sprague-Dawley rats. In: *Journal of hypertension* 27 (8), S. 1664–1671. DOI: 10.1097/HJH.0b013e32832c419a.

Guo, Yi; Zhang, Yuning; Yang, Xunjun; Lu, Panpan; Yan, Xijuan; Xiao, Fanglan et al. (2016): Effects of methylglyoxal and glyoxalase I inhibition on breast cancer cells proliferation, invasion, and apoptosis through modulation of MAPKs, MMP9, and Bcl-2. In: *Cancer biology & therapy* 17 (2), S. 169–180. DOI: 10.1080/15384047.2015.1121346.

Hagenhaus, Vanessa; Gorenflos López, Jacob L.; Rosenstengel, Rebecca; Neu, Carolin; Hackenberger, Christian P. R.; Celik, Arif et al. (2023): Glycation Interferes with the Activity of the Bi-Functional UDP-N-Acetylglucosamine 2-Epimerase/N-Acetyl-mannosamine Kinase (GNE). In: *Biomolecules* 13 (3). DOI: 10.3390/biom13030422.

Hait, Nitai C.; Maiti, Aparna; Wu, Rongrong; Andersen, Valerie L.; Hsu, Chang-Chieh; Wu, Yun et al. (2022): Extracellular sialyltransferase st6gal1 in breast tumor cell growth and invasiveness. In: *Cancer Gene Therapy* 29 (11), S. 1662–1675. DOI: 10.1038/s41417-022-00485-y.

Hakomori, Sen-Itiroh; Handa, Kazuko (2015): GM3 and cancer. In: *Glycoconjugate journal* 32 (1-2), S. 1–8. DOI: 10.1007/s10719-014-9572-4.

Hanahan, Douglas; Weinberg, Robert A. (2011): Hallmarks of cancer: the next generation. In: *Cell* 144 (5), S. 646–674. DOI: 10.1016/j.cell.2011.02.013.

Harazi, A.; Yakovlev, L.; Selke, P.; Horstkorte, R.; Mitrani-Rosenbaum, S. (2023): P152 Post weaning Gne knock out results in dramatic reduction of sialic acid levels in postnatal mouse life but no phenotype. In: *Neuromuscular Disorders* 33, S137. DOI: 10.1016/j.nmd.2023.07.284.

Harduin-Lepers, A.; Vallejo-Ruiz, V.; Krzewinski-Recchi, M. A.; Samyn-Petit, B.; Julien, S.; Delannoy, P. (2001): The human sialyltransferase family. In: *Biochimie* 83 (8), S. 727–737. DOI: 10.1016/s0300-9084(01)01301-3.

Häuselmann, Irina; Borsig, Lubor (2014): Altered tumor-cell glycosylation promotes metastasis. In: *Front. Oncol.* 4, S. 28. DOI: 10.3389/fonc.2014.00028.

Hawkins, Brian T.; Davis, Thomas P. (2005): The blood-brain barrier/neurovascular unit in health and disease. In: *Pharmacological reviews* 57 (2), S. 173–185. DOI: 10.1124/pr.57.2.4.

Hildebrandt, Herbert; Mühlenhoff, Martina; Gerardy-Schahn, Rita (2010): Polysialylation of NCAM. In: *Advances in experimental medicine and biology* 663, S. 95–109. DOI: 10.1007/978-1-4419-1170-4_6.

Hofmann, Britt; Adam, Anne-Catrin; Jacobs, Kathleen; Riemer, Marcus; Erbs, Christian; Bushnaq, Hasan et al. (2013): Advanced glycation end product associated skin autofluorescence: a mirror of vascular function? In: *Experimental gerontology* 48 (1), S. 38–44. DOI: 10.1016/j.exger.2012.04.011.

Hoonhorst, Susan J. M.; Lo Tam Loi, Adèle T.; Pouwels, Simon D.; Faiz, Alen; Telenga, Eef D.; van den Berge, Maarten et al. (2016): Advanced glycation endproducts and their receptor in different body compartments in COPD. In: *Respiratory research* 17, S. 46. DOI: 10.1186/s12931-016-0363-2.

Hu, Feng; Dzaye, Omar Dildar; Hahn, Alexander; Yu, Yong; Scavetta, Rick Joey; Dittmar, Gunnar et al. (2015): Glioma-derived versican promotes tumor expansion via glioma-associated microglial/macrophages Toll-like receptor 2 signaling. In: *Neuro-oncology* 17 (2), S. 200–210. DOI: 10.1093/neuonc/nou324.

Huang, Jianmei; Huang, Jianming; Zhang, Guonan (2022a): Insights into the Role of Sialylation in Cancer Metastasis, Immunity, and Therapeutic Opportunity. In: *Cancers* 14 (23). DOI: 10.3390/cancers14235840.

Huang, Tian-Lan; Mei, Yi-Wen; Li, Yang; Chen, Xin; Yu, Si-Xun; Kuang, Yong-Qin; Shu, Hai-Feng (2022b): Thrombospondin-2 promotes the proliferation and migration of glioma cells and contributes to the progression of glioma. In: *Chinese neurosurgical journal* 8 (1), S. 39. DOI: 10.1186/s41016-022-00308-x.

International Agency for Research on Cancer (1994): Some industrial chemicals. Lyon: IARC (IARC monographs on the evaluation of carcinogenic risks to humans, 60).

Ivanova, Ekaterina L.; Costa, Barbara; Eisemann, Tanja; Lohr, Sabrina; Boskovic, Pavle; Eichwald, Viktoria et al. (2022): CD44 expressed by myeloid cells promotes glioma invasion. In: *Front. Oncol.* 12, S. 969787. DOI: 10.3389/fonc.2022.969787.

Jaisson, Stéphane; Gillery, Philippe (2021): Methods to assess advanced glycation end-products. In: *Current opinion in clinical nutrition and metabolic care* 24 (5), S. 411–415. DOI: 10.1097/MCO.0000000000000774.

Jarahian, Mostafa; Marofi, Faroogh; Maashi, Marwah Suliman; Ghaebi, Mahnaz; Khezri, Abdolrahman; Berger, Martin R. (2021): Re-Expression of Poly/Oligo-Sialylated Adhesion Molecules on the Surface of Tumor Cells Disrupts Their Interaction with Immune-Effector Cells and Contributes to Pathophysiological Immune Escape. In: *Cancers* 13 (20). DOI: 10.3390/cancers13205203.

John, W. Garry; Mosca, Andrea; Weykamp, Cas; Goodall, Ian (2007): HbA1c standardisation: history, science and politics. In: *The Clinical Biochemist Reviews* 28 (4), S. 163–168.

Jules, Joel; Maiguel, Dony; Hudson, Barry I. (2013): Alternative splicing of the RAGE cytoplasmic domain regulates cell signaling and function. In: *PloS one* 8 (11), e78267. DOI: 10.1371/journal.pone.0078267.

Kalapos, M. P.; Groot, H. de (1992): Morphological changes of cultured rat hepatocytes exposed to methylglyoxal. Calcium-independence of injury. In: *Acta morphologica Hungarica* 40 (1-4), S. 87–94.

Kaminska, Bozena; Kocyk, Marta; Kijewska, Magdalena (2013): TGF beta signaling and its role in glioma pathogenesis. In: *Advances in experimental medicine and biology* 986, S. 171–187. DOI: 10.1007/978-94-007-4719-7_9.

Kang, Qingzheng; Dai, Haiyu; Jiang, Suwei; Yu, Li (2022): Advanced glycation end products in diabetic retinopathy and phytochemical therapy. In: *Frontiers in nutrition* 9, S. 1037186. DOI: 10.3389/fnut.2022.1037186.

Kemerdere, Rahsan; Akgun, Mehmet Yigit; Toklu, Sureyya; Aydin, Seckin; Orhan, Bagnu; Inal, Berrin Bercik et al. (2021): Circulating Levels of Thrombospondin-1 and Thrombospondin-2 in Patients with Common Brain Tumors. In: *Turkish neurosurgery* 31 (3), S. 399–403. DOI: 10.5137/1019-5149.JTN.28624-20.3.

Kesanakurti, Divya; Chetty, Chandramu; Bhoopathi, Praveen; Lakka, Sajani S.; Gorantla, Bharathi; Tsung, Andrew J.; Rao, Jasti S. (2011): Suppression of MMP-2 attenuates TNF-α induced NF-κB

activation and leads to JNK mediated cell death in glioma. In: *PloS one* 6 (5), e19341. DOI: 10.1371/journal.pone.0019341.

Khalid, Mariyam; Petroianu, Georg; Adem, Abdu (2022): Advanced Glycation End Products and Diabetes Mellitus: Mechanisms and Perspectives. In: *Biomolecules* 12 (4). DOI: 10.3390/biom12040542.

Kim, Chan-Sik; Park, Sok; Kim, Junghyun (2017): The role of glycation in the pathogenesis of aging and its prevention through herbal products and physical exercise. In: *Journal of exercise nutrition & biochemistry* 21 (3), S. 55–61. DOI: 10.20463/jenb.2017.0027.

Kim, Junghyun; Kim, Ohn Soon; Kim, Chan-Sik; Kim, Nan Hee; Kim, Jin Sook (2010): Cytotoxic role of methylglyoxal in rat retinal pericytes: Involvement of a nuclear factor-kappaB and inducible nitric oxide synthase pathway. In: *Chemico-biological interactions* 188 (1), S. 86–93. DOI: 10.1016/j.cbi.2010.07.002.

Kishikawa, Hirofumi; Mine, Shinichiro; Kawahara, Chie; Tabata, Takahiro; Hirose, Akiko; Okada, Yosuke; Tanaka, Yoshiya (2006): Glycated albumin and cross-linking of CD44 induce scavenger receptor expression and uptake of oxidized LDL in human monocytes. In: *Biochemical and biophysical research communications* 339 (3), S. 846–851. DOI: 10.1016/j.bbrc.2005.11.091.

Kontou, Maria; Weidemann, Wenke; Bauer, Christian; Reutter, Werner; Horstkorte, Rüdiger (2008): The key enzyme of sialic acid biosynthesis (GNE) promotes neurite outgrowth of PC12 cells. In: *Neuroreport* 19 (12), S. 1239–1242. DOI: 10.1097/WNR.0b013e32830b368a.

Koorman, Thijs; Jansen, Karin A.; Khalil, Antoine; Haughton, Peter D.; Visser, Daan; Rätze, Max A. K. et al. (2022): Spatial collagen stiffening promotes collective breast cancer cell invasion by reinforcing extracellular matrix alignment. In: *Oncogene* 41 (17), S. 2458–2469. DOI: 10.1038/s41388-022-02258-1.

Krakhmal, N. V.; Zavyalova, M. V.; Denisov, E. V.; Vtorushin, S. V.; Perelmuter, V. M. (2015): Cancer Invasion: Patterns and Mechanisms. In: *Acta naturae* 7 (2), S. 17–28.

Kroemer, Guido; Pouyssegur, Jacques (2008): Tumor cell metabolism: cancer's Achilles' heel. In: *Cancer cell* 13 (6), S. 472–482. DOI: 10.1016/j.ccr.2008.05.005.

Kuhla, Björn; Lüth, Hans-Joachim; Haferburg, Dietrich; Boeck, Katharina; Arendt, Thomas; Münch, Gerald (2005): Methylglyoxal, glyoxal, and their detoxification in Alzheimer's disease. In: *Annals of the New York Academy of Sciences* 1043, S. 211–216. DOI: 10.1196/annals.1333.026.

Lai, Seigmund Wai Tsuen; Lopez Gonzalez, Edwin De Jesus; Zoukari, Tala; Ki, Priscilla; Shuck, Sarah C. (2022): Methylglyoxal and Its Adducts: Induction, Repair, and Association with Disease. In: *Chemical research in toxicology* 35 (10), S. 1720–1746. DOI: 10.1021/acs.chemrestox.2c00160.

Läubli, Heinz; Borsig, Lubor (2019): Altered Cell Adhesion and Glycosylation Promote Cancer Immune Suppression and Metastasis. In: *Frontiers in immunology* 10, S. 2120. DOI: 10.3389/fimmu.2019.02120.

Lee, Eun Ji; Park, Jong Hoon (2013): Receptor for Advanced Glycation Endproducts (RAGE), Its Ligands, and Soluble RAGE: Potential Biomarkers for Diagnosis and Therapeutic Targets for Human Renal Diseases. In: *Genomics & informatics* 11 (4), S. 224–229. DOI: 10.5808/GI.2013.11.4.224.

Lee, Hee-Weon; Gu, Min Ji; Lee, Jee-Young; Lee, Seungju; Kim, Yoonsook; Ha, Sang Keun (2021): Methylglyoxal-Lysine Dimer, an Advanced Glycation End Product, Induces Inflammation via

Interaction with RAGE in Mesangial Cells. In: *Molecular nutrition & food research* 65 (13), e2000799. DOI: 10.1002/mnfr.202000799.

Lee, Hyun Kyoung; Seo, In Ae; Suh, Duk Joon; Lee, Hye Jeong; Park, Hwan Tae (2009): A novel mechanism of methylglyoxal cytotoxicity in neuroglial cells. In: *Journal of neurochemistry* 108 (1), S. 273–284. DOI: 10.1111/j.1471-4159.2008.05764.x.

Lee, Ji Min; Hammarén, Henrik M.; Savitski, Mikhail M.; Baek, Sung Hee (2023): Control of protein stability by post-translational modifications. In: *Nature Communications* 14 (1), S. 201. DOI: 10.1038/s41467-023-35795-8.

Leone, Alessia; Nigro, Cecilia; Nicolò, Antonella; Prevenzano, Immacolata; Formisano, Pietro; Beguinot, Francesco; Miele, Claudia (2021): The Dual-Role of Methylglyoxal in Tumor Progression - Novel Therapeutic Approaches. In: *Frontiers in oncology* 11, S. 645686. DOI: 10.3389/fonc.2021.645686.

Lewis-Tuffin, Laura J.; Rodriguez, Fausto; Giannini, Caterina; Scheithauer, Bernd; Necela, Brian M.; Sarkaria, Jann N.; Anastasiadis, Panos Z. (2010): Misregulated E-cadherin expression associated with an aggressive brain tumor phenotype. In: *PloS one* 5 (10), e13665. DOI: 10.1371/journal.pone.0013665.

Li, Hong; Zhang, Xiaoyun; Guan, Xiumei; Cui, Xiaodong; Wang, Yuliang; Chu, Hairong; Cheng, Min (2012): Advanced glycation end products impair the migration, adhesion and secretion potentials of late endothelial progenitor cells. In: *Cardiovascular diabetology* 11, S. 46. DOI: 10.1186/1475-2840-11-46.

Li, Qinying; Sun, Mei; Yu, Mingsheng; Fu, Qianyun; Jiang, Hao; Yu, Guangli; Li, Guoyun (2019): Gangliosides profiling in serum of breast cancer patient: GM3 as a potential diagnostic biomarker. In: *Glycoconjugate journal* 36 (5), S. 419–428. DOI: 10.1007/s10719-019-09885-z.

Liang, Huasheng (2020): Advanced glycation end products induce proliferation, invasion and epithelial-mesenchymal transition of human SW480 colon cancer cells through the PI3K/AKT signaling pathway. In: *Oncology letters* 19 (4), S. 3215–3222. DOI: 10.3892/ol.2020.11413.

Liao, Tsai-Tsen; Yang, Muh-Hwa (2017): Revisiting epithelial-mesenchymal transition in cancer metastasis: the connection between epithelial plasticity and stemness. In: *Molecular oncology* 11 (7), S. 792–804. DOI: 10.1002/1878-0261.12096.

Lim, Ee Wei; Aarsland, Dag; Ffytche, Dominic; Taddei, Raquel Natalia; van Wamelen, Daniel J.; Wan, Yi-Min et al. (2019): Amyloid-β and Parkinson's disease. In: *Journal of neurology* 266 (11), S. 2605–2619. DOI: 10.1007/s00415-018-9100-8.

Lima, M.; Baynes, J. W. (2013): Glycation. In: Encyclopedia of Biological Chemistry: Elsevier, S. 405–411.

Lin, Jer-An; Wu, Chi-Hao; Yen, Gow-Chin (2018): Methylglyoxal displays colorectal cancer-promoting properties in the murine models of azoxymethane and CT26 isografts. In: *Free radical biology & medicine* 115, S. 436–446. DOI: 10.1016/j.freeradbiomed.2017.12.020.

Lisowski, Dominik; Hartrampf, Philipp E.; Hasenauer, Natalie; Nickl, Vera; Monoranu, Camelia-Maria; Tamihardja, Jörg (2023): Complete loss of E-cadherin expression in a rare case of metastatic malignant meningioma: a case report. In: *BMC neurology* 23 (1), S. 398. DOI: 10.1186/s12883-023-03450-w.

Loarca, Lorena; Sassi-Gaha, Sihem; Artlett, Carol M. (2013): Two α-dicarbonyls downregulate migration, invasion, and adhesion of liver cancer cells in a p53-dependent manner. In: *Digestive and liver disease : official journal of the Italian Society of Gastroenterology and the Italian Association for the Study of the Liver* 45 (11), S. 938–946. DOI: 10.1016/j.dld.2013.05.005.

Logsdon, Craig D.; Fuentes, Maren K.; Huang, Emina H.; Arumugam, Thiruvengadam (2007): RAGE and RAGE ligands in cancer. In: *Current molecular medicine* 7 (8), S. 777–789. DOI: 10.2174/156652407783220697.

Louis, David N.; Perry, Arie; Wesseling, Pieter; Brat, Daniel J.; Cree, Ian A.; Figarella-Branger, Dominique et al. (2021): The 2021 WHO Classification of Tumors of the Central Nervous System: a summary. In: *Neuro-oncology* 23 (8), S. 1231–1251. DOI: 10.1093/neuonc/noab106.

Lu, Renquan; Wu, Chengsheng; Guo, Lin; Liu, Yingchao; Mo, Wei; Wang, Huijie et al. (2012): The role of brevican in glioma: promoting tumor cell motility in vitro and in vivo. In: *BMC cancer* 12, S. 607. DOI: 10.1186/1471-2407-12-607.

Maeta, Kazuhiro; Izawa, Shingo; Inoue, Yoshiharu (2005): Methylglyoxal, a metabolite derived from glycolysis, functions as a signal initiator of the high osmolarity glycerol-mitogen-activated protein kinase cascade and calcineurin/Crz1-mediated pathway in Saccharomyces cerevisiae. In: *The Journal of biological chemistry* 280 (1), S. 253–260. DOI: 10.1074/jbc.M408061200.

Maeta, Kazuhiro; Izawa, Shingo; Okazaki, Shoko; Kuge, Shusuke; Inoue, Yoshiharu (2004): Activity of the Yap1 transcription factor in Saccharomyces cerevisiae is modulated by methylglyoxal, a metabolite derived from glycolysis. In: *Molecular and cellular biology* 24 (19), S. 8753–8764. DOI: 10.1128/MCB.24.19.8753-8764.2004.

Matou-Nasri, Sabine; Sharaf, Hana; Wang, Qiuyu; Almobadel, Nasser; Rabhan, Zaki; Al-Eidi, Hamad et al. (2017): Biological impact of advanced glycation endproducts on estrogen receptor-positive MCF-7 breast cancer cells. In: *Biochimica et biophysica acta. Molecular basis of disease* 1863 (11), S. 2808–2820. DOI: 10.1016/j.bbadis.2017.07.011.

Medeiros, Matheus L.; Oliveira, Akila L.; Oliveira, Mariana G. de; Mónica, Fabíola Z.; Antunes, Edson (2021): Methylglyoxal Exacerbates Lipopolysaccharide-Induced Acute Lung Injury via RAGE-Induced ROS Generation: Protective Effects of Metformin. In: *Journal of inflammation research* 14, S. 6477–6489. DOI: 10.2147/JIR.S337115.

Mehta, Kruti A.; Patel, Kinjal A.; Pandya, Shashank J.; Patel, Prabhudas S. (2020): "Aberrant sialylation plays a significant role in oral squamous cell carcinoma progression". In: *Journal of oral pathology & medicine : official publication of the International Association of Oral Pathologists and the American Academy of Oral Pathology* 49 (3), S. 253–259. DOI: 10.1111/jop.12976.

Menini, Stefano; Iacobini, Carla; Latouliere, Luisa de; Manni, Isabella; Vitale, Martina; Pilozzi, Emanuela et al. (2020): Diabetes promotes invasive pancreatic cancer by increasing systemic and tumour carbonyl stress in KrasG12D/+ mice. In: *Journal of experimental & clinical cancer research : CR* 39 (1), S. 152. DOI: 10.1186/s13046-020-01665-0.

Michel, Maurice; Hollenbach, Marcus; Pohl, Sabine; Ripoll, Cristina; Zipprich, Alexander (2019): Inhibition of Glyoxalase-I Leads to Reduced Proliferation, Migration and Colony Formation, and Enhanced Susceptibility to Sorafenib in Hepatocellular Carcinoma. In: *Front. Oncol.* 9, S. 785. DOI: 10.3389/fonc.2019.00785.

Midwood, Kim S.; Chiquet, Matthias; Tucker, Richard P.; Orend, Gertraud (2016): Tenascin-C at a glance. In: *Journal of cell science* 129 (23), S. 4321–4327. DOI: 10.1242/jcs.190546.

Miró, Laura; López, Júlia; Guerrero, Pedro E.; Martínez-Bosch, Neus; Manero-Rupérez, Noemí; Moreno, Mireia et al. (2022): Sialyltransferase Inhibitor Ac53FaxNeu5Ac Reverts the Malignant Phenotype of Pancreatic Cancer Cells, and Reduces Tumor Volume and Favors T-Cell Infiltrates in Mice. In: *Cancers* 14 (24). DOI: 10.3390/cancers14246133.

Miyata, T.; Ueda, Y.; Horie, K.; Nangaku, M.; Tanaka, S.; van Ypersele de Strihou, C.; Kurokawa, K. (1998): Renal catabolism of advanced glycation end products: the fate of pentosidine. In: *Kidney international* 53 (2), S. 416–422. DOI: 10.1046/j.1523-1755.1998.00756.x.

Munkley, Jennifer (2022): Aberrant Sialylation in Cancer: Therapeutic Opportunities. In: *Cancers* 14 (17). DOI: 10.3390/cancers14174248.

Nagai, Ryoji; Mera, Katsumi; Nakajou, Keisuke; Fujiwara, Yukio; Iwao, Yasunori; Imai, Hiroki et al. (2007): The ligand activity of AGE-proteins to scavenger receptors is dependent on their rate of modification by AGEs. In: *Biochimica et biophysica acta* 1772 (11-12), S. 1192–1198. DOI: 10.1016/j.bbadis.2007.09.001.

Nairn, Alison V.; York, William S.; Harris, Kyle; Hall, Erica M.; Pierce, J. Michael; Moremen, Kelley W. (2008): Regulation of glycan structures in animal tissues: transcript profiling of glycan-related genes. In: *The Journal of biological chemistry* 283 (25), S. 17298–17313. DOI: 10.1074/jbc.M801964200.

Nam, Han-Kyul; Jeong, So-Ra; Pyo, Min Cheol; Ha, Sang-Keun; Nam, Mi-Hyun; Lee, Kwang-Won (2021): Methylglyoxal-Derived Advanced Glycation End Products (AGE4) Promote Cell Proliferation and Survival in Renal Cell Carcinoma Cells through the RAGE/Akt/ERK Signaling Pathways. In: *Biological & pharmaceutical bulletin* 44 (11), S. 1697–1706. DOI: 10.1248/bpb.b21-00382.

Nardy, Ana Flávia Fernandes Ribas; Freire-de-Lima, Leonardo; Freire-de-Lima, Célio Geraldo; Morrot, Alexandre (2016): The Sweet Side of Immune Evasion: Role of Glycans in the Mechanisms of Cancer Progression. In: *Frontiers in oncology* 6, S. 54. DOI: 10.3389/fonc.2016.00054.

Nokin, Marie-Julie; Bellier, Justine; Durieux, Florence; Peulen, Olivier; Rademaker, Gilles; Gabriel, Maude et al. (2019): Methylglyoxal, a glycolysis metabolite, triggers metastasis through MEK/ERK/SMAD1 pathway activation in breast cancer. In: *Breast cancer research : BCR* 21 (1), S. 11. DOI: 10.1186/s13058-018-1095-7.

Nokin, Marie-Julie; Durieux, Florence; Bellier, Justine; Peulen, Olivier; Uchida, Koji; Spiegel, David A. et al. (2017): Hormetic potential of methylglyoxal, a side-product of glycolysis, in switching tumours from growth to death. In: *Scientific reports* 7 (1), S. 11722. DOI: 10.1038/s41598-017-12119-7.

Nokin, Marie-Julie; Durieux, Florence; Peixoto, Paul; Chiavarina, Barbara; Peulen, Olivier; Blomme, Arnaud et al. (2016): Methylglyoxal, a glycolysis side-product, induces Hsp90 glycation and YAP-mediated tumor growth and metastasis. In: *eLife* 5. DOI: 10.7554/eLife.19375.

Nomura, Wataru; Aoki, Miho; Inoue, Yoshiharu (2020): Methylglyoxal inhibits nuclear division through alterations in vacuolar morphology and accumulation of Atg18 on the vacuolar membrane in Saccharomyces cerevisiae. In: *Scientific reports* 10 (1), S. 13887. DOI: 10.1038/s41598-020-70802-8.

Oh, Eun-Joo; Ryu, Hye-Myung; Choi, Soon-Youn; Yook, Ju-Min; Kim, Chan-Duck; Park, Sun-Hee et al. (2010): Impact of Low Glucose Degradation Product Bicarbonate/Lactate-Buffered Dialysis Solution on the Epithelial-Mesenchymal Transition of Peritoneum. In: *Am J Nephrol* 31 (1), S. 58–67. DOI: 10.1159/000256658.

Oliveira, Akila L.; Medeiros, Matheus L.; Oliveira, Mariana G. de; Teixeira, Caio Jordão; Mónica, Fabíola Z.; Antunes, Edson (2022): Enhanced RAGE Expression and Excess Reactive-Oxygen Species

Production Mediates Rho Kinase-Dependent Detrusor Overactivity After Methylglyoxal Exposure. In: *Frontiers in physiology* 13, S. 860342. DOI: 10.3389/fphys.2022.860342.

Olzscha, Heidi (2019): Posttranslational modifications and proteinopathies: how guardians of the proteome are defeated. In: *Biological chemistry* 400 (7), S. 895–915. DOI: 10.1515/hsz-2018-0458.

Onken, Julia; Moeckel, Sylvia; Leukel, Petra; Leidgens, Verena; Baumann, Fusun; Bogdahn, Ulrich et al. (2014): Versican isoform V1 regulates proliferation and migration in high-grade gliomas. In: *Journal of neuro-oncology* 120 (1), S. 73–83. DOI: 10.1007/s11060-014-1545-8.

Osuka, Satoru; Zhu, Dan; Zhang, Zhaobin; Li, Chaoxi; Stackhouse, Christian T.; Sampetrean, Oltea et al. (2021): N-cadherin upregulation mediates adaptive radioresistance in glioblastoma. In: *The Journal of clinical investigation* 131 (6). DOI: 10.1172/JCI136098.

Ott, Christiane; Jacobs, Kathleen; Haucke, Elisa; Navarrete Santos, Anne; Grune, Tilman; Simm, Andreas (2014): Role of advanced glycation end products in cellular signaling. In: *Redox biology* 2, S. 411–429. DOI: 10.1016/j.redox.2013.12.016.

Oya-Ito, Tomoko; Naito, Yuji; Takagi, Tomohisa; Handa, Osamu; Matsui, Hirofumi; Yamada, Masaki et al. (2011): Heat-shock protein 27 (Hsp27) as a target of methylglyoxal in gastrointestinal cancer. In: *Biochimica et biophysica acta* 1812 (7), S. 769–781. DOI: 10.1016/j.bbadis.2011.03.017.

Pan, Shuo; Guan, Yitong; Ma, Yanpeng; Cui, Qianwei; Tang, Zhiguo; Li, Jingyuan et al. (2022): Advanced glycation end products correlate with breast cancer metastasis by activating RAGE/TLR4 signaling. In: *BMJ open diabetes research & care* 10 (2). DOI: 10.1136/bmjdrc-2021-002697.

Patel, Kinjal D.; De, Maitri; Jethva, Disha D.; Rathod, Bharati S.; Patel, Prabhudas S. (2022): Alterations in Sialylation Patterns are Significantly Associated with Imatinib Mesylate Resistance in Chronic Myeloid Leukemia. In: *Archives of medical research* 53 (1), S. 51–58. DOI: 10.1016/j.arcmed.2021.06.003.

Paul-Samojedny, Monika; Łasut, Barbara; Pudełko, Adam; Fila-Daniłow, Anna; Kowalczyk, Małgorzata; Suchanek-Raif, Renata et al. (2016): Methylglyoxal (MGO) inhibits proliferation and induces cell death of human glioblastoma multiforme T98G and U87MG cells. In: *Biomedicine & pharmacotherapy = Biomedecine & pharmacotherapie* 80, S. 236–243. DOI: 10.1016/j.biopha.2016.03.021.

Perez, Ser John Lynon P.; Fu, Chih-Wei; Li, Wen-Shan (2021): Sialyltransferase Inhibitors for the Treatment of Cancer Metastasis: Current Challenges and Future Perspectives. In: *Molecules (Basel, Switzerland)* 26 (18). DOI: 10.3390/molecules26185673.

Perrone, Anna; Giovino, Antonio; Benny, Jubina; Martinelli, Federico (2020): Advanced Glycation End Products (AGEs): Biochemistry, Signaling, Analytical Methods, and Epigenetic Effects. In: *Oxidative medicine and cellular longevity* 2020, S. 3818196. DOI: 10.1155/2020/3818196.

Poulsen, Malene W.; Hedegaard, Rikke V.; Andersen, Jeanette M.; Courten, Barbora de; Bügel, Susanne; Nielsen, John et al. (2013): Advanced glycation endproducts in food and their effects on health. In: *Food and chemical toxicology : an international journal published for the British Industrial Biological Research Association* 60, S. 10–37. DOI: 10.1016/j.fct.2013.06.052.

Prestes Fallavena, Lucas; Poerner Rodrigues, Naira; Damasceno Ferreira Marczak, Ligia; Domeneghini Mercali, Giovana (2022): Formation of advanced glycation end products by novel food processing technologies: A review. In: *Food chemistry* 393, S. 133338. DOI: 10.1016/j.foodchem.2022.133338.

Pucci, M.; Aria, F.; Premoli, M.; Maccarinelli, G.; Mastinu, A.; Bonini, S. et al. (2021): Methylglyoxal affects cognitive behaviour and modulates RAGE and Presenilin-1 expression in hippocampus of aged mice. In: *Food and chemical toxicology : an international journal published for the British Industrial Biological Research Association* 158, S. 112608. DOI: 10.1016/j.fct.2021.112608.

Qi, Chunxiao; Lei, Lei; Hu, Jinqu; Wang, Gang; Liu, Jiyuan; Ou, Shaowu (2021): Thrombospondin-1 is a prognostic biomarker and is correlated with tumor immune microenvironment in glioblastoma. In: *Oncology letters* 21 (1), S. 22. DOI: 10.3892/ol.2020.12283.

Rabbani, Naila; Thornalley, Paul J. (2012): Methylglyoxal, glyoxalase 1 and the dicarbonyl proteome. In: *Amino acids* 42 (4), S. 1133–1142. DOI: 10.1007/s00726-010-0783-0.

Rabbani, Naila; Xue, Mingzhan; Weickert, Martin O.; Thornalley, Paul J. (2018): Multiple roles of glyoxalase 1-mediated suppression of methylglyoxal glycation in cancer biology-Involvement in tumour suppression, tumour growth, multidrug resistance and target for chemotherapy. In: *Seminars in cancer biology* 49, S. 83–93. DOI: 10.1016/j.semcancer.2017.05.006.

Raghavan, Cibin T.; Smuda, Mareen; Smith, Andrew J. O.; Howell, Scott; Smith, Dawn G.; Singh, Annapurna et al. (2016): AGEs in human lens capsule promote the TGFβ2-mediated EMT of lens epithelial cells: implications for age-associated fibrosis. In: *Aging cell* 15 (3), S. 465–476. DOI: 10.1111/acel.12450.

Reiter, Michael J.; Costello, Justin E.; Schwope, Ryan B.; Lisanti, Christopher J.; Osswald, Michael B. (2015): Review of Commonly Used Serum Tumor Markers and Their Relevance for Image Interpretation. In: *Journal of computer assisted tomography* 39 (6), S. 825–834. DOI: 10.1097/RCT.0000000000000297.

Rosenstock, Philip; Kaufmann, Thomas (2021): Sialic Acids and Their Influence on Human NK Cell Function. In: *Cells* 10 (2). DOI: 10.3390/cells10020263.

Ross, Christopher A.; Poirier, Michelle A. (2004): Protein aggregation and neurodegenerative disease. In: *Nature medicine* 10 Suppl, S10-7. DOI: 10.1038/nm1066.

Rowe, Matthew M.; Wang, Wenjun; Taufalele, Paul V.; Reinhart-King, Cynthia A. (2022): AGE-breaker ALT711 reverses glycation-mediated cancer cell migration. In: *Soft matter* 18 (44), S. 8504–8513. DOI: 10.1039/d2sm00004k.

Rupp, Tristan; Langlois, Benoit; Koczorowska, Maria M.; Radwanska, Agata; Sun, Zhen; Hussenet, Thomas et al. (2016): Tenascin-C Orchestrates Glioblastoma Angiogenesis by Modulation of Pro- and Anti-angiogenic Signaling. In: *Cell reports* 17 (10), S. 2607–2619. DOI: 10.1016/j.celrep.2016.11.012.

Rutkowski, Robert; Chrzanowski, Robert; Trwoga, Magdalena; Kochanowicz, Jan; Turek, Grzegorz; Mariak, Zenon; Reszeć, Joanna (2018): Expression of N-cadherin and β-catenin in human meningioma in correlation with peritumoral edema. In: *The International journal of neuroscience* 128 (9), S. 805–810. DOI: 10.1080/00207454.2018.1424153.

Sato, Chihiro; Kitajima, Ken (2021): Polysialylation and disease. In: *Molecular aspects of medicine* 79, S. 100892. DOI: 10.1016/j.mam.2020.100892.

Schalkwijk, C. G.; Stehouwer, C. D. A. (2020): Methylglyoxal, a Highly Reactive Dicarbonyl Compound, in Diabetes, Its Vascular Complications, and Other Age-Related Diseases. In: *Physiological reviews* 100 (1), S. 407–461. DOI: 10.1152/physrev.00001.2019.

Schalkwijk, Casper G.; Micali, Linda Renata; Wouters, Kristiaan (2023): Advanced glycation endproducts in diabetes-related macrovascular complications: focus on methylglyoxal. In: *Trends in endocrinology and metabolism: TEM* 34 (1), S. 49–60. DOI: 10.1016/j.tem.2022.11.004.

Scheer, Maximilian; Bork, Kaya; Simon, Frieder; Nagasundaram, Manimozhi; Horstkorte, Rüdiger; Gnanapragassam, Vinayaga Srinivasan (2020): Glycation Leads to Increased Polysialylation and Promotes the Metastatic Potential of Neuroblastoma Cells. In: *Cells* 9 (4). DOI: 10.3390/cells9040868.

Schildhauer, Paola; Selke, Philipp; Scheller, Christian; Strauss, Christian; Horstkorte, Rüdiger; Leisz, Sandra; Scheer, Maximilian (2023a): Glycation Leads to Increased Invasion of Glioblastoma Cells. In: *Cells* 12 (9), S. 1219. DOI: 10.3390/cells12091219.

Schildhauer, Paola; Selke, Philipp; Staege, Martin S.; Harder, Anja; Scheller, Christian; Strauss, Christian et al. (2023b): Glycation Interferes with the Expression of Sialyltransferases and Leads to Increased Polysialylation in Glioblastoma Cells. In: *Cells* 12 (23), S. 2758. DOI: 10.3390/cells12232758.

Schnaar, Ronald L.; Gerardy-Schahn, Rita; Hildebrandt, Herbert (2014): Sialic acids in the brain: gangliosides and polysialic acid in nervous system development, stability, disease, and regeneration. In: *Physiological reviews* 94 (2), S. 461–518. DOI: 10.1152/physrev.00033.2013.

Seifert, Anja; Glanz, Dagobert; Glaubitz, Nicole; Horstkorte, Rüdiger; Bork, Kaya (2012): Polysialylation of the neural cell adhesion molecule: interfering with polysialylation and migration in neuroblastoma cells. In: *Archives of biochemistry and biophysics* 524 (1), S. 56–63. DOI: 10.1016/j.abb.2012.04.011.

Selke, Philipp; Bork, Kaya; Zhang, Tao; Wuhrer, Manfred; Strauss, Christian; Horstkorte, Rüdiger; Scheer, Maximilian (2021a): Glycation Interferes with the Expression of Sialyltransferases in Meningiomas. In: *Cells* 10 (12). DOI: 10.3390/cells10123298.

Selke, Philipp; Rosenstock, Philip; Bork, Kaya; Strauss, Christian; Horstkorte, Rüdiger; Scheer, Maximilian (2021b): Glycation of benign meningioma cells leads to increased invasion. In: *Biological chemistry* 402 (7), S. 849–859. DOI: 10.1515/hsz-2020-0376.

Selvik, Linn-Karina M.; Rao, Shalini; Steigedal, Tonje S.; Haltbakk, Ildri; Misund, Kristine; Bruland, Torunn et al. (2014): Salt-inducible kinase 1 (SIK1) is induced by gastrin and inhibits migration of gastric adenocarcinoma cells. In: *PloS one* 9 (11), e112485. DOI: 10.1371/journal.pone.0112485.

Sharaf, Hana; Matou-Nasri, Sabine; Wang, Qiuyu; Rabhan, Zaki; Al-Eidi, Hamad; Al Abdulrahman, Abdulkareem; Ahmed, Nessar (2015): Advanced glycation endproducts increase proliferation, migration and invasion of the breast cancer cell line MDA-MB-231. In: *Biochimica et biophysica acta* 1852 (3), S. 429–441. DOI: 10.1016/j.bbadis.2014.12.009.

Silsirivanit, Atit (2019): Glycosylation markers in cancer. In: *Advances in clinical chemistry* 89, S. 189–213. DOI: 10.1016/bs.acc.2018.12.005.

Singh, R.; Barden, A.; Mori, T.; Beilin, L. (2001): Advanced glycation end-products: a review. In: *Diabetologia* 44 (2), S. 129–146. DOI: 10.1007/s001250051591.

Singh, Sanjiv; Siva, Boddu Veerabadra; Ravichandiran, V. (2022): Advanced Glycation End Products: key player of the pathogenesis of atherosclerosis. In: *Glycoconjugate journal* 39 (4), S. 547–563. DOI: 10.1007/s10719-022-10063-x.

Sisay, Mekonnen; Edessa, Dumessa; Ali, Tilahun; Mekuria, Abraham Nigussie; Gebrie, Alemu (2020): The relationship between advanced glycation end products and gestational diabetes: A systematic review and meta-analysis. In: *PloS one* 15 (10), e0240382. DOI: 10.1371/journal.pone.0240382.

Smedsrød, B.; Melkko, J.; Araki, N.; Sano, H.; Horiuchi, S. (1997): Advanced glycation end products are eliminated by scavenger-receptor-mediated endocytosis in hepatic sinusoidal Kupffer and endothelial cells. In: *The Biochemical journal* 322 (Pt 2) (Pt 2), S. 567–573. DOI: 10.1042/bj3220567.

Smithson, Mary; Irwin, Regina; Williams, Gregory; Alexander, Katie L.; Smythies, Lesley E.; Nearing, Marie et al. (2022): Sialyltransferase ST6GAL-1 mediates resistance to chemoradiation in rectal cancer. In: *The Journal of biological chemistry* 298 (3), S. 101594. DOI: 10.1016/j.jbc.2022.101594.

Sparvero, Louis J.; Asafu-Adjei, Denise; Kang, Rui; Tang, Daolin; Amin, Neilay; Im, Jaehyun et al. (2009): RAGE (Receptor for Advanced Glycation Endproducts), RAGE ligands, and their role in cancer and inflammation. In: *Journal of translational medicine* 7, S. 17. DOI: 10.1186/1479-5876-7-17.

Srikanth, Velandai; Maczurek, Annette; Phan, Thanh; Steele, Megan; Westcott, Bernadette; Juskiw, Damian; Münch, Gerald (2011): Advanced glycation endproducts and their receptor RAGE in Alzheimer's disease. In: *Neurobiology of aging* 32 (5), S. 763–777. DOI: 10.1016/j.neurobiolaging.2009.04.016.

Stäsche, R.; Hinderlich, S.; Weise, C.; Effertz, K.; Lucka, L.; Moormann, P.; Reutter, W. (1997): A bifunctional enzyme catalyzes the first two steps in N-acetylneuraminic acid biosynthesis of rat liver. Molecular cloning and functional expression of UDP-N-acetyl-glucosamine 2-epimerase/N-acetylmannosamine kinase. In: *The Journal of biological chemistry* 272 (39), S. 24319–24324. DOI: 10.1074/jbc.272.39.24319.

Stefanowicz-Hajduk, Justyna; Ochocka, J. Renata (2020): Real-time cell analysis system in cytotoxicity applications: Usefulness and comparison with tetrazolium salt assays. In: *Toxicology Reports* 7, S. 335–344. DOI: 10.1016/j.toxrep.2020.02.002.

Steinberg, D.; Parthasarathy, S.; Carew, T. E.; Khoo, J. C.; Witztum, J. L. (1989): Beyond cholesterol. Modifications of low-density lipoprotein that increase its atherogenicity. In: *The New England journal of medicine* 320 (14), S. 915–924. DOI: 10.1056/NEJM198904063201407.

Stirban, Alin; Gawlowski, Thomas; Roden, Michael (2014): Vascular effects of advanced glycation endproducts: Clinical effects and molecular mechanisms. In: *Molecular metabolism* 3 (2), S. 94–108. DOI: 10.1016/j.molmet.2013.11.006.

Suh, Young Joon; Hall, Matthew S.; Huang, Yu Ling; Moon, So Youn; Song, Wei; Ma, Minglin et al. (2019): Glycation of collagen matrices promotes breast tumor cell invasion. In: *Integrative biology : quantitative biosciences from nano to macro*. DOI: 10.1093/intbio/zyz011.

Sutariya, Brijesh; Jhonsa, Dimple; Saraf, Madhusudan N. (2016): TGF-β: the connecting link between nephropathy and fibrosis. In: *Immunopharmacology and immunotoxicology* 38 (1), S. 39–49. DOI: 10.3109/08923973.2015.1127382.

Takeuchi, M.; Makita, Z.; Yanagisawa, K.; Kameda, Y.; Koike, T. (1999): Detection of noncarboxymethyllysine and carboxymethyllysine advanced glycation end products (AGE) in serum of diabetic patients. In: *Molecular medicine (Cambridge, Mass.)* 5 (6), S. 393–405.

Taniguchi, Naoyuki; Murata, Masatsune (2021): Advances in Glycation: from food to human health and disease. In: *Glycoconjugate journal* 38 (3), S. 273–275. DOI: 10.1007/s10719-021-09981-z.

Tarbell, J. M.; Cancel, L. M. (2016): The glycocalyx and its significance in human medicine. In: *Journal of internal medicine* 280 (1), S. 97–113. DOI: 10.1111/joim.12465.

Thiesler, Hauke; Küçükerden, Melike; Gretenkort, Lina; Röckle, Iris; Hildebrandt, Herbert (2022): News and Views on Polysialic Acid: From Tumor Progression and Brain Development to Psychiatric

Disorders, Neurodegeneration, Myelin Repair and Immunomodulation. In: *Frontiers in cell and developmental biology* 10, S. 871757. DOI: 10.3389/fcell.2022.871757.

Thomsen, Maj S.; Routhe, Lisa J.; Moos, Torben (2017): The vascular basement membrane in the healthy and pathological brain. In: *Journal of cerebral blood flow and metabolism : official journal of the International Society of Cerebral Blood Flow and Metabolism* 37 (10), S. 3300–3317. DOI: 10.1177/0271678X17722436.

Thornalley, Paul J. (2005): Dicarbonyl intermediates in the maillard reaction. In: *Annals of the New York Academy of Sciences* 1043, S. 111–117. DOI: 10.1196/annals.1333.014.

Touré, Fatouma; Zahm, Jean-Marie; Garnotel, Roselyne; Lambert, Elise; Bonnet, Noel; Schmidt, Ann Marie et al. (2008): Receptor for advanced glycation end-products (RAGE) modulates neutrophil adhesion and migration on glycoxidated extracellular matrix. In: *The Biochemical journal* 416 (2), S. 255–261. DOI: 10.1042/BJ20080054.

Trepat, Xavier; Chen, Zaozao; Jacobson, Ken (2012): Cell migration. In: *Comprehensive Physiology* 2 (4), S. 2369–2392. DOI: 10.1002/cphy.c110012.

Tupe, Rashmi S.; Vishwakarma, Anjali; Solaskar, Anamika; Prajapati, Anali (2019): Methylglyoxal induces glycation and oxidative stress in Saccharomyces cerevisiae. In: *Ann Microbiol* 69 (11), S. 1165–1175. DOI: 10.1007/s13213-019-01498-z.

Twarda-Clapa, Aleksandra; Olczak, Aleksandra; Białkowska, Aneta M.; Koziołkiewicz, Maria (2022): Advanced Glycation End-Products (AGEs): Formation, Chemistry, Classification, Receptors, and Diseases Related to AGEs. In: *Cells* 11 (8). DOI: 10.3390/cells11081312.

Uribarri, Jaime; Peppa, Melpomeni; Cai, Weijing; Goldberg, Teresia; Lu, Min; He, Cijiang; Vlassara, Helen (2003): Restriction of dietary glycotoxins reduces excessive advanced glycation end products in renal failure patients. In: *Journal of the American Society of Nephrology : JASN* 14 (3), S. 728–731. DOI: 10.1097/01.asn.0000051593.41395.b9.

Uribarri, Jaime; Woodruff, Sandra; Goodman, Susan; Cai, Weijing; Chen, Xue; Pyzik, Renata et al. (2010): Advanced glycation end products in foods and a practical guide to their reduction in the diet. In: *Journal of the American Dietetic Association* 110 (6), 911-16.e12. DOI: 10.1016/j.jada.2010.03.018.

Utsuki, S.; Oka, H.; Sato, Y.; Kawano, N.; Tsuchiya, B.; Kobayashi, I.; Fujii, K. (2005): Invasive meningioma is associated with a low expression of E-cadherin and beta-catenin. In: *Clinical neuropathology* 24 (1), S. 8–12.

Valiente, M.; Sepúlveda, J. M.; Pérez, A. (2023): Emerging targets for cancer treatment: S100A9/RAGE. In: *ESMO open* 8 (1), S. 100751. DOI: 10.1016/j.esmoop.2022.100751.

van der Bruggen, Myrthe M.; Spronck, Bart; Delhaas, Tammo; Reesink, Koen D.; Schalkwijk, Casper G. (2021): The Putative Role of Methylglyoxal in Arterial Stiffening: A Review. In: *Heart, lung & circulation* 30 (11), S. 1681–1693. DOI: 10.1016/j.hlc.2021.06.527.

Veillon, Lucas; Fakih, Christina; Abou-El-Hassan, Hadi; Kobeissy, Firas; Mechref, Yehia (2018): Glycosylation Changes in Brain Cancer. In: *ACS chemical neuroscience* 9 (1), S. 51–72. DOI: 10.1021/acschemneuro.7b00271.

Vlassara, H. (2001): The AGE-receptor in the pathogenesis of diabetic complications. In: *Diabetes/metabolism research and reviews* 17 (6), S. 436–443. DOI: 10.1002/dmrr.233.

Vlassara, Helen; Cai, Weijing; Crandall, Jill; Goldberg, Teresia; Oberstein, Robert; Dardaine, Veronique et al. (2002): Inflammatory mediators are induced by dietary glycotoxins, a major risk factor for

diabetic angiopathy. In: *Proceedings of the National Academy of Sciences of the United States of America* 99 (24), S. 15596–15601. DOI: 10.1073/pnas.242407999.

Voet, Donald (2006): Fundamentals of biochemistry. Life at the molecular level. 2. ed. Hoboken, NJ: Wiley. Online verfügbar unter http://bcs.wiley.com/he-bcs/Books?action=index&itemId=0471214957&itemTypeId=BKS&bcsId=2261.

Vollmann-Zwerenz, Arabel; Leidgens, Verena; Feliciello, Giancarlo; Klein, Christoph A.; Hau, Peter (2020): Tumor Cell Invasion in Glioblastoma. In: *International journal of molecular sciences* 21 (6). DOI: 10.3390/ijms21061932.

Waghela, Bhargav N.; Vaidya, Foram U.; Ranjan, Kishu; Chhipa, Abu Sufiyan; Tiwari, Budhi Sagar; Pathak, Chandramani (2021): AGE-RAGE synergy influences programmed cell death signaling to promote cancer. In: *Molecular and cellular biochemistry* 476 (2), S. 585–598. DOI: 10.1007/s11010-020-03928-y.

Wallesch, Maren; Pachow, Doreen; Blücher, Christina; Firsching, Raimund; Warnke, Jan-Peter; Braunsdorf, Werner E. K. et al. (2017): Altered expression of E-Cadherin-related transcription factors indicates partial epithelial-mesenchymal transition in aggressive meningiomas. In: *Journal of the neurological sciences* 380, S. 112–121. DOI: 10.1016/j.jns.2017.07.009.

Wang, Bowen; Vashishth, Deepak (2023): Advanced glycation and glycoxidation end products in bone. In: *Bone* 176, S. 116880. DOI: 10.1016/j.bone.2023.116880.

Wang, J.; Chang, T. (2010): Methylglyoxal content in drinking coffee as a cytotoxic factor. In: *Journal of food science* 75 (6), H167-71. DOI: 10.1111/j.1750-3841.2010.01658.x.

Wang, Lu; Xu, Haojie; Yang, Huaxia; Zhou, Jiaxin; Zhao, Lidan; Zhang, Fengchun (2022): Glucose metabolism and glycosylation link the gut microbiota to autoimmune diseases. In: *Frontiers in immunology* 13, S. 952398. DOI: 10.3389/fimmu.2022.952398.

Wang, Ning; Song, Qian; Yu, Hai; Bao, Gang (2021): Overexpression of FBXO17 Promotes the Proliferation, Migration and Invasion of Glioma Cells Through the Akt/GSK-3β/Snail Pathway. In: *Cell transplantation* 30, 9636897211007395. DOI: 10.1177/09636897211007395.

Waqas, Komal; Muller, Max; Koedam, Marijke; el Kadi, Youssra; Zillikens, M. Carola; van der Eerden, B. C. J. (2022): Methylglyoxal - an advanced glycation end products (AGEs) precursor - Inhibits differentiation of human MSC-derived osteoblasts in vitro independently of receptor for AGEs (RAGE). In: *Bone* 164, S. 116526. DOI: 10.1016/j.bone.2022.116526.

Wu, En-Ting; Liang, Jin-Tung; Wu, Ming-Shiou; Chang, Kuo-Chu (2011): Pyridoxamine prevents age-related aortic stiffening and vascular resistance in association with reduced collagen glycation. In: *Experimental gerontology* 46 (6), S. 482–488. DOI: 10.1016/j.exger.2011.02.001.

Wu, Xin; Zhao, Junda; Ruan, Yuanyuan; Sun, Li; Xu, Congjian; Jiang, Hua (2018): Sialyltransferase ST3GAL1 promotes cell migration, invasion, and TGF-β1-induced EMT and confers paclitaxel resistance in ovarian cancer. In: *Cell death & disease* 9 (11), S. 1102. DOI: 10.1038/s41419-018-1101-0.

Xia, Shuli; Lal, Bachchu; Tung, Brian; Wang, Shervin; Goodwin, C. Rory; Laterra, John (2016): Tumor microenvironment tenascin-C promotes glioblastoma invasion and negatively regulates tumor proliferation. In: *Neuro-oncology* 18 (4), S. 507–517. DOI: 10.1093/neuonc/nov171.

Xu, Gaoran; Chen, Junzhu; Wang, Guorong; Xiao, Junhong; Zhang, Ning; Chen, Yanyu et al. (2020): Resveratrol Inhibits the Tumorigenesis of Follicular Thyroid Cancer via ST6GAL2-Regulated Activation

of the Hippo Signaling Pathway. In: *Molecular Therapy Oncolytics* 16, S. 124–133. DOI: 10.1016/j.omto.2019.12.010.

Yamagishi, Sho-ichi; Imaizumi, Tsutomu (2005): Diabetic vascular complications: pathophysiology, biochemical basis and potential therapeutic strategy. In: *Current pharmaceutical design* 11 (18), S. 2279–2299. DOI: 10.2174/1381612054367300.

Yan, Tengfeng; Tan, Yinqiu; Deng, Gang; Sun, Zhiqiang; Liu, Baohui; Wang, Yixuan et al. (2022): TGF-β induces GBM mesenchymal transition through upregulation of CLDN4 and nuclear translocation to activate TNF-α/NF-κB signal pathway. In: *Cell death & disease* 13 (4), S. 339. DOI: 10.1038/s41419-022-04788-8.

Yang, Zeyong; Zhang, Wangping; Lu, Han; Cai, Shu (2022): Methylglyoxal in the Brain: From Glycolytic Metabolite to Signalling Molecule. In: *Molecules (Basel, Switzerland)* 27 (22). DOI: 10.3390/molecules27227905.

Yu, Fengbo; Li, Guihong; Gao, Junxia; Sun, Yuxue; Liu, Pengfei; Gao, Haijun et al. (2016): SPOCK1 is upregulated in recurrent glioblastoma and contributes to metastasis and Temozolomide resistance. In: *Cell proliferation* 49 (2), S. 195–206. DOI: 10.1111/cpr.12241.

Yuan, Ye; Li, Shi-Lin; Cao, Yu-Lin; Li, Jun-Jun; Wang, Qiang-Ping (2019): LKB1 suppresses glioma cell invasion via NF-κB/Snail signaling repression. In: *OncoTargets and therapy* 12, S. 2451–2463. DOI: 10.2147/OTT.S193736.

Yuen, Amy; Laschinger, Carol; Talior, Ilana; Lee, Wilson; Chan, Matthew; Birek, Juliana et al. (2010): Methylglyoxal-modified collagen promotes myofibroblast differentiation. In: *Matrix biology : journal of the International Society for Matrix Biology* 29 (6), S. 537–548. DOI: 10.1016/j.matbio.2010.04.004.

Zhang, Qibin; Ames, Jennifer M.; Smith, Richard D.; Baynes, John W.; Metz, Thomas O. (2009): A perspective on the Maillard reaction and the analysis of protein glycation by mass spectrometry: probing the pathogenesis of chronic disease. In: *Journal of proteome research* 8 (2), S. 754–769. DOI: 10.1021/pr800858h.

Zhao, Chu-Biao; Bao, Ji-Ming; Lu, Yong-Jie; Zhao, Tong; Zhou, Xin-Hua; Zheng, Da-Yong; Zhao, Shan-Chao (2014): Co-expression of RAGE and HMGB1 is associated with cancer progression and poor patient outcome of prostate cancer. In: *American Journal of Cancer Research* 4 (4), S. 369–377.

Zhao, Xiangdong; Sun, Qian; Dou, Changwu; Chen, Qianxue; Liu, Baohui (2019): BMP4 inhibits glioblastoma invasion by promoting E-cadherin and claudin expression. In: *Frontiers in bioscience (Landmark edition)* 24 (6), S. 1060–1070. DOI: 10.2741/4768.

Zheng, Changping; Terreni, Marco; Sollogoub, Matthieu; Zhang, Yongmin (2019): Ganglioside GM3 and Its Role in Cancer. In: *Current medicinal chemistry* 26 (16), S. 2933–2947. DOI: 10.2174/0929867325666180129100619.

Zhong, Chuanhong; Tao, Bei; Chen, Yitian; Guo, Zhangchao; Yang, Xiaobo; Peng, Lilei et al. (2020): B7-H3 Regulates Glioma Growth and Cell Invasion Through a JAK2/STAT3/Slug-Dependent Signaling Pathway. In: *OncoTargets and therapy* 13, S. 2215–2224. DOI: 10.2147/OTT.S237841.

Zhou, Keiyu; Wang, Guangtao; Wang, Yirong; Jin, Hanghuang; Yang, Shuxu; Liu, Chibo (2010): The potential involvement of E-cadherin and beta-catenins in meningioma. In: *PloS one* 5 (6), e11231. DOI: 10.1371/journal.pone.0011231.

Zhou, Wei; Yu, Xuejuan; Sun, Shuang; Zhang, Xuehai; Yang, Wenjing; Zhang, Junpeng et al. (2019): Increased expression of MMP-2 and MMP-9 indicates poor prognosis in glioma recurrence. In:

Biomedicine & pharmacotherapy = Biomedecine & pharmacotherapie 118, S. 109369. DOI: 10.1016/j.biopha.2019.109369.

Zunkel, Katja; Simm, Andreas; Bartling, Babett (2020): Long-term intake of the reactive metabolite methylglyoxal is not toxic in mice. In: *Food and chemical toxicology : an international journal published for the British Industrial Biological Research Association* 141, S. 111333. DOI: 10.1016/j.fct.2020.111333.

5. Thesen

1. Eine Behandlung mit MGO zeigt in allen verwendeten Zelllinien einen konzentrationsabhängigen, zytotoxischen Effekt.
2. Neben einer konzentrationsabhängigen, zelltypunabhängigen Induktion von Glykierung, konnte die Behandlung mit MGO außerdem eine Modifikation der Glykosylierung hervorrufen.
3. Neben der Induktion von Glykosylierung führte eine Behandlung mit MGO eine zelltypspezifische Modifikation der Expression von Sialyltransferasen.
4. Die durch MGO induzierte Glykierung und Glykosylierung ging mit einer Modifikation des Verhaltens der Zellen einher. Abhängig vom Zelltyp kam es teilweise zu einem aggressiveren Phänotyp durch Steigerung der Migration sowie Invasion.
5. Die Modifikation des Verhaltens der Zellen war mit einer Modulation der Expression von Extrazellulären Matrixproteinen sowie Transkriptionsfaktoren vergesellschaftet.

6. Publikationsteil

cells

MDPI

Article

Glycation Leads to Increased Polysialylation and Promotes the Metastatic Potential of Neuroblastoma Cells

Maximilian Scheer [1,2], Kaya Bork [1], Frieder Simon [1], Manimozhi Nagasundaram [1], Rüdiger Horstkorte [1,*] and Vinayaga Srinivasan Gnanapragassam [1]

[1] Institute for Physiological Chemistry, Medical Faculty, Martin-Luther-University Halle-Wittenberg, 06114 Halle (Saale), Germany; Maximilian.Scheer@uk-halle.de (M.S.); kaya.bork@medizin.uni-halle.de (K.B.); frieder.simon@uk-halle.de (F.S.); manimozhi.nagasundaram@medizin.uni-halle.de (M.N.); vinayaga.gnanapragassam@medizin.uni-halle.de (V.S.G.)

[2] Department for Neurosurgery, University Hospital Halle, 06120 Halle (Saale), Germany

* Correspondence: ruediger.horstkorte@medizin.uni-halle.de; Tel.: +49-0-345-557-3873

Received: 2 March 2020; Accepted: 1 April 2020; Published: 2 April 2020

Abstract: Neuroblastoma is the second most frequent extracranial tumor, affecting young children worldwide. One hallmark of tumors such as neuroblastomas, is the expression of polysialic acid, which interferes with adhesion and may promote invasion and metastasis. Since tumor cells use glycolysis for energy production, they thereby produce as side product methylglyoxal (MGO), which reacts with proteins to advanced glycation end products in a mechanism called glycation. Here we analyzed the expression of (poly) sialic acid and adhesion of Kelly neuroblastoma cells after glycation with MGO. We found that both sialylation and polysialylation is increased after glycation. Furthermore, glycated Kelly neuroblastoma cells had a much higher potential for migration and invasion compared with non-glycated cells.

Keywords: (poly) sialic acid; NCAM; adhesion; migration; methylglyoxal; Kelly cells

1. Introduction

Neuroblastoma is a malignant embryonic tumor and arises from immature cells of the sympathetic nervous system. Neuroblastomas represent neuroendocrine tumors because they synthesize catecholamines. They are among the most common extracranial solid tumor forms in childhood. Neuroblastoma is responsible for approximately 7.3% of childhood tumors and the cause of death in around 15% of childhood cancer. The mean age of onset of the disease is 14 months, whereas adults are rarely affected [1].

Characterization of genetic alterations in neuroblastoma revealed that MYCN amplification is an independent prognostic factor for identifying rapid tumor progression and predicting a poor prognosis irrespective of age and clinical stage [2]. The clinical picture depends also on the location of the tumor. In most cases, the primary tumors are located in the area of the adrenal gland, paravertebral or in the abdominal midline. About 50% of all patients already have distant metastases when diagnosed. These mostly affect the bone marrow (86% of all patients with metastatic disease), the bone (62%), the lymph nodes (19%) and the liver (17%) [1]. Neuroblastoma is a sporadic disease; family cases make up only about 1% of all patients. In a large part of these familial neuroblastomas, germline mutations of the ALK (anaplastic lymphoma kinase) gene can be detected [3]. Despite this frequent metastasis, spontaneous remission of the tumor including metastases has often been described. Spontaneous remissions occur in 50% of cases of stage 2a—and even in 80% of all cases in the rare stage 4 S [4–6]. As many tumors, also neuroblastomas express polysialylated neural cell adhesion molecule (NCAM) [7]. Polysialylation is a posttranslational modification of NCAM, in which long

linear polymers of sialic acid are built [8]. Both, polysialic acid and NCAM expression are prognostic markers for neuroblastoma [9,10]. In addition to its role in cell migration and axonal growth during development, polysialic acid is closely related to tumor malignancy. The level of polysialic acid correlates with the malignant potential of several tumors, such as undifferentiated neuroblastoma and is significantly more abundant in high-grade tumors than in low-grade tumors [7]. It has been shown that also in aggressive brain tumors, such as glioblastoma, polysialylation is a negative prognostic marker, since the expression of long chains of negatively charged sialic acids interferes with cell adhesion and promotes metastasis [11–13].

Nearly all tumors including neuroblastoma use primarily glycolysis to generate energy [14]. Besides ATP and NADH, glycolysis produces dicarbonyl compounds that are highly reactive and react with amino groups [15]. One of the most common byproducts of glycolysis is methylglyoxal (MGO) [16]. Approximately 0.1–0.4% of the glucose is converted to MGO during glycolysis. MGO is 20,000 times more reactive than glucose reacting with amino groups [17]. This non-enzymatic chemical reaction of MGO with amino groups is also called glycation and stable advanced glycation end products (AGEs) are formed in further steps. AGEs represent a heterogeneous group of often unknown structures. However, some of these structures are well characterized, such as carboxymethyllysine (CML) and carboxylethyllysine (CEL), which are formed by glyoxal or MGO [18]. Those and other AGEs interfere with protein function, solubility and degradation [19]. The dicarbonyl compound MGO occurs in high concentrations in the human cerebrospinal fluid [20]. In this study, we analyzed Kelly neuroblastoma cells, which express both NCAM and polysialic acid [7] before and after glycation with MGO. We found an upregulation of polysialylation and in agreement with this observation, reduced cellular adhesion and increased invasion.

2. Materials and Methods

2.1. Chemicals and Reagents

Cell culture medium Dulbecco's Modified Eagle Medium, serum, penicillin and streptomycin were purchased from Gibco (Darmstadt, Germany). Laminin, fibronectin and vitronectin were purchased from Sigma Aldrich (Hamburg, Germany). E- and CIM-plates were purchased from OLS (Bremen, Germany). Protease and phosphatase inhibitors were purchased from Sigma Aldrich (Hamburg, Germany). Biotinylated Maackia Amurensis Lectin II, Sambucus nigra lectin and DyLight 488 Streptavidin (Vector labs, Burlingame, CA, USA). Beta tubulin anti mouse antibody were purchased from Thermofisher (Darmstadt, Germany).

2.2. Cell Culture

Kelly cells were cultured in RPMI medium containing 10% FCS with L-glutamine, minimum essential medium, non-essential amino acids, penicillin and streptomycin. Cultured cells were treated with 0, 5, 10, 25, 50 and 100 µM methylglyoxal dissolved in medium. After 48 h, cells were washed two times with PBS and dissociated with PBS/EDTA. Cells were further washed with PBS and pelleted by centrifugation at 1000 rpm (82× *g*) for 5 min for further analysis.

2.3. Cell Viability Assay by MTT

Kelly cells (10,000/well) were seeded in 96-well plates and treated with MGO at various concentrations (0–100 µM) for 48 h. Cultured cells were replaced with fresh medium for every 24 h. After 48 h 200 µL of fresh medium were replaced, to that 20 µL of 5 mg/mL of 3-[4,5-Dimethylthiazol-2-yl]-2,5 diphenyl tetrazolium bromide (MTT) reagent was added and incubated for 4 h at 37 °C. After removal of the media, 150 µL of DMSO was added to each well. The plates were kept in a plate shaker for 20 min for solubilization of the formazan crystals followed by measuring the absorbance at 560 nm in the ELISA plate reader (Thermo Scientific Multiskan EX, Langenselbold, Germany).

2.4. HPLC Analysis of Sialic Acid

Kelly cells were incubated with MGO for 48 h, followed by PBS washing and dissociation using PBS/EDTA buffer. Cells were pelleted by centrifugation and further processed for sialic acid analysis. Briefly cell pellets were homogenized and followed by mild acid hydrolysis of Sia with an equal volume of 2 M propionic acid at 80 °C, for 4 h. After hydrolysis the total lysate was cooled on ice for 10 min, followed by centrifugation at 16,000× *g* for 20 min at 4 °C. The supernatant was subjected to centrifugation using Amicon®Ultra-0.5 centrifugal filter devices at 16,000× *g* at 4 °C, for 30 min. The flow through was collected, freeze-dried and lyophilized overnight to remove the acid. The samples were dissolved in 100 µL of water to which an equal volume of 1,2-diamino-4,5-methylenedioxybenzene (DMB) was added and incubated in the dark at 50 °C, for 2.5 h. Samples were cooled briefly on ice followed by short centrifugation at 10,600× *g* for 1 min. Then, 20 µL of DMB labeled samples were injected into the HPLC column and eluted the sialic acids using isocratic solvent, acetonitrile:methanol:water at 8:6:86 ratios at a flow rate of 0.6 mL/min. Neu5Ac standard was labeled with DMB and used as a reference.

2.5. Immunoblotting

Kelly cells were seeded in the 6-well plates and cultured for 48 h with the respective concentrations of MGO. Fresh medium containing MGO was replaced every 24 h. After 48 h, cells were washed with PBS and dissociated with PBS/EDTA. Cells were washed once again with PBS and pelleted by centrifugation. Cell pellets were lysed and solubilized with RIPA buffer containing protease and phosphatase inhibitors. A total of 50 µg of protein was loaded on the 10% SDS PAGE gels and separated at 80 V for 3 h. Resolved proteins were transferred onto nitrocellulose membranes and blocked overnight with TBS containing 5% milk for 1 h at room temperature. Blots were incubated with anti-polySia (mab 735; 1:1000); anti-NCAM (mab 123C3; 1:1000); anti-RAGE (mab ab3611; 1:1000); anti-CML-AGE (mab CML56; 1:10,000); anti-tubulin (mab BT7R; 1:5000) overnight at 4 °C. Blots were washed 3 times with TBS-Tween (TBST) and incubated with HRP conjugated anti-mouse secondary antibody at 1:10,000 dilution in TBST containing 3% milk for 1 h at RT. Again, blots were further washed 3 times with TBST for 10 min each. PolySia bands were developed using chemiluminescence reagent (Immobilon Forte Western HRP substrate: Merck, Darmstadt, Germany) and detected by ChemiDoc XRS system (Bio-Rad Laboratories GmbH, München, Germany).

2.6. Adhesion Assay

E-plates were coated with fibronectin, laminin or vitronectin, respectively at 20 µg/mL concentration and incubated for 60 min at 37 °C. The wells were blocked with 0.1% BSA for 1 h at 37 °C. The wells were washed with PBS and 0.1×10^6 cells from MGO treatment were added to the respective E plate wells and allowed to settle the cells. Afterwards the E-plate was kept in the xCELLigence device (RTCA, OLS xCELLigence, Bremen, Germany) and the adhesion was quantified by monitoring the impedance for each 5 min for 4 h.

2.7. Migration Assay

The migration assay was performed in a real-time cell analyzer (RTCA, OLS xCELLigence, Bremen, Germany). Cells were treated with MGO for 48 h, washed twice with 10 mL of PBS and dislodged with PBS/EDTA buffer and washed once with PBS. Cells (0.5×10^6/well) were added to the upper chamber of the 16-well CIM plate (OLS xCELLigence, Bremen, Germany). The lower chamber was previously filled with 160 µL of complete medium. After the cells were settled in the upper plate the CIM plate was placed in the station. The impedance was measured for every 15 min up to 24 h for monitoring the migration of the cells.

2.8. Invasion Assay

Kelly cells were treated with MGO for 48 h, washed twice with PBS and dislodged with PBS/EDTA buffer and washed once with serum-free medium. Cells were (0.5×10^6/well) added to the upper chamber of the 16-well CIM-plate previously coated ECM gel (Engelbrecht-Holm-Swarm murine sarcoma) at 1:50 dilution. The lower chamber had been previously filled with 160 µL of complete medium. After the cells were settled in the upper plate (kept in the cell culture hood for 30 min), the CIM-plate was placed in the station (RTCA, OLS xCELLigence, Bremen, Germany). Invasion of the cells was monitored, by measuring the impedance for every 15 min up to 24 h.

3. Results

3.1. Glycation of Neuroblastoma Cells

In the first series of experiments, we analyzed the effect of MGO on the viability of neuroblastoma cells. We decided to use Kelly cells, since these cells are known to express both NCAM and polysialic acids [7]. We therefore investigated whether glycation was affecting the metabolic activity of the Kelly cells. An MTT assay was performed after growing Kelly cells in the absence or presence MGO for 48 h. Various concentrations up to 100 µM MGO did not significantly alter the metabolic activity of Kelly cells (Figure 1). However, at 250 µM MGO, the metabolic activity was reduced by about 50%, whereas treatment of Kelly cells with 1 mM MGO for 48 h was toxic for the cells (Figure 1). Therefore, we decided to use 100 µM MGO for all further experiments—a concentration that can also be reached in the cerebrospinal fluid of diabetic patients. Next, we analyzed whether treatment of Kelly cells leads to glycation or AGE formation. For this, Kelly cells were grown in the presence of 100 µM MGO for 48 h and analyzed by Western blot using a specific AGE-antibody. The blot indicated that treatment of Kelly cells with 100 µM MGO leads to increased AGE signals on the entire membrane (Figure 2A) Quantification reveals a 5-fold increase of the overall signal intensity (Figure 2B).

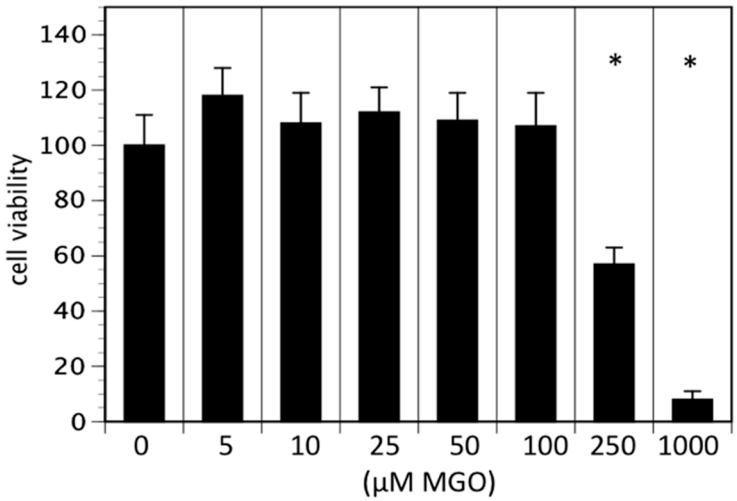

Figure 1. Cell viability in the presence of MGO. Kelly cells were grown in the absence or presence of various MGO concentrations for 48 h and an 3-[4,5-Dimethylthiazol-2-yl]-2,5 diphenyl tetrazolium bromide (MTT) assay was performed. Cells without MGO treatment were normalized to 100%. Bars represent means of +/− SEM of 3 independent experiments (* $p < 0.05$).

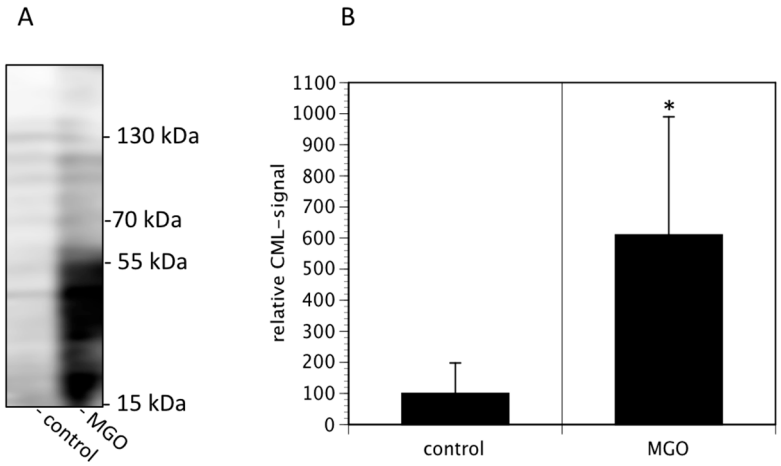

Figure 2. MGO treatment of Kelly cells leads to increased glycation. Kelly cells were grown in the absence or presence of 100 µM MGO for 48 h. Cells were washed and proteins were isolated, separated by SDS-PAGE and stained using an anti-CML-AGE antibody (**A**). The entire membrane is shown. (**B**) Bands of 3 independent experiments were scanned and the intensities analyzed by Image J. Bars represent means +/− SEM of 3 independent experiments (* $p < 0.05$).

3.2. Glycation Leads to Increased Sialylation and Increased Expression of Polysialic Acids

Since cell surface sialylation and polysialylation are prognostic markers of several tumors [21], we then quantified membrane bound sialic acids and polysialic acids of Kelly cells cultured in the absence or presence of 100 µM MGO. We found that MGO treatment increased the total sialic acids on cell surface proteins by nearly 50% (Figure 3A). Analysis of polysialic acid expression revealed a dramatic increase in polysialylation after MGO treatment (Figure 3B, topmost bands). This was not due to increased NCAM expression, since the NCAM expression was not increased after MGO treatment (Figure 3B). For control reasons, we also determined the RAGE and tubulin expression, which are also not altered (Figure 3B).

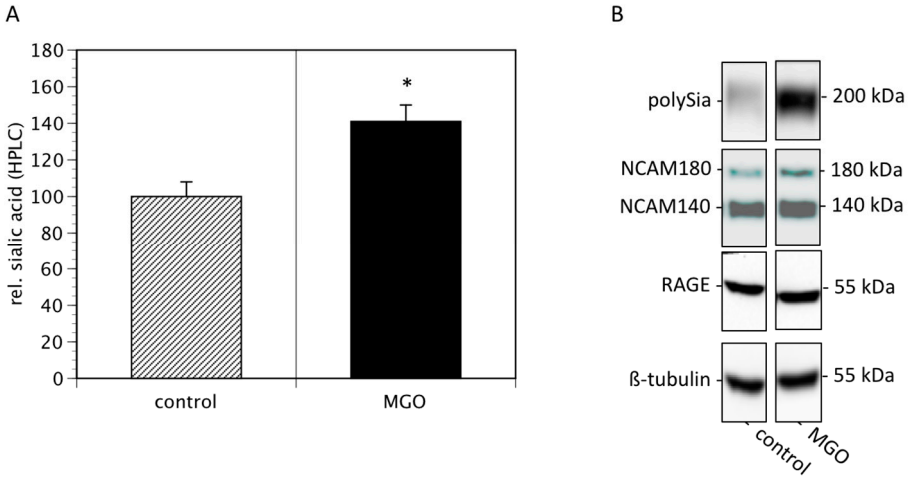

Figure 3. MGO treatment of Kelly cells leads to increased (poly)sialylation. Kelly cells were grown in the absence or presence of 100 µM MGO for 48 h. Cells were washed and proteins were isolated. (**A**) Proteins were dried, sialic acids were cleaved, labeled with DMB and analyzed by HPLC. Bars represent means +/− SEM of 3 independent experiments (* $p < 0.05$). (**B**). Proteins were separated by SDS-PAGE and transferred to a nitrocellulose membrane. Polysialylation was detected using monoclonal 735 antibody. NCAM expression was analyzed using the monoclonal 123C3 antibody. For control, RAGE and ß-tubulin staining was used.

3.3. MGO-Induced Polysialylation Interferes with Adhesion

Because polysialylation is often involved in the regulation of adhesion, we performed real time cell adhesion assays with Kelly cells on several substrates cultured in the absence or presence of MGO. First, we compared several substrates and found, that Kelly cells prefer laminin as substrate over vitronectin and fibronectin (Figure 4A). We then compared adhesion of Kelly cells to all three substrates grown presence of 100 µM MGO for 48 h. We measured a reduction of adhesion of about 30% on all tested substrates (laminin, vitronectin or fibronectin) (Figure 4B). Please note that we normalized all the data for comparison.

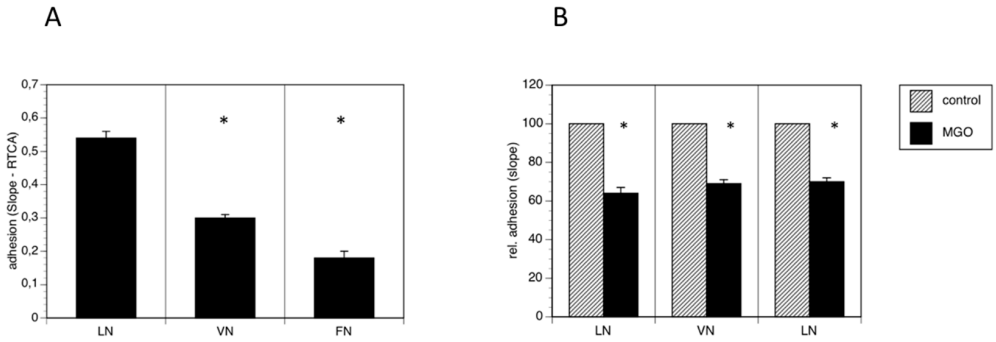

Figure 4. MGO-induced polysialylation interferes with adhesion. A total of 0.1×10^6 Kelly cells were allowed bind to E-plates coated with laminin (LN), vitronectin (VN) or fibronectin (FN). (**A**) Adhesion was continuously quantified by RTCA measurement. Bars represent means +/− SEM of 3 independent experiments (* $p < 0.05$). (**B**) Kelly cells were grown in the absence (control) or presence of 100 µM MGO for 48 h prior to the adhesion assay. Adhesion in the absence of MGO was set to 100% (control) and in the presence of MGO in percent of the control. Bars represent means +/− SEM of 3 independent experiments (* $p < 0.05$).

3.4. MGO-Induced Polysialylation Promotes Migration and Invasion

Reduced cell adhesion correlates with cell migration or invasion into tissue and increased invasion of tumor cells often promotes metastasis. We therefore analyzed cell migration and invasion using the real time cell analyzer. Migration was measured using serum as chemoattractant, whereas invasion was quantified using EHS extra cellular matrix gels. When cells were grown in the presence of MGO, migration to the chemoattractant was dramatically increased (Figure 5). A similar effect was observed when the cellular invasion into EHS extra cellular matrix gels was analyzed (Figure 5).

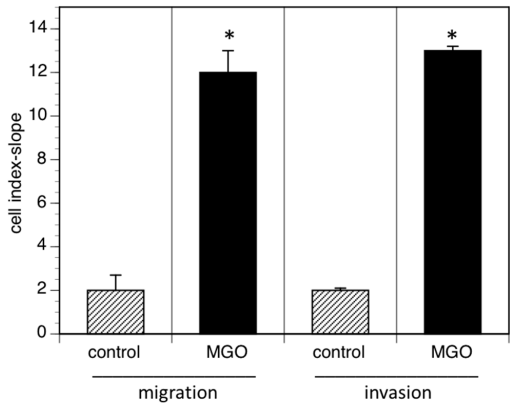

Figure 5. MGO-induced polysialylation promotes migration and invasion. A total of 0.5×10^6 Kelly cells were grown in the absence (control) or presence of 100 µM MGO for 48 h prior to the migration or invasion assay. Migration/invasion in the absence of MGO was set to 100% (control) and in the presence of MGO in percent of the control. Bars represent means +/− SEM of 3 independent experiments (* $p < 0.05$).

4. Discussion

Methylglyoxal (MGO) is a regular byproduct of glycolysis [16], which is the major energy-generating pathway in the brain, since fatty acids cannot path the blood brain barrier [22,23]. Tumor cells are also known to use glucose as their primary energy source [14]. Therefore, many tumors such as neuroblastomas produce high amounts of MGO. MGO is a dicarbonyl-compound, and is known to be, in comparison to glucose, a very strong glycating agent [17].

In this study, we analyzed the effect of MGO on neuroblastoma cells and could demonstrate that neuroblastoma exhibited characteristics consistent with more aggressive disease, e.g., less adhesive and more invasive after glycation with MGO. One possible explanation for the reduced adhesion and enhanced migration could be the upregulation of polysialic acids after MGO treatment. Polysialic acid is nearly exclusively expressed on the neural cell adhesion molecule NCAM. Two polysialyltransferase (ST8Sia2 and ST8Sia4) are capable to polysialylate NCAM. Since we could demonstrate that NCAM expression is not altered after glycation e.g., treatment with MGO, we speculate that the increased expression of polysialic acid may be due to increased polysialyltransferase expression.

In this context it would be also important to know, how MGO or glycation alter the expression of polysialyltransferases. Although recent studies demonstrate that MGO alters gene expression profiles [24], the mechanism how MGO interfere with transcription is still unknown. It is conceivable that glycation of transcription factors is the major cause for this observation. In addition, it is also possible that polysialylation is only indirectly responsible for the reduced adhesion. The major adhesion molecules binding to ECM proteins such as laminin, vitronectin or fibronectin are integrins. It has been shown that glycation of ECM proteins interferes with integrin function [25,26], however whether the glycation of integrins itself interfere with its function is not known. However, not only adhesion, but also migration is affected by polysialylation. In this context, Li et al. (2011) proposed that polysialylation could act via an FGF-receptor dependent mechanism [27]. Further experiments including enzymatic removal of polysialic acid by Endo N after MGO treatment are necessary to finally answer these questions.

MGO is generated under physiological conditions in all cells including tumor cells. In our experiments we added additional MGO to the cell culture medium. The question arises: How physiological is this procedure? To answer this question, one has to keep in mind that under physiological conditions the oxygen concentrations are much lower than cell culture conditions, and therefore, the glycolysis rate is probably much higher than cell cultures. Therefore, it is well accepted to increase the MGO concentrations in cell culture to mimic the physiological conditions, in which such concentrations are reached.

Glycation of cells results in upregulation of RAGE and thereby stimulating inflammatory cascades in a positive feedback loop [28,29]. In this study we present data that RAGE expression is not changed after treatment of Kelly cells with 100 µM MGO. Therefore, we conclude that RAGE is not directly involved in neuroblastoma progression. However, there are studies suggesting an involvement of RAGE in tumor progression [30–32]. We have also performed FACS and Western blot experiments showing increased RAGE expression after MGO treatment (data not shown). However, we observed an increase in RAGE expression only after treatment with more than 300 µM MGO and these concentrations interfere with the viability of Kelly cells (see Figure 1).

Further arguments that glycation may promote tumor growth arises from data from diabetic patients. It is well known that both patients with diabetes type I and II have significant higher risks of developing cancer and have poorer prognosis [33,34]. As already mentioned, diabetes patients also have increased levels of MGO. Therefore, one could argue that at least the elevated levels of MGO are partially responsible on the molecular level for the increased tumor risk of diabetic patients.

Recently, we could demonstrate that glycation of immune cells has a negative impact on their function [35,36]. For example, NK-cells are less active to kill tumor cells after being glycated. This opens a further line of evidence that increase MGO levels due to diabetes or increased blood glucose promotes tumor progression.

In summary, we propose that glycation seems to be a negative event for tumor patients and increased production of MGO during tumor progression can alter its properties. Unfortunately, there is no treatment for "de-glycation" available at the moment there is a need to develop anti-glycation strategies in the future.

5. Conclusions

Methylglyoxal (MGO) is regular byproduct of glycolysis and occurs in high concentration in the brain. MGO is a dicarbonyl and highly reactive. It glycates proteins and advanced glycation end products are formed. In this study, we could demonstrate that glycation had several severe effects on neuroblastoma cells. It leads to increased expression of polysialic acid, a negative prognostic marker and interferes with adhesion and migration of neuroblastoma cells.

Author Contributions: Conceptualization, V.S.G., R.H. and K.B.; methodology, M.S. and M.N.; validation, V.S.G.; investigation, M.S., M.N. and F.S.; writing—original draft preparation, R.H.; writing—review and editing, R.H.; supervision, V.S.G.; funding acquisition, R.H. All authors have read and agreed to the published version of the manuscript.

Funding: This research was funded by the Deutsche Forschungsgemeinschaft RTG 2155 (ProMoAge) and the Roland and Elfriede Schauer Foundation (T 0391-32.368).

Acknowledgments: We thank Rita Gerardy-Schahn (Hannover, Germany) for the 735 anti-polysialic acid antibody.

Conflicts of Interest: The authors declare no conflict of interest.

References

1. Cohn, S.L.; Pearson, A.D.; London, W.B.; Monclair, T.; Ambros, P.; Brodeur, G.M.; Faldum, A.; Hero, B.; Iehara, T.; Machin, D.; et al. The International Neuroblastoma Risk Group (INRG) Classification System: An INRG Task Force Report. *J. Clin. Oncol.* **2009**, *27*, 289–297. [CrossRef] [PubMed]
2. Brodeur, G.; Seeger, R.; Schwab, M.; Varmus, H.; Bishop, J. Amplification of N-myc in untreated human neuroblastomas correlates with advanced disease stage. *Science* **1984**, *224*, 1121–1124. [CrossRef] [PubMed]
3. Mossé, Y.P.; Laudenslager, M.; Longo, L.; Cole, K.A.; Wood, A.; Attiyeh, E.F.; Laquaglia, M.J.; Sennett, R.; Lynch, J.E.; Perri, P.; et al. Identification of ALK as a major familial neuroblastoma predisposition gene. *Nature* **2008**, *455*, 930–935. [CrossRef] [PubMed]
4. Hero, B.; Simon, T.; Spitz, R.; Ernestus, K.; Gnekow, A.K.; Scheel-Walter, H.-G.; Schwabe, D.; Schilling, F.H.; Benz-Bohm, G.; Berthold, F. Localized Infant Neuroblastomas Often Show Spontaneous Regression: Results of the Prospective Trials NB95-S and NB97. *J. Clin. Oncol.* **2008**, *26*, 1504–1510. [CrossRef]
5. De Bernardi, B.; Gerrard, M.; Boni, L.; Rubie, H.; Cañete, A.; Di Cataldo, A.; Castel, V.; De Lacerda, A.F.; Ladenstein, R.; Ruud, E.; et al. Excellent Outcome with Reduced Treatment for Infants with Disseminated Neuroblastoma without MYCN Gene Amplification. *J. Clin. Oncol.* **2009**, *27*, 1034–1040. [CrossRef]
6. Maris, J.M. Recent advances in neuroblastoma. *N. Engl. J. Med.* **2010**, *362*, 2202–2211. [CrossRef]
7. Seifert, A.; Glanz, D.; Glaubitz, N.; Horstkorte, R.; Bork, K. Polysialylation of the neural cell adhesion molecule: Interfering with polysialylation and migration in neuroblastoma cells. *Arch. Biochem. Biophys.* **2012**, *524*, 56–63. [CrossRef]
8. Finne, J.; Finne, U.; Deagostini-Bazin, H.; Goridis, C. Occurrence of α2–8 linked polysialosyl units in a neural cell adhesion molecule. *Biochem. Biophys. Res. Commun.* **1983**, *112*, 482–487. [CrossRef]
9. Glüer, S.; Zense, M.; Radtke, E.; von Schweinitz, D. Polysialylated neural cell adhesion molecule in childhood ganglioneuroma and neuroblastoma of different histological grade and clinical stage. *Langenbeck's Arch. Surg.* **1998**, *383*, 340–344. [CrossRef]
10. Moolenaar, C.E.; Muller, E.J.; Schol, D.J.; Figdor, C.G.; Bock, E.; Bitter-Suermann, D.; Michalides, R.J. Expression of neural cell adhesion molecule-related sialoglycoprotein in small cell lung cancer and neuroblastoma cell lines H69 and CHP-212. *Cancer Res.* **1990**, *50*, 1102–1106.
11. Amoureux, M.-C.; Coulibaly, B.; Chinot, O.; Loundou, A.; Metellus, P.; Rougon, G.; Figarella-Branger, D. Polysialic Acid Neural Cell Adhesion Molecule (PSA-NCAM) is an adverse prognosis factor in glioblastoma, and regulates olig2 expression in glioma cell lines. *BMC Cancer* **2010**, *10*, 91. [CrossRef]

12. Autelitano, F.; Loyaux, D.; Roudières, S.; Deon, C.; Guette, F.; Fabre, P.; Ping, Q.; Wang, S.; Auvergne, R.; Badarinarayana, V.; et al. Identification of Novel Tumor-Associated Cell Surface Sialoglycoproteins in Human Glioblastoma Tumors Using Quantitative Proteomics. *PLOS ONE* **2014**, *9*, e110316. [CrossRef]
13. Petushkova, N.A.; Zgoda, V.G.; Pyatnitskiy, M.A.; Larina, O.V.; Teryaeva, N.B.; Potapov, A.A.; Lisitsa, A.V. Post-translational modifications of FDA-approved plasma biomarkers in glioblastoma samples. *PLOS ONE* **2017**, *12*, e0177427. [CrossRef]
14. Fang, E.; Wang, X.; Wang, J.; Hu, A.; Song, H.; Yang, F.; Li, D.; Xiao, W.; Chen, Y.; Guo, Y.; et al. Therapeutic targeting of YY1/MZF1 axis by MZF1-uPEP inhibits aerobic glycolysis and neuroblastoma progression. *Theranostics* **2020**, *10*, 1555–1571. [CrossRef] [PubMed]
15. Thornalley, P.J. Dicarbonyl Intermediates in the Maillard Reaction. *Ann. N. Y. Acad. Sci.* **2005**, *1043*, 111–117. [CrossRef] [PubMed]
16. Angeloni, C.; Zambonin, L.; Hrelia, S. Role of Methylglyoxal in Alzheimer's Disease. *BioMed Res. Int.* **2014**, *2014*, 1–12. [CrossRef] [PubMed]
17. Kalapos, M.P. Methylglyoxal and Glucose Metabolism: A Historical Perspective and Future Avenues for Research. *Drug Metab. Drug Interact.* **2008**, *23*, 69–91. [CrossRef] [PubMed]
18. Brownlee, M.M. Advanced Protein Glycosylation in Diabetes and Aging. *Annu. Rev. Med.* **1995**, *46*, 223–234. [CrossRef] [PubMed]
19. Thornalley, P.J. Pharmacology of methylglyoxal: Formation, modification of proteins and nucleic acids, and enzymatic detoxification—A role in pathogenesis and antiproliferative chemotherapy. *Gen. Pharmacol. Vasc. Syst.* **1996**, *27*, 565–573. [CrossRef]
20. Kuhla, B.; Lüth, H.-J.; Haferburg, D.; Boeck, K.; Arendt, T.; Münch, G. Methylglyoxal, Glyoxal, and Their Detoxification in Alzheimer's Disease. *Ann. N. Y. Acad. Sci.* **2005**, *1043*, 211–216. [CrossRef]
21. Elkashef, S.M.; Allison, S.J.; Sadiq, M.; Basheer, H.A.; Morais, G.R.; Loadman, P.M.; Pors, K.; Falconer, R. Polysialic acid sustains cancer cell survival and migratory capacity in a hypoxic environment. *Sci. Rep.* **2016**, *6*, 33026. [CrossRef] [PubMed]
22. Schönfeld, P.; Reiser, G. Why does brain metabolism not favor burning of fatty acids to provide energy? Reflections on disadvantages of the use of free fatty acids as fuel for brain. *Br. J. Pharmacol.* **2013**, *33*, 1493–1499.
23. Hussain, M.; Bork, K.; Gnanapragassam, V.S.; Bennmann, D.; Jacobs, K.; Navarette-Santos, A.; Hofmann, B.; Simm, A.; Danker, K.; Horstkorte, R. Novel insights in the dysfunction of human blood-brain barrier after glycation. *Mech. Ageing Dev.* **2016**, *155*, 48–54. [CrossRef] [PubMed]
24. Braun, J.D.; Pastene, D.O.; Breedijk, A.; Rodriguez, A.; Hofmann, B.B.; Sticht, C.; Von Ochsenstein, E.; Allgayer, H.; Born, J.V.D.; Bakker, S.; et al. Methylglyoxal down-regulates the expression of cell cycle associated genes and activates the p53 pathway in human umbilical vein endothelial cells. *Sci. Rep.* **2019**, *9*, 1152. [CrossRef] [PubMed]
25. Talior-Volodarsky, I.; Arora, P.D.; Wang, Y.; Zeltz, C.; Connelly, K.; Gullberg, D.; McCulloch, C. Glycated Collagen Induces α11 Integrin Expression Through TGF-β2 and Smad3. *J. Cell. Physiol.* **2014**, *230*, 327–336. [CrossRef]
26. Bennmann, D.; Horstkorte, R.; Hofmann, B.; Jacobs, K.; Navarrete-Santos, A.; Simm, A.; Bork, K.; Gnanapragassam, V. Advanced Glycation Endproducts Interfere with Adhesion and Neurite Outgrowth. *PLOS ONE* **2014**, *9*, e112115. [CrossRef]
27. Li, J.; Dai, G.; Cheng, Y.-B.; Qi, X.; Geng, M. Polysialylation promotes neural cell adhesion molecule-mediated cell migration in a fibroblast growth factor receptor-dependent manner, but independent of adhesion capability. *Glycobiology* **2011**, *21*, 1010–1018. [CrossRef]
28. Gkogkolou, P.; Böhm, M. Advanced glycation end products: Key players in skin aging? *Dermato-Endocrinology* **2012**, *4*, 259–270. [CrossRef]
29. Schalkwijk, C.G.; Miyata, T. Early- and advanced non-enzymatic glycation in diabetic vascular complications: The search for therapeutics. *Amino Acids* **2010**, *42*, 1193–1204. [CrossRef]
30. Medapati, M.R.; Dahlmann, M.; Ghavami, S.; Pathak, K.A.; Lucman, L.; Klonisch, T.; Hoang-Vu, C.; Stein, U.; Hombach-Klonisch, S. RAGE Mediates the Pro-Migratory Response of Extracellular S100A4 in Human Thyroid Cancer Cells. *Thyroid* **2015**, *25*, 514–527. [CrossRef]
31. Takino, J.-I.; Yamagishi, S.-I.; Takeuchi, M. Cancer Malignancy Is Enhanced by Glyceraldehyde-Derived Advanced Glycation End-Products. *J. Oncol.* **2010**, *2010*, 1–8. [CrossRef] [PubMed]

32. Sharaf, H.; Matou-Nasri, S.; Wang, Q.; Rabhan, Z.; Al-Eidi, H.; Al Abdulrahman, A.; Ahmed, N. Advanced glycation endproducts increase proliferation, migration and invasion of the breast cancer cell line MDA-MB-231. *Biochim. Biophys. Acta* **2015**, *1852*, 429–441. [CrossRef]
33. Suh, S.; Kim, K.-W. Diabetes and Cancer: Is Diabetes Causally Related to Cancer? *Diabetes Metab. J.* **2011**, *35*, 193–198. [CrossRef]
34. Habib, S.L.; Rojna, M. Diabetes and risk of cancer. *ISRN Oncol.* **2013**, *2013*, 583786. [CrossRef] [PubMed]
35. Bezold, V.; Rosenstock, P.; Scheffler, J.; Geyer, H.; Horstkorte, R.; Bork, K. Glycation of macrophages induces expression of pro-inflammatory cytokines and reduces phagocytic efficiency. *Aging* **2019**, *11*, 5258–5275. [CrossRef] [PubMed]
36. Rosenstock, P.; Bezold, V.; Bork, K.; Scheffler, J.; Horstkorte, R. Glycation interferes with natural killer cell function. *Mech. Ageing Dev.* **2019**, *178*, 64–71. [CrossRef]

Philipp Selke, Philip Rosenstock, Kaya Bork, Christian Strauss, Rüdiger Horstkorte* and Maximilian Scheer

Glycation of benign meningioma cells leads to increased invasion

https://doi.org/10.1515/hsz-2020-0376
Received November 25, 2020; accepted February 26, 2021; published online March 17, 2021

Abstract: Meningiomas are the most common non-malignant intracranial tumors. Like most tumors, meningiomas prefer anaerobic glycolysis for energy production (Warburg effect). This leads to an increased synthesis of the metabolite methylglyoxal (MGO). This metabolite is known to react with amino groups of proteins. This reaction is called glycation, thereby building advanced glycation endproducts (AGEs). In this study, we investigated the influence of glycation on two meningioma cell lines, representing the WHO grade I (BEN-MEN-1) and the WHO grade III (IOMM-Lee). Increasing MGO concentrations led to the formation of AGEs and decreased growth in both cell lines. When analyzing the influence of glycation on adhesion, chemotaxis and invasion, we could show that the glycation of meningioma cells resulted in increased invasive potential of the benign meningioma cell line, whereas the invasive potential of the malignant cell line was reduced. In addition, glycation increased the E-cadherin- and decreased the N-cadherin-expression in BEN-MEN-1 cells, but did not affect the cadherin-expression in IOMM-Lee cells.

Keywords: glycation; intracranial tumor; invasion; meningioma; methylglyoxal; MGO.

***Corresponding author: Rüdiger Horstkorte**, Medical Faculty, Institute for Physiological Chemistry, Martin-Luther-University Halle-Wittenberg, D-06114 Halle/Saale, Germany,
E-mail: ruediger.horstkorte@medizin.uni-halle.de
Philipp Selke, Philip Rosenstock and Kaya Bork, Medical Faculty, Institute for Physiological Chemistry, Martin-Luther-University Halle-Wittenberg, D-06114 Halle/Saale, Germany. https://orcid.org/0000-0001-7862-2713 (P. Selke)
Christian Strauss, Department for Neurosurgery, University Hospital Halle, D-06120 Halle/Saale, Germany
Maximilian Scheer, Medical Faculty, Institute for Physiological Chemistry, Martin-Luther-University Halle-Wittenberg, D-06114 Halle/Saale, Germany; and Department for Neurosurgery, University Hospital Halle, D-06120 Halle/Saale, Germany. https://orcid.org/0000-0003-3149-0797

Introduction

Meningioma represents the most common non-malignant intracranial tumor (Goldbrunner et al. 2016; Holleczek et al. 2019; Ostrom et al. 2018, 2019).

Like many tumors, meningiomas need large amounts of glucose as primary energy source, because they mainly metabolize glucose to lactate during anaerobic glycolysis (Warburg effect) (Bharadwaj et al. 2015), which generates only low amounts of adenosine triphosphate (ATP). This changed (anaerobic) energy metabolism is one of the "hallmarks of cancer" (Gill et al. 2016). In line with this, there is a correlation between serum glucose levels and meningioma risk (Edlinger et al. 2012; Michaud et al. 2011; Niedermaier et al. 2015; Wiedmann et al. 2013). However, there are many inconsistent data suggesting a positive (Schneider et al. 2005; Schwartzbaum et al. 2005) or inverse (Bernardo et al. 2016) relationship between diabetes and serum glucose levels and the risk of meningioma. Patients with type 2 diabetes have a decreased survival after surgical resection of a WHO grade I meningioma (Nayeri et al. 2016).

Methylglyoxal (MGO) has been discussed as a possible linker between diabetes and serum glucose levels and cancer (Bellier et al. 2019), since diabetic patients and aged individuals have elevated MGO concentrations (Rabbani and Thornalley 2015). Some authors even propose MGO as a tumor promoting agent (Antognelli et al. 2019; Bellahcène et al. 2018). Approximately 0.1–0.4% of the glucose is transformed to MGO during glycolysis as a regular side product from dihydroxyacetone phosphate or glyceraldehyde-3-phosphate (Allaman et al. 2015). Importantly, MGO is 20,000 times more reactive than glucose and reacts mainly with proteins (through arginine, lysine, and cysteine residues) or to a lower degree also with DNA or lipids, thereby forming advanced glycation endproducts (AGEs) (Falone et al. 2012; Kalapos 2008; Schalkwijk 2015). This non-enzymatic reaction between the carbonyl groups of dicarbonyls (like MGO or glyoxal) or sugars (like glucose or fructose) and the amino groups of proteins is called glycation (Ahmed 2005; Rabbani and Thornalley 2008). Electrophilic carbonyl groups of glucose or other reactive sugars react with free amino groups of amino acids and forming a non-stable Schiff base. This reaction is called

classical Maillard reaction. Further rearrangement leads to formation of a more stable ketosamine (Amadori product). The formation of Schiff bases and Amadori products are reversible reactions. In later reactions, they form irreversible adducts or protein crosslinks (Ahmed 2005; Paul and Bailey 1996). The process of producing AGEs affects all proteins including cell adhesion molecules or receptors and proteins of the extracellular matrix (Pedchenko et al. 2005; Rabbani and Thornalley 2012).

It was previously suggested that application of MGO lead to altered adhesion and migration (Antognelli et al. 2019; Loarca et al. 2013; Nokin et al. 2019).

Cadherins represent cell adhesion molecules that mediate Ca^{2+}-dependent homophilic interaction with cadherin molecules on the surface of neighboring cells. The cytoplasmic domain binds downstream to members of the catenin protein family and regulates functions like cell–cell interactions (Harrison et al. 2011; Mège and Ishiyama 2017). Cadherins also play an important role in the epithelial–mesenchymal-transition (EMT). The EMT describes the change of epithelial markers like E-cadherin to mesenchymal markers like N-cadherin or Vimentin and can promote migration of transformed cells (Gloushankova et al. 2017; Mendonsa et al. 2018). Decreasing E-cadherin expression is mostly associated with weakening of cell–cell adhesion in tumor progression (Rodriguez et al. 2012). Expression of N-cadherin is closely related to tumor invasion and metastasis (Cao et al. 2019).

In the present study, we analyzed differences between benign and malignant meningioma cell lines before and after glycation using MGO. We could show that physiological MGO concentrations had no effect on cell morphology, metabolic activity, chemotaxis and adhesion. However, the invasiveness of the benign meningioma cells was increased whereas the invasiveness of the malignant meningioma cells was reduced in the presence of MGO, which means that glycation resulted in a switch of benign tumor to a more aggressive tumor cell. Furthermore, glycation led to increased E-cadherin and reduced N-cadherin-expression in the benign meningioma cells.

Results

MGO-treatment of meningioma cells interferes with their morphology

First of all, we analyzed whether treatment with MGO affects meningioma cells by comparing their morphology. Therefore, we cultured both cell lines in absence or presence of MGO for 24 h. Representative micrographs for the benign BEN-MEN-1 cells are shown in Figure 1A and for the malignant IOMM-Lee cells in Figure 1B. When cells were cultured in the presence of 0.1 or 0.3 mM MGO, we could not observe any changes in the morphology compared with untreated control cells. BEN-MEN-1 cells had a typical meningothelial shape and grew in monolayers. IOMM-Lee cells were more epithelial-like and grew as multilayers. After treatment with 0.6 mM MGO, we observed less cells and morphological differences compared with the controls. When culturing cells in presence of 1.0 mM MGO, cells became round and we observed less cells and less spreading in both cultures.

High concentrations of MGO interfere with the cell viability of meningioma cells

Since morphology was changed in presence of 0.6 mM MGO or more, we examined the cell viability of both meningioma cell lines, after culturing in absence or presence of different

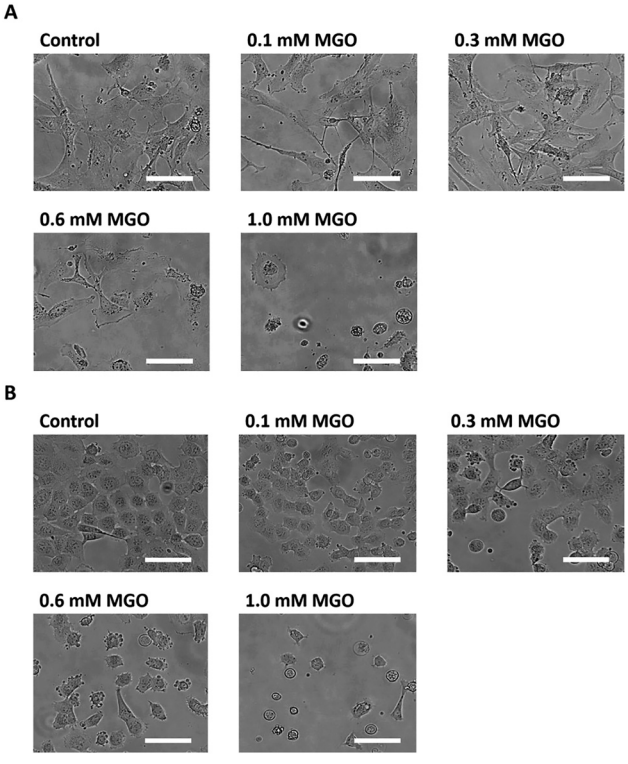

Figure 1: Micrographs of meningioma cells after 24 h MGO-treatment.
Cells (A = BEN-MEN-1 and B = IOMM-Lee) were cultured in the absence (control) or presence of different concentrations (0.1, 0.3, 0.6 and 1.0 mM) of MGO. Scale bar in white: 50 µm.

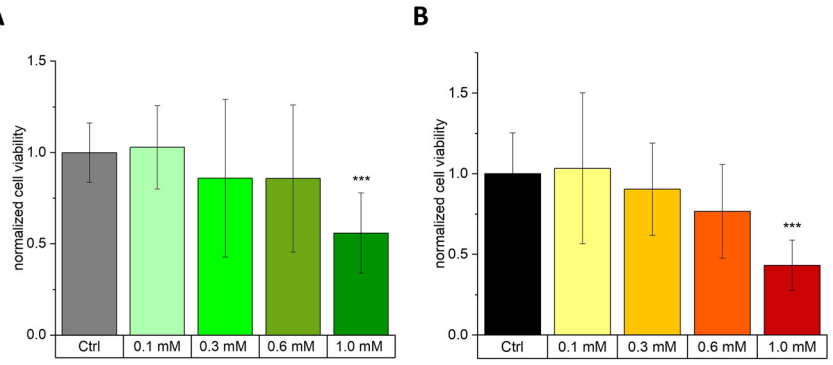

Figure 2: Cell viability of meningioma cell lines after 24 h MGO-treatment.
Cell viability was analyzed using an MTT-assay for BEN-MEN-1 (A) and IOMM–Lee cells (B). Cells were seeded in absence (Ctrl) or presence of MGO (0.1, 0.3, 0.6 and 1.0 mM). Both cell lines showed a decreasing metabolic activity with increasing concentration of MGO. Statistical analysis was performed using *t*-test and error bars represent SD ($n = 7$; ***$p < 0.005$; (BEN-MEN-1: $p = 0.0027$; IOMM-Lee: $p = 0.00045$)).

concentrations of MGO (Figure 2). We measured decreased cell viability after incubation with high concentrations of MGO. For the benign cell line, we could not show significant differences at MGO concentrations up to 0.6 mM. Only at 1.0 mM MGO, cell viability was significantly reduced compared with untreated controls (BEN-MEN-1; Figure 2A). For the malignant cell line (IOMM-Lee; Figure 2B), we observed similar effects. Only at 1.0 mM MGO, there was a significant difference compared with control, which confirmed our microscopic observations presented in Figure 1A and B. Furthermore, we analyzed caspase 3 expression by Western blot analysis. Caspase 3 was only expressed in cultures treated with 1.0 mM MGO and not in cultures treated with 0.1, 0.3 or 0.6 mM MGO (data not shown), indicating that only very high concentrations of MGO induce apoptosis in our experiments.

Increased glycation with increasing concentrations of MGO

Next, we wanted to examine whether treatment of meningioma cells with MGO led to glycation. For this, we cultured both meningioma cell lines in the presence (0.1, 0.3, 0.6 and 1.0 mM) or absence of MGO for 24 h. To verify the effect of the treatment, we performed immunoblotting using anti-AGE antibodies. We could show that increasing MGO concentrations led to increasing AGE-signals, which is shown in Figure 3A and C for BEN-MEN-1 and in Figure 3B and D for IOMM-Lee cells. Glycation is quantified in Figure 3B and D. We found significant increase of glycation already at concentrations of 0.3 mM MGO (Figure 3E).

MGO has no effect on the adhesion of meningioma cells to ECM components

We then analyzed the effect of glycation on adhesion of the two meningioma cell lines. Since 0.3 mM MGO had no effect on the cell viability of both meningioma cell lines and led to significant formation of AGEs, we decided to use 0.3 mM MGO for all further experiments. To quantify adhesion, we cultured both meningioma cell lines in E-plates. Cells were seeded in absence or presence of MGO on two different matrices (collagen IV or fibronectin) which were in addition preincubated with or without MGO. Figure 4A and B shows the adhesion of both meningioma cell lines on the two different matrices. No significant difference in adhesion could be detected in both cell lines after MGO treatment. Please note, that we observed that BEN-MEN-1 cells adhere much better on both substrates compared to IOMM-Lee cells and that both cancer cells prefer fibronectin to collagen IV as substrate.

MGO has no effect on chemotaxis of meningioma cells

Since MGO leads to glycation of almost all cellular proteins, we next wanted to analyze whether cell surface receptors are in general inactivated after glycation. We therefore investigated the impact of glycation on the chemotaxis, which is mediated by cell surface receptors. We cultured both meningioma cell lines in CIM-plates for 24 h. Cells were cultured again in the absence or presence of 0.3 mM MGO. Figure 5A and B shows the chemotactic cell migration after

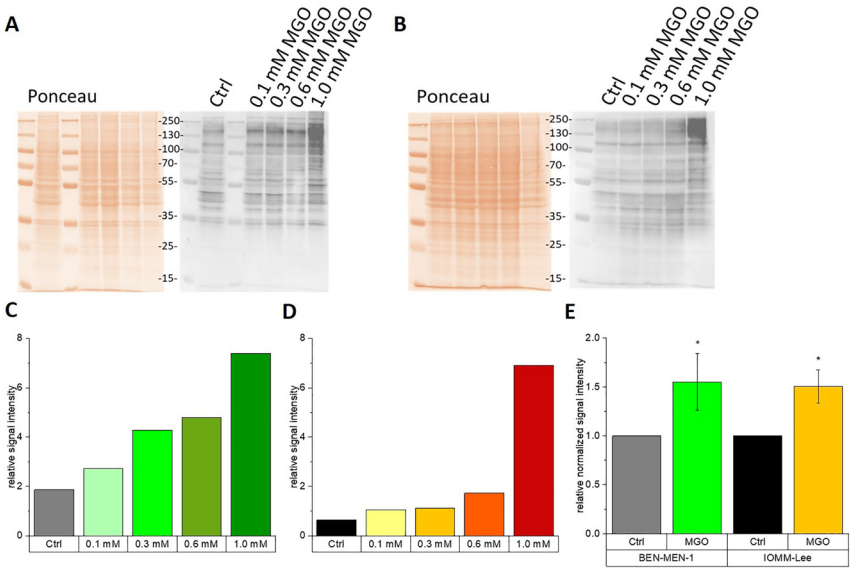

Figure 3: Glycation of meningioma cells.
(A) Ponceau S staining of the total proteins (left side) and immunoblot (right side) of BEN-MEN-1 with different MGO concentrations. Controls (Ctrl) were cells without MGO treatment. We used an anti-AGE antibody to verify cellular glycation. (B) Ponceau S staining of the total proteins (left side) and immunoblot (right side) of IOMM-Lee cells with different MGO concentrations. Controls (Ctrl) were cells without MGO treatment. We used an anti-AGE antibody to verify cellular glycation (C) Representative quantification of the blot of BEN-MEN-1 cells shown in panel (A). (D) Representative quantification of the blot of IOMM-Lee cells shown in panel (B). (E) Quantification of glycation of BEN-MEN-1 and IOMM-Lee after treatment with 0.3 mM MGO. Non-glycated cells were used as controls (Ctrl). Statistical analysis was performed using *t*-test and error bars represent SD ($n = 4$; (BEN-MEN-1: $p = 0.0452$; IOMM-Lee: $p = 0.0143$)).

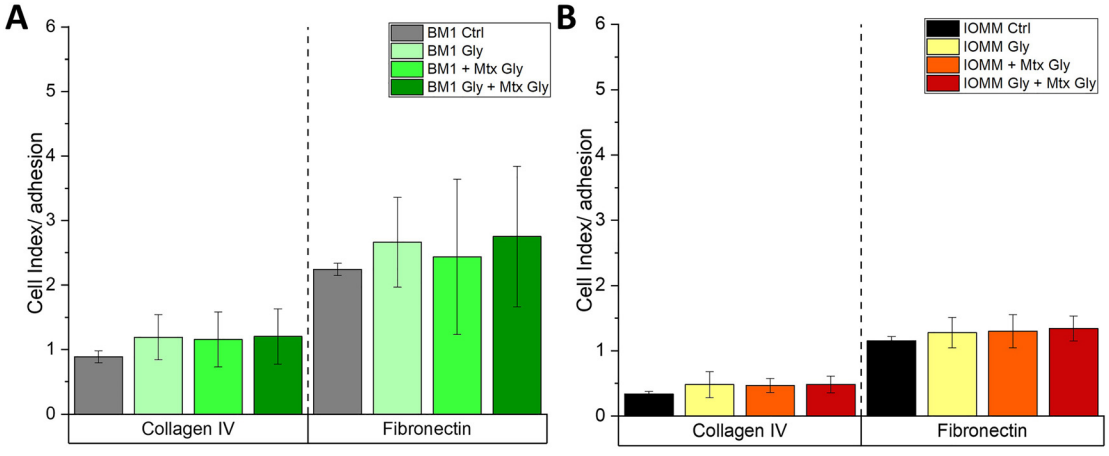

Figure 4: Adhesion of meningioma cells with MGO-treatment.
BEN-MEN-1 (BM1) (A) and IOMM-Lee (IOMM) (B) cells were seeded in absence (Ctrl) or presence of 0.3 mM MGO on collagen IV (left) or fibronectin (right). Graphs display adhesion on collagen IV and fibronectin with or without treatment with untreated or treated cells after 2 h. Gray and black bars in (A) and (B) represent the untreated matrix with untreated cells as control. Untreated matrix and treated BEN-MEN-1 cells (BM1 Gly; light green bar) or treated IOMM cells (IOMM Gly; yellow bar). The green (BM1 + Mtx Gly) and orange (IOMM + Mtx Gly) bars show cell adhesion of treated matrix with untreated BEN-MEN-1 and IOMM-Lee cells. Dark green (BM1 Gly + Mtx Gly) and red (IOMM Gly + Mtx Gly) bars represent treated matrix with treated BEN-MEN-1 and IOMM-Lee cells. Error bars represent SD ($n = 4$), (Mtx = Matrix; Gly = MGO treatment).

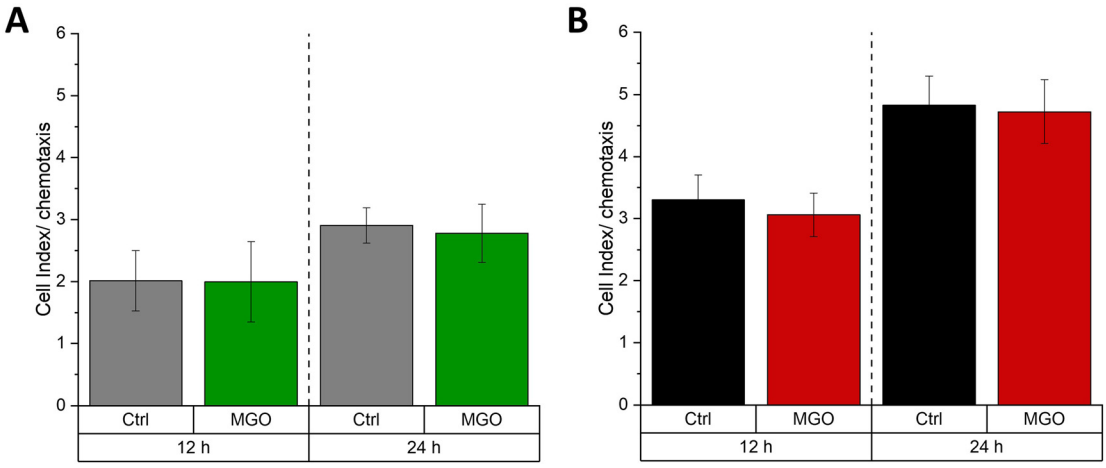

Figure 5: Chemotaxis of meningioma cells.
BEN-MEN-1 (A) and IOMM-Lee (B) were cultured for 24 h in the absence (Ctrl) or presence of 0.3 mM MGO. Graphs display relative chemotaxis (presented as cell indices) with treatment (MGO) or without treatment (Ctrl) for 12 and 24 h. Error bars represent SD (n = 4).

12 h or 24 h. Treatment with MGO had no effect, neither on BEN-MEN-1 (Figure 5A) nor on IOMM-Lee cells (Figure 5B). Please note that chemotaxis of malignant IOMM-Lee cells is higher in contrast to benign BEN-MEN-1 cells.

Glycation increases invasiveness of the benign cell line and decreases the invasiveness of malignant cell line

Since invasiveness is the most important parameter in most tumors, we finally wanted to examine whether there are changes in invasiveness due to glycation. From our chemotaxis experiments, we knew already that glycation does not interfere with the function of cellular receptors in general. We therefore cultured meningioma cell lines in CIM-plates for 48 h on matrigel in absence or presence of 0.3 mM MGO. Figure 6A displays the invasion over 48 h for both cell lines. Untreated IOMM-Lee cells are more invasive compared with BEN-MEN-1 cells. BEN-MEN-1 (Figure 6B) cells had a significantly increased invasion after MGO-treatment after 24, 36 and 48 h compared with the untreated controls. This effect could be also observed in another benign meningioma cell line (HBL-52) (data not shown). Interestingly, the malignant cell line (IOMM-Lee, Figure 6C) showed a significant reduction in their invasiveness over 48 h.

Glycation influences the expression of E- and N-cadherin in benign meningioma cells

Finally, we wanted to investigate whether MGO treatment influences the expression of members of the cadherin family, which are involved in epithelial-mesenchymal or mesenchymal-epithelial-transition. Therefore, we cultured meningioma cells in absence or presence of 0.3 mM MGO for 24 h and performed immunoblotting using anti-E- and N-cadherin antibodies (Figure 7). The expression of E- and N-cadherin in IOMM-Lee was not changed after glycation (Figure 7A–D). However, glycation of BEN-MEN-1 cell line resulted in increasing expression of E-cadherin (Figure 7A and B) and decreasing expression of N-cadherin (Figure 7C and D).

Discussion

Little is known about the role of MGO and glycation on meningioma cells. In this study, we analyzed the effect of MGO-treatment and glycation on two meningioma cell lines, representing the WHO grade I (BEN-MEN1) and the WHO grade III (IOMM-Lee). We could show that treatment with MGO led to glycation and modulated the invasiveness of both meningioma cell lines. However, glycation did not affect cell adhesion and chemotaxis of these cell lines.

Up to 90–99% of cellular MGO is bound *in vivo* to macromolecules; however, cellular concentrations up to 0.3 mM have been reported (Chaplen 1998; Chaplen et al. 1998; Thornalley 1996). Our data on cell viability using the methylthiazolyldiphenyl-tetrazolium bromide (MTT) assay showed that meningioma cells have no significantly reduced metabolism at physiological concentration of 0.3 mM MGO, but are influenced by MGO at high non-physiological concentrations. This could be confirmed via microscopy, where fewer cells and less cell spreading were observed and in immunoblotting in high concentrations,

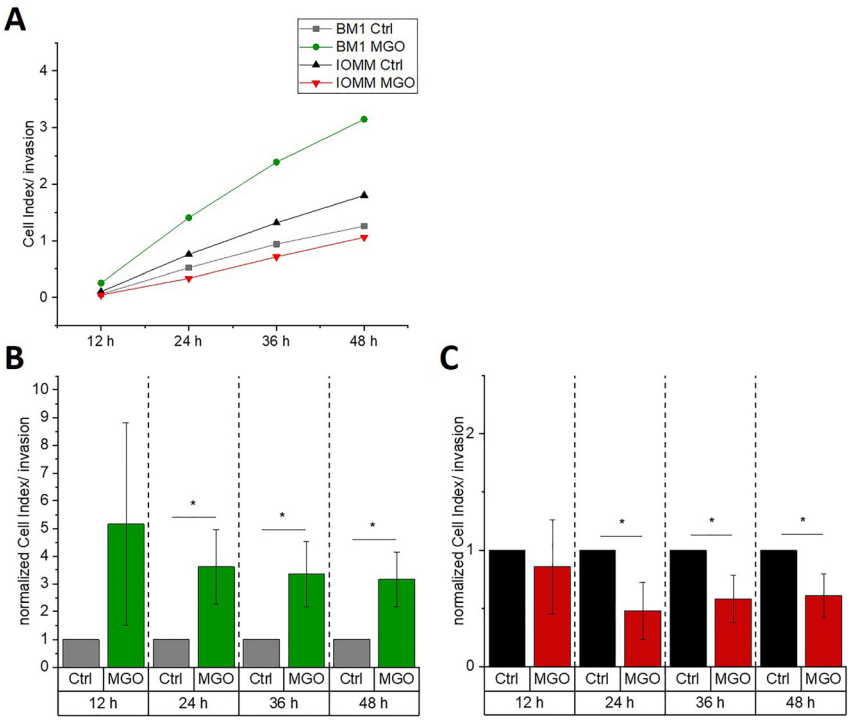

Figure 6: Invasion of meningioma cells.
BEN-MEN-1 (A, B) and IOMM-Lee (A, C) were cultivated for 48 h in absence (Ctrl) or presence of 0.3 mM MGO. Graphs display invasion (presented as cell indices) with treatment (MGO) or without treatment (Ctrl) for 12 h, 24 h (BEN-MEN-1: $p = 0.012$; IOMM-Lee: $p = 0.0347$), 36 h (BEN-MEN-1: $p = 0.0112$; IOMM-Lee: $p = 0.0377$) and 48 h (BEN-MEN-1: $p = 0.0324$; IOMM-Lee: $p = 0.0374$). In the graphs (B) and (C) normalized cell indices were shown for both cell lines relative to the controls. Statistical analysis was performed using *t*-test. Error bars represent SD ($n = 4$; $*p < 0.05$).

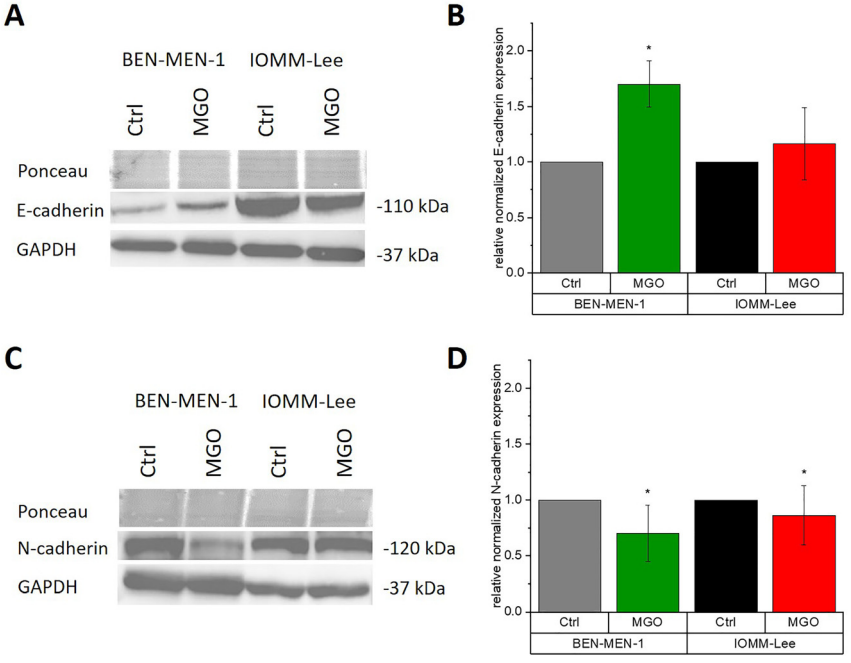

Figure 7: Cadherin expression of meningioma cells with and without MGO-treatment.
(A) BEN-MEN-1 and IOMM-Lee were cultured in the absence or presence of 0.3 mM MGO and E-cadherin was analyzed by Western blotting. (B) Quantification of E-cadherin expression in BEN-MEN-1 ($p = 0.0406$) and IOMM-Lee cells before (Ctrl) and after treatment with 0.3 mM MGO ($n = 3$). (C) BEN-MEN-1 and IOMM-Lee were cultured in the absence or presence of 0.3 mM MGO and N-cadherin was analyzed by Western blotting. (D) Quantification of N-cadherin expression in BEN-MEN-1 ($p = 0.0276$) and IOMM-Lee cells before (Ctrl) and after treatment with 0.3 mM MGO ($n = 7$). All statistical analysis (B, D) were performed using *t*-test. Error bars represent SD ($*p < 0.05$).

we could detect the cleaved- caspase-3 activity, which is one of the key player of programmed cell death (i.e. apoptosis) (data not shown). Similar observations have been shown in human glioblastoma multiforme T98G, U87MG cells and SH-SY5Y neuroblastoma cells, where MGO interfered with proliferation (Paul-Samojedny et al. 2016; Yin et al. 2012). Another study showed that MGO affects rat schwannoma RT4 cells, PC12 cells and U87 glioma cells in cell viability by decreasing of the key signaling pathway for cell survival (gp130/STAT3 signaling) and as a consequence promotes cytotoxicity (Lee et al. 2009).

MGO led in our hands to detectable glycation of meningioma cell proteins. The influence of glycation on adhesion, migration, invasion and apoptosis of cancer cells could be demonstrated in several recent studies (He et al. 2016; Loarca et al. 2013; Scheer et al. 2020). Our data show that cell adhesion of meningioma cells is not altered at physiological relevant MGO concentrations. Meningioma cells prefer fibronectin as substrate, what is in line with their integrin expression (α4, 5, 6 and β1, 3, 4) (preliminary data not shown), which are also known to be involved in proliferation, adhesion, migration and invasion in meningiomas (Bello et al. 2000; Chen et al. 2009; Gogineni et al. 2011; Nigim et al. 2019).

Our data on chemotaxis indicate that glycation of meningioma cells does not lead to a general loss of function. MGO-treatment seems to have cell-specific effects on behavior, since migration was reduced in liver and colon cancer cells and increased in neuroblastoma cells (He et al. 2016; Loarca et al. 2013; Scheer et al. 2020).

However, our results from the invasion of the meningioma cells indicate that MGO-treatment leads to a higher degree of invasiveness in benign meningioma cells, consequently to increased aggressiveness of meningioma cells. Antognelli et al. have shown that MGO treatment increases the invasion in anaplastic thyroid cancer (ATC) cells (Antognelli et al. 2019). This observation was also confirmed in neuroblastoma cells (Scheer et al. 2020). In liver cancer, it has been shown that invasion was inhibited by MGO treatment (Loarca et al. 2013). However, one has to keep in mind that the concentrations of MGO treatments were different in most studies. Low concentration of 5 μM MGO resulted in an increased invasion in ATC cells and a decreased invasion in liver cancer cells (Antognelli et al. 2019; Loarca et al. 2013). In neuroblastoma cells, increased invasiveness occurred after treatment with 0.1 mM MGO (Scheer et al. 2020).

Canel et al. proposed an E-cadherin–integrin crosstalk during cancer invasion and metastasis (Canel et al. 2013). Although Utsuki and colleagues have shown that low expression of E-cadherin is associated with invasive meningioma (Utsuki et al. 2005), we found high expression of E-cadherin in the malignant grade III IOMM-Lee cells and low expression in the benign grade I BEN-MEN-1 cells (see blots in Figure 7). Glycation led to increased expression of E-cadherin in BEN-MEN-1 cells, which fits nicely to the increased invasiveness after glycation. On the other hand, we found decreased expression of N-cadherin in BEN-MEN-1 cells. Asano and colleagues reported for gliomas, that an increased expression of N-cadherin correlated with a decreased invasiveness (Asano et al. 2004). Another study has shown that a decreased expression of N-cadherin resulted in a faster and less-directed migration of tumor cells (Camand et al. 2012). In our model, it appears that increased expression of E-cadherin and a decreased expression of N-cadherin are associated with a more invasive behavior. Many studies suggest a correlation between N-cadherin expression and matrix metalloproteinase-9 (MMP-9) (Hsu et al. 2016; Suyama et al. 2002; Walker et al. 2014). Preliminary data suggest an up-regulation of MMP-9 in BEN-MEN-1 cells after treatment with 0.3 mM MGO (data not shown). Although this has to be validated, one could speculate this as one reason for the increased invasion of this cell line.

Further studies should include expression analysis of the receptor of advanced glycation endproducts (RAGE), since Dai and colleagues showed that the AGE-induced RAGE-signaling pathways promotes development and progression of meningiomas (Dai et al. 2018) and several other studies suggested also an involvement of RAGE in tumor progression (Abe and Yamagishi 2008; Ahmad et al. 2018; Takino et al. 2010). In our hands, RAGE expression was increased in both cell lines after glycation (data not shown).

In summary, we propose that glycation has a specific effect on different cancer cells. Glycation promotes invasiveness of a WHO grade I meningioma cell line *in vitro*, but decreases invasive behavior in a WHO grade III meningioma cell line. Further studies are necessary, which could include strategies for “de-glycation”, which may be important for future cancer treatment.

Materials and methods

Cell culture

The human benign meningioma cell line BEN-MEN-1 was obtained from Leibniz-Institute DSMZ (Deutsche Sammlung von Mikroorganismen und Zellkulturen GmbH, Braunschweig, Germany) and the human malignant meningioma cell line IOMM-Lee (ATCC® CRL-3370™) was obtained from American Type Culture Collection (ATCC, Manassas, USA). Both cell lines were cultured in Dulbecco’s

modified Eagle's medium (DMEM) supplemented with 100 µg/mL of streptomycin, 100 U/mL of penicillin, 4 mM glutamine and 10% fetal bovine serum (FBS, Sigma Aldrich, St. Louis, MO, USA) at 37 °C in a 5% CO_2 incubator. The cell lines were split every 2–3 days with 0.1% Trypsin-ethylenediaminetetraacetic acid (EDTA) solution for 2 min.

Cell viability and cell morphology assays

The cell viability of glycated BEN-MEN-1 and IOMM-Lee cells was measured using an MTT (Sigma Aldrich) assay. Both cell lines were seeded into 96-well plates at a density of $7.8 \times 10^4/cm^2$ cells per well in DMEM with 1% FBS. After 2 h of attachment, cells were treated with different concentrations of MGO (Sigma Aldrich, 40% aqueous solution; diluted in 1× PBS; 0.1, 0.3, 0.6 and 1.0 mM). Controls (Ctrl) were cells (BEN-MEN-1, IOMM-Lee) without MGO treatment. Cell lines were cultivated for 24 h. Morphology of the cells was acquired with bright field microscopy (Axiovert 100, Carl Zeiss AG, Oberkochen, Germany). MTT was diluted to a final concentration of 0.5 mg/mL in normal growth medium and cells were incubated for 2 h with 100 µL MTT solution per well. After elimination of MTT-containing medium, residual formazan crystals were dissolved in 150 µL dimethyl sulfoxide (DMSO). The absorption values were measured (Plate-Reader, Clariostar, BMG Labtech GmbH, Ortenberg, Germany) at a wavelength of 570 nm (background 630 nm). The untreated control cells were set to 1 of cell viability. The changes in cell viability of the treated cells were calculated in relation to the untreated control.

Glycation and immunoblotting

Cells were seeded in 12-well plates at a density of $3.95 \times 10^4/cm^2$ in DMEM with 1% FBS. After 2 h of attachment, the cells were treated with different concentrations of MGO (0.1, 0.3, 0.6 and 1.0 mM). Controls (Ctrl) were cells (BEN-MEN-1, IOMM-Lee) without MGO treatment. The cell lines were cultivated for 24 h. Cells were directly lysed in hot SDS-sample buffer (2.5% sodium dodecyl sulfate, 0.06 M TRIS (tris(hydroxymethyl)aminomethane) pH 6.8, 10% glycerin, 0.01% bromophenol blue, 10 mM dithiothreitol in TBS-T (TRIS-buffered saline/0.1% Tween)) to isolate the total protein. Proteins were separated by sodium dodecyl sulfate polyacrylamide gel electrophoresis (SDS-PAGE, 10%) and transferred to a nitrocellulose membrane using Western blot techniques. The monoclonal anti-AGE antibody Carboxymethyllysine (CML)-26 (0.05 µg/mL, Abcam, Cambridge, UK) together with the secondary peroxidase-coupled antibody (ImmunoResearch Inc., Eagan, USA) was used to detect the glycation. Detection of E- and N-cadherin expression were done with monoclonal anti-E-cadherin antibody (0.05 µg/mL, Abcam, Cambridge, UK) and with monoclonal anti-N-cadherin antibody (0.0483 µg/mL, Abcam, Cambridge, UK) and a secondary peroxidase-coupled antibody (ImmunoResearch Inc., Eagan, USA). Images were taken using Chemidoc MP imaging system (Bio-Rad Laboratories, Hercules, USA). Ponceau S staining (0.1% Ponceau S, 3% trichloroacetic acid and 3% sulfosalicylic acid) of total loaded protein and glyceraldehyde 3-phosphate dehydrogenase (GAPDH) (0.04 µg/mL, Santa Cruz Biotechnology Inc., Dallas, USA) were used as loading controls. Band intensity of proteins of interest were transformed into numeric values using Image lab software (Bio-Rad Laboratories, Hercules) and normalized to the corresponding ponceau S staining to quantify the results.

Examination of adhesion with real time cell analysis

Fibronectin and collagen IV at a concentration of 10 µg/mL were used for each experiment and were added to the wells of the 96X E-plates® (ACEA Biosciences, San Diego, USA) and incubated for 1 h at 37 °C. E-plates® have gold microelectrode biosensors in each well of ACEA's electronic microtiter plates. After a washing step with PBS, the wells were incubated with 0.5% BSA solution in PBS for 20 min. Before the cells and media were added, the wells were washed with PBS. The cells were trypsinized and detached. The reaction was stopped and the cells were resuspended in media with 1% FBS. 50 µL serum-free media was added to every well in order to measure the background signal. Cells were added in density of $1.5625 \times 10^4/cm^2$. The adhesion of cell lines was measured as changes in impedance with the Real Time cell electronic sensing (RT-CES®) system (ACEA Biosciences) and monitored every 15 min for a period of 4 h. The measurement was done with the Real Time Cell Analyzer dual purpose (RTCA DP) Analyzer (ACEA Biosciences,) and displayed with the Real Time Cell Analyzer (RTCA) program 2.0 (ACEA Biosciences,) as Cell Index (CI). The index is calculated as follows: CI = (impedance at time point n – impedance in the absence of cells)/nominal impedance value.

Examination of chemotaxis with real time cell analysis

Chemotaxis was analyzed in 96X Cellular invasion and migration (CIM)-plates (ACEA Biosciences). The CIM-plates are composed of an upper and a lower chamber. The bottom surface of the upper chamber consists of a microporous membrane where cells can migrate through. Underneath the membrane, a gold electrode detects the presence of adherent cells. 160 µL DMEM with 20% FBS were added in the lower chamber. 50 µL DMEM with 1% FBS were added in the upper chamber. CIM-plates were incubated for 1 h at 37 °C, followed by background measurement. Cells were trypsinized, detached, the reaction was stopped and the cells were resuspended in media with 1% FBS. Cells were added to the upper chamber in density of $7.8 \times 10^4/cm^2$. The chemotaxis on every label was measured as changes in impedance with the RT-CES® system and monitored every 15 min for a period of 24 h. The measurement was conducted with the RTCA DP Analyzer (ACEA Biosciences) and displayed with the RTCA program 2.0 (ACEA Biosciences).

Examination of invasion with real time cell analysis

Invasion was analyzed in 96X CIM-plates (ACEA Biosciences). The CIM-plates are composed of an upper and a lower chamber. The bottom surface of the upper chamber consists of a microporous membrane where cells can migrate through. On the underside of this membrane a gold electrode detects the presence of adherent cells. To investigate the invasion, 800 µg/mL Basement Membrane Matrix, lactose dehydrogenase-elevating virus (LDEV)-free Matrigel® (Corning, Minneapolis, MN, USA) were added in the upper chamber. After an incubation for 4 h at 37 °C, 160 µL DMEM with 20% FBS were added in the lower chamber and 50 µL DMEM with 1% FBS were added in the upper chamber. The CIM-plates were incubated for 1 h at 37 °C. Afterwards, the background signal was measured. Cells were trypsinized and detached. The reaction was stopped by adding media with 1% FBS and the cells were resuspended. Cells were added to the upper chamber in density of $1.1 \times 10^5/cm^2$. Invasion was measured as

changes in impedance with the RT-CES® system and monitored every 15 min for a period of 48 h. The measurement was carried out with the RTCA DP Analyzer (ACEA Biosciences) and displayed with the RTCA program 2.0 (ACEA Biosciences).

Statistical analysis

All analyses and visualizations were performed using OriginPro 2019 software (OriginLab Corporation, Northampton, USA). Paired student's *t*-test against the control group, both cell lines or a theoretical value of 1 (due to data normalization) were executed. Figures show the average mean with standard deviation (SD) and levels of significance are represented within the Figures.

Acknowledgment: Special thanks to Dr. Heidi Olzscha for critical reading of the manuscript.
Author contributions: All the authors have accepted responsibility for the entire content of this submitted manuscript and approved submission.
Research funding: This research was funded by Wilhelm Roux-program, FKZ 31/21 and Deutsche Forschungsgemeinschaft (DFG, ProMoAge RTG 2155).
Conflict of interest statement: The authors declare no conflict of interest. The funders had no role in the design of the study; in the collection, analyses, or interpretation of data; in the writing of the manuscript, or in the decision to publish the results.

References

Abe, R. and Yamagishi, S.-i. (2008). AGE-RAGE system and carcinogenesis. Curr. Pharmaceut. Des. 14: 940–945.

Ahmad, S., Khan, H., Siddiqui, Z., Khan, M.Y., Rehman, S., Shahab, U., Godovikova, T., Silnikov, V., and Moinuddin (2018). AGEs, RAGEs and s-RAGE; friend or foe for cancer. Semin. Cancer Biol. 49: 44–55.

Ahmed, N. (2005). Advanced glycation endproducts–role in pathology of diabetic complications. Diabetes Res. Clin. Pract. 67: 3–21.

Allaman, I., Bélanger, M., and Magistretti, P.J. (2015). Methylglyoxal, the dark side of glycolysis. Front. Neurosci. 9: 23.

Antognelli, C., Moretti, S., Frosini, R., Puxeddu, E., Sidoni, A., and Talesa, V.N. (2019). Methylglyoxal acts as a tumor-promoting factor in anaplastic thyroid cancer. Cells 8. https://doi.org/10.3390/cells8060547.

Asano, K., Duntsch, C.D., Zhou, Q., Weimar, J.D., Bordelon, D., Robertson, J.H., and Pourmotabbed, T. (2004). Correlation of N-cadherin expression in high grade gliomas with tissue invasion. J. Neurooncol. 70: 3–15.

Bellahcène, A., Nokin, M.-J., Castronovo, V., and Schalkwijk, C. (2018). Methylglyoxal-derived stress: an emerging biological factor involved in the onset and progression of cancer. Semin. Cancer Biol. 49: 64–74.

Bellier, J., Nokin, M.-J., Lardé, E., Karoyan, P., Peulen, O., Castronovo, V., and Bellahcène, A. (2019). Methylglyoxal, a potent inducer of AGEs, connects between diabetes and cancer. Diabetes Res. Clin. Pract. 148: 200–211.

Bello, L., Zhang, J., Nikas, D.C., Strasser, J.F., Villani, R.M., Cheresh, D.A., Carroll, R.S., and Black, P.M. (2000). Alpha(v)beta3 and alpha(v)beta5 integrin expression in meningiomas. Neurosurgery 47: 1185–1195.

Bernardo, B.M., Orellana, R.C., Weisband, Y.L., Hammar, N., Walldius, G., Malmstrom, H., Ahlbom, A., Feychting, M., and Schwartzbaum, J. (2016). Association between prediagnostic glucose, triglycerides, cholesterol and meningioma, and reverse causality. Br. J. Cancer 115: 108–114.

Bharadwaj, S., Venkatraghavan, L., Mariappan, R., Ebinu, J., Meng, Y., Khan, O., Tung, T., Reyhani, S., Bernstein, M., and Zadeh, G. (2015). Serum lactate as a potential biomarker of non-glial brain tumors. J. Clin. Neurosci. 22: 1625–1627.

Camand, E., Peglion, F., Osmani, N., Sanson, M., and Etienne-Manneville, S. (2012). N-cadherin expression level modulates integrin-mediated polarity and strongly impacts on the speed and directionality of glial cell migration. J. Cell Sci. 125: 844–857.

Canel, M., Serrels, A., Frame, M.C., and Brunton, V.G. (2013). E-cadherin-integrin crosstalk in cancer invasion and metastasis. J. Cell Sci. 126: 393–401.

Cao, Z.-Q., Wang, Z., and Leng, P. (2019). Aberrant N-cadherin expression in cancer. Biomed. Pharmacother. 118: 109320.

Chaplen, F.W. (1998). Incidence and potential implications of the toxic metabolite methylglyoxal in cell culture: a review. Cytotechnology 26: 173–183.

Chaplen, F.W., Fahl, W.E., and Cameron, D.C. (1998). Evidence of high levels of methylglyoxal in cultured Chinese hamster ovary cells. Proc. Natl. Acad. Sci. U. S. A. 95: 5533–5538.

Chen, J., Xu, X., and Wang, H. (2009). Expression of integrin-alpha(3) mRNA in meningiomas and its correlation with proliferation and invasion. J. Huazhong Univ. Sci. Technol. 29: 94–96.

Dai, J., Ma, Y., Chu, S., Le, N., Cao, J., and Wang, Y. (2018). Identification of key genes and pathways in meningioma by bioinformatics analysis. Oncol. Lett. 15: 8245–8252.

Edlinger, M., Strohmaier, S., Jonsson, H., Bjørge, T., Manjer, J., Borena, W.T., Häggström, C., Engeland, A., Tretli, S., Concin, H., et al. (2012). Blood pressure and other metabolic syndrome factors and risk of brain tumour in the large population-based Me-Can cohort study. J. Hypertens. 30: 290–296.

Falone, S., D'Alessandro, A., Mirabilio, A., Petruccelli, G., Cacchio, M., Di Ilio, C., Di Loreto, S., and Amicarelli, F. (2012). Long term running biphasically improves methylglyoxal-related metabolism, redox homeostasis and neurotrophic support within adult mouse brain cortex. PLoS One 7: e31401.

Gill, K.S., Fernandes, P., O'Donovan, T.R., McKenna, S.L., Doddakula, K.K., Power, D.G., Soden, D.M., and Forde, P.F. (2016). Glycolysis inhibition as a cancer treatment and its role in an anti-tumour immune response. Biochim. Biophys. Acta 1866: 87–105.

Gloushankova, N.A., Rubtsova, S.N., and Zhitnyak, I.Y. (2017). Cadherin-mediated cell-cell interactions in normal and cancer cells. Tissue Barriers 5: e1356900.

Gogineni, V.R., Nalla, A.K., Gupta, R., Gujrati, M., Klopfenstein, J.D., Mohanam, S., and Rao, J.S. (2011). α3β1 integrin promotes radiation-induced migration of meningioma cells. Int. J. Oncol. 38: 1615–1624.

Goldbrunner, R., Minniti, G., Preusser, M., Jenkinson, M.D., Sallabanda, K., Houdart, E., von Deimling, A., Stavrinou, P., Lefranc, F., Lund-Johansen, M., et al. (2016). EANO guidelines for

the diagnosis and treatment of meningiomas. Lancet Oncol. 17: e383–e391.

Harrison, O.J., Jin, X., Hong, S., Bahna, F., Ahlsen, G., Brasch, J., Wu, Y., Vendome, J., Felsovalyi, K., Hampton, C.M., et al. (2011). The extracellular architecture of adherens junctions revealed by crystal structures of type I cadherins. Structure 19: 244–256.

He, T., Zhou, H., Li, C., Chen, Y., Chen, X., Li, C., Mao, J., Lyu, J., and Meng, Q.H. (2016). Methylglyoxal suppresses human colon cancer cell lines and tumor growth in a mouse model by impairing glycolytic metabolism of cancer cells associated with down-regulation of c-Myc expression. Cancer Biol. Ther. 17: 955–965.

Holleczek, B., Zampella, D., Urbschat, S., Sahm, F., von Deimling, A., Oertel, J., and Ketter, R. (2019). Incidence, mortality and outcome of meningiomas: a population-based study from Germany. Cancer Epidemiol. 62: 101562.

Hsu, C.-C., Huang, S.-F., Wang, J.-S., Chu, W.-K., Nien, J.-E., Chen, W.-S., and Chow, S.-E. (2016). Interplay of N-cadherin and matrix metalloproteinase 9 enhances human nasopharyngeal carcinoma cell invasion. BMC Cancer 16: 800.

Kalapos, M.P. (2008). Methylglyoxal and glucose metabolism: a historical perspective and future avenues for research. Drug Metabol. Drug Interact. 23: 69–91.

Lee, H.K., Seo, I.A., Suh, D.J., Lee, H.J., and Park, H.T. (2009). A novel mechanism of methylglyoxal cytotoxicity in neuroglial cells. J. Neurochem. 108: 273–284.

Loarca, L., Sassi-Gaha, S., and Artlett, C.M. (2013). Two α-dicarbonyls downregulate migration, invasion, and adhesion of liver cancer cells in a p53-dependent manner. Dig. Liver Dis. 45: 938–946.

Mège, R.M. and Ishiyama, N. (2017). Integration of cadherin adhesion and cytoskeleton at adherens junctions. Cold Spring Harb. Perspect. Biol. 9. https://doi.org/10.1101/cshperspect.a028738.

Mendonsa, A.M., Na, T.-Y., and Gumbiner, B.M. (2018). E-cadherin in contact inhibition and cancer. Oncogene 37: 4769–4780.

Michaud, D.S., Bové, G., Gallo, V., Schlehofer, B., Tjønneland, A., Olsen, A., Overvad, K., Dahm, C.C., Teucher, B., Boeing, H., et al. (2011). Anthropometric measures, physical activity, and risk of glioma and meningioma in a large prospective cohort study. Cancer Prev. Res. 4: 1385–1392.

Nayeri, A., Chotai, S., Prablek, M.A., Brinson, P.R., Douleh, D.G., Weaver, K.D., Thompson, R.C., and Chambless, L. (2016). Type 2 diabetes is an independent negative prognostic factor in patients undergoing surgical resection of a WHO grade I meningioma. Clin. Neurol. Neurosurg. 149: 6–10.

Niedermaier, T., Behrens, G., Schmid, D., Schlecht, I., Fischer, B., and Leitzmann, M.F. (2015). Body mass index, physical activity, and risk of adult meningioma and glioma: a meta-analysis. Neurology 85: 1342–1350.

Nigim, F., Kiyokawa, J., Gurtner, A., Kawamura, Y., Hua, L., Kasper, E.M., Brastianos, P.K., Cahill, D.P., Rabkin, S.D., Martuza, R.L., et al. (2019). A monoclonal antibody against β1 integrin inhibits proliferation and increases survival in an orthotopic model of high-grade meningioma. Target. Oncol. 14: 479–489.

Nokin, M.-J., Bellier, J., Durieux, F., Peulen, O., Rademaker, G., Gabriel, M., Monseur, C., Charloteaux, B., Verbeke, L., van Laere, S., et al. (2019). Methylglyoxal, a glycolysis metabolite, triggers metastasis through MEK/ERK/SMAD1 pathway activation in breast cancer. Breast Cancer Res. 21: 11.

Ostrom, Q.T., Cioffi, G., Gittleman, H., Patil, N., Waite, K., Kruchko, C., and Barnholtz-Sloan, J.S. (2019). CBTRUS statistical report: primary brain and other central nervous system tumors diagnosed in the United States in 2012-2016. Neuro Oncol 21: v1–v100.

Ostrom, Q.T., Gittleman, H., Truitt, G., Boscia, A., Kruchko, C., and Barnholtz-Sloan, J.S. (2018). CBTRUS statistical report: primary brain and other central nervous system tumors diagnosed in the United States in 2011-2015. Neuro Oncol. 20: iv1–iv86.

Paul, R.G. and Bailey, A.J. (1996). Glycation of collagen: the basis of its central role in the late complications of ageing and diabetes. Int. J. Biochem. Cell Biol. 28: 1297–1310.

Paul-Samojedny, M., Łasut, B., Pudełko, A., Fila-Daniłow, A., Kowalczyk, M., Suchanek-Raif, R., Zieliński, M., Borkowska, P., and Kowalski, J. (2016). Methylglyoxal (MGO) inhibits proliferation and induces cell death of human glioblastoma multiforme T98G and U87MG cells. Biomed. Pharmacother. 80: 236–243.

Pedchenko, V.K., Chetyrkin, S.V., Chuang, P., Ham, A.-J.L., Saleem, M.A., Mathieson, P.W., Hudson, B.G., and Voziyan, P.A. (2005). Mechanism of perturbation of integrin-mediated cell-matrix interactions by reactive carbonyl compounds and its implication for pathogenesis of diabetic nephropathy. Diabetes 54: 2952–2960.

Rabbani, N. and Thornalley, P.J. (2008). The dicarbonyl proteome: proteins susceptible to dicarbonyl glycation at functional sites in health, aging, and disease. Ann. N. Y. Acad. Sci. 1126: 124–127.

Rabbani, N. and Thornalley, P.J. (2012). Methylglyoxal, glyoxalase 1 and the dicarbonyl proteome. Amino Acids 42: 1133–1142.

Rabbani, N. and Thornalley, P.J. (2015). Dicarbonyl stress in cell and tissue dysfunction contributing to ageing and disease. Biochem. Biophys. Res. Commun. 458: 221–226.

Rodriguez, F.J., Lewis-Tuffin, L.J., and Anastasiadis, P.Z. (2012). E-cadherin's dark side: possible role in tumor progression. Biochim. Biophys. Acta 1826: 23–31.

Schalkwijk, C.G. (2015). Vascular AGE-ing by methylglyoxal: the past, the present and the future. Diabetologia 58: 1715–1719.

Scheer, M., Bork, K., Simon, F., Nagasundaram, M., Horstkorte, R., and Gnanapragassam, V.S. (2020). Glycation leads to increased polysialylation and promotes the metastatic potential of neuroblastoma cells. Cells 9. https://doi.org/10.3390/cells9040868.

Schneider, B., Pülhorn, H., Röhrig, B., and Rainov, N.G. (2005). Predisposing conditions and risk factors for development of symptomatic meningioma in adults. Cancer Detect. Prev. 29: 440–447.

Schwartzbaum, J., Jonsson, F., Ahlbom, A., Preston-Martin, S., Malmer, B., Lönn, S., Söderberg, K., and Feychting, M. (2005). Prior hospitalization for epilepsy, diabetes, and stroke and subsequent glioma and meningioma risk. Cancer Epidemiol. Biomarkers Prev. 14: 643–650.

Suyama, K., Shapiro, I., Guttman, M., and Hazan, R.B. (2002). A signaling pathway leading to metastasis is controlled by N-cadherin and the FGF receptor. Cancer Cell 2: 301–314.

Takino, J.-I., Yamagishi, S.-i., and Takeuchi, M. (2010). Cancer malignancy is enhanced by glyceraldehyde-derived advanced glycation end-products. J. Oncol. 2010: 739852.

Thornalley, P.J. (1996). Pharmacology of methylglyoxal: formation, modification of proteins and nucleic acids, and enzymatic

detoxification - a role in pathogenesis and antiproliferative chemotherapy. Gen. Pharmacol. Vasc. Syst. 27: 565–573.

Utsuki, S., Oka, H., Sato, Y., Kawano, N., Tsuchiya, B., Kobayashi, I., and Fujii, K. (2005). Invasive meningioma is associated with a low expression of E-cadherin and beta-catenin. Clin. Neuropathol. 24: 8–12.

Walker, A., Frei, R., and Lawson, K.R. (2014). The cytoplasmic domain of N-cadherin modulates MMP-9 induction in oral squamous carcinoma cells. Int. J. Oncol. 45: 1699–1706.

Wiedmann, M., Brunborg, C., Lindemann, K., Johannesen, T.B., Vatten, L., Helseth, E., and Zwart, J.A. (2013). Body mass index and the risk of meningioma, glioma and schwannoma in a large prospective cohort study (The HUNT Study). Br. J. Cancer 109: 289–294.

Yin, Q.-Q., Dong, C.-F., Dong, S.-Q., Dong, X.-L., Hong, Y., Hou, X.-Y., Luo, D.-Z., Pei, J.-J., and Liu, X.-P. (2012). AGEs induce cell death via oxidative and endoplasmic reticulum stresses in both human SH-SY5Y neuroblastoma cells and rat cortical neurons. Cell. Mol. Neurobiol. 32: 1299–1309.

cells

MDPI

Article

Glycation Interferes with the Expression of Sialyltransferases in Meningiomas

Philipp Selke [1,*], Kaya Bork [1], Tao Zhang [2], Manfred Wuhrer [2], Christian Strauss [3], Rüdiger Horstkorte [1] and Maximilian Scheer [1,3]

[1] Medical Faculty, Institute for Physiological Chemistry, Martin-Luther-University Halle-Wittenberg, 06114 Halle (Saale), Germany; kaya.bork@medizin.uni-halle.de (K.B.); Ruediger.horstkorte@medizin.uni-halle.de (R.H.); maximilian.scheer@uk-halle.de (M.S.)
[2] Center for Proteomics and Metabolomics, Leiden University Medical Center, 2333 ZA Leiden, The Netherlands; t.zhang@lumc.nl (T.Z.); m.wuhrer@lumc.nl (M.W.)
[3] Department of Neurosurgery, University Hospital Halle, 06120 Halle (Saale), Germany; Christian.strauss@uk-halle.de
* Correspondence: philipp.selke@uk-halle.de; Tel.: +49-0-345-557-3814

Abstract: Meningiomas are the most common non-malignant intracranial tumors and prefer, like most tumors, anaerobic glycolysis for energy production (Warburg effect). This anaerobic glycolysis leads to an increased synthesis of the metabolite methylglyoxal (MGO) or glyoxal (GO), which is known to react with amino groups of proteins. This reaction is called glycation, thereby building advanced glycation end products (AGEs). In this study, we investigated the influence of glycation on sialylation in two meningioma cell lines, representing the WHO grade I (BEN-MEN-1) and the WHO grade III (IOMM-Lee). In the benign meningioma cell line, glycation led to differences in expression of sialyltransferases (*ST3GAL1/2/3/5/6*, *ST6GAL1/2*, *ST6GALNAC2/6*, and *ST8SIA1/2*), which are known to play a role in tumor progression. We could show that glycation of BEN-MEN-1 cells led to decreased expression of ST3Gal5. This resulted in decreased synthesis of the ganglioside GM3, the product of ST3Gal5. In the malignant meningioma cell line, we observed changes in expression of sialyltransferases (*ST3GAL1/2/3*, *ST6GALNAC5*, and *ST8SIA1*) after glycation, which correlates with less aggressive behavior.

Keywords: intracranial tumor; methylglyoxal; MGO; sialylation; tumorigenesis; posttranslational modification

Citation: Selke, P.; Bork, K.; Zhang, T.; Wuhrer, M.; Strauss, C.; Horstkorte, R.; Scheer, M. Glycation Interferes with the Expression of Sialyltransferases in Meningiomas. *Cells* **2021**, *10*, 3298. https://doi.org/10.3390/cells10123298

Academic Editor: Javier S. Castresana

Received: 5 November 2021
Accepted: 22 November 2021
Published: 25 November 2021

1. Introduction

Meningiomas arise from the arachnoid and are the most common non-malignant intracranial tumor [1–5]. They are classified according to WHO (World Health Organization) in grades I, II, and III. The benign grade I represents the most frequent subtype (>80%), and has a low risk of recurrence and slow growth [5,6]. As opposed to benign meningioma, grade III meningiomas (anaplastic, rhabdoid, and papillary subtype) are rare (1–3%) and little is known about factors that influence their survival and malignity. The present surgical, medicinal, and radiotherapeutic treatments are not adequate to manage the morbidity and mortality in this subtype [7–10].

Like many other tumors, meningiomas use glucose as a primary energy source (Warburg effect), which is considered as one of the "hallmarks of cancer" [11–13].

During glycolysis, up to 0.4% of the glucose is converted into methylglyoxal (MGO). MGO is a typical side product of glyceraldehyde-3-phosphate, which is generated by the aldolase reaction from fructose-1,6-bisphosphate. Please note that MGO is more than 20,000 times more reactive than glucose [11]. Previous studies showed that MGO concentrations are elevated in diabetic and or aged individuals [14]. Many studies suggest that diabetes is linked to an increased risk of cancer [15,16]. In line with this, there is a correlation

between serum glucose levels and meningioma risk [17,18]. However, there are contrary data suggesting a positive [19,20] or inverse [21] correlation between diabetes and serum glucose levels and the risk of meningioma. For example, patients with type 2 diabetes have a decreased survival after surgical resection of a WHO grade I meningioma [22].

The dicarbonyl MGO reacts primarily with proteins (through arginine, lysine, and cysteine residues) or to a small extent also with DNA and lipids. This non-enzymatic reaction between the carbonyl groups of dicarbonyls (i.e., MGO) or monosaccharides (i.e., glucose) and the amino groups of proteins is called glycation [23,24]. Another important glycating agent is glyoxal (GO), which is formed by degradation of glucose or autoxidation of glycoaldehyde to glyoxal [25]. Glycation is much stronger with dicarbonyls than with monosaccharides [26]. The end products of this reaction are called advanced glycation end products (AGEs) [27–29]. Recently, we demonstrated that glycation through MGO led to an increased invasive behavior in benign meningioma cells [30]. Several other studies propose MGO as a tumor-promoting agent [31,32].

Another common posttranslational modification is glycosylation. In contrast to glycation, glycosylation is an enzymatic addition of carbohydrates, glycans to a non-carbohydrate-structure, commonly a lipid or protein in the endoplasmatic reticulum (ER)/Golgi. Sialylation is of deep interest and describes the addition of sialic acids (Sia) to lipids (i.e., gangliosides) or proteins (i.e., neural cell adhesion molecule (NCAM)) through sialyltransferases (ST) [33].

N-acetyl neuraminic acid (Neu_5Ac) represents the major Sia of mammals. It is synthesized from UDP-*N*-acetyl glucosamine (UDP-GlcNAc) in the cytosol [34]. The key enzyme of the Sia biosynthesis is the bifunctional UDP-*N*-acetyl glucosamine 2-epimerase/*N*-acetyl mannosamine kinase (GNE) [35]. Sialylation is taking place in the Golgi and is catalyzed by STs. They are 20 known STs in humans, which use CMP-activated Sia as substrate (Figure 1). These STs are subdivided into 4 families dedicated to the carbohydrate linkages they synthesize: beta-galactoside alpha 2,3-sialyltransferases (ST3Gal1-6), beta-galactoside alpha 2,6-sialyltransferases (ST6Gal1-2), *N*-acetyl galactosamine (GalNAc) alpha 2,6-sialyltransferases (ST6GalNAc1-6) and alpha 2,8-sialyltransferases (ST8Sia1-6) [36,37]. The members of the ST3Gal family transfer Sia from CMP-Sia to terminal galactose residues through 2,3 linkages, whereas the two known members of the ST6Gal family do this through 2,6 linkages. The six members of the ST6GalNAc family transfer Sia from CMP-Sia to GalNAc residues via 2,6 linkages. In addition, the ST8Sia-family transfer Sia from CMP-Sia to other terminal Sia residues by 2,8-linkages [36,37]. High blood glucose concentrations in individuals with diabetes result in a UDP-GlcNAc-dependent change to more complex *N*-glycans [38]. Especially, glycoproteins with only few *N*-glycosylation sites such as transforming growth factor β (TGFβ) or glucose transporter 4 (GLUT4) show rapid response to increasing GlcNAc concentrations causing complex glycan formation and branching [39]. Gangliosides are glycosphingolipids that contain Sias. The synthesis of gangliosides begins with ceramide (Cer) in the ER. During GM3-synthesis, Cer will be glucosylated by the glucosylceramid synthase. After this step in the cis-golgi, glucosylceramide is converted in the trans-golgi to lactosylceramide [40]. This is the substrate for GM3-synthase (ST3Gal5). It is known that GM3 plays a role during several diseases (chronic inflammation, insulin resistance or cancer) [41–43].

In this study, we compared the expression of STs in benign and malignant meningioma cells and found significant differences between these two. Furthermore, we investigated the role of the glycating metabolite MGO on the expression of STs in both benign and malignant meningioma cells. Thereby, we could show that glycation has a dramatic effect on the expression of STs and consequently on the GM3 expression. As a result, this could change sialylation-dependent tumor progression in meningioma.

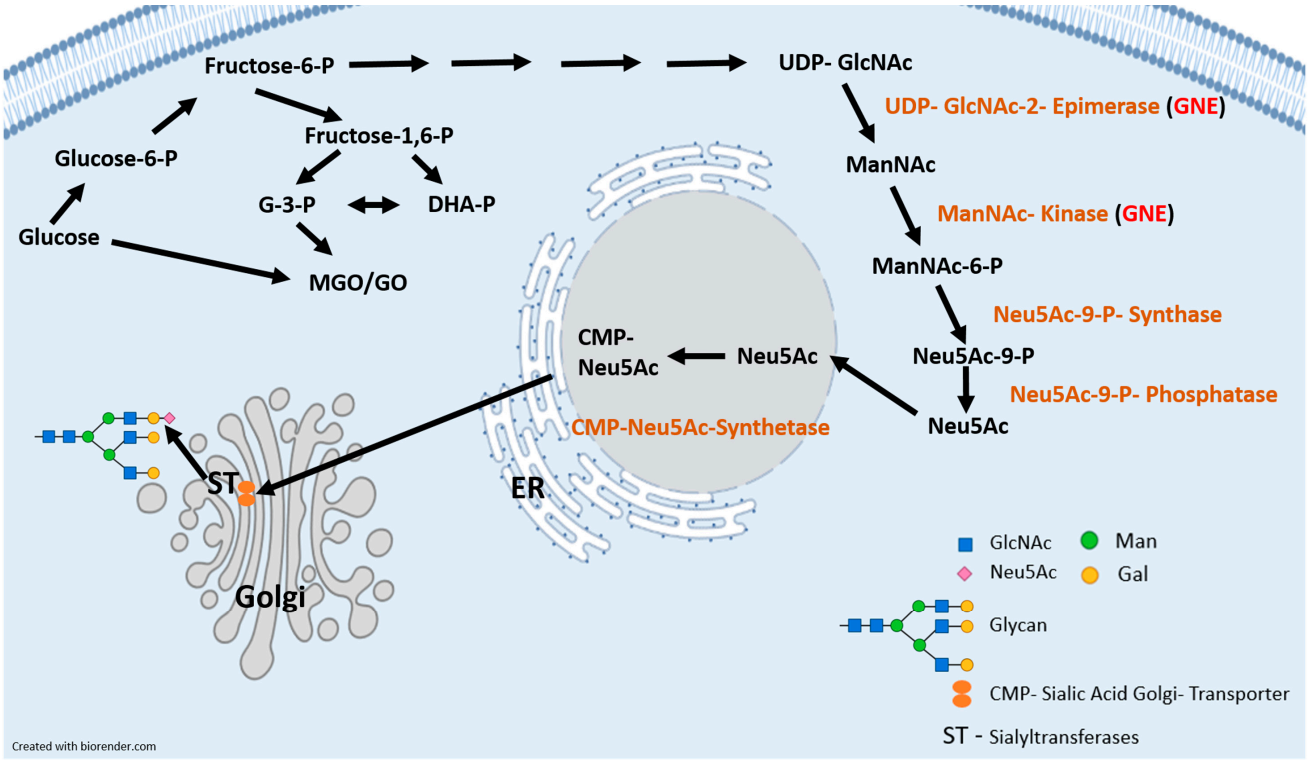

Figure 1. Schematic representation of the Sia biosynthesis from glucose to Sia and glycation agents (MGO/GO) and sialylation of glycoproteins (i.e., *N*-glycans, *O*-glycans or gangliosides) in the endoplasmatic reticulum and Golgi. G-3-P = glyceraldehyde-3-phosphate; DHA-P = Dihydroxyaceton phosphate; MGO = methylglyoxal; GO = glyoxal; GlcNAc = *N*-acetyl-glucosamine; Man = Mannose; Gal = Galactose; Neu5Ac = *N*-acetyl-neuraminic acid; GNE = UDP-*N*-acetyl glucosamine 2-epimerase/*N*-acetyl mannosamine kinase; ER = Endoplasmatic reticulum.

2. Materials and Methods

2.1. Cell Culture

The human benign meningioma cell line BEN-MEN-1 was obtained from Leibniz-Institute DSMZ (Deutsche Sammlung von Mikroorganismen und Zellkulturen GmbH, Braunschweig, Germany) and the human malignant meningioma cell line IOMM-Lee (ATCC® CRL-3370™) was obtained from American Type Culture Collection (ATCC, Manassas, VA, USA). Both cell lines were cultured in Dulbecco's Modified Eagle's Medium (DMEM) supplemented with 100 µg/mL of streptomycin, 100 U/mL of penicillin, 4 mM of glutamine, and 10% fetal bovine serum (FBS, Sigma-Aldrich, St. Louis, MO, USA) at 37 °C in a 5% CO_2 incubator. The cell lines were split every 2–3 days with 0.1% Trypsin-EDTA (Ethylenediaminetetraacetic acid) solution for 2 min.

2.2. Glycation and Real-Time PCR Analysis

Cells were seeded in 12-well plates at a density of $3.95 \times 10^4/cm^2$ in DMEM with 1% FBS. After 2 h of attachment, the cells were treated with 0.3 mM MGO or GO. Controls (Ctrl) were cells (BEN-MEN-1, IOMM-Lee) without MGO or GO treatment. The cell lines were cultivated for 24 h. RNA was isolated using the Quick-RNA™ MiniPrep Kit (Zymo Research, Irvine, CA, USA) according to the manufacturer's instructions. The quality and concentration of the RNA were analyzed using the NanoDrop 1000 Spectrophotometer (Thermo Fisher Scientific, Waltham, MA, USA). RNA (2 µg) was transcribed into cDNA using SuperScript™ II Reverse Transcriptase according to the manufacturer's instructions. PCR reactions were performed using DreamTaq DNA polymerase (Thermo Fisher Scientific), and products were separated on a 1.5% agarose gel. The following conditions were used: initial denaturation for 2 min at 95 °C, 35 cycles (30 s at 95 °C, 30 s at 55 °C, 30 s at

72 °C), final elongation for 5 min at 72 °C. We use for all sialyltransferases the same primer pairs which were used in a previous study [44].

The sialyltransferase expression of untreated meningioma cell lines (BEN-MEN-1; IOMM- Lee) and after 24 h of glycation with 0.3 mM MGO were measured via quantitative real-time PCR (qPCR) using the iQ™ 5 Multicolor Real-Time PCR Detection System (Biorad, Hercules, CA, USA) and qPCR GreenMaster (Jena Bioscience, Jena, Germany) with the same primer pairs used for normal PCR. The following conditions were used for qPCR: initial denaturation for 1:30 min at 95 °C, 40 cycles (10 s at 95 °C, 10 s at 62 °C, 25 s at 72 °C), final elongation for 1 min at 72 °C, followed by a melting curve analysis. The expression level of sialyltransferases in control and glycated cell lines was determined relative to GAPDH (165 bp; fw: GGAGCGAGATCCCTCCAAA; rv: ATGACGAACATGGGGGCATC), calculated as ΔCT. The control was relatively computed to glycated cell line ($2^{-\Delta\Delta CT}$). All reactions were performed in triplicate.

2.3. Cultivation of BEN-MEN-1 Cells and Preparation of GSL-Glycan Alditols Released from BEN-MEN-1 Cells

Extraction of GSLs and preparation of GSL-glycan alditols from cells were performed in triplicate as previously described [45]. The cells were cultivated until 80% of confluence and followed by 24 h treatment with and without 0.3 mM MGO. Shortly, 2×10^6 cells were harvested, washed and resuspended with 200 µL of water. The cell samples were lysed by vortexing and sonication for 30 min. In this step, 2.5 µL of 0.5 µM ganglioside GT1b in ethanol were added as a spiked internal standard to monitor sample preparation and to normalize roughly absolute quantification. Chloroform (550 µL) was added to the samples followed by 15 min sonication. Methanol (350 µL) was added to the cell pellets and incubated for 4 h with shaking at room temperature. The upper phase containing GSLs was collected after centrifugation at 2700× g for 20 min. Then, 400 µL of chloroform/methanol (2:1, v/v) was added, followed by adding 400 µL of methanol/water (1:1, v/v). After sonication and centrifugation, the upper phase was collected and pooled to the previous sample. The process of adding methanol/water (1:1, v/v), sonication, centrifugation and removing the upper phase was repeated another two times. In each replicate, the upper phase was collected and replaced by the same volume of methanol/water (1:1, v/v). The combined upper phases were dried under vacuum in an Eppendorf Concentrator 5301 (Eppendorf, Hamburg, Germany) at 30 °C.

Before the purification of the GSLs using reverse-phase (RP) SPE, the samples were dissolved in 100 µL methanol followed by the addition of 100 µL water. TC18-RP-cartridges were prewashed with 2 mL of chloroform/methanol (2:1, v/v), 2 mL of methanol followed by equilibration with 2 mL methanol/water (1:1, v/v). The extracted GSLs were loaded to the cartridge and washed with 2 mL methanol/water (1:1, v/v). The GSLs were eluted from the column with 2 mL methanol and 2 mL chloroform/methanol (2:1, v/v). The samples were dried under vacuum in an Eppendorf Concentrator at 30 °C.

To release the glycans from the GSLs, a mixture of EGCase I (12 mU, 2 µL), EGCase I buffer (4 µL) and water (34 µL) (pH 5.2) was added to each sample and incubated for 36 h at 37 °C. The released glycans were collected and loaded on TC18-RP-cartridges, which had been preconditioned with 2 mL of methanol and 2 mL of water. The samples were washed with 200 µL of water and residual glycans were loaded to the cartridge. Then, 500 µL of water were added to the cartridge to wash the glycans from the column. The flow-through and wash fractions were pooled and dried in an Eppendorf Concentrator at 30 °C.

The reduction was carried out with slight modifications following the same procedure as described in previous work [45,46]. In brief, GSL-glycans were reduced to alditols in 20 µL of sodium borohydride (500 mM) in potassium hydroxide (50 mM) for 2 h at 50 °C. Subsequently, 2 µL of glacial acetic acid were added to acidify the solution and quench the reaction. The desalting of GSL-glycans was performed as previously described. Glycan alditols were eluted with 50 µL of water twice. The combined flow-through and eluate were pooled and dried under vacuum in an Eppendorf Concentrator at 30 °C. The

carbon SPE clean-up was performed and the purified glycan alditols were re-suspended in 20 µL of water prior to Porous Graphitized Carbon (PGC) nano-Liquid Chromatography (LC)-Electro Spray Ionization (ESI)-Mass Spectrometry (MS)/MS/MS analysis.

2.4. Analysis of GSL-Glycan Alditols Using PGC Nano-LC-ESI-MS/MS

The analysis of glycan alditols was performed using PGC nano-LC-ESI-MS/MS following a method described previously [45,46]. Measurements were performed on an Ultimate 3000 Ultra-High-Performance Liquid Chromatography (UHPLC) system (Thermo Fisher Scientific) equipped with a home-packed PGC trap column (5 µm Hypercarb, 320 µm × 30 mm) and a home-packed PGC nano-column (3 µm Hypercarb 100 µm × 150 mm) coupled to an amaZon ETD speed ion trap (Bruker, Bremen, Germany). Mobile phase A consisted of 10 mM ABC, while mobile phase B was 60% (*v*/*v*) acetonitrile/10 mM ABC. The trap column was packed with 5 µm particle size PGC stationary phase from Hypercarb PGC analytical column (size 100 × 4.6 mm, 5 µm particle size, Thermo), while the PGC nano-column was packed with 3 µm particle size PGC stationary phase from Hypercarb PGC analytical column (size 30 × 4.6 mm, 3 µm particle size, Thermo).

To analyze glycans, 2 µL injections were performed and trapping was achieved on the trap column using a 6 µL/min loading flow in 1% solvent B for 5 min. Separation was achieved with a linear gradient from 1% to 50% solvent B over 73 min, applied followed by a 10 min wash step using 95% of B at a 0.6 µL/min flow rate. The column was held at a constant temperature of 35 °C.

Ionization was achieved using the nanoBooster source (Bruker) with a capillary voltage of 1000 V applied and a dry gas temperature of 280 °C at 3 L/min and isopropanol enriched nitrogen at 3 psi. MS spectra were acquired within an *m/z* range of 340–1850 in enhanced mode using negative ion mode, smart parameter setting was set to *m/z* 900. MS/MS spectra were recorded using the top 3 highest intensity peaks.

Structures of detected glycans were studied by MS/MS in negative mode. Glycan structures were assigned based on the known MS/MS fragmentation patterns in negative-ion mode [47,48], elution order, and general glycobiological knowledge, with the help of Glycoworkbench [49] and Glycomod [50] software. To get an estimate of the glycan amount per cell, glycan intensity was normalized to the intensity of the internal standard GT1b. Then, assuming complete release of glycans and similar response factors between released glycan and GT1b standard, the number of glycans per cell was estimated.

Structures are depicted according to the Consortium of Functional Glycomics (CFG). Blue square is *N*-acetylglucosamine; yellow square is *N*-acetylgalactosamine; blue circle is glucose; yellow circle is galactose; red triangle is fucose; purple diamond is *N*-acetylneuraminic acid, grey diamond is *N*-glycolylneuraminic acid.

2.5. Statistical Analysis

All analyses and visualizations were performed using OriginPro 2019 software (OriginLab Corporation, Northampton, MA, USA). Paired Student *t*-test against the control group, both cell lines of a theoretical value of 1 (due to data normalization), were executed. Figures show the average mean with standard deviation (SD) and levels of significance are represented within the figures.

3. Results

3.1. Expression of Sialyltransferases in Meningioma Cell Lines

Since there is evidence that sialyltransferases have an impact on tumorigenesis, we analyzed benign (BEN-MEN-1) and malignant (IOMM-Lee) meningioma cell lines regarding differences in expression of sialyltransferases (Figure 2, Table 1). Figure 2A shows the expression of *ST3GAL1–6* in BEN-MEN-1 and IOMM-Lee. *ST3GAL1–ST3GAL3* and ST3GAL5–ST3GAL6 were detected in both cell lines. The band intensity of ST3GAL2 was higher in the malignant cell line compared with the benign cell line, whereas the *ST3GAL3, ST3GAL5–6* band intensities were higher in BEN-MEN-1 compared to the malignant cell

line. Agarose gel of *ST6GAL1–2* is shown in Figure 2B for both cell lines. *ST6GAL2* was only expressed in the benign cell line. In contrast, no differences could be found in terms of band intensity of *ST6GAL1* in both cell lines. The expression of *ST6GALNAC1–6* for both cell lines is shown in Figure 2C. In contrast to IOMM-Lee, a weak band in *ST6GALNAC2* was detectable in BEN-MEN-1. Expression of *ST6GALNAC4–6* was detectable in both cell lines. The band intensities of *ST6GALNAC5* and *ST6GALNAC6* were higher in IOMM-Lee compared to BEN-MEN-1. The expression of *ST8SIA1–6* in both cell lines is shown in Figure 2D. For *ST8SIA1–2* and *ST8SIA5–6*, the expression has been detected in both meningioma cell lines. In BEN-MEN-1, we observed a higher expression of *ST8SIA2* and *ST8SIA6* compared to the malignant cell line. Again, the band intensity of *ST8SIA5* was stronger in IOMM-Lee compared to the benign cell line.

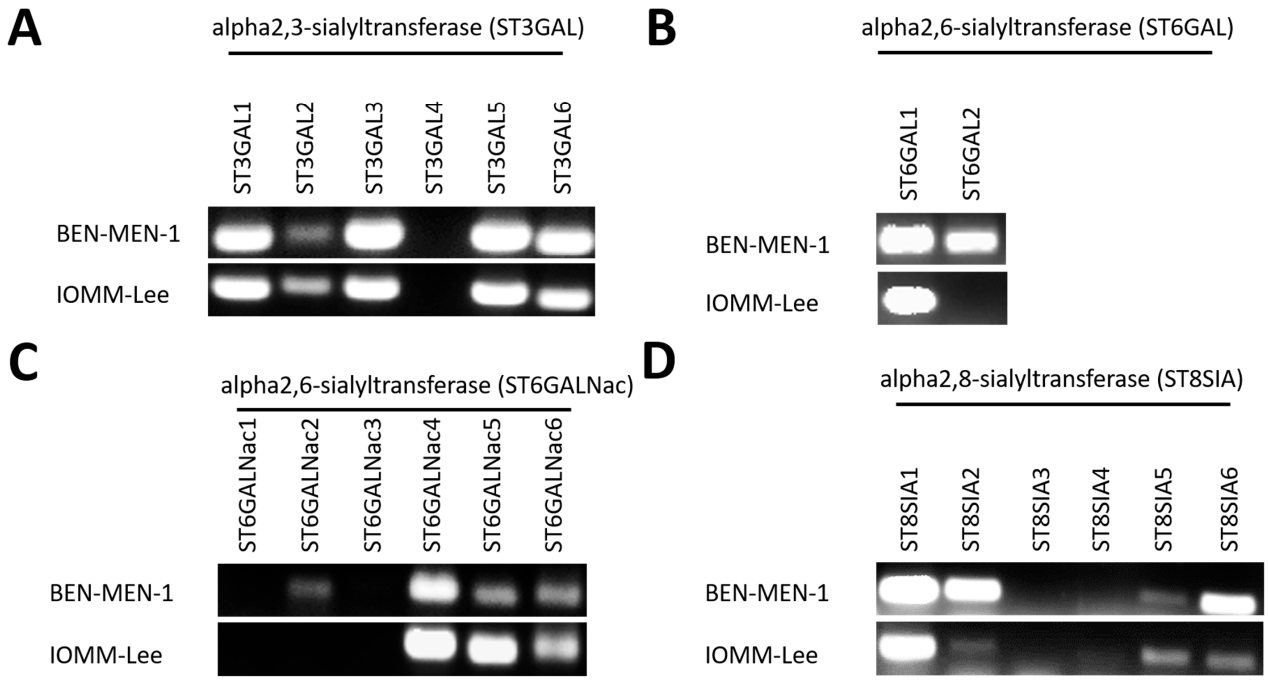

Figure 2. Expression of 20 Sialyltransferases (agarose gel) in BEN-MEN-1 and IOMM-Lee. (**A**): Expression of *ST3GAL1–6*. (**B**)**:** Expression of *ST6GAL1–2*. (**C**)**:** Expression of *ST6GALNAC1–6*. (**D**)**:** Expression of *ST8SIA1–6*.

3.2. Sialyltransferases Are More Affected by MGO in Benign Cell Line

Since the expression of sialyltransferases is different in the benign and malignant meningioma cell lines, we quantified the sialyltransferase mRNA expression level after 24 h of glycation of the cells to verify the influence of glycation on sialylation. Figure 3 displays the different mRNA expressions of *ST3GAL1–6* in BEN-MEN-1 (Figure 3A) and IOMM-Lee (Figure 3B). Glycation led to changes in ST expression. In the benign cell line, we observed an increased overall expression, whereas we noticed a decreased overall expression of STs in the malignant cell line. *ST3GAL1* (1.4812 ± 0.115 fold change), *ST3GAL2* (3.143 ± 0.476 fold change), and *ST3GAL3* (1.28 ± 0.189 fold change) expression were increased in contrast to non-glycated cells in BEN-MEN-1. Furthermore, the relative expression of *ST3GAL5* (0.7863 ± 0.0933 fold change) and *ST3GAL6* (0.572 ± 0.126 fold change) were decreased in contrast to non-glycated cells. The relative expression of *ST3GAL1* (0.601 ± 0.223 fold change), *ST3GAL2* (0.288 ± 0.0535 fold change), *ST3GAL3* (0.6175 ± 0.217 fold change), *ST3GAL5* (0.4561 ± 0.1271 fold change), *ST3GAL6* (0.502 ± 0.1325 fold change) were decreased in contrast to non-glycated cells in the malignant cell line.

Table 1. Overview of sialyltransferase expressions in both meningioma cell lines.

GENE	BEN-MEN-1	IOMM-Lee
ST3GAL1	+++	+++
ST3GAL2	+	++
ST3GAL3	+++	+++
ST3GAL4	-	-
ST3GAL5	+++	+++
ST3GAL6	+++	+++
ST6GAL1	+++	+++
ST6GAL2	++	-
ST6GALNAC1	-	-
ST6GALNAC2	+	-
ST6GALNAC3	-	-
ST6GALNAC4	+++	+++
ST6GALNAC5	++	+++
ST6GALNAC6	++	++
ST8SIA1	+++	+++
ST8SIA2	+++	+
ST8SIA3	-	-
ST8SIA4	-	-
ST8SIA5	+	+
ST8SIA6	+++	+

Table 1 shows overview of sialyltransferase expression in both meningioma cell lines. The expression levels are displayed in +++ = high expression level; ++ = middle expression level; + = low expression level; - = no expression.

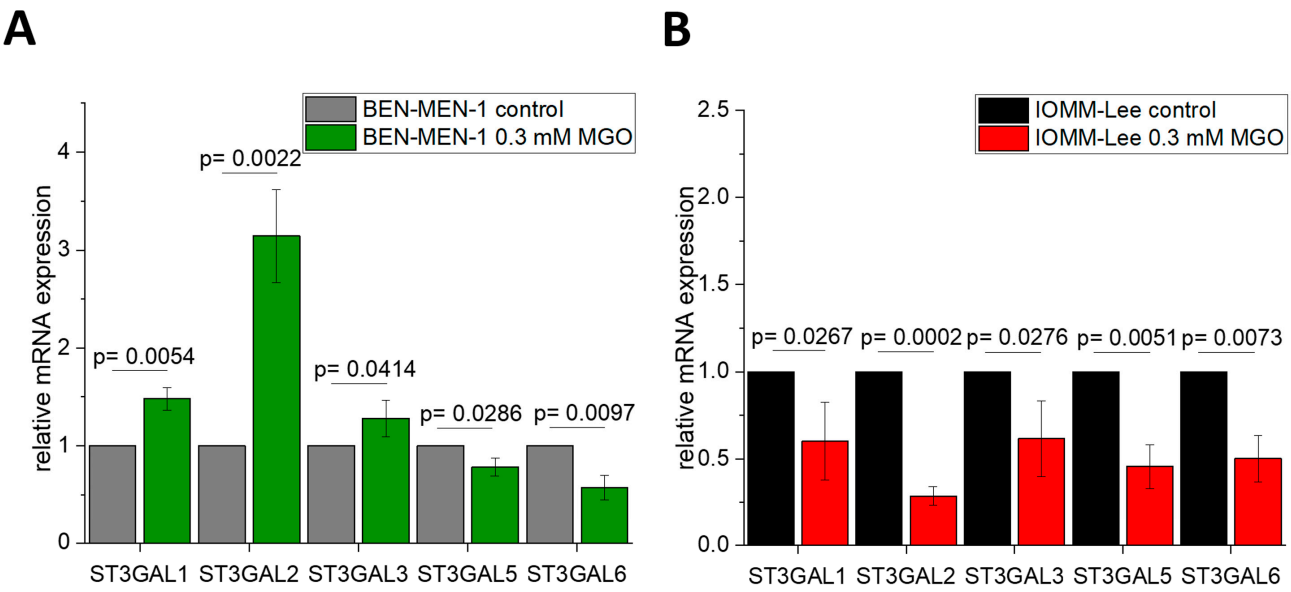

Figure 3. Relative mRNA expression of *ST3GAL1–6* in BEN-MEN-1 (**A**) and IOMM-Lee (**B**). (**A**): Normalized control (grey) and mRNA expression after 24 h treatment with 0.3 mM MGO (green). (**B**): Normalized control (black) and mRNA expression after 24 h treatment with 0.3 mM MGO (red). Statistical analysis was performed using *t*-test and error bars represent SD (n = 4; *ST3GAL1*: $p = 0.0054$ (**A**), $p = 0.0267$ (**B**); *ST3GAL2*: $p = 0.0022$ (**A**), $p = 0.0002$ (**B**); *ST3GAL3*: $p = 0.0414$ (**A**), $p = 0.0276$ (**B**); *ST3GAL5*: $p = 0.0286$ (**A**), $p = 0.0051$ (**B**); *ST3GAL6*: $p = 0.0097$ (**A**), $p = 0.0073$ (**B**)).

Figure 4 shows the expression of the *ST6GAL*-family in BEN-MEN-1 (Figure 4A) and IOMM-Lee (Figure 4B). Glycation led to opposing changes in the expression of this sialyltransferase. We observed a higher expression in the benign cell line after treatment with MGO (3.2402 ± 0.962 fold change), whereas no changes could be measured in the glycated malignant cell line (1.018 ± 0.164 fold change). The expression of *ST6GAL2* was only detected in BEN-MEN-1 and increased after treatment with MGO (1.624 ± 0.188 fold change).

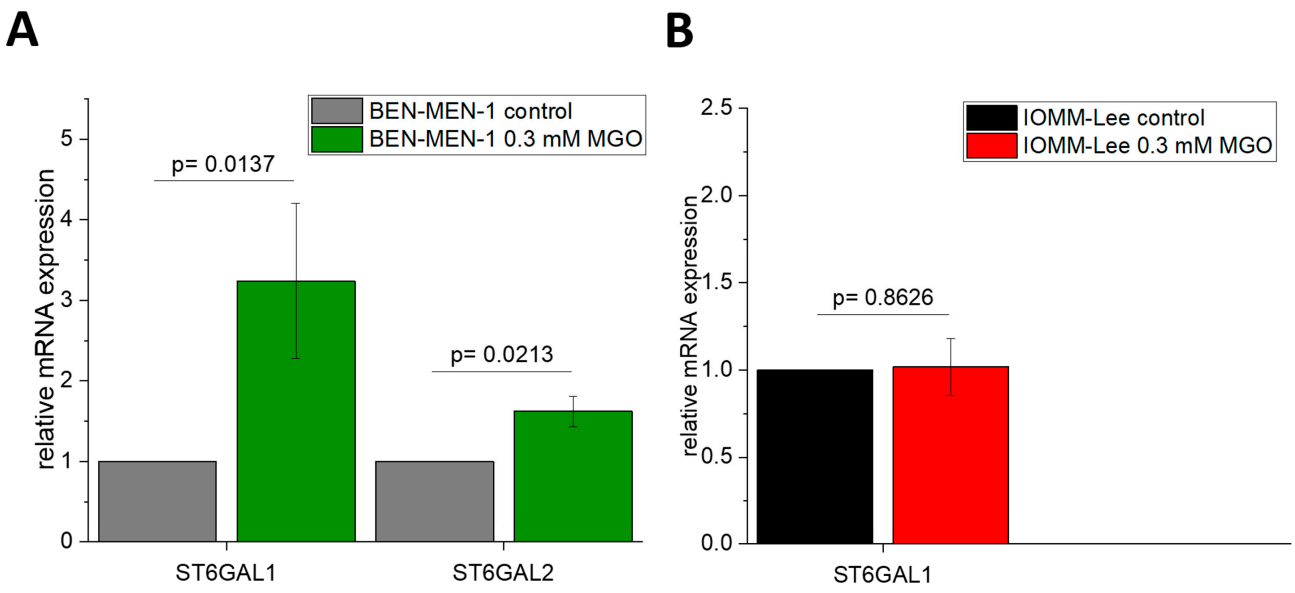

Figure 4. Relative mRNA expression of *ST6GAL1–2* in BEN-MEN-1 (**A**) and IOMM- Lee (**B**). (**A**): Normalized control (grey) and mRNA expression after 24 h treatment with 0.3 mM MGO (green). (**B**): Normalized control (black) and the mRNA expression after 24 h treatment with 0.3 mM MGO (red). Statistical analysis was performed using *t*-test and error bars represent SD (n = 4; *ST6GAL1*: p = 0.0274 (**A**), p = 0.863 (**B**); *ST6GAL2*: p = 0.0213 (**A**)).

Moreover, the mRNA expression of *ST6GALNAC1–6* in BEN-MEN-1 (Figure 5A) and IOMM-Lee (Figure 5B) is also differently altered after glycation. *ST6GALNAC2* expression decreased after glycation in contrast to the untreated benign cell line (0.6807 ± 0.1106 fold change). *ST6GALNAC4* expression is not affected in BEN-MEN-1 (2.556 ± 1.232 fold change) and IOMM-Lee (1.005 ± 0.2552 fold change), but glycation decreased the mRNA expression of *ST6GALNAC5* in both cell lines (0.5575 ± 0.283; 0.5991 ± 0.2174). Glycation led to a higher expression of *ST6GALNAC6* in the benign cell line (1.5141 ± 0.1999). *ST6GALNAC6* expression is not influenced by glycation in the malignant cell line (0.839 ± 0.203).

Finally, we quantified the expression of *ST8SIA 1–6*. Glycation influenced more strongly the expression level of these sialyltransferases in BEN-MEN-1 cells compared to the malignant IOMM-Lee cell line. The expression of *ST8SIA1* was highly increased (2.696 ± 0.627 fold change) after glycation in the benign cell line (Figure 6A) and decreased (0.744 ± 0.07712 fold change) in the glycated malignant cell line (Figure 6B). The expression of *ST8SIA2* (3.2171 ± 0.6837 fold change) and *ST8SIA5* (1.696 ± 0.3475 fold change) were both increased in BEN-MEN-1 (Figure 6A). *ST8SIA5* expression was not influenced by glycation in IOMM-Lee cells. The expression of *ST8SIA6* was not influenced by glycation in both cell lines.

3.3. MGO-Treatment Decreases Ganglioside GM3 Expression in BEN-MEN-1

To prove that MGO-induced reduction of ST3GAL5 expression has an impact on BEN-MEN-1 cells, we quantified ganglioside GM3 by PGC nano-LC-ESI-MS/MS. Figure 7A summarizes the biosynthesis of GM3. Figure 7B shows the signal intensity of GM3 before and after glycation in comparison to the internal standard of GT1b in BEN-MEN-1 cells. The absolute quantification of GM3 is shown in Figure 7C. We could show a decreased GM3 expression after glycation (p = 0.00314), which is in line with the decreasing expression of *ST3GAL5* (see: Figure 3A). The normalized copy numbers of GM3 per cell in the untreated BEN-MEN-1 cell line ($1.32 \times 10^8 \pm 9.15 \times 10^6$) were decreased by 235% compared to the glycated cells ($5.61 \times 10^7 \pm 3.89 \times 10^6$).

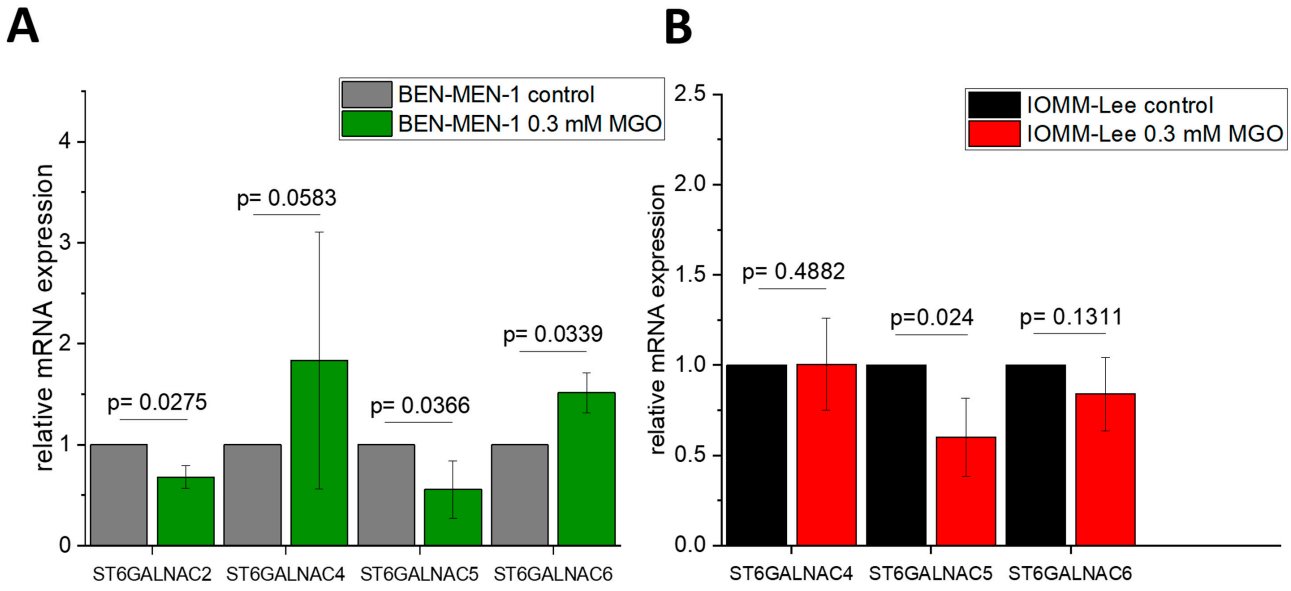

Figure 5. Relative mRNA expression of *ST6GALNAC1–6* in BEN-MEN-1 (**A**) and IOMM- Lee (**B**). (**A**): Normalized control (grey) and mRNA expression after 24 h treatment with 0.3 mM MGO (green). (**B**): Normalized control (black) and mRNA expression after 24 h treatment with 0.3 mM MGO (**red**). Statistical analysis was performed using *t*-test and error bars represent SD (n = 4; *ST6GALNAC2*: $p = 0.0275$ (**A**); *ST6GALNAC4*: $p = 0.0583$ (**A**), $p = 0.4882$ (**B**); *ST6GALNAC5*: $p = 0.0366$ (**A**), $p = 0.024$ (**B**); *ST6GALNAC6*: $p = 0.0339$ (**A**), $p = 0.1311$ (**B**)).

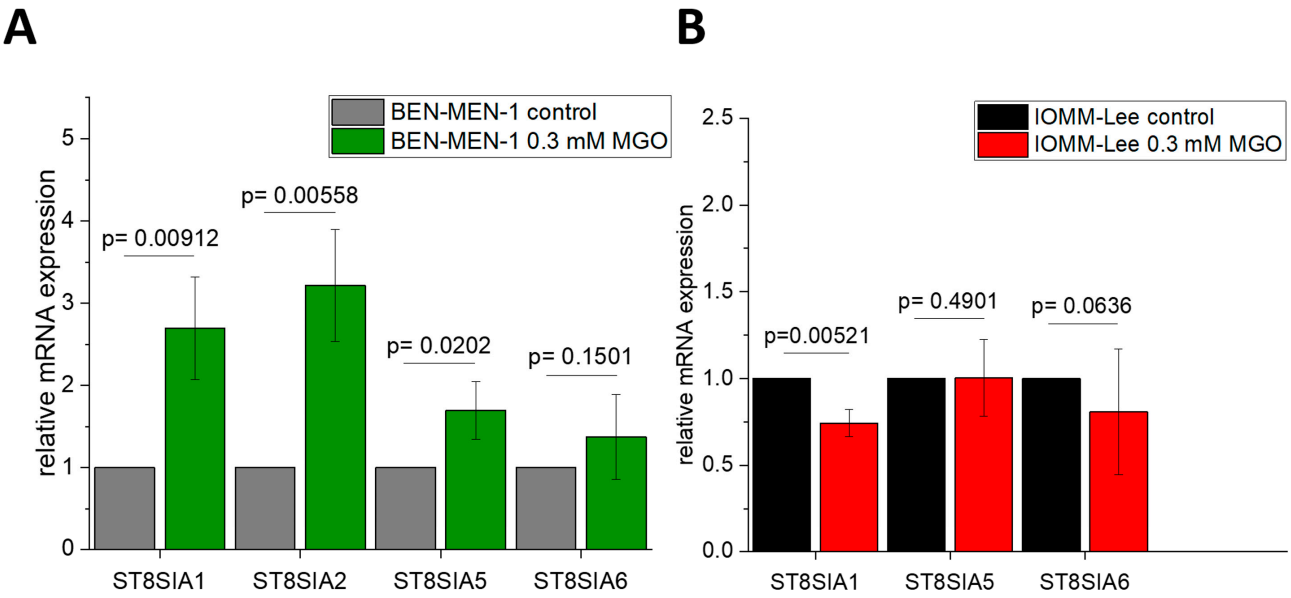

Figure 6. Relative mRNA expression of *ST8SIA1–6* in BEN-MEN-1 (**A**) and IOMM- Lee (**B**). (**A**): Normalized control (grey) and mRNA expression after 24 h treatment with 0.3 mM MGO (green). (**B**): Normalized control (black) and mRNA expression after 24 h treatment with 0.3 mM MGO (red). Statistical analysis was performed using *t*-test and error bars represent SD (n = 4; *ST8SIA1*: $p = 0.00912$ (**A**), $p = 0.00521$ (**B**); *ST8SIA2*: $p = 0.00558$ (**A**); *ST8SIA5*: $p = 0.0202$ (**A**), $p = 0.4901$ (**B**); *ST8SIA6*: $p = 0.1501$ (**A**), $p = 0.0636$ (**B**)).

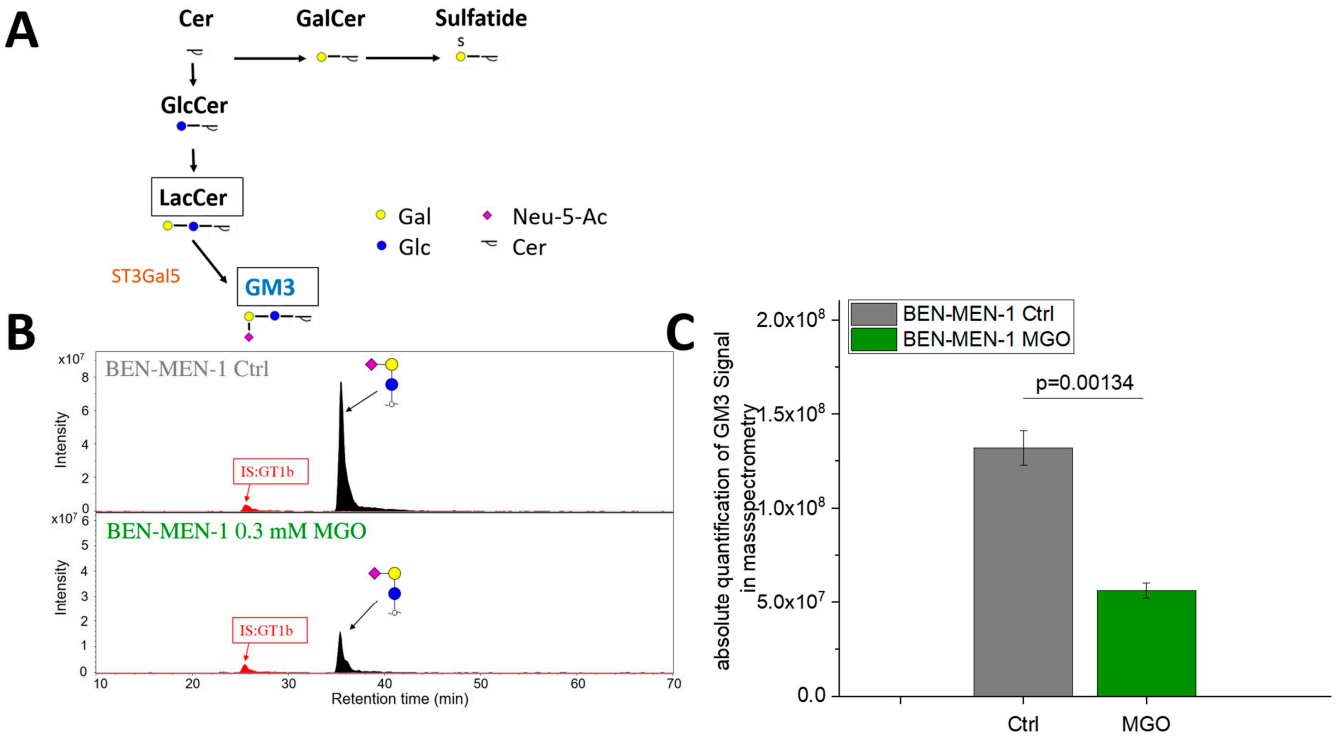

Figure 7. Absolute quantification of GM3 signal by PGC nano-LC-ESI-MS/MS. (**A**): Schematic representation of the GM3 biosynthesis. Cer = Ceramide; GalCer = Galactosylceramide; GlcCer = Glucosylceramide; LacCer = Lactosylceramide; GM3 = Monosialoganglioside 3. (**B**): Signal intensity of GM3 in BEN-MEN-1 Ctrl and BEN-MEN-1 0.3 mM MGO in comparison to the internal standard GT1b. (**C**): Absolute quantification of GM3 signal by PGC nano-LC-ESI-MS/MS of Ctrl (grey) and 0.3 mM MGO-treated BEN-MEN-1 (green). Statistical analysis was performed using *t*-test and error bars represent SD (n = 3; $p = 0.00134$).

3.4. Glyoxal-Treatment Has Different Effects in ST3GAL5

Finally, we analyzed whether another glycation agent than MGO has the same effect on *ST3GAL5* expression as MGO. We could show by Western blot analysis that 0.3 mM glyoxal (GO) leads to glycation in both cell lines (data not shown). Using qPCR of cDNA of BEN-MEN-1 cells (Figure 8A) or IOMM-Lee (Figure 8B), which were grown for 24 h in the presence of 0.3 mM GO, we could show that GO-induced glycation had the same effect on *ST3GAL5* expression as MGO treatment in BEN-MEN-1 cells. However, GO did not alter the expression of *ST3GAL5* in malignant IOMM-Lee cells, which is in contrast to MGO. This suggests a glycation agent-specific change of *ST3GAL5* expression.

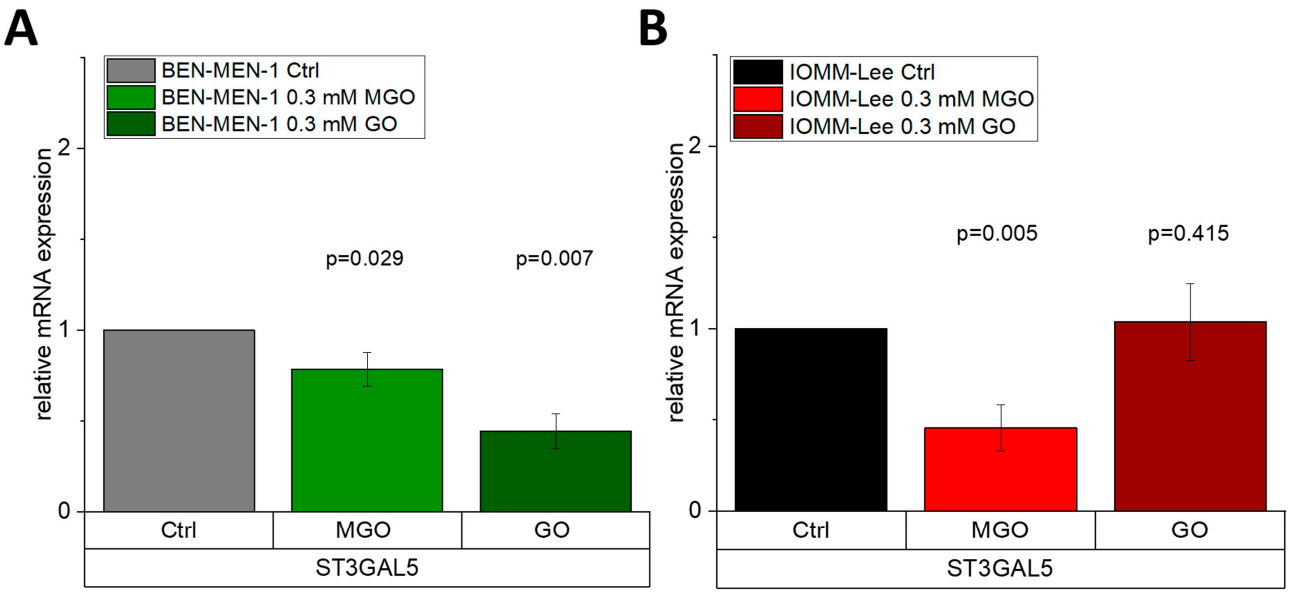

Figure 8. Relative mRNA expression of *ST3GAL5* in BEN-MEN-1 (**A**) and IOMM-Lee (**B**). A shows the relative expression of *ST3GAL5* in untreated (grey), 0.3 mM MGO (green)- and 0.3 mM GO (dark green)-treated BEN-MEN-1. B shows the relative expression of *ST3GAL5* in untreated (black), 0.3 mM MGO (red)- and 0.3 mM GO (dark red)-treated IOMM-Lee. Statistical analysis was performed using *t*-test and error bars represent SD (n = 4; *ST3GAL5* GO (**A**) $p = 0.007$; (**B**) $p = 0.415$).

4. Discussion

Many studies demonstrated that sialylation has an impact on tumorigenesis [51–55]. Abnormal levels of different glycosyltransferases were found in different types of human cancers [56,57]. In addition, high serum levels of sialyltransferases are associated with the progression of advanced breast cancer [58].

However, little is known about the influence on glycosylation by glycation, which is increased in several cancers because of the Warburg effect [59,60]. In this study, we could show, that glycation affects sialylation by modulating ST expression, which could have an impact on different ganglioside patterns and thereby on tumor development. Most of the STs were expressed in both BEN-MEN-1 and IOMM-Lee cell lines. Glycation of both cell lines resulted in an increasing level of STs in the benign meningioma cells and decreasing level in the malignant cells.

There are many reports of changes in ST expression in cancer. Overexpression of *ST3GAL1* in ovarian cancer led to transforming growth factor (TGF)-β1-induced epithelial-mesenchymal-transition, migration, and invasion, and a knockdown resulted in the opposite [61]. Another study by Mehta et al. has revealed that *ST3GAL2* and *ST6GAL1* were significantly upregulated in tumors with positive perineural invasion status [62], which we observed in the glycated benign cell line. *ST3GAL3* was increased in the glycated BEN-MEN-1 cell line but decreased in glycated IOMM-Lee cells. Expression of *ST3GAL3* is important for the regulation of biosynthesis of brain disialoganglioside (GD)1a and trisialoganglioside (GT)1b [57]. In several studies, the altered expression of *ST3GAL3* has an impact on cell adhesion and invasion. Glycation of meningioma cell lines resulted in decreased *ST3GAL5* expression in both cell lines. This sialyltransferase is also known as monosialoganglioside (GM3) synthase [63] and suppresses the epidermal growth factor receptor (EGFR) phosphorylation, which influences the cell proliferation [64] and the cellular resistance to oxidative stress and radiation therapy through upregulation of extracellular signal-regulated kinases (ERK) [42]. The total amount of GM3 was decreased in BEN-MEN-1 cells after glycation. Yamashita and colleagues reported that GM3 synthase knockout mice displayed enhanced ligand-induced insulin receptor phosphorylation. Furthermore, they could show that an increased sensitivity in glucose and insulin tolerance consequently results in an elevated insulin signaling response [65]. Other studies show that

decreasing expression of GM3 leads to decreased cell motility and cell adhesion through ERK phosphorylation along with Ras upregulation. This regulates migration through mitogen-activated protein kinase (MAPK) [41,42,66,67]. The glycating agent GO has the same effect in BEN-MEN-1 cells (downregulation of *ST3GAL5*) as MGO. However, in IOMM-Lee cells, we observed no effect after glycation with GO, which could be explained by higher glyoxalase 1 activity, which degrades dicarbonyls and has been described in many studies on cancer and glycation [68–70]. The expression of *ST3GAL6* was reduced in both glycated meningioma cell lines, which is known to play a key role in the generation of functional Sialyl Lewis X [71]. Decreasing levels of *ST3GAL6* can lead to decreasing migration and invasion in 5637 and J82 UBC cells as well as decreasing adhesion and migration in multiple myeloma cells [72,73].

Increased *ST6GAL1* expression, as we have shown in glycated BEN-MEN-1 cells, was also found in lung, colon, glioma, prostate, cervical, and breast cancer tissues [74–80]. The downregulation of *ST6GAL1* decreased metalloproteinases (MMPs) expression and suppressed invasive potential of A549 and H1299 cells in vitro [79], whereas bladder cancer has *ST6GAL1* upregulation, a tumor-suppressive role [81]. The upregulation of *ST6GAL2* was found in different types of cancer and was associated with breast cancer with higher expression of intracellular adhesion molecule (ICAM)-1, vascular adhesion molecule (VCAM)-1, CD24, MMP2, MMP9 and C-X-C motif chemokine receptor (CXCR)4 [82,83].

ST6GALNAC2 is known as a metastasis suppressor in breast cancer and a low expression of it, as we observed in glycated BEN-MEN-1 cells, is associated with a bad prognosis [84,85]. In Colorectal Carcinoma, Venkitachalam et al. have observed the same [86]. In contrast, Schneider et al. could show, that a high expression of *ST6GALNAC2* correlates with metastases to the lymph system [87]. The expression level may be a prognostic marker, but it seems that the mutation of the gene is more important. In our study, *ST6GALNAC4* expression was elevated in glycated BEN-MEN-1. High expression of *ST6GALNAC4* leads to the prevention of O-glycan chain elongation [88]. In another study of Follicular Thyroid Carcinoma (FTC)-238 cells, the suppression of the *ST6GALNAC4* gene led to an inhibition of invasive behavior in vitro and in vivo [89]. The lower expression of *ST6GALNAC5* in both glycated meningioma cell lines in our study could be a sign of transformation, because it is restricted to the brain and synthesizes GD1alpha in the nervous tissues [90,91]. We have observed an increased expression of *ST6GALNAC6* in glycated BEN-MEN-1 cells. A study in colon cancer has shown that *ST6GALNAC6* is responsible for the synthesis of sialyl Lewis (a), which is a significant inductive mechanism in cancer progression [92,93].

The increased expression of *ST8SIA1* in glycated BEN-MEN-1 cells could lead to a weak prognosis for patients. In contrast, we observed decreased expression of *ST8SIA1* after glycation in IOMM-Lee cells. In melanoma brain metastases, it was shown that *ST8SIA1* (GD3 synthases) is upregulated and the GD3 expression is increased, which was associated with a bad prognosis [94]. In gliomas, malignancy increased by higher GD3 and GD2 expression [95]. In addition, *ST8SIA1* is one of the key drivers for malignancy in glioblastoma [96]. Mennel et al. reported on different expression levels of GD3 and GD2 in meningiomas, depending on the tumor origin [97]. A study for neuroblastoma and melanoma cells demonstrated that most neuroblastoma cells had a high expression of GD2 and melanoma cells had high expression of GD3 [98]. The increased expression of *ST8SIA2*, as we observed in glycated BEN-MEN-1 cells, plays a role in the invasive behavior and was significantly associated with the risk of relapse in non-small-cell lung carcinoma [99]. The sialyltransferase ST8Sia5, which is increased in glycated BEN-MEN-1 cells, is known to synthesize GD1c/GT1a/Tetrasialogangliotetraosyl-ceramide (GQ)1b from GM1b/GD1a/GT1b. The group of Schiopu et al. has identified thirty-four distinct glycosphingolipid components (one GM4, nine GM3, two GM2, two GD3, nine GM1, and six GD1) differing in their ceramide compositions [100].

The glycation of meningioma cell lines has opposite effects in benign or malignant meningioma cells. Overall, glycated BEN-MEN-1 cells express more sialyltransferases than unglycated, whereas glycation of IOMM-Lee cells leads to a downregulation of the

sialyltransferase expression. These observations support our recent observations that glycation of BEN-MEN-1 cells lead to increased invasive potential [30].

5. Conclusions

To sum up, glycation of meningioma cell lines has cell line-specific effects. The glycated BEN-MEN-1 cell line is affected in a different expression of *ST3GAL1/2/3/5/6; ST6GAL1/2; ST6GALNAC2/6* and *ST8SIA1/2*. These STs have a direct or indirect impact on tumor progression. The decreased expression of *ST3GAL5* after glycation results in a decreasing expression of GM3 in benign meningioma cells. The expression levels of some sialyltransferases (*ST3GAL1/2/3; ST6GALNAC5* and *ST8SIA1*) of the glycated IOMM-Lee cell line were inhibited, which indicates less aggressive behavior.

Author Contributions: Conceptualization, P.S.; methodology, P.S., K.B., M.W. and T.Z.; software, K.B. and P.S.; validation, P.S.; formal analysis, P.S., M.W. and T.Z.; investigation, P.S.; resources, P.S., K.B. and R.H.; data curation, P.S.; writing—original draft preparation, P.S.; writing—review and editing, M.S., R.H. and P.S.; visualization, P.S. and M.S.; supervision, R.H. and C.S.; project administration, R.H., C.S. and M.S.; funding acquisition, R.H., M.S. and C.S. All authors have read and agreed to the published version of the manuscript.

Funding: This research was funded by the Wilhelm Roux Program, FKZ 31/21 and Deutsche Forschungsgemeinschaft (DFG, ProMoAge RTG 2155).

Institutional Review Board Statement: Not applicable.

Informed Consent Statement: Not applicable.

Data Availability Statement: The data presented in this study are available in this article.

Conflicts of Interest: The authors declare no conflict of interest. The funders had no role in the design of the study; in the collection, analyses, or interpretation of data; in the writing of the manuscript, or in the decision to publish the results.

References

1. Goldbrunner, R.; Minniti, G.; Preusser, M.; Jenkinson, M.D.; Sallabanda, K.; Houdart, E.; von Deimling, A.; Stavrinou, P.; Lefranc, F.; Lund-Johansen, M.; et al. EANO guidelines for the diagnosis and treatment of meningiomas. *Lancet Oncol.* **2016**, *17*, e383–e391. [CrossRef]
2. Ostrom, Q.T.; Gittleman, H.; Truitt, G.; Boscia, A.; Kruchko, C.; Barnholtz-Sloan, J.S. CBTRUS Statistical Report: Primary Brain and Other Central Nervous System Tumors Diagnosed in the United States in 2011–2015. *Neuro Oncol.* **2018**, *20*, iv1–iv86. [CrossRef]
3. Holleczek, B.; Zampella, D.; Urbschat, S.; Sahm, F.; von Deimling, A.; Oertel, J.; Ketter, R. Incidence, mortality and outcome of meningiomas: A population-based study from Germany. *Cancer Epidemiol.* **2019**, *62*, 101562. [CrossRef] [PubMed]
4. Ostrom, Q.T.; Cioffi, G.; Gittleman, H.; Patil, N.; Waite, K.; Kruchko, C.; Barnholtz-Sloan, J.S. CBTRUS Statistical Report: Primary Brain and Other Central Nervous System Tumors Diagnosed in the United States in 2012–2016. *Neuro Oncol.* **2019**, *21*, v1–v100. [CrossRef] [PubMed]
5. Maier, A.D.; Bartek, J.; Eriksson, F.; Ugleholdt, H.; Juhler, M.; Broholm, H.; Mathiesen, T.I. Clinical and histopathological predictors of outcome in malignant meningioma. *Neurosurg. Rev.* **2020**, *43*, 643–653. [CrossRef] [PubMed]
6. Buerki, R.A.; Horbinski, C.M.; Kruser, T.; Horowitz, P.M.; James, C.D.; Lukas, R.V. An overview of meningiomas. *Future Oncol.* **2018**, *14*, 2161–2177. [CrossRef]
7. Champeaux, C.; Jecko, V. World Health Organization grade III meningiomas. A retrospective study for outcome and prognostic factors assessment. *Neurochirurgie* **2016**, *62*, 203–208. [CrossRef]
8. Peyre, M.; Gauchotte, G.; Giry, M.; Froehlich, S.; Pallud, J.; Graillon, T.; Bielle, F.; Cazals-Hatem, D.; Varlet, P.; Figarella-Branger, D.; et al. De novo and secondary anaplastic meningiomas: A study of clinical and histomolecular prognostic factors. *Neuro Oncol.* **2018**, *20*, 1113–1121. [CrossRef]
9. Claus, E.B.; Bondy, M.L.; Schildkraut, J.M.; Wiemels, J.L.; Wrensch, M.; Black, P.M. Epidemiology of intracranial meningioma. *Neurosurgery* **2005**, *57*, 1088–1095. [CrossRef]
10. Pasquier, D.; Bijmolt, S.; Veninga, T.; Rezvoy, N.; Villa, S.; Krengli, M.; Weber, D.C.; Baumert, B.G.; Canyilmaz, E.; Yalman, D.; et al. Atypical and malignant meningioma: Outcome and prognostic factors in 119 irradiated patients. A multicenter, retrospective study of the Rare Cancer Network. *Int. J. Radiat. Oncol. Biol. Phys.* **2008**, *71*, 1388–1393. [CrossRef]
11. Allaman, I.; Bélanger, M.; Magistretti, P.J. Methylglyoxal, the dark side of glycolysis. *Front. Neurosci.* **2015**, *9*, 23. [CrossRef] [PubMed]

12. Bharadwaj, S.; Venkatraghavan, L.; Mariappan, R.; Ebinu, J.; Meng, Y.; Khan, O.; Tung, T.; Reyhani, S.; Bernstein, M.; Zadeh, G. Serum lactate as a potential biomarker of non-glial brain tumors. *J. Clin. Neurosci.* **2015**, *22*, 1625–1627. [CrossRef] [PubMed]
13. Gill, K.S.; Fernandes, P.; O'Donovan, T.R.; McKenna, S.L.; Doddakula, K.K.; Power, D.G.; Soden, D.M.; Forde, P.F. Glycolysis inhibition as a cancer treatment and its role in an anti-tumour immune response. *Biochim. Biophys. Acta* **2016**, *1866*, 87–105. [CrossRef]
14. Rabbani, N.; Thornalley, P.J. Dicarbonyl stress in cell and tissue dysfunction contributing to ageing and disease. *Biochem. Biophys. Res. Commun.* **2015**, *458*, 221–226. [CrossRef]
15. Giovannucci, E.; Harlan, D.M.; Archer, M.C.; Bergenstal, R.M.; Gapstur, S.M.; Habel, L.A.; Pollak, M.; Regensteiner, J.G.; Yee, D. Diabetes and cancer: A consensus report. *CA Cancer J. Clin.* **2010**, *60*, 207–221. [CrossRef] [PubMed]
16. Chowdhury, T.A. Diabetes and cancer. *QJM* **2010**, *103*, 905–915. [CrossRef]
17. Michaud, D.S.; Bové, G.; Gallo, V.; Schlehofer, B.; Tjønneland, A.; Olsen, A.; Overvad, K.; Dahm, C.C.; Teucher, B.; Boeing, H.; et al. Anthropometric measures, physical activity, and risk of glioma and meningioma in a large prospective cohort study. *Cancer Prev. Res.* **2011**, *4*, 1385–1392. [CrossRef]
18. Edlinger, M.; Strohmaier, S.; Jonsson, H.; Bjørge, T.; Manjer, J.; Borena, W.T.; Häggström, C.; Engeland, A.; Tretli, S.; Concin, H.; et al. Blood pressure and other metabolic syndrome factors and risk of brain tumour in the large population-based Me-Can cohort study. *J. Hypertens.* **2012**, *30*, 290–296. [CrossRef]
19. Schneider, B.; Pülhorn, H.; Röhrig, B.; Rainov, N.G. Predisposing conditions and risk factors for development of symptomatic meningioma in adults. *Cancer Detect. Prev.* **2005**, *29*, 440–447. [CrossRef]
20. Schwartzbaum, J.; Jonsson, F.; Ahlbom, A.; Preston-Martin, S.; Malmer, B.; Lönn, S.; Söderberg, K.; Feychting, M. Prior hospitalization for epilepsy, diabetes, and stroke and subsequent glioma and meningioma risk. *Cancer Epidemiol. Biomark. Prev.* **2005**, *14*, 643–650. [CrossRef]
21. Bernardo, B.M.; Orellana, R.C.; Weisband, Y.L.; Hammar, N.; Walldius, G.; Malmstrom, H.; Ahlbom, A.; Feychting, M.; Schwartzbaum, J. Association between prediagnostic glucose, triglycerides, cholesterol and meningioma, and reverse causality. *Br. J. Cancer* **2016**, *115*, 108–114. [CrossRef]
22. Nayeri, A.; Chotai, S.; Prablek, M.A.; Brinson, P.R.; Douleh, D.G.; Weaver, K.D.; Thompson, R.C.; Chambless, L. Type 2 diabetes is an independent negative prognostic factor in patients undergoing surgical resection of a WHO grade I meningioma. *Clin. Neurol. Neurosurg.* **2016**, *149*, 6–10. [CrossRef] [PubMed]
23. Ahmed, N. Advanced glycation endproducts–role in pathology of diabetic complications. *Diabetes Res. Clin. Pract.* **2005**, *67*, 3–21. [CrossRef] [PubMed]
24. Rabbani, N.; Thornalley, P.J. The dicarbonyl proteome: Proteins susceptible to dicarbonyl glycation at functional sites in health, aging, and disease. *Ann. N. Y. Acad. Sci.* **2008**, *1126*, 124–127. [CrossRef]
25. Thornalley, P.J.; Langborg, A.; Minhas, H.S. Formation of glyoxal, methylglyoxal and 3-deoxyglucosone in the glycation of proteins by glucose. *Biochem. J.* **1999**, *344 Pt 1*, 109–116. [CrossRef]
26. Brings, S.; Fleming, T.; Freichel, M.; Muckenthaler, M.U.; Herzig, S.; Nawroth, P.P. Dicarbonyls and Advanced Glycation End-Products in the Development of Diabetic Complications and Targets for Intervention. *Int. J. Mol. Sci.* **2017**, *18*, 984. [CrossRef] [PubMed]
27. Kalapos, M.P. Methylglyoxal and glucose metabolism: A historical perspective and future avenues for research. *Drug Metabol. Drug Interact.* **2008**, *23*, 69–91. [CrossRef] [PubMed]
28. Falone, S.; D'Alessandro, A.; Mirabilio, A.; Petruccelli, G.; Cacchio, M.; Di Ilio, C.; Di Loreto, S.; Amicarelli, F. Long term running biphasically improves methylglyoxal-related metabolism, redox homeostasis and neurotrophic support within adult mouse brain cortex. *PLoS ONE* **2012**, *7*, e31401. [CrossRef]
29. Schalkwijk, C.G. Vascular AGE-ing by methylglyoxal: The past, the present and the future. *Diabetologia* **2015**, *58*, 1715–1719. [CrossRef]
30. Selke, P.; Rosenstock, P.; Bork, K.; Strauss, C.; Horstkorte, R.; Scheer, M. Glycation of benign meningioma cells leads to increased invasion. *Biol. Chem.* **2021**. [CrossRef]
31. Bellahcène, A.; Nokin, M.-J.; Castronovo, V.; Schalkwijk, C. Methylglyoxal-derived stress: An emerging biological factor involved in the onset and progression of cancer. *Semin. Cancer Biol.* **2018**, *49*, 64–74. [CrossRef] [PubMed]
32. Antognelli, C.; Moretti, S.; Frosini, R.; Puxeddu, E.; Sidoni, A.; Talesa, V.N. Methylglyoxal Acts as a Tumor-Promoting Factor in Anaplastic Thyroid Cancer. *Cells* **2019**, *8*, 547. [CrossRef] [PubMed]
33. Takashima, S.; Tsuji, S.; Tsujimoto, M. Characterization of the second type of human beta-galactoside alpha 2,6-sialyltransferase (ST6Gal II), which sialylates Galbeta 1,4GlcNAc structures on oligosaccharides preferentially. Genomic analysis of human sialyltransferase genes. *J. Biol. Chem.* **2002**, *277*, 45719–45728. [CrossRef] [PubMed]
34. Comb, D.G.; Roseman, S. The sialic acids. I. The structure and enzymatic synthesis of N-acetylneuraminic acid. *J. Biol. Chem.* **1960**, *235*, 2529–2537. [CrossRef]
35. Stäsche, R.; Hinderlich, S.; Weise, C.; Effertz, K.; Lucka, L.; Moormann, P.; Reutter, W. A bifunctional enzyme catalyzes the first two steps in N-acetylneuraminic acid biosynthesis of rat liver. Molecular cloning and functional expression of UDP-N-acetylglucosamine 2-epimerase/N-acetylmannosamine kinase. *J. Biol. Chem.* **1997**, *272*, 24319–24324. [CrossRef]
36. Harduin-Lepers, A.; Vallejo-Ruiz, V.; Krzewinski-Recchi, M.-A.; Samyn-Petit, B.; Julien, S.; Delannoy, P. The human sialyltransferase family. *Biochimie* **2001**, *83*, 727–737. [CrossRef]

37. Datta, A.K. Comparative sequence analysis in the sialyltransferase protein family: Analysis of motifs. *Curr. Drug Targets* **2009**, *10*, 483–498. [CrossRef]
38. Lau, K.S.; Partridge, E.A.; Grigorian, A.; Silvescu, C.I.; Reinhold, V.N.; Demetriou, M.; Dennis, J.W. Complex N-glycan number and degree of branching cooperate to regulate cell proliferation and differentiation. *Cell* **2007**, *129*, 123–134. [CrossRef]
39. Taganna, J.; de Boer, A.R.; Wuhrer, M.; Bouckaert, J. Glycosylation changes as important factors for the susceptibility to urinary tract infection. *Biochem. Soc. Trans.* **2011**, *39*, 349–354. [CrossRef]
40. Uemura, S.; Go, S.; Shishido, F.; Inokuchi, J.-i. Expression machinery of GM4: The excess amounts of GM3/GM4S synthase (ST3GAL5) are necessary for GM4 synthesis in mammalian cells. *Glycoconj. J.* **2014**, *31*, 101–108. [CrossRef]
41. Hakomori, S.-I.; Handa, K. GM3 and cancer. *Glycoconj. J.* **2015**, *32*, 1–8. [CrossRef] [PubMed]
42. Shimizu, T.; Nagane, M.; Suzuki, M.; Yamauchi, A.; Kato, K.; Kawashima, N.; Nemoto, Y.; Maruo, T.; Kawakami, Y.; Yamashita, T. Tumor hypoxia regulates ganglioside GM3 synthase, which contributes to oxidative stress resistance in malignant melanoma. *Biochim. Biophys. Acta Gen. Subj.* **2020**, *1864*, 129723. [CrossRef]
43. Inokuchi, J.-i.; Inamori, K.-I.; Kabayama, K.; Nagafuku, M.; Uemura, S.; Go, S.; Suzuki, A.; Ohno, I.; Kanoh, H.; Shishido, F. Biology of GM3 Ganglioside. *Prog. Mol. Biol. Transl. Sci.* **2018**, *156*, 151–195. [CrossRef] [PubMed]
44. Rosenstock, P.; Bork, K.; Massa, C.; Selke, P.; Seliger, B.; Horstkorte, R. Sialylation of Human Natural Killer (NK) Cells is Regulated by IL-2. *J. Clin. Med.* **2020**, *9*, 1816. [CrossRef] [PubMed]
45. Zhang, T.; van Die, I.; Tefsen, B.; van Vliet, S.J.; Laan, L.C.; Zhang, J.; ten Dijke, P.; Wuhrer, M.; Belo, A.I. Differential O- and Glycosphingolipid Glycosylation in Human Pancreatic Adenocarcinoma Cells With Opposite Morphology and Metastatic Behavior. *Front. Oncol.* **2020**, *10*, 732. [CrossRef]
46. Jensen, P.H.; Karlsson, N.G.; Kolarich, D.; Packer, N.H. Structural analysis of N- and O-glycans released from glycoproteins. *Nat. Protoc.* **2012**, *7*, 1299–1310. [CrossRef]
47. Anugraham, M.; Everest-Dass, A.V.; Jacob, F.; Packer, N.H. A platform for the structural characterization of glycans enzymatically released from glycosphingolipids extracted from tissue and cells. *Rapid Commun. Mass Spectrom.* **2015**, *29*, 545–561. [CrossRef]
48. Karlsson, N.G.; Wilson, N.L.; Wirth, H.-J.; Dawes, P.; Joshi, H.; Packer, N.H. Negative ion graphitised carbon nano-liquid chromatography/mass spectrometry increases sensitivity for glycoprotein oligosaccharide analysis. *Rapid Commun. Mass Spectrom.* **2004**, *18*, 2282–2292. [CrossRef]
49. Ceroni, A.; Maass, K.; Geyer, H.; Geyer, R.; Dell, A.; Haslam, S.M. GlycoWorkbench: A tool for the computer-assisted annotation of mass spectra of glycans. *J. Proteome Res.* **2008**, *7*, 1650–1659. [CrossRef]
50. Cooper, C.A.; Gasteiger, E.; Packer, N.H. GlycoMod—A software tool for determining glycosylation compositions from mass spectrometric data. *Proteomics* **2001**, *1*, 340–349. [CrossRef]
51. Pihikova, D.; Kasak, P.; Kubanikova, P.; Sokol, R.; Tkac, J. Aberrant sialylation of a prostate-specific antigen: Electrochemical label-free glycoprofiling in prostate cancer serum samples. *Anal. Chim. Acta* **2016**, *934*, 72–79. [CrossRef]
52. Yoneyama, T.; Ohyama, C.; Hatakeyama, S.; Narita, S.; Habuchi, T.; Koie, T.; Mori, K.; Hidari, K.I.P.J.; Yamaguchi, M.; Suzuki, T.; et al. Measurement of aberrant glycosylation of prostate specific antigen can improve specificity in early detection of prostate cancer. *Biochem. Biophys. Res. Commun.* **2014**, *448*, 390–396. [CrossRef]
53. Vučković, F.; Theodoratou, E.; Thaçi, K.; Timofeeva, M.; Vojta, A.; Štambuk, J.; Pučić-Baković, M.; Rudd, P.M.; Đerek, L.; Servis, D.; et al. IgG Glycome in Colorectal Cancer. *Clin. Cancer Res.* **2016**, *22*, 3078–3086. [CrossRef] [PubMed]
54. Fleming, S.C.; Smith, S.; Knowles, D.; Skillen, A.; Self, C.H. Increased sialylation of oligosaccharides on IgG paraproteins–A potential new tumour marker in multiple myeloma. *J. Clin. Pathol.* **1998**, *51*, 825–830. [CrossRef] [PubMed]
55. Saldova, R.; Wormald, M.R.; Dwek, R.A.; Rudd, P.M. Glycosylation changes on serum glycoproteins in ovarian cancer may contribute to disease pathogenesis. *Dis. Markers* **2008**, *25*, 219–232. [CrossRef]
56. Suzuki, O.; Abe, M.; Hashimoto, Y. Sialylation by β-galactoside α-2,6-sialyltransferase and N-glycans regulate cell adhesion and invasion in human anaplastic large cell lymphoma. *Int. J. Oncol.* **2015**, *46*, 973–980. [CrossRef] [PubMed]
57. Cui, H.-X.; Wang, H.; Wang, Y.; Song, J.; Tian, H.; Xia, C.; Shen, Y. ST3Gal III modulates breast cancer cell adhesion and invasion by altering the expression of invasion-related molecules. *Oncol. Rep.* **2016**, *36*, 3317–3324. [CrossRef]
58. Dao, T.L.; Ip, C.; Patel, J. Serum sialyltransferase and 5′-nucleotidase as reliable biomarkers in women with breast cancer. *J. Natl. Cancer Inst.* **1980**, *65*, 529–534.
59. Ahmad, S.; Khan, H.; Siddiqui, Z.; Khan, M.Y.; Rehman, S.; Shahab, U.; Godovikova, T.; Silnikov, V. AGEs, RAGEs and s-RAGE; friend or foe for cancer. *Semin. Cancer Biol.* **2018**, *49*, 44–55. [CrossRef]
60. Bellier, J.; Nokin, M.-J.; Lardé, E.; Karoyan, P.; Peulen, O.; Castronovo, V.; Bellahcène, A. Methylglyoxal, a potent inducer of AGEs, connects between diabetes and cancer. *Diabetes Res. Clin. Pract.* **2019**, *148*, 200–211. [CrossRef]
61. Wu, X.; Zhao, J.; Ruan, Y.; Sun, L.; Xu, C.; Jiang, H. Sialyltransferase ST3GAL1 promotes cell migration, invasion, and TGF-β1-induced EMT and confers paclitaxel resistance in ovarian cancer. *Cell Death Dis.* **2018**, *9*, 1102. [CrossRef] [PubMed]
62. Mehta, K.A.; Patel, K.A.; Pandya, S.J.; Patel, P.S. Aberrant sialylation plays a significant role in oral squamous cell carcinoma progression. *J. Oral Pathol. Med.* **2020**, *49*, 253–259. [CrossRef] [PubMed]
63. Trinchera, M.; Parini, R.; Indellicato, R.; Domenighini, R.; dall'Olio, F. Diseases of ganglioside biosynthesis: An expanding group of congenital disorders of glycosylation. *Mol. Genet. Metab.* **2018**, *124*, 230–237. [CrossRef]
64. Kawashima, N.; Nishimiya, Y.; Takahata, S.; Nakayama, K.-I. Induction of Glycosphingolipid GM3 Expression by Valproic Acid Suppresses Cancer Cell Growth. *J. Biol. Chem.* **2016**, *291*, 21424–21433. [CrossRef]

65. Yamashita, T.; Hashiramoto, A.; Haluzik, M.; Mizukami, H.; Beck, S.; Norton, A.; Kono, M.; Tsuji, S.; Daniotti, J.L.; Werth, N.; et al. Enhanced insulin sensitivity in mice lacking ganglioside GM3. *Proc. Natl. Acad. Sci. USA* **2003**, *100*, 3445–3449. [CrossRef]
66. Kojima, N.; Hakomori, S. Cell adhesion, spreading, and motility of GM3-expressing cells based on glycolipid-glycolipid interaction. *J. Biol. Chem.* **1991**, *266*, 17552–17558. [CrossRef]
67. Hashiramoto, A.; Mizukami, H.; Yamashita, T. Ganglioside GM3 promotes cell migration by regulating MAPK and c-Fos/AP-1. *Oncogene* **2006**, *25*, 3948–3955. [CrossRef] [PubMed]
68. Hu, X.; Yang, X.; He, Q.; Chen, Q.; Yu, L. Glyoxalase 1 is up-regulated in hepatocellular carcinoma and is essential for HCC cell proliferation. *Biotechnol. Lett.* **2014**, *36*, 257–263. [CrossRef] [PubMed]
69. Peng, H.-T.; Chen, J.; Liu, T.-Y.; Wu, Y.-Q.; Lin, X.-H.; Lai, Y.-H.; Huang, Y.-F. Up-regulation of the tumor promoter Glyoxalase-1 indicates poor prognosis in breast cancer. *Int. J. Clin. Exp. Pathol.* **2017**, *10*, 10852–10862.
70. Burdelski, C.; Shihada, R.; Hinsch, A.; Angerer, A.; Göbel, C.; Friedrich, E.; Hube-Magg, C.; Burdak-Rothkamm, S.; Kluth, M.; Simon, R.; et al. High-Level Glyoxalase 1 (GLO1) expression is linked to poor prognosis in prostate cancer. *Prostate* **2017**, *77*, 1528–1538. [CrossRef]
71. Chachadi, V.B.; Bhat, G.; Cheng, P.-W. Glycosyltransferases involved in the synthesis of MUC-associated metastasis-promoting selectin ligands. *Glycobiology* **2015**, *25*, 963–975. [CrossRef]
72. Dalangood, S.; Zhu, Z.; Ma, Z.; Li, J.; Zeng, Q.; Yan, Y.; Shen, B.; Yan, J.; Huang, R. Identification of glycogene-type and validation of ST3GAL6 as a biomarker predicts clinical outcome and cancer cell invasion in urinary bladder cancer. *Theranostics* **2020**, *10*, 10078–10091. [CrossRef]
73. Glavey, S.V.; Manier, S.; Natoni, A.; Sacco, A.; Moschetta, M.; Reagan, M.R.; Murillo, L.S.; Sahin, I.; Wu, P.; Mishima, Y.; et al. The sialyltransferase ST3GAL6 influences homing and survival in multiple myeloma. *Blood* **2014**, *124*, 1765–1776. [CrossRef] [PubMed]
74. Lin, S.; Kemmner, W.; Grigull, S.; Schlag, P.M. Cell surface alpha 2,6 sialylation affects adhesion of breast carcinoma cells. *Exp. Cell Res.* **2002**, *276*, 101–110. [CrossRef] [PubMed]
75. Lu, J.; Isaji, T.; Im, S.; Fukuda, T.; Hashii, N.; Takakura, D.; Kawasaki, N.; Gu, J. β-Galactoside α2,6-sialyltranferase 1 promotes transforming growth factor-β-mediated epithelial-mesenchymal transition. *J. Biol. Chem.* **2014**, *289*, 34627–34641. [CrossRef]
76. Swindall, A.F.; Bellis, S.L. Sialylation of the Fas death receptor by ST6Gal-I provides protection against Fas-mediated apoptosis in colon carcinoma cells. *J. Biol. Chem.* **2011**, *286*, 22982–22990. [CrossRef]
77. Wang, P.-H.; Lee, W.-L.; Lee, Y.-R.; Juang, C.-M.; Chen, Y.-J.; Chao, H.-T.; Tsai, Y.-C.; Yuan, C.-C. Enhanced expression of α 2,6-sialyltransferase ST6Gal I in cervical squamous cell carcinoma. *Gynecol. Oncol.* **2003**, *89*, 395–401. [CrossRef]
78. Wei, A.; Fan, B.; Zhao, Y.; Zhang, H.; Wang, L.; Yu, X.; Yuan, Q.; Yang, D.; Wang, S. ST6Gal-I overexpression facilitates prostate cancer progression via the PI3K/Akt/GSK-3β/β-catenin signaling pathway. *Oncotarget* **2016**, *7*, 65374–65388. [CrossRef] [PubMed]
79. Yuan, Q.; Chen, X.; Han, Y.; Lei, T.; Wu, Q.; Yu, X.; Wang, L.; Fan, Z.; Wang, S. Modification of α2,6-sialylation mediates the invasiveness and tumorigenicity of non-small cell lung cancer cells in vitro and in vivo via Notch1/Hes1/MMPs pathway. *Int. J. Cancer* **2018**, *143*, 2319–2330. [CrossRef]
80. Yamamoto, H.; Oviedo, A.; Sweeley, C.; Saito, T.; Moskal, J.R. Alpha2,6-sialylation of cell-surface N-glycans inhibits glioma formation in vivo. *Cancer Res.* **2001**, *61*, 6822–6829.
81. Antony, P.; Rose, M.; Heidenreich, A.; Knüchel, R.; Gaisa, N.T.; Dahl, E. Epigenetic inactivation of ST6GAL1 in human bladder cancer. *BMC Cancer* **2014**, *14*, 901. [CrossRef] [PubMed]
82. Cheng, J.; Wang, R.; Zhong, G.; Chen, X.; Cheng, Y.; Li, W.; Yang, Y. ST6GAL2 Downregulation Inhibits Cell Adhesion and Invasion and is Associated with Improved Patient Survival in Breast Cancer. *Onco. Targets. Ther.* **2020**, *13*, 903–914. [CrossRef] [PubMed]
83. Xu, G.; Chen, J.; Wang, G.; Xiao, J.; Zhang, N.; Chen, Y.; Yu, H.; Wang, G.; Zhao, Y. Resveratrol Inhibits the Tumorigenesis of Follicular Thyroid Cancer via ST6GAL2-Regulated Activation of the Hippo Signaling Pathway. *Mol. Ther. Oncolytics* **2020**, *16*, 124–133. [CrossRef] [PubMed]
84. Ferrer, C.M.; Reginato, M.J. Sticking to sugars at the metastatic site: Sialyltransferase ST6GalNAc2 acts as a breast cancer metastasis suppressor. *Cancer Discov.* **2014**, *4*, 275–277. [CrossRef]
85. Murugaesu, N.; Iravani, M.; van Weverwijk, A.; Ivetic, A.; Johnson, D.A.; Antonopoulos, A.; Fearns, A.; Jamal-Hanjani, M.; Sims, D.; Fenwick, K.; et al. An in vivo functional screen identifies ST6GalNAc2 sialyltransferase as a breast cancer metastasis suppressor. *Cancer Discov.* **2014**, *4*, 304–317. [CrossRef]
86. Venkitachalam, S.; Revoredo, L.; Varadan, V.; Fecteau, R.E.; Ravi, L.; Lutterbaugh, J.; Markowitz, S.D.; Willis, J.E.; Gerken, T.A.; Guda, K. Biochemical and functional characterization of glycosylation-associated mutational landscapes in colon cancer. *Sci. Rep.* **2016**, *6*, 23642. [CrossRef]
87. Schneider, F.; Kemmner, W.; Haensch, W.; Franke, G.; Gretschel, S.; Karsten, U.; Schlag, P.M. Overexpression of sialyltransferase CMP-sialic acid:Galbeta1,3GalNAc-R alpha6-Sialyltransferase is related to poor patient survival in human colorectal carcinomas. *Cancer Res.* **2001**, *61*, 4605–4611.
88. Reticker-Flynn, N.E.; Bhatia, S.N. Aberrant glycosylation promotes lung cancer metastasis through adhesion to galectins in the metastatic niche. *Cancer Discov.* **2015**, *5*, 168–181. [CrossRef]

89. Miao, X.; Jia, L.; Zhou, H.; Song, X.; Zhou, M.; Xu, J.; Zhao, L.; Feng, X.; Zhao, Y. miR-4299 mediates the invasive properties and tumorigenicity of human follicular thyroid carcinoma by targeting ST6GALNAC4. *IUBMB Life* **2016**, *68*, 136–144. [CrossRef]
90. Bos, P.D.; Zhang, X.H.-F.; Nadal, C.; Shu, W.; Gomis, R.R.; Nguyen, D.X.; Minn, A.J.; van de Vijver, M.J.; Gerald, W.L.; Foekens, J.A.; et al. Genes that mediate breast cancer metastasis to the brain. *Nature* **2009**, *459*, 1005–1009. [CrossRef]
91. Okajima, T.; Fukumoto, S.; Ito, H.; Kiso, M.; Hirabayashi, Y.; Urano, T.; Furukawa, K. Molecular cloning of brain-specific GD1alpha synthase (ST6GalNAc V) containing CAG/Glutamine repeats. *J. Biol. Chem.* **1999**, *274*, 30557–30562. [CrossRef] [PubMed]
92. Kannagi, R. Carbohydrate antigen sialyl Lewis a–its pathophysiological significance and induction mechanism in cancer progression. *Chang Gung Med. J.* **2007**, *30*, 189–209.
93. Tsuchida, A.; Okajima, T.; Furukawa, K.; Ando, T.; Ishida, H.; Yoshida, A.; Nakamura, Y.; Kannagi, R.; Kiso, M.; Furukawa, K. Synthesis of disialyl Lewis a (Le(a)) structure in colon cancer cell lines by a sialyltransferase, ST6GalNAc VI, responsible for the synthesis of alpha-series gangliosides. *J. Biol. Chem.* **2003**, *278*, 22787–22794. [CrossRef]
94. Ramos, R.I.; Bustos, M.A.; Wu, J.; Jones, P.; Chang, S.C.; Kiyohara, E.; Tran, K.; Zhang, X.; Stern, S.L.; Izraely, S.; et al. Upregulation of cell surface GD3 ganglioside phenotype is associated with human melanoma brain metastasis. *Mol. Oncol.* **2020**, *14*, 1760–1778. [CrossRef]
95. Iwasawa, T.; Zhang, P.; Ohkawa, Y.; Momota, H.; Wakabayashi, T.; Ohmi, Y.; Bhuiyan, R.H.; Furukawa, K.; Furukawa, K. Enhancement of malignant properties of human glioma cells by ganglioside GD3/GD2. *Int. J. Oncol.* **2018**, *52*, 1255–1266. [CrossRef] [PubMed]
96. Yeh, S.-C.; Wang, P.-Y.; Lou, Y.-W.; Khoo, K.-H.; Hsiao, M.; Hsu, T.-L.; Wong, C.-H. Glycolipid GD3 and GD3 synthase are key drivers for glioblastoma stem cells and tumorigenicity. *Proc. Natl. Acad. Sci. USA* **2016**, *113*, 5592–5597. [CrossRef] [PubMed]
97. Mennel, H.D.; Bosslet, K.; Geissel, H.; Bauer, B.L. Immunohistochemically visualized localisation of gangliosides Glac2 (GD3) and Gtri2 (GD2) in cells of human intracranial tumors. *Exp. Toxicol. Pathol.* **2000**, *52*, 277–285. [CrossRef]
98. Ruan, S.; Raj, B.K.; Lloyd, K.O. Relationship of glycosyltransferases and mRNA levels to ganglioside expression in neuroblastoma and melanoma cells. *J. Neurochem.* **1999**, *72*, 514–521. [CrossRef] [PubMed]
99. Hao, J.; Zeltz, C.; Pintilie, M.; Li, Q.; Sakashita, S.; Wang, T.; Cabanero, M.; Martins-Filho, S.N.; Wang, D.Y.; Pasko, E.; et al. Characterization of Distinct Populations of Carcinoma-Associated Fibroblasts from Non-Small Cell Lung Carcinoma Reveals a Role for ST8SIA2 in Cancer Cell Invasion. *Neoplasia* **2019**, *21*, 482–493. [CrossRef]
100. Schiopu, C.; Vukelić, Z.; Capitan, F.; Kalanj-Bognar, S.; Sisu, E.; Zamfir, A.D. Chip-nanoelectrospray quadrupole time-of-flight tandem mass spectrometry of meningioma gangliosides: A preliminary study. *Electrophoresis* **2012**, *33*, 1778–1786. [CrossRef]

cells

MDPI

Article

Glycation Leads to Increased Invasion of Glioblastoma Cells

Paola Schildhauer [1], Philipp Selke [2], Christian Scheller [1], Christian Strauss [1], Rüdiger Horstkorte [2], Sandra Leisz [1,†] and Maximilian Scheer [1,*,†]

[1] Department of Neurosurgery, Medical Faculty, Martin-Luther-University Halle-Wittenberg, Ernst-Grube-Str. 40, 06120 Halle (Saale), Germany
[2] Institute for Physiological Chemistry, Medical Faculty, Martin-Luther-University Halle-Wittenberg, 06114 Halle (Saale), Germany
* Correspondence: maximilian.scheer@uk-halle.de; Tel.: +49-0-345-557-1656
† These authors contributed equally to this work.

Abstract: Glioblastoma (GBM) is a highly aggressive and invasive brain tumor with a poor prognosis despite extensive treatment. The switch to aerobic glycolysis, known as the Warburg effect, in cancer cells leads to an increased production of methylglyoxal (MGO), a potent glycation agent with pro-tumorigenic characteristics. MGO non-enzymatically reacts with proteins, DNA, and lipids, leading to alterations in the signaling pathways, genomic instability, and cellular dysfunction. In this study, we investigated the impact of MGO on the LN229 and U251 (WHO grade IV, GBM) cell lines and the U343 (WHO grade III) glioma cell line, along with primary human astrocytes (hA). The results showed that increasing concentrations of MGO led to glycation, the accumulation of advanced glycation end-products, and decreasing cell viability in all cell lines. The invasiveness of the GBM cell lines increased under the influence of physiological MGO concentrations (0.3 mmol/L), resulting in a more aggressive phenotype, whereas glycation decreased the invasion potential of hA. In addition, glycation had differential effects on the ECM components that are involved in the invasion progress, upregulating TGFβ, brevican, and tenascin C in the GBM cell lines LN229 and U251. These findings highlight the importance of further studies on the prevention of glycation through MGO scavengers or glyoxalase 1 activators as a potential therapeutic strategy against glioma and GBM.

Keywords: glycation; invasion; glioblastoma; glioma; astrocytes; methylglyoxal; advanced glycation end-products

Citation: Schildhauer, P.; Selke, P.; Scheller, C.; Strauss, C.; Horstkorte, R.; Leisz, S.; Scheer, M. Glycation Leads to Increased Invasion of Glioblastoma Cells. *Cells* **2023**, *12*, 1219. https://doi.org/10.3390/cells12091219

Academic Editors: Javier S. Castresana, Bárbara Meléndez and Pablo Martín-Vasallo

Received: 20 February 2023
Revised: 11 April 2023
Accepted: 20 April 2023
Published: 23 April 2023

1. Introduction

Glioblastoma (GBM, WHO grade IV glioma) is the most common and aggressive astrocytic brain tumor in adults with a high recurrence and mortality. Despite extensive treatment, including surgical resection, radiotherapy, and temozolomide chemotherapy, the median survival for patients diagnosed with GBM is 12–20 months [1]. The invasive nature of GMB leads to cells infiltrating diffusely into the brain parenchyma, making complete surgical resection difficult and promoting recurrence. For GBM cells to infiltrate and disseminate within a tumor, key changes in the energy metabolism, cell adhesion, and remodeling of the extracellular matrix (ECM) are required [2].

The ECM is a complex network of proteins and components, such as laminin, collagen, and proteoglycans, which provide anchorage of the cells and shape the consistency of the tissue [3]. Several ECM molecules involved in migration and invasion are proteoglycans (versican, brevican, cadherins) and glycoproteins (CD44, tenascin C, fibrinogen), which were found upregulated in higher grade gliomas [4]. GBM cells are known to secrete matrix metalloproteinase (MMP) to degrade the ECM, penetrating the surrounding parenchyma [5,6]. Moreover, GBM cells increase their invasiveness by upregulating tenascin C and brevican, thus creating a migration-promoting environment [7,8]. Through the upregulation of integrin receptors, GBM cells are able to bind other ECM molecules,

which facilitates migration [9]. Another mechanism that enhances migratory capacities is the epithelial-mesenchymal transition (EMT). GBM cells undergoing EMT lose epithelial characteristics and become more spindle-shaped and motile, with a downregulation of epithelial proteins such as E-cadherin and an upregulation of mesenchymal proteins such as N-cadherin and vimentin [10,11].

As is known for many cancer cells, GBM reprograms their metabolism to gain energy through aerobic glycolysis (Warburg effect) [12]. Due to the inefficient means of generating adenosine triphosphate (ATP) this way, the aerobic glycolysis occurs 10 to 100 times faster in cancer cells [13]. This produces an increased amount of by-products, which are favorable for tumor growth and progression [14]. During glycolysis, 0.1–0.4% of glucose are turned into methylglyoxal (MGO), a regular by-product, through the non-enzymatic elimination of the phosphate group of glyceraldehyde-3-phosphate [15].

MGO is a reactive dicarbonyl and one of the most potent glycation agents known to cause vascular complications of diabetes (neuropathy, retinopathy, nephropathy, and atherosclerosis) and central nervous system disorders [15]. Being 20,000 times more reactive than glucose, MGO reacts with the amino acids lysine, cysteine, and arginine to form advanced glycation end products (AGEs) [13]. This non-enzymatic reaction between the carbonyl groups of dicarbonyls (MGO or glyoxal) or sugars (glucose, fructose) with amino groups of proteins, lipids, and DNA is called glycation. The process of glycation affects all proteins and can cause protein crosslinking, which alters tertiary structures and protein functions [16,17]. In total, 90–99% of MGO is bound to macromolecules and the cellular concentration can reach up to 0.3 mmol/L [18]. Elevated MGO and AGE levels were found to be associated with Alzheimer's and cardiovascular disease and mortality in type 1 and 2 diabetes [19,20]. AGEs function through various transmembrane receptors inducing oxidative stress, inflammation, dysregulation of signaling pathways, and genomic instability, which can trigger the initiation and progression of cancer [21]. The activation of the receptor for AGEs (RAGE) can, for example, trigger the JNK/AP1 signaling pathway, which promotes cell survival, invasion, and metastasis [21]. In breast cancer tumors, an accumulation of MGO adducts have been found and studies have shown that MGO induces the remodeling of the ECM and the activation of migratory-signaling pathways, enhancing metastatic dissemination [22].

Our preliminary work showed that MGO led to glycation and increased invasion in benign meningioma cells [23]. Similar results were obtained after the glycation of neuroblastoma cells [24]. Here, an increase in cell migration and invasion associated with a reduction in adhesion was detected.

In this study, we analyzed the effect of MGO on the glioma (WHO grade III and IV) cell lines compared to normal human astrocytes (hAs). We focused on the effect of glycation on chemotaxis, adhesion, and invasion. Our results showed that glycation led to an increase in invasion in the GBM cell lines and a decrease in the hA. In addition, we analyzed the effect of glycation on ECM proteins and their potential role in the observed increased invasion.

2. Materials and Methods

2.1. Cell Lines and Cultivation

The human glioma cell lines U343, U251, and LN229 have been kindly provided by Jacqueline Kessler (Department of Radiotherapy, Martin Luther University Halle-Wittenberg, Halle (Saale), Germany). All three of the cell lines were cultured in RPMI 1640 (Gibco, Thermo Fisher Scientific, Waltham, MA, USA) supplemented with 1% Penicillin-Streptomycin (10,000 U/mL Penicillin/10,000 µg/mL Streptomycin) (Gibco, Thermo Fisher Scientific, Waltham, MA, USA) and 10% fetal bovine serum (FBS, Gibco, Thermo Fisher Scientific, Waltham, MA, USA) at 37 °C in a 5% CO_2 incubator. The hAs were obtained from ScienCell Research Laboratories (Carlsbad, CA, USA) and cultured with astrocyte media (ScienCell Research Laboratories, Carlsbad, CA, USA)), as recommended by the manufacturer. All plates for hA were coated prior to use with a poly-L-Lysine solution (0.01%, EMD Millipore Corporation, Burlington, VT, USA).

2.2. MGO Treatment

The cell lines were seeded and incubated at 37 °C and 5% CO_2 in an incubator. After 4 h of attachment, the cells were treated with different concentrations of MGO (Merck, Sigma-Aldrich, St. Louis, MO, USA) (0.1, 0.3, 0.6, and 1.0 mmol/L), depending on the experiment. After the treatment, the cells were incubated again at 37 °C 5% CO_2 for 24–96 h. The untreated cells served as the control.

2.3. XTT Assay

The cellular metabolic activity of the glycated glioma cell lines LN229, U343, and U251, and the hAs were measured with a XTT assay (Roche, Sigma-Aldrich, St. Louis, MO, USA) as an indicator of cell vitality. In total, 5×10^4 cells were seeded in 96-well plates (Techno Plastic Products, TPP, Trasadingen, Switzerland) in 100 µL, incubated, and treated with MGO. As a control, a cell-free media without MGO was used. The XTT assay was performed after 24, 48, 72, and 96 h of MGO treatment. After each incubation period, 50 µL of the XTT labelling mixture was added to each well, according to the kit's instructions. The plate was incubated for 4 h in a humidified atmosphere, 37 °C, 5.0% CO_2 and then measured at a wavelength of 492 nm using the Tecan Infinite F200 Pro. (Tecan, Männedorf, Switzerland). The XTT assay was also performed using media with only 1% FBS.

2.4. Cell Microscopy

In total, 5×10^4 cells were seeded in 24-well plates (TPP) and treated with different MGO concentrations as described above. Microscope imaging was taken 24 and 48 h after treatment. The cells were stained with a propidium iodide solution (PI, 1.0 mg/mL, Sigma-Aldrich) and NucBlue Live Cell Stain ReadyProbes reagent (Thermo Fisher Scientific). The cells were washed with Dulbecco's phosphate-buffered saline (DPBS, Gibco, Thermo Fisher Scientific) and covered with FluoroBriteTM DMEM (Gibco, Thermo Fisher Scientific) and imaged with a Keyence BZ-800E microscope (Keyence, Neu-Isenburg, Germany). The quantification of PI and DAPI stained cells was performed using the IndentifyPrimaryObjects function of the software CellProfiler (Version 4.2.4, Broad Institute, Cambridge, MA, USA).

2.5. Glycation and Immunoblotting

The cells were seeded in 100 mm × 21 mm petri dishes (TPP) and treated with different concentrations of MGO accordingly. After 24 h, the cells were washed twice with ice cold PBS (Thermo Fisher Scientific) and harvested with PBS containing one diluted Pierce™ Protease Inhibitor Mini Tablet EDTA-free (Thermo Fisher Scientific). Benzonase Nuclease (Merck, Sigma Aldrich) was added to cleave the nucleic acid bonds. The proteins were extracted with 1× LDS sample buffer (Invitrogen, Thermo Fisher Scientific, Waltham, MA USA) and heated at 70 °C for 10 min. The protein concentration measurement was performed using the Pierce BCA Protein Assay Kit (Thermo Fisher Scientific) according to the manufacturer's instructions. Furthermore, 5% β-mercaptoethanol (Carl Roth, Karlsruhe, Germany) and 1× LDS sample buffer was added to the proteins and afterwards heated at 70 °C for 10 min.

The proteins were separated by sodium dodecyl sulphate polyacrylamide gel electrophoresis (SDS-PAGE) using the NuPAGE™ 4–12%, Bis-Tris, 1.5 mm, Mini-Protein-Gels and NuPAGE™ MES SDS Running Buffer (both Thermo Fisher Scientific). Blotting was performed using the iBlot 2 Dry Blotting System (Thermo Fisher Scientific) with iBlot™ 2 NC Regular Stacks (Thermo Fisher Scientific) followed by Ponceau S staining (0.1% Ponceau S, 3% trichloroacetic acid, and 3% sulfosalicylic acid).

The membranes were blocked with 5% skim milk powder (Carl Roth) in TRIS-buffered saline with 0.1% Tween (TBS-T, Sigma-Aldrich). The primary antibodies were added (Table 1) overnight at 4 °C and, after washing with TBS-T 5 times, the secondary antibodies were added for 60 min at room temperature. The protein level of glyceraldehyde 3-phosphate dehydrogenase (GAPDH) was used as the loading control.

Table 1. Antibodies used for immunofluorescence staining.

Antibody	Species	Dilution	Dilution Buffer	Manufacture
Anti-Carboxymethyl Lysine antibody (ab125145)	Mouse IgG	1:1000	5% MP in TBS-T	Abcam (Cambridge, UK)
Anti-E Cadherin antibody Intercellular Junction Marker (ab15148)	Rabbit IgG	1:1000	5% BSA in TBS-T	
Recombinant Anti-N Cadherin antibody (ab245117)	Rabbit IgG	1:1000	5% BSA in TBS-T	
GAPDH (14C10) (#2118)	Rabbit IgG	1:1000	5% BSA in TBS-T	Cell Signaling Technology Inc. (Danvers, MA, USA)
Anti-rabbit IgG, HRP-linked Antibody (#7074)	Goat	1:1000	2% MP in TBS-T	
Anti-mouse IgG, HRP-linked Antibody (#7076)	Horse	1:1000	2% MP in TBS-T	

Abbreviations: BSA, bovine serum albumin; IgG, immunoglobulin G; MP, milk powder.

The membranes were developed using the SuperSignal West Femto Chemiluminescent Substrate (Thermo Fisher Scientific) and signals were detected with a CCD camera (ImageQuant LAS4000, GE Healthcare, Freiburg, Germany). The quantification of the band intensity was performed using the ImageQuant TL software version 3.0 (GE Healthcare, Freiburg, Germany) and normalized to the corresponding GAPDH bands. All of the bands identified by the CML antibody, which indicate glycated protein, were included in the quantification process.

2.6. mRNA Isolation and qPCR

In total, 5×10^5 cells were seeded in 6-well plates (TPP) and treated with 0, 0.3, and 0.6 mmol/L MGO accordingly. After 24 h, the cells were washed twice with ice cold PBS. Afterwards, the cells were harvested in 300 µL of lysis buffer LBP (MACHEREY-NAGEL, Düren, Germany) and the lysate was stored at −20 °C. RNA was isolated using the NucleoSpin® RNA Plus Kit (MACHEREY-NAGEL, Düren, Germany), according to the manufacturer's instructions. Using the RevertAid First Strand cDNA Synthesis Kit (Thermo Fisher Scientific) 2 µg of RNA was transcribed into cDNA.

Using the Platinum® SYBR® Green qPCR SuperMix-UDG (Invitrogen, Thermo Fisher Scientific,), 0.5 µL of the respective reverse and forward primers (Table 2) and 1 µL of cDNA were prepared in a total volume of 20 µL. qPCR was performed with the Rotor-Gene Q (Qiagen, Hilden, Germany).

Table 2. Primers used for real-time quantitative PCR.

Gene Name (Protein)	Oligo Sequence 5′ to 3′ (Forward, Reverse)	Annealing Temperature (°C)	Product Length	Reference Sequence	Species
CD44	ACGCTTCAGCCTACTGCAAA GGTCCTGCTTTCCTTCGTGT	60	279	NM_000610.4	Homo sapiens
MMP2	ATGTCGCCCCCAAAACGG CCGCATGGTCTCGATGGTAT	60	176	NM_004530.6	Homo sapiens
MMP9	TCTATGGTCCTCGCCCTGAA CATCGTCCACCGGACTCAAA	60	219	NM_004994.3	Homo sapiens
MMP14	GGAGAATTTTGTGCTGCCCG TTGGTTATTCCTCACCCGCC	60	247	NM_004995.4	Homo sapiens
Versican	GCAGAAACTGCATCACCCAG TCCCAGGGCTTCTTGGTACT	60	227	NM_004385.5	Homo sapiens
Brevican	ATGGTGGGACATGCTTGGAG GAAGTCCTGTTCCTCGGGTG	60	233	NM_021948.5	Homo sapiens
Tensacin C	GAAACTGCAGAGACCAGCCT CAGGGGCTTGTTCAGTGGAT	60	244	NM_001410991.1	Homo sapiens
Fibronectin	GGTCCGGGACTCAATCCAAA GACAGAGTTGCCCACGGTAA	60	279	NM_212482.4	Homo sapiens
Integrin β1	AGCAACGGACAGATCTGCAA GCTGGGGTAATTTGTCCCGA	60	241	NM_002211.4	Homo sapiens
Integrin α3	GGCCTGCCAAGCTAATGAGA GACTCACCCATCACTGTCCC	60	273	NM_002204.4	Homo sapiens
Integrin α5	TCTCAGTGGAGTTTTACCGGC CCGAGAGCCTTTGCTGTCAA	60	173	NM_002205.5	Homo sapiens
Fibulin 3	TGTATGTGCCCCCAGGGATA ATTGACTGGGGCAGTTCTCG	60	227	XM_005264205.5	Homo sapiens
Vimentin	GGAGTCCACTGAGTACCGGA AGGTGACGAGCCATTTCCTC	60	198	NM_003380.5	Homo sapiens
Snail (SNAI1)	CTCGAAAGGCCTTCAACTGC GACATTCGGGAGAAGGTCCG	60	298	NM_005985.4	Homo sapiens
Slug (SNAI2)	TTTCAGACCCCCATGCCATT GAAAAAGGCTTCTCCCCCGT	60	292	NM_003068.5	Homo sapiens
Thrombospondin 1	ATCCTGGACTCGCTGTAGGT AGAAAGGCCCGAGTATCCCT	60	209	NM_003246.4	Homo sapiens
GAPDH	TCGTGGAAGGACTCATGACC TTCCCGTTCAGCTCAGGGAT	60	172	NM_002046.7	Homo sapiens

2.7. Real-Time Cell Analysis

The chemotactic migration was measured using the Real-Time Cell Analyzer Dual Purpose (RTCA DP) Analyzer (ACEA Biosciences Inc., San Diego, CA, USA), along with the cell invasion and migration plate (CIM-plate 16, ACEA Biosciences Inc.).

In total, 160 µL of media with 20% FBS was added to the lower chamber and 50 µL of media containing 1% FBS was added to the upper chamber. The CIM-plates were assembled according to the manufacturer's instructions and incubated for 1 h at 37 °C, followed by background measurements. The cells were detached using Accutase (Capricorn Scientific GmbH, Ebsdorfergrund, Germany) and resuspended with 1% FBS media. In total, 2×10^4 cells in 100 µL were added to each well. After 30 min of incubation at room temperature, 0.3 mmol/L or 0.6 mmol/L MGO were added. The cell migration was measured with the RTCA DP Analyzer as a change in impedance every 15 min for 48 h and displayed with the RTCA program 2.0 (ACEA Biosciences Inc.). To analyze the invasion, the upper chamber of the CIM-plate was coated with 20 µL of Geltrex TM LDEV-FREE Reduced Growth Factor Basement Membrane Matrix (Thermo Fisher Scientific). The Geltrex Matrix solution gels were kept at 37 °C, forming a basement membrane and acting as a barrier through which the cells have to invade. The coated upper chambers were incubated for one hour at 37 °C for the Geltrex to polymerize. Afterwards, the CIM-plates were assembled and measured as described above.

For the adhesion assay, 96× E-plates (ACEA Biosciences Inc.) were coated with 10 µg/mL of Fibronectin (EMD Millipore Corporation) or collagen IV (collagen from human placenta, Bornstein and Traub Type IV, Sigma Aldrich) and incubated for 1 h at 37 °C. Afterwards, the wells were washed with PBS and incubated with media for 20 min. To acquire the background measurements, 50 µL of media with 1% FBS was added to each well. Furthermore, 2×10^4 cells in 100 µL were added to each well. After 30 min of incubation at room temperature, 0.3 mmol/L or 0.6 mmol/L of MGO were added. Adhesion was measured every 15 min for 24 h with the RTCA.

2.8. Statistical Analysis

All analyses were performed using Excel Software (Microsoft Corporation, Redmond, WA, USA) and GraphPad Prism 4.9.1 (GraphPad Software Inc., San Diego, CA, USA). The half maximal inhibitory effect (IC50) was calculated using GraphPad Prisms nonlinear regression analysis and the dose-response inhibition equations.

An unpaired two-sided Student's *t*-test was performed for all cell lines compared to the untreated cells. The figures depict the mean and standard deviation (SD), respectively. At least three biological replicates were performed for each experiment.

3. Results

3.1. High MGO Concentrations Lead to Decreased Cell Vitality

The influence of MGO on the cell vitality of LN229, U343, U251, and hA after 24, 48, 72, and 96 h was investigated using an XTT assay (Supplementary Materials Figure S1). MGO showed concentration-dependent cytotoxic effects in all cell lines after 24 h (Figure 1). In LN229, the cell vitality decreased in a concentration-dependent manner, with a reduction in the cell vitality of 18.53 ± 2.71%; $p < 0.001$with 0.1 mmol/L, 34.15 ± 15.07%; $p < 0.001$ with 0.3 mmol/L, 58.28 ± 14.90%; $p < 0.001$ with 0.6 mmol/L; and the strongest effect with 1 mmol/L with a reduction of 64.53 ± 10.11%; $p < 0.001$ (Figure 1A). Equivalent results were observed in the U251 and U343 cell lines (Figure 1B,C). The treatment with 0.1 mmol/L MGO did not affect the cell vitality of the U251 cells and 0.3 mmol/L MGO showed a 20.54 ± 10.21%; $p = 0.047$ reduction in the cell vitality. The 0.6 mmol/L MGO decreased the cell vitality by 51.13 ± 0.34%; $p < 0.001$ and 1 mmol/L by 57.69 ± 4.00%; $p < 0.001$ (Figure 1B). In the U343 cells, 0.1 mmol/L reduced the cell vitality by 17.43 ± 11.47%; $p = 0.018$, 0.3 mmol/L reduced it by 35.96 ± 10.36%; $p < 0.001$, and 0.6 mmol/L MGO reduced it by 47.86 ± 15.86%; $p < 0.001$. A 53.82 ± 17.02%; $p < 0.001$ reduction in the cell vitality was observed at 1 mmol/L MGO (Figure 1C). In the hA cell line, the cell vitality was not

affected by treatment with 0.1 and 0.3 mmol/L MGO, but a 51.78 ± 2.53%; $p < 0.001$ reduction in the cell vitality was observed at concentrations of 0.6 mmol/L and a 53.97 ± 2.05%; $p < 0.001$ reduction was observed with 1 mmol/L MGO (Figure 1D). The IC50 of MGO treatment measured 0.384 ± 0.040 mmol/L in the LN229 and 0.4379 ± 0.037 mmol/L in the U251 cells. For the U343 cells, the IC50 was slightly lower at 0.368 ± 0.099 mmol/L and for the hA cells it was slightly lower at 0.333 ± 0.032 mmol/L MGO.

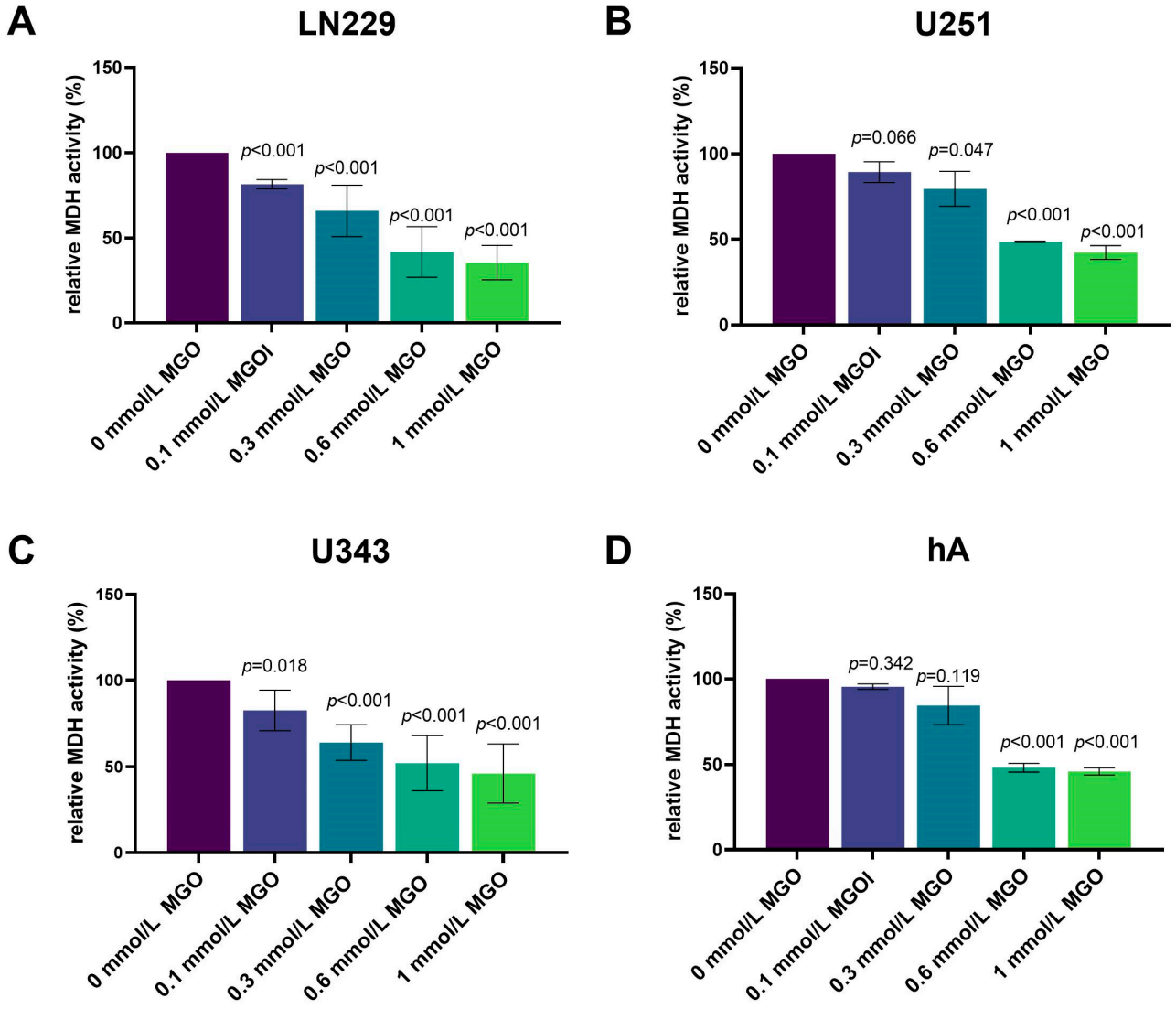

Figure 1. Cell vitality of glioma cell lines and hA after MGO treatment. The cell vitality of LN229 (**A**), U251 (**B**), U343 (**C**), and hA (**D**) cells was determined using an XTT assay after MGO treatment. Graphs show intracellular mitochondrial dehydrogenase (MDH) activity normalized to untreated cells after 24 h. Student's *t*-test was performed for statistical analysis. Graphs represent the means and SDs of three independent biological replicates.

3.2. High MGO Concentration Induce Altered Cell Morphology and Cell Death

In addition, we investigated the influence of MGO on the cell morphology. The cells were cultivated in the absence or in the presence of different concentrations of MGO (0.1–1 mmol/L) for 24 h (Figure 2) and 48 h (Supplementary Materials Figure S2). LN229 and U251 did not exhibit any changes in their morphology when cultured with MGO up to a concentration of 0.6 mmol/L. However, at 1 mmol/L MGO, there was a reduction in the cell amount and the cells became more spherical (Figure 2A,B). U343 and hA displayed a reduction in cell numbers already at 0.3 mmol/L MGO and changes in the morphology at

0.6 mmol/L MGO, appearing more granular and sporadic (Figure 2C,D). An increase in the number of dead cells, as indicated by PI staining, was observed at both 0.6 mmol/L and 1 mmol/L MGO for hA. The quantification of PI-stained cells showed a higher cell death with increasing concentrations of MGO (Supplementary Material Table S1).

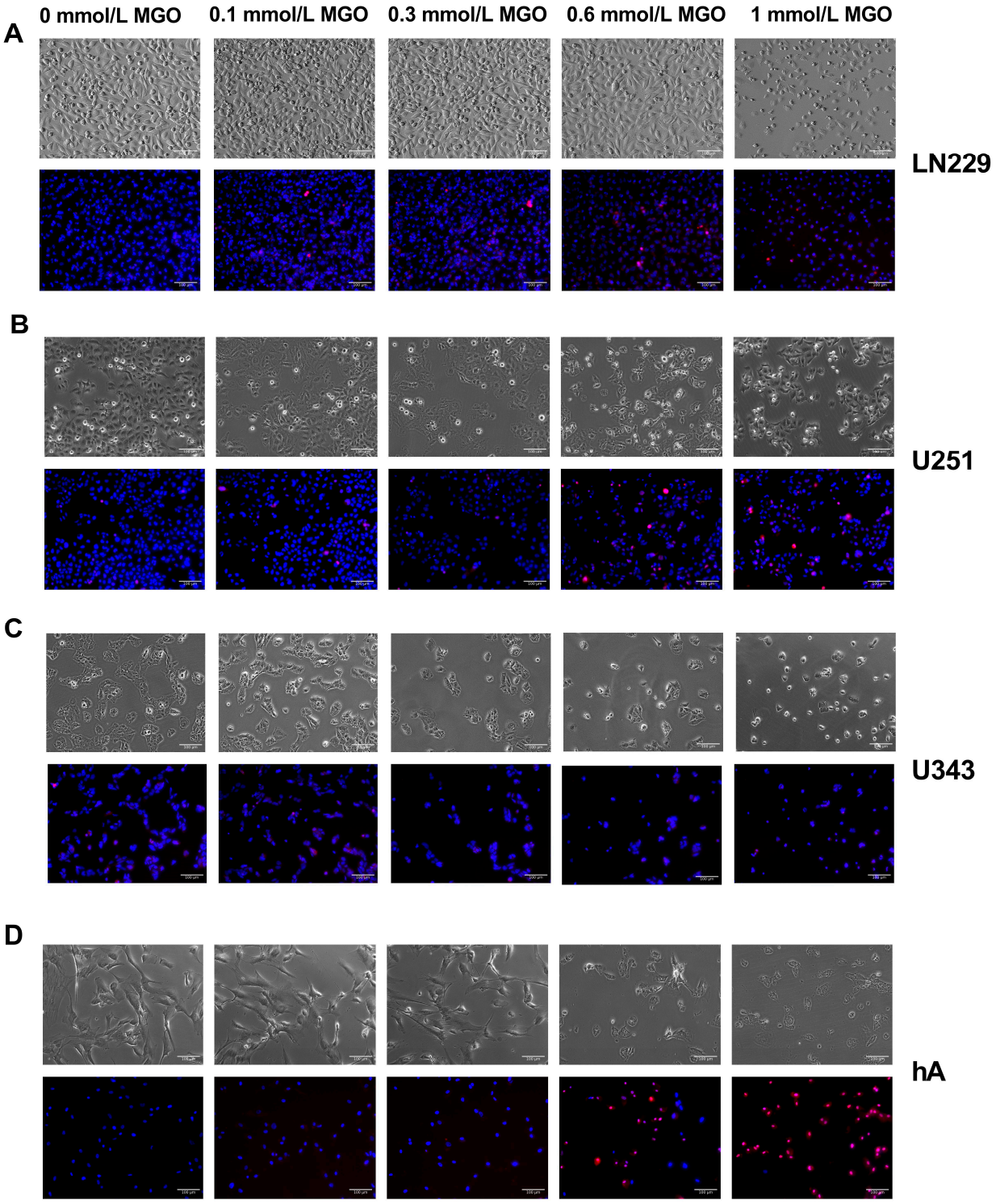

Figure 2. Microscope imaging of glioma cell lines and hA 24 h after MGO treatment. Bright field (above) and fluorescence (below) microscope imaging of LN229 (**A**), U251 (**B**), U343 (**C**), and hA (**D**) 24 h after MGO treatment. Cells were stained with DAPI (blue) and propidium iodide (red). Scale bar = 100 µm.

In addition, for the LN229 and U251 cells a higher confluency compared to the U343 and hA cell lines was observed. This difference can be attributed to the higher proliferation rate of the GBM cell lines, such as LN229 and U251, in contrast to the grade III glioma cell line U343, and primary normal hA, which have slower growth rates. Additionally, the hA cells have a distinct morphology characterized by spindle-shaped cells with a larger cell body, which further contributes to their lower confluency.

3.3. MGO Treatment Increases Glycation in a Concentration-Dependent Manner

To evaluate the level of glycation with the increasing MGO concentration, immunoblotting was performed. The cells were treated with various concentrations of MGO (0.3, 0.6 and 1 mmol/L), and proteins were extracted and separated using SDS PAGE. Carboxymethyl Lysine antibody was used to verify glycation. An increase in glycation could be observed in all four cell lines in a concentration-dependent manner (Figure 3). In the LN229 cell line, protein glycation increased slightly after treatment with 0.3 and 0.6 mmol/L MGO and a 76.77 ± 24.75%; $p = 0.011$ increase was observed with 1 mmol/L (Figure 3A). Similar results were detected in the U251, where 1 mmol/l led to an increase in glycation of 53.09 ± 30.97%; $p = 0.072$ (Figure 3B). In the U343 cell line, 0.3 mmol/L MGO led to no increase in glycation but glycation increased with 0.6 mmol/L MGO by 34.06 ± 14.85%; $p = 0.032$ and with 1 mmol/L by 63.43 ± 33.89%; $p = 0.057$ (Figure 3C). The hA showed the strongest effect of glycation, with an increase of 72.30 ± 62.41%; $p = 0.231$ with 0.3 mmol/L MGO, 93.80 ± 77.57%; $p < 0.001$ with 0.6 mmol/L; and 152.21 ± 81.69%; $p = 0.223$ with 1 mmol/L (Figure 3D). Interestingly, a distinct pattern of glycated proteins was observed in the cell lines.

3.4. Chemotactic Cell Migration after MGO Treatment

As chemotactic cell migration plays a crucial role in the dissemination and progression of tumors, we investigated the effect of MGO on chemotaxis. The LN229 cell line exhibited a decrease in cell migration in response to the MGO treatment in a dose-dependent manner, with a reduction of 26.66 ± 10.92%; $p = 0.043$ observed after 48 h of treatment with 0.6 mmol/L MGO (Figure 4A). The treatment with MGO did not result in changes in the chemotactic migration of U251 cells after 24 and 48 h (Figure 4B). The U343 cell line showed a decrease in chemotactic migration activity after treatment with 0.3 mmol/L MGO for 24 and 48 h (Figure 4C). The hA cell line exhibited a reduction in chemotactic migration activity by 11.26 ± 7.53%; $p = 0.041$ with 0.3 mmol/L after 24 h, but no other alterations in chemotactic migration were observed (Figure 4D). The effect of glycation on the cell motility was additionally analyzed using time-lapse microscopy. No significant changes were observed in the migration after MGO treatment compared to the untreated cells.

3.5. MGO Increases Invasion of GBM Cell Lines

Since invasiveness is one of the hallmarks of cancer cells, next we analyzed the influence of glycation on invasion. The invasion of the LN229 cells increased significantly with higher MGO concentrations, showing an increase of 23.06 ± 14.46%; $p = 0.033$ after treatment with 0.3 mmol/L and 45.35 ± 18.24%; $p = 0.025$ after treatment with 0.6 mmol/L MGO after 24 h (Figure 5A). Interestingly, the U251 cells only showed an increase in invasion after treatment with 0.3 mmol/L MGO. The enhancement of invasion with 0.6 mmol/L was not significant compared to the control cells (Figure 5B). The U343 cell line showed increased invasiveness with 0.6 mmol/L MGO. No difference was observed between the treatment with 0.3 mmol/L and the untreated cells (Figure 5C). The invasiveness of the hA decreased after MGO treatment in a concentration-dependent manner, showing a reduction of 21.02 ± 8.37%; $p = 0.023$ with 0.3 mmol/L and 35.75 ± 4.54%; $p < 0.001$ with 0.6 mmol/L MGO after 24 h (Figure 5D).

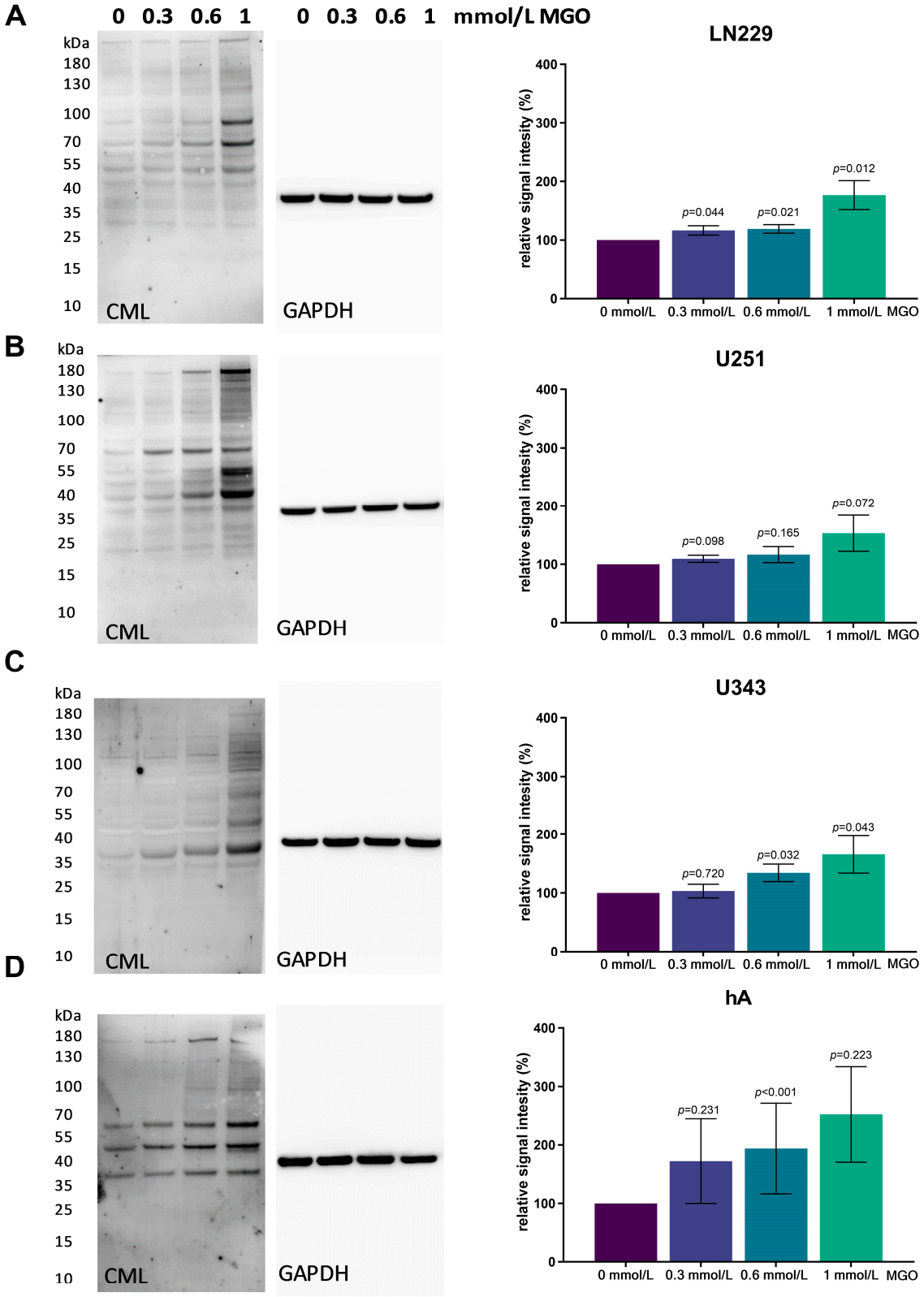

Figure 3. Glycation of glioma cell lines and hA. Immunoblot of LN229 (**A**), U251 (**B**), U343 (**C**), and hA (**D**) with different MGO concentrations (left). Antibody against carboxymethyl lysine (CML) was used to detect glycation. Graphs (right) show representative quantification of the blot, normalized to the untreated cells. GAPDH was used as loading control. Student's *t*-test was performed for statistical analysis. Graphs represent the means and SDs of three independent biological replicates.

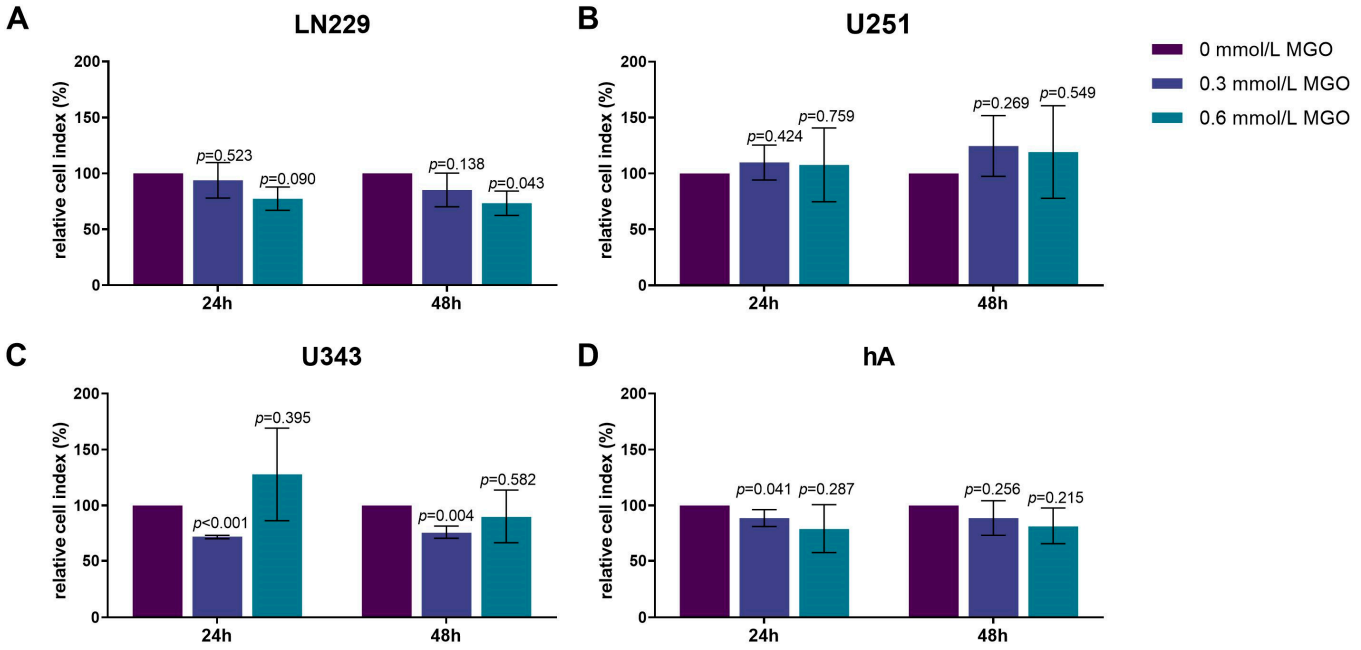

Figure 4. Chemotactic cell migration of glioma cell lines and hA after MGO treatment. Graphs display chemotaxis of LN229 (**A**), U251 (**B**), U343 (**C**), and hA (**D**) after 24 h and 48 h normalized to control cells, after treatment with 0.3 or 0.6 mmol/L MGO. Statistical analysis was performed using Student's *t*-test. Graphs represent the means and SDs of three independent biological replicates.

3.6. MGO Has No Effect on the Adhesion of Glioma Cell Lines or hA

Since the invasion was altered after glycation, we analyzed the effect of MGO on adhesion. The cells were seeded on different matrices (without coating, fibronectin, and collagen IV) and treated with MGO (0.3 or 0.6 mmol/L). No significant changes of adhesion were observed after glycation in any of the cell lines (Figure 6). However, differences in adhesion to the different matrices were observed. LN229, U343, and hA adhered best to fibronectin, followed by collagen IV and adhered least to the uncoated plates (Figure 6A,C,D). Surprisingly, U251 showed the least adhesion to collagen IV and no difference was measured between the uncoated plates and the fibronectin coating (Figure 6B).

3.7. Glycation Alters the Expression of ECM Components

Since cell-cell adhesion molecules, matrix-degrading enzymes, and various ECM components typically modulate invasion, we analyzed the effect of glycation on: versican, tenascin C, MMP 2, MMP 9, MMP 14, fibulin 3, thrombospondin, integrin β1, integrin α3, integrin α5, brevican, fibronectin, vimentin, TGF-β, and transcription factors slug (SNAI2) and snail (SNAI1) (Figure 7).

The effect of glycation on various ECM components, cell-cell adhesion molecules, and matrix-degrading enzymes was analyzed in the LN299, U251, U343, and hA cell lines using qPCR. The mRNA expression levels of these components were found to be lower expressed in the malignant cell lines compared to hA, with the exception of CD44, SNAI1, and fibulin 3 (Figure 7B). The U251 showed a significantly higher expression of CD44 (3.612 ± 1.397, $p = 0.041$) compared to the hA. SNAI1 and fibulin 3 were significantly higher expressed in LN229 (1.794 ± 0.488, $p = 0.030$; 1.712 ± 0.379, $p < 0.001$) (Figure 7B).

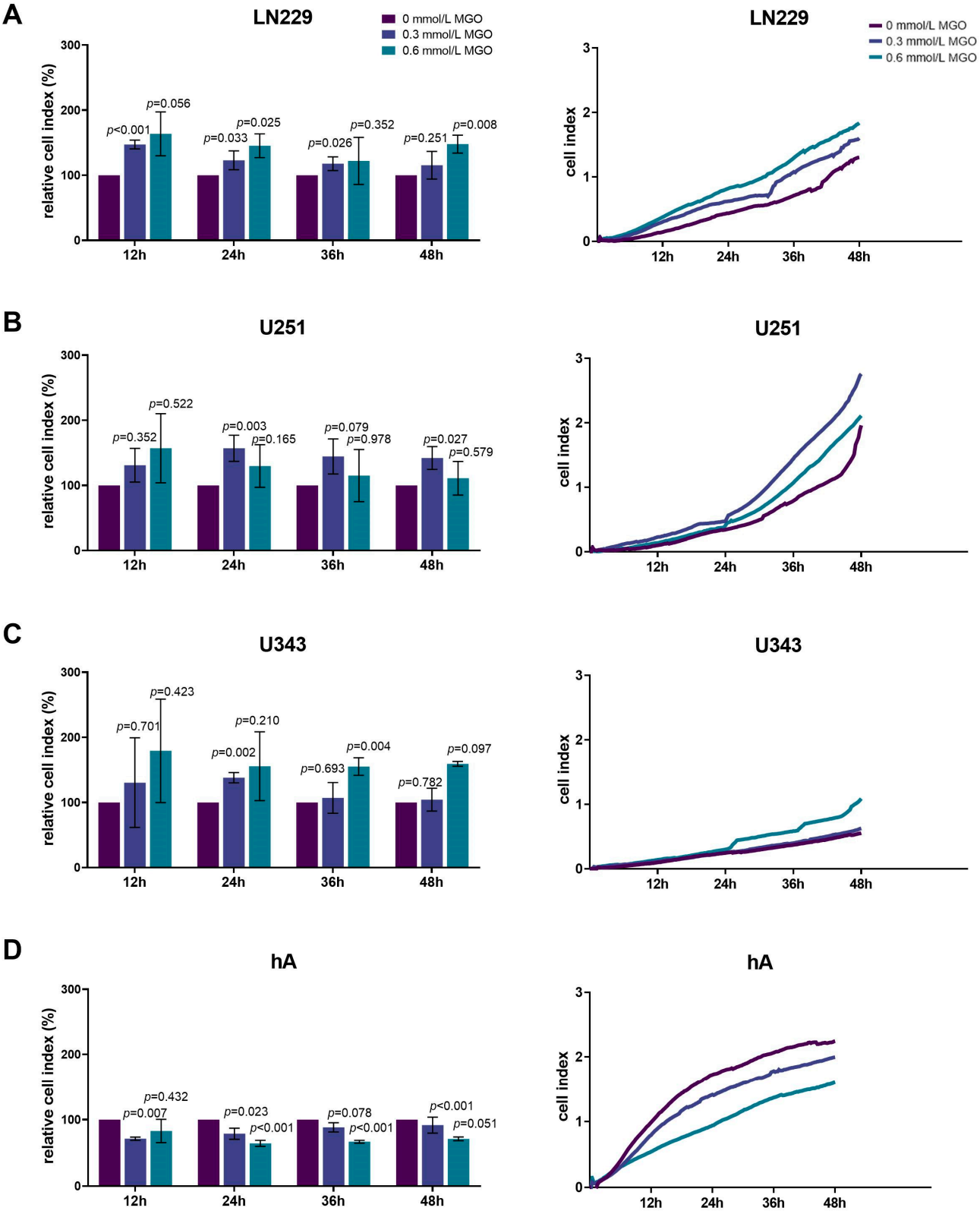

Figure 5. Invasion of glioma cell lines and hA after MGO treatment. LN229 (**A**), U251 (**B**), U343 (**C**), and hA (**D**) were cultivated in absence or presence of MGO (0.3 mmol/L or 0.6 mmol/L) on CIM-plates, coated with Geltrex to imitate basement membranes. Invasion was measured every 15 min for 48 h. Graphs (left column) show cell indices normalized to the untreated cells and graphs (right column) show measured cell indices for 12, 24, 36, and 48 h. Student's *t*-test was performed for statistical analysis. Graphs represent the means and SDs of three independent biological replicates.

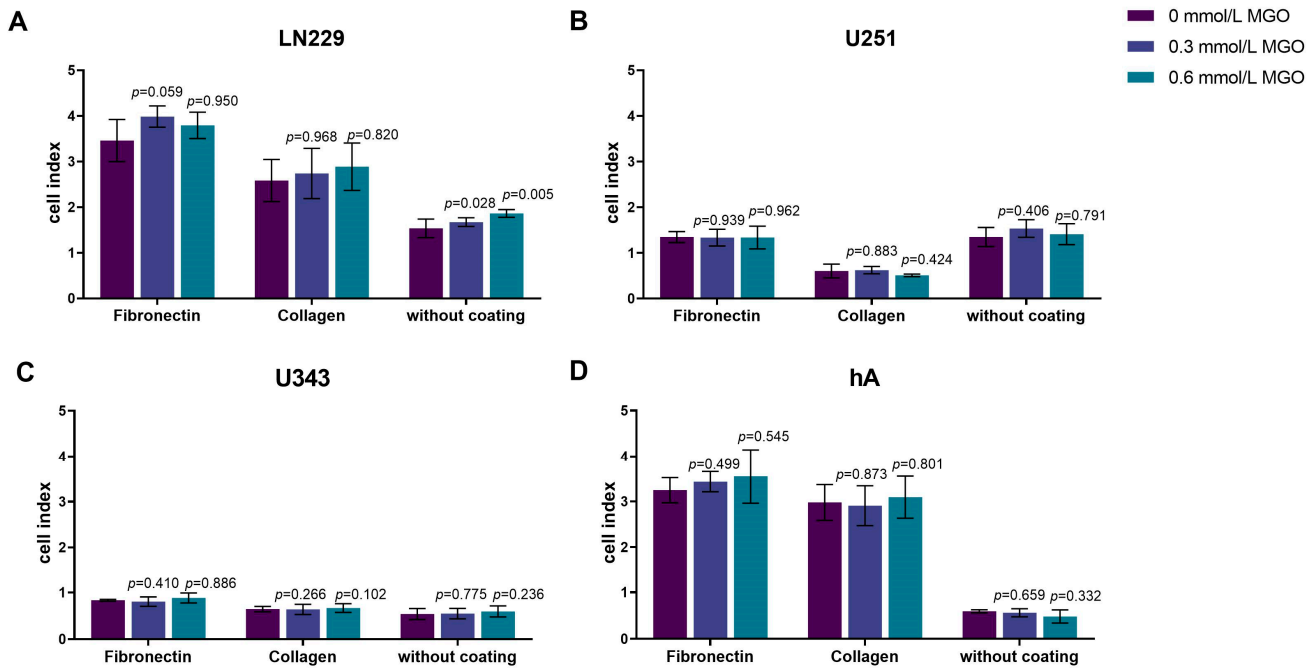

Figure 6. Adhesion of glioma cell lines and hA after MGO treatment. LN229 (**A**), U251 (**B**), U343 (**C**), and hA (**D**) were seeded at concentrations of 0.3 mmol/L and 0.6 mmol/L MGO on plates either coated with fibronectin, collagen, or left uncoated. Graphs display measured cell index after 4 h. Absolute cell index was used to show the different adherence to the different matrices and to illustrate the differences between the cells. Student's *t*-test was performed for statistical analysis. Graphs represent the means and SDs of three independent biological replicates.

The effect of glycation on the ECM components varied among the cell lines, with an overall upregulation in the LN229 cells. The strongest effect of glycation was observed on the expression of CD44, which was upregulated in the U251 (1.655 ± 0.259, $p = 0.023$), U343 (1.548 ± 0.562, $p = 0.240$), and hA (1.641 ± 0.657, $p = 0.058$) cells, but remained unchanged in the LN229 cells (1.055 ± 0.145, $p = 0.539$). Brevican expression was upregulated in the LN229 (1.498 ± 0.369, $p = 0.057$) and U251 cells (1.303 ± 0.074, $p = 0.004$) and downregulated in the U343 cells (0.725 ± 0.302, $p = 0.166$). Similar results were observed with tenascin C, as the expression increased in the LN229 (1.203 ± 0.140, $p = 0.046$) and U251 cells (1.655 ± 0.238, $p = 0.018$). In the LN229 cells, versican and thrombospondin were upregulated (1.358 ± 0.174, $p = 0.012$; 1.392 ± 0.151, $p = 0.021$), as well as SNAI1 and SNAI2 (1.335 ± 0.160, $p = 0.011$; 1.491 ± 0.294, $p = 0.027$). The TGF-β expression increased in the LN229 and U251 cells (1.229 ± 0.099, $p = 0.007$; 1.328 ± 0.596, $p = 0.281$). The MMP2 expression decreased after glycation in the U251 cells (0.625 ± 0.094, $p < 0.001$). On the contrary, the MMP2 expression increased in the LN229 and U343 cells after glycation (1.518 ± 0.294, $p = 0.022$; 1.544 ± 0.466, $p = 0.089$). No expression of MMP9 was detected in any of the analyzed cells. The remaining components were not differentially expressed by glycation.

In addition, we examined E- and N-cadherin, as they are involved in the epithelial mesenchymal transition (EMT). Therefore, the cells were treated with MGO and immunoblotting was performed using E- and N-cadherin antibodies (Figure 8).

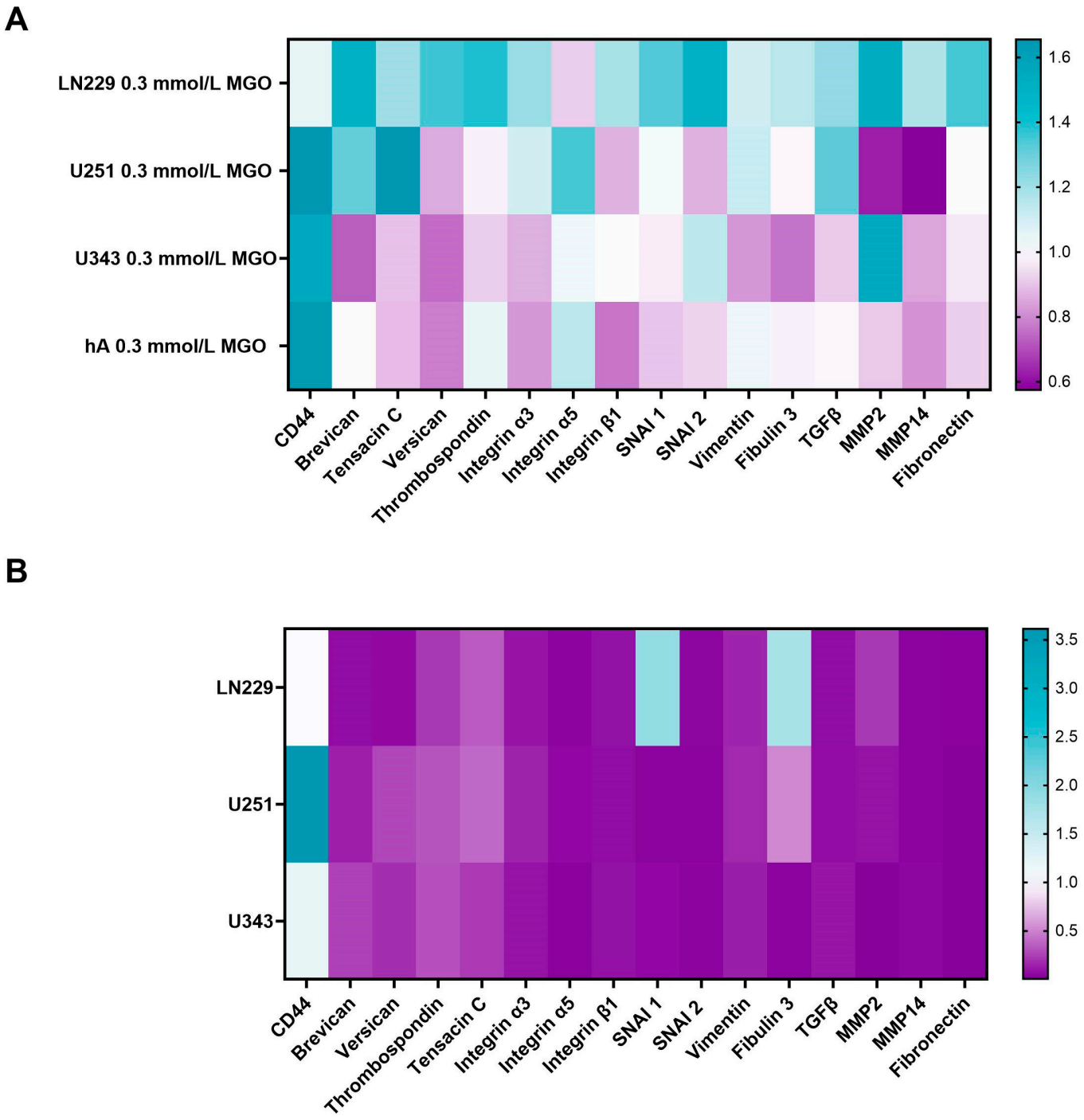

Figure 7. mRNA expression of invasion-associated ECM molecules and transcription factors. Heat map of mRNA expression of LN229, U251, U343, and hA after treatment with 0.3 mmol/L MGO normalized to untreated cells (**A**). Heatmap of mRNA expression of LN229, U251, and U343 cells normalized to the expression of hA (**B**). Three independent biological replicates of the mRNA were analyzed by qPCR.

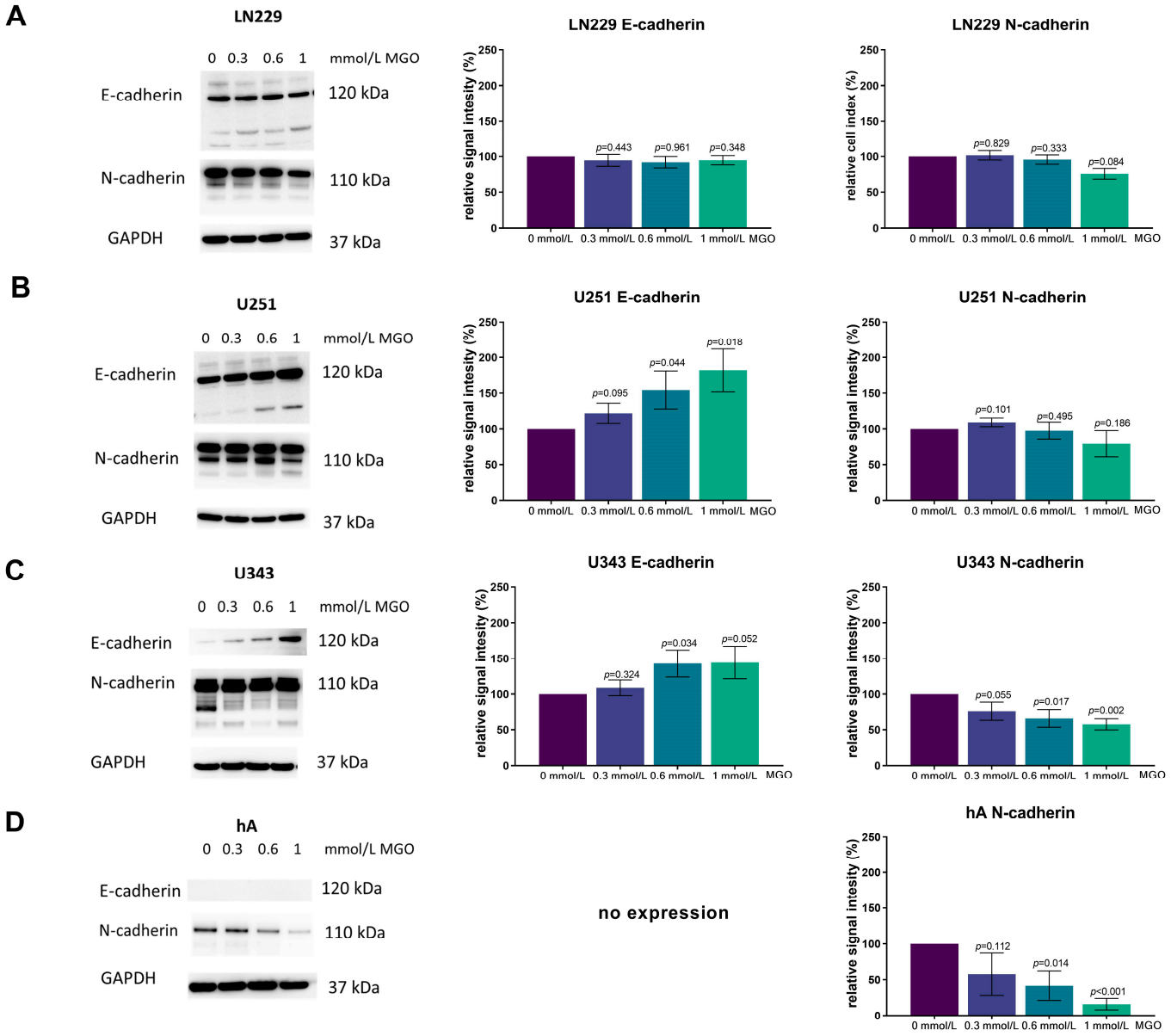

Figure 8. E- and N-cadherin expression after MGO treatment. Immunoblot of LN229 (**A**), U251 (**B**), U343 (**C**), and hA (**D**) cells with different MGO concentrations (0.3, 0.6, and 1 mmol/L) (left column) and antibody against E- and N-cadherin. GAPDH was used as loading control. Graphs show representative quantification of E-cadherin (middle column) and N-cadherin (right column) Western blots from three independent biological replicates, normalized to the untreated cells. Student's *t*-test was performed for statistical analysis. Graphs represent the means and SDs.

In the LN229 cell line, the expression of both E- and N-cadherin remained unchanged after MGO treatment (Figure 8A). In the U251 cell line, the E-cadherin expression increased in a concentration-dependent manner, with an increase of 21.74 ± 14.15%; $p = 0.095$, 54.26 ± 26.53%; $p = 0.044$ and 81.86 ± 30.09%; $p = 0.018$ observed with 0.3 mmol/L, 0.6 mmol/L, and 1 mmol/L MGO treatment, respectively. The N-cadherin expression was not affected by MGO treatment (Figure 8B). In the U343 cell line, both the E-cadherin and N-cadherin expressions were altered in a concentration-dependent manner, with E-cadherin increasing and N-cadherin decreasing. The E-cadherin expression increased by about 44.25 ± 22.90; $p = 0.052$ with 1 mmol/L MGO treatment and the N-cadherin expression decreased by about 42.36 ± 7.79%; $p = 0.002$ with 1 mmol/L MGO treatment (Figure 8C). In the hA cell line, the E-cadherin expression was not detected and was not induced after

glycation. The N-cadherin expression was reduced in a concentration-dependent manner in the hA cells, with a reduction of 42.27 ± 29.44%; $p = 0.112$ with 0.3 mmol/L, 58.27 ± 20.45; $p = 0.014$ with 0.6 mmol/L; and 83.93 ± 8.11; $p < 0.001$ with 1 mmol/L MGO (Figure 8D).

4. Discussion

In earlier studies, MGO was initially thought to be toxic to cancer cells and, thus, considered as a therapeutic agent. However, recent studies have revealed that sub-toxic low doses of MGO can promote tumor development, as cancer cells acquire resistance to apoptosis and enhanced growth properties [25–32]. The glycolytic switch of cancer cells (Warburg effect) and increased glycation could positively impact signaling pathways, promoting tumor invasion and uncontrolled cell proliferation. In our study, we analyzed the effect of MGO on GBM and glioma cell behavior. High MGO concentrations (1 mmol/L) led to cytotoxic effects in all cell lines, but low doses increased invasion in the GBM and glioma cell lines, resulting in a more aggressive phenotype.

Similar outcomes were observed in human meningioma (BEN-MEN-1, WHO grade I) and neuroblastoma (Kelly) cells, where elevated levels of MGO inhibited cell growth and low levels boosted cell invasion [23,24]. Our findings are supported by Nokin et al. The authors implanted U87MG GBM cells on a chicken chorioallantoic membrane and exposed them to increasing MGO concentrations. Low doses of MGO (0.1 and 0.3 mmol/L) significantly increased the tumor volume compared to the untreated tumors, while higher doses (0.5–3 mmol/L) significantly reduced it [33]. According to Lee et al., high MGO doses reduce the crucial cell survival signaling pathway, gp130/STAT3, leading to an increased cytotoxicity in rat schwannoma RT4 cells, PC12 cells, and U87MG GBM cells. Lee did not observe significant harm to cell viability at a concentration of 0.5 mmol/L of MGO [34].

The pro-tumorigenic effect of MGO has been extensively studied previously [31]. One of the key mechanisms supporting cancer progression is the evasion of programmed cell death and the inhibition of tumor suppressors. This can occur as a result of the glycation of heat-shock proteins; for instance, MGO-modified heat-shock protein 27 prevents apoptosis of cancer cells in lung and gastrointestinal cancer [25,35]. In breast cancer, the MGO-altered heat shock protein 90 decreased the LATS1 expression, a kinase of the Hippo tumor suppressor pathway, enhancing growth and metastatic potential in vivo [27].

Sufficient evidence suggests that MGO increases invasion through various mechanisms. In anaplastic thyroid cancer, MGO promotes migration and EMT through modulation of the TGF-β1/FAK signaling pathway [36]. Additionally, glycation has been linked to activating the RAGE/TLR4/MyD88 signaling pathway and upregulating MMP9 expression in breast cancer, thus increasing migration and invasion [37]. Moreover, MGO adduct accumulation, which is a consistent feature of high-stage colon carcinomas, has been linked to the promotion of proliferation, invasion, and EMT through the PI3K/AKT signaling pathway [38].

However, the regulations by glycation in cancer cells are described as differential. In hepatocellular carcinoma, glycation impaired migration and adhesion [39]. Interestingly, Selke et al. showed that glycation reduced the invasiveness of WHO grade III IOMM-Lee meningioma cells [23]. Our study also observed a decrease in the invasiveness of normal primary human astrocytes. This implies that the effects of glycation are cell-type specific. Furthermore, the effect of glycation on the ECM components can also be differential. While there is strong evidence for an EMT-like process in GBMs through well-described EMT-promoting pathways, such as ZEB1/ZEB2, SNAI1, SNAI2, TWIST, and the WNT-catenin pathway, we did not observe EMT to be the primary reason for increased invasion in our data [11]. Instead, we propose a reverse process of the mesenchymal-epithelial transition (MET) in the WHO grade III glioma cell line U343 (E-cadherin increase and N-cadherin decrease). Interestingly, Selke et al. also found an upregulation of E-cadherin and a downregulation of N-cadherin in meningioma cells (BEN-MEN-1, WHO grade I), in which increased invasion was observed, suggesting MET potentially having a role in the increased invasion [23]. According to Their et al., carcinoma cells sometimes undergo

MET after dissemination to distant tissue sites and ensuing extravasation in order to efficiently form metastases [40]. In the GBM cell line LN229, even though SNAI1 and SNAI2 was upregulated, E- and N-cadherin remained unaffected while also showing no EMT promoting expression pattern.

While E-cadherin expression is commonly described as non-abundant or absent in gliomas and GBM [41], our data showed E-cadherin expression in all three malignant cell lines (LN229, U251, U343) and an absence in the hA. Additionally, glycation even increased the E-cadherin expression in the U343 and U251 cell lines, where invasion was increased. The E-cadherin expression has been found in certain subtypes of glioblastoma with epithelial and pseudo-epithelial differentiation, where E-cadherin levels even correlated with a worse prognosis [42]. In a Xenograft mouse model by Lewis-Tuffin et al., the E-cadherin expression also correlated with the increased invasiveness of glioma cells. Additionally, endogenous E-cadherin expression promoted the growth and migration of the SF767 glioma cell line [42]. Together with these findings, our results could suggest a currently unknown role for E-cadherin in GBM.

Aberrant N-cadherin expression has been reported in many types of cancer, such as lung-, breast-, prostate-, and squamous cell cancer and has been linked to cell transformation, adhesion, apoptosis, angiogenesis, and invasion [43]. In some studies, N-cadherin expression was found to be upregulated in GBM and linked to the extracellular signal-regulated kinase (ERK) pathway, promoting cancer stem cell invasion [44]. Other researchers reported an inverse correlation between N-cadherin expression and invasion and that the downregulation of N-cadherin was linked to changes in cell polarization and abnormal motile behavior, resulting in increased tumor cell migration and invasiveness [45]. However, no consistent association between N-cadherin and invasiveness has been found in glioblastoma and glioma. We also did not find a correlation between invasiveness and N-cadherin expression.

Glycation also made cell line specific alterations on other ECM components. In our study, we found that glycation increased the expression of CD44 in the U343, U251, and hA cell lines. CD44 is a transmembrane glycoprotein which binds hyaluronic acid in the ECM and is recognized as a molecular marker for cancer stem cells. The binding of hyaluronic acid activates various signaling pathways, leading to cell proliferation, adhesion, migration, and invasion [46]. In GBM, CD44 has been linked to increasing tumor invasiveness, proliferation, and chemotherapy resistance [47]. However, in our study, CD44 upregulation was not associated with the increased invasion of the GBM cell lines.

Brevican and tenascin-C were upregulated in the LN229 and U251 cells, where the strongest increase in invasion was observed. Both brevican and tenascin-C are glycoproteins in the human brain that are overexpressed in glioma cells and associated with a later tumor stage [48,49]. Brevican promotes glioma cell motility through the upregulation of integrins and proteolytic cleavage by ADAMTS4 [50]. According to Xia et al., tenascin-C increases the GBM invasion of MMP12 and ADAM9 and negatively regulates proliferation [51]. Although strong evidence suggests that versican and thrombospondin play a role in tumor invasion [4,8,52], our study found that they were only upregulated in the LN229 cells. For example, versican enhances locomotion and reduces cell adhesion of astrocytoma cells through the binding of its G1 domain to hyaluronan [53]. Interestingly, thrombospondin is upregulated upon TFG-β stimulation and enhances microtube formation, which form important structural cell networks of GBM contributing to invasion and treatment resistance [54]. The upregulation of MMP2, which we observed in the LN229 and U343 cells, could increase invasion through remodeling and degradation of ECM.

Despite the differential gene expression of the ECM components, we did not observe any effects of glycation on chemotactic cell migration or adhesion at physiological concentrations. Notably, we only analyzed cell-matrix adhesion and not cell-cell adhesion. Invasion, however, is a fine balance between cell-cell and cell-extracellular matrix adhesions. We concluded that the GBM and glioma cell lined preferred fibronectin as substrate more than collagen IV. Fibronectin is a glycoprotein in the brain parenchyma and its expression is

increased in brain malignancies [55]. Collagen IV is less common in the brain and presence is usually restricted to the basement membrane of blood vessels or the glia limitants, which explains the poorer adherence [56].

In summary, our study found that high concentrations of MGO are cytotoxic to cells and sub-toxic levels lead to an increase in glycation, resulting in a more invasive phenotype of GBM cells (Figure 9). The underlying mechanism behind this correlation is not yet well understood and further analyses are necessary. Additionally, deglycation could present potential for novel therapeutic approaches, such as utilizing MGO scavengers or activating glyoxalase 1. In the case of colon cancer, the use of an MGO scavenger, carnosine, has shown promising results by enhancing the efficacy of cetuximab therapy in KRAS-mutated cancer cells [57].

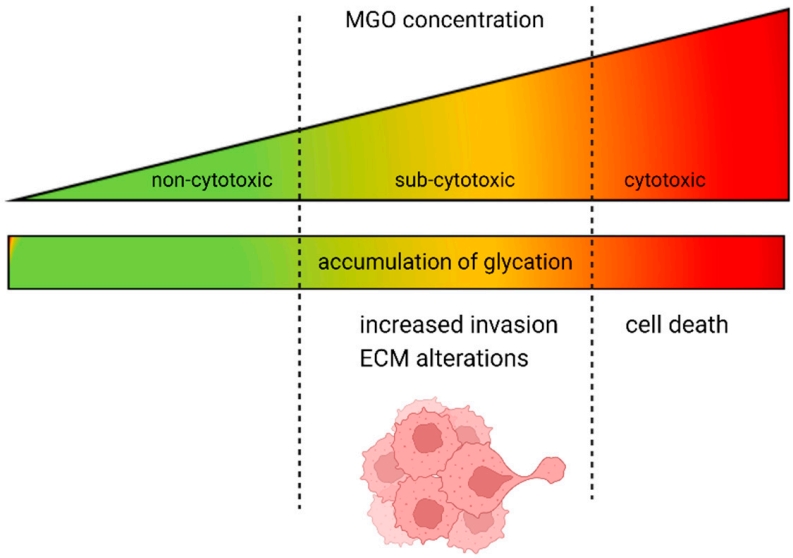

Figure 9. Dual role of MGO in GBM and glioma cells. The increase in glycation is proportional to the rising concentration of MGO. At high doses, MGO has a cytotoxic effect on GBM and glioma cells; however, when present at lower, physiological concentrations, it causes alterations in the ECM and increased invasion.

Limitations

Our study is limited by the fact that we used two glioblastoma cell lines and one glioma cell line. Different cell lines have unique genetic and epigenetic characteristics that affect their responses to glycation. The results may not necessarily apply to primary glioma cells and further analysis is needed to evaluate the effect of glycation in these contexts. Another limiting factor is that the invasion was only analyzed in vitro. The in vitro model does not accurately depict the complexity of the tumor microenvironment, including the impact of immune cell infiltration, physiological parameters (oxygen and pH), growth and angiogenic factors, and the unique composition and stiffness of the ECM.

5. Conclusions

In our study, we show that MGO leads to glycation in a concentration-dependent manner. While high concentrations of MGO were cytotoxic, lower concentrations increased the invasiveness of the GBM cell lines. In addition, glycation had differential effects on the ECM components that are involved in the invasion progress, upregulating TGFβ, brevican, and tenascin C in the GBM cell lines.

Supplementary Materials: The following supporting information can be downloaded at: https://www.mdpi.com/article/10.3390/cells12091219/s1, Figure S1. Cell vitality of glioma cell lines and hA after MGO treatment; Figure S2. Microscope imaging of glioma cell lines and hA 48 h after MGO treatment; Table S1. Quantification of microscope imaging of glioma cell lines and hA after 24 h.

Author Contributions: Conceptualization, R.H. and M.S.; methodology, P.S. (Philipp Selke), R.H. and M.S.; formal analysis, P.S. (Paola Schildhauer) and S.L.; investigation, P.S. (Paola Schildhauer); resources, P.S. (Paola Schildhauer), C.S. (Christian Scheller), C.S. (Christian Strauss) and R.H.; data curation, P.S. (Paola Schildhauer), S.L. and M.S.; writing—original draft preparation, P.S. (Paola Schildhauer); writing—review and editing, P.S. (Philipp Selke), C.S. (Christian Scheller), R.H., S.L. and M.S.; visualization, P.S. (Paola Schildhauer); supervision, C.S. (Christian Scheller), R.H., S.L. and M.S.; project administration, P.S. (Paola Schildhauer) and M.S.; funding acquisition, P.S. (Paola Schildhauer), C.S. (Christian Scheller), C.S. (Christian Strauss) and R.H. All authors have read and agreed to the published version of the manuscript for the term explanation.

Funding: P.S. (Paola Schildhauer) was funded by a fellowship from the Halle Doctoral College in Medicine (HaPKoM). M.S. was supported by the clinician scientist program of the Medical Faculty of Martin Luther University Halle-Wittenberg. R.H. and P.S. (Philipp Selke) received funding from the DFG (RTG 2155; ProMoAge and research consortium ProDGNE). We acknowledge the financial support within the funding programme Open Access Publishing by the German Research Foundation (DFG).

Institutional Review Board Statement: Not applicable.

Informed Consent Statement: Not applicable.

Data Availability Statement: The dataset is available from the corresponding author upon reasonable request.

Acknowledgments: We would like to thank Jacqueline Kessler (Department of Radiotherapy, Martin Luther University Halle-Wittenberg, Germany) for providing the glioma cell lines.

Conflicts of Interest: The authors declare no conflict of interest.

References

1. Stathis, A. *Treatment Overview. Handbook of Lymphoma*; Springer: Cham, Switzerland, 2016; Volume 20, pp. 33–44. [CrossRef]
2. Cuddapah, V.A.; Robel, S.; Watkins, S.; Sontheimer, H. REVIEWS A Neurocentric Perspective on Glioma Invasion. *Nat. Rev. Neurosci.* **2014**, *15*, 455–465. [CrossRef] [PubMed]
3. Yue, B. Biology of the Extracellular Matrix an Overview. *J. Glaucoma* **2014**, *23*, S20–S23. [CrossRef]
4. So, J.S.; Kim, H.; Han, K.S. Mechanisms of Invasion in Glioblastoma: Extracellular Matrix, Ca^{2+} Signaling, and Glutamate. *Front. Cell. Neurosci.* **2021**, *15*, 663092. [CrossRef] [PubMed]
5. Joester, A.; Faissner, A. The Structure and Function of Tenascins in the Nervous System. *Matrix Biol.* **2001**, *20*, 13–22. [CrossRef] [PubMed]
6. Demuth, T.; Berens, M.E. Molecular Mechanisms of Glioma Cell Migration and Invasion. *J. Neurooncol.* **2004**, *70*, 217–228. [CrossRef]
7. Zhang, H.; Kelly, G.; Zeritlo, C.; Jaworski, D.M.; Hockfield, S. Expression of a Cleaved Brain-Specific Extracellular Matrix Protein Mediates Glioma Cell Invasion in Vivo. *J. Neurosci.* **1998**, *18*, 2370–2376. [CrossRef]
8. Mentlein, R.; Hattermann, K.; Held-Feindt, J. Lost in Disruption: Role of Proteases in Glioma Invasion and Progression. *Biochim. Biophys. Acta* **2012**, *1825*, 178–185. [CrossRef]
9. Wolfenson, H.; Lavelin, I.; Geiger, B. Dynamic Regulation of the Structure and Functions of Integrin Adhesions. Dev. *Cell* **2013**, *24*, 447–458. [CrossRef]
10. Dongre, A.; Weinberg, R.A. New Insights into the Mechanisms of Epithelial–Mesenchymal Transition and Implications for Cancer. *Nat. Rev. Mol. Cell Biol.* **2019**, *20*, 69–84. [CrossRef]
11. Iwadate, Y. Epithelial-Mesenchymal Transition in Glioblastoma Progression. *Oncol. Lett.* **2016**, *11*, 1615–1620. [CrossRef]
12. Nguyen, T.T.T.; Shang, E.; Shu, C.; Kim, S.; Mela, A.; Humala, N.; Mahajan, A.; Yang, H.W.; Akman, H.O.; Quinzii, C.M.; et al. Aurora Kinase A Inhibition Reverses the Warburg Effect and Elicits Unique Metabolic Vulnerabilities in Glioblastoma. *Nat. Commun.* **2021**, *12*, 5203. [CrossRef] [PubMed]
13. Allaman, I.; Bélanger, M.; Magistretti, P.J. Methylglyoxal, the Dark Side of Glycolysis. *Front. Neurosci.* **2015**, *9*, 23. [CrossRef] [PubMed]
14. Manuscript, A. Spinothalamic Tract. *Encycl. Neurosci.* **2008**, *324*, 3828. [CrossRef]
15. Schalkwijk, C.G.; Stehouwer, C.D.A. Methylglyoxal, a Highly Reactive Dicarbonyl Compound, in Diabetes, Its Vascular Complications, and Other Age-Related Diseases. *Physiol. Rev.* **2020**, *100*, 407–461. [CrossRef]

16. Verzijl, N.; DeGroot, J. Crosslinking by Advanced Glycation End Products Increases the Stiffness of the Collagen Network in Human Articular Cartilage. *Arthritis Rheum.* **2002**, *46*, 114–123. [CrossRef] [PubMed]
17. Kass, D.A. Getting Better without Age: New Insights into the Diabetic Heart. *Circ. Res.* **2003**, *92*, 704–706. [CrossRef] [PubMed]
18. Chaplen, F.W.R. Incidence and Potential Implications of the Toxic Metabolite Methylglyoxal in Cell Culture: A Review. *Cytotechnology* **1998**, *26*, 173–183. [CrossRef]
19. Hanssen, N.M.J.; Westerink, J.; Scheijen, J.L.J.M.; Van Der Graaf, Y.; Stehouwer, C.D.A.; Schalkwijk, C.G. Higher Plasma Methylglyoxal Levels Are Associated with Incident Cardiovascular Disease and Mortality in Individuals with Type 2 Diabetes. *Diabetes Care* **2018**, *41*, 1689–1695. [CrossRef]
20. Dariya, B.; Nagaraju, G.P. Advanced Glycation End Products in Diabetes, Cancer and Phytochemical Therapy. *Drug Discov. Today* **2020**, *25*, 1614–1623. [CrossRef]
21. Muthyalaiah, Y.S.; Jonnalagadda, B.; John, C.M.; Arockiasamy, S. Impact of Advanced Glycation End Products (AGEs) and Its Receptor (RAGE) on Cancer Metabolic Signaling Pathways and Its Progression. *Glycoconj. J.* **2021**, *38*, 717–734. [CrossRef]
22. Chiavarina, B.; Nokin, M.J.; Durieux, F.; Bianchi, E.; Turtoi, A.; Peulen, O.; Peixoto, P.; Irigaray, P.; Uchida, K.; Belpomme, D.; et al. Triple Negative Tumors Accumulate Significantly Less Methylglyoxal Specific Adducts than Other Human Breast Cancer Subtypes. *Oncotarget* **2014**, *5*, 5472–5482. [CrossRef] [PubMed]
23. Selke, P.; Rosenstock, P.; Bork, K.; Strauss, C.; Horstkorte, R.; Scheer, M. Glycation of Benign Meningioma Cells Leads to Increased Invasion. *Biol. Chem.* **2021**, *402*, 849–859. [CrossRef] [PubMed]
24. Scheer, M.; Bork, K.; Simon, F.; Nagasundaram, M.; Horstkorte, R.; Gnanapragassam, V.S. Glycation Leads to Increased Polysialylation and Promotes the Metastatic Potential of Neuroblastoma Cells. *Cells* **2020**, *9*, 868. [CrossRef]
25. van Heijst, J.W.J.; Niessen, H.W.M.; Musters, R.J.; van Hinsbergh, V.W.M.; Hoekman, K.; Schalkwijk, C.G. Argpyrimidine-Modified Heat Shock Protein 27 in Human Non-Small Cell Lung Cancer: A Possible Mechanism for Evasion of Apoptosis. *Cancer Lett.* **2006**, *241*, 309–319. [CrossRef] [PubMed]
26. Lin, J.A.; Wu, C.H.; Yen, G.C. Methylglyoxal Displays Colorectal Cancer-Promoting Properties in the Murine Models of Azoxymethane and CT26 Isografts. *Free Radic. Biol. Med.* **2018**, *115*, 436–446. [CrossRef] [PubMed]
27. Nokin, M.J.; Durieux, F.; Peixoto, P.; Chiavarina, B.; Peulen, O.; Blomme, A.; Turtoi, A.; Costanza, B.; Smargiasso, N.; Baiwir, D.; et al. Methylglyoxal, a Glycolysis Side-Product, Induces Hsp90 Glycation and YAP- Mediated Tumor Growth and Metastasis. *Elife* **2016**, *5*, e19375. [CrossRef] [PubMed]
28. Chiavarina, B.; Nokin, M.J.; Bellier, J.; Durieux, F.; Bletard, N.; Sherer, F.; Lovinfosse, P.; Peulen, O.; Verset, L.; Dehon, R.; et al. Methylglyoxal-Mediated Stress Correlates with High Metabolic Activity and Promotes Tumor Growth in Colorectal Cancer. *Int. J. Mol. Sci.* **2017**, *18*, 213. [CrossRef]
29. Sharaf, H.; Matou-Nasri, S.; Wang, Q.; Rabhan, Z.; Al-Eidi, H.; Al Abdulrahman, A.; Ahmed, N. Advanced Glycation Endproducts Increase Proliferation, Migration and Invasion of the Breast Cancer Cell Line MDA-MB-231. *Biochim. Biophys. Acta-Mol. Basis Dis.* **2015**, *1852*, 429–441. [CrossRef]
30. Suh, Y.J.; Hall, M.S.; Huang, Y.L.; Moon, S.Y.; Song, W.; Ma, M.; Bonassar, L.J.; Segall, J.E.; Wu, M. Glycation of Collagen Matrices Promotes Breast Tumor Cell Invasion. *Integr. Biol.* **2019**, *11*, 109–117. [CrossRef]
31. Leone, A.; Nigro, C.; Nicolò, A.; Prevenzano, I.; Formisano, P.; Beguinot, F.; Miele, C. The Dual-Role of Methylglyoxal in Tumor Progression—Novel Therapeutic Approaches. *Front. Oncol.* **2021**, *11*, 645686. [CrossRef]
32. Bellahcène, A.; Nokin, M.J.; Castronovo, V.; Schalkwijk, C. Methylglyoxal-Derived Stress: An Emerging Biological Factor Involved in the Onset and Progression of Cancer. *Semin. Cancer Biol.* **2018**, *49*, 64–74. [CrossRef]
33. Nokin, M.; Durieux, F.; Bellier, J.; Peulen, O.; Uchida, K.; David, A.; Cochrane, J.R.; Hutton, C.A.; Castronovo, V.; Bellahcène, A. Hormetic Potential of Methylglyoxal, a Side-Product of Glycolysis, in Switching Tumours from Growth to Death. *Sci. Rep.* **2017**, *7*, 11722. [CrossRef]
34. Lee, H.K.; Seo, I.A.; Suh, D.J.; Lee, H.J.; Park, H.T. A Novel Mechanism of Methylglyoxal Cytotoxicity in Neuroglial Cells. *J. Neurochem.* **2009**, *108*, 273–284. [CrossRef]
35. Oya-Ito Tomoko, T.; Naito, Y.; Takagi, T.; Handa, O.; Matsui, H.; Yamada, M.; Shima, K.; Yoshikawa, T. Heat-Shock Protein 27 (Hsp27) as a Target of Methylglyoxal in Gastrointestinal Cancer. *Biochim. Biophys. Acta-Mol. Basis Dis.* **2011**, *1812*, 769–781. [CrossRef]
36. Antognelli, C.; Moretti, S.; Frosini, R.; Puxeddu, E.; Sidoni, A.; Talesa, V.N. Methylglyoxal Acts as a Tumor-Promoting Factor in Anaplastic Thyroid Cancer. *Cells* **2019**, *8*, 547. [CrossRef] [PubMed]
37. Pan, S.; Guan, Y.; Ma, Y.; Cui, Q.; Tang, Z.; Li, J.; Zu, C.; Zhang, Y.; Zhu, L.; Jiang, J.; et al. Advanced Glycation End Products Correlate with Breast Cancer Metastasis by Activating RAGE/TLR4 Signaling. *BMJ Open Diabetes Res. Care* **2022**, *10*, e002697. [CrossRef]
38. Liang, H. Advanced Glycation End Products Induce Proliferation, Invasion and Epithelial-Mesenchymal Transition of Human SW480 Colon Cancer Cells through the PI3K/AKT Signaling Pathway. *Oncol. Lett.* **2020**, *19*, 3215–3222. [CrossRef]
39. Loarca, L.; Sassi-gaha, S.; Artlett, C.M. Two α-Dicarbonyls Downregulate Migration, Invasion, and Adhesion of Liver Cancer Cells in a P53-Dependent Manner. *Dig. Liver Dis.* **2013**, *45*, 938–946. [CrossRef]
40. Their, J.P. Epithelial-Mesenchymal Transitions in Tumor Progression. *Nat. Rev. Cancer* **2002**, *2*, 442–454. [CrossRef]
41. Howng, S.L.; Wu, C.H.; Cheng, T.S.; Sy, W.D.; Lin, P.C.K.; Wang, C.; Hong, Y.R. Differential Expression of Wnt Genes, β-Catenin and E-Cadherin in Human Brain Tumors. *Cancer Lett.* **2002**, *183*, 95–101. [CrossRef] [PubMed]

42. Lewis-Tuffin, L.J.; Rodriguez, F.; Giannini, C.; Scheithauer, B.; Necela, B.M.; Sarkaria, J.N.; Anastasiadis, P.Z. Misregulated E-Cadherin Expression Associated with an Aggressive Brain Tumor Phenotype. *PLoS ONE* **2010**, *5*, e13665. [CrossRef] [PubMed]
43. Cao, Z.Q.; Wang, Z.; Leng, P. Aberrant N-Cadherin Expression in Cancer. *Biomed. Pharmacother.* **2019**, *118*, 109320. [CrossRef]
44. Velpula, K.K.; Rehman, A.A.; Chelluboina, B.; Dasari, V.R.; Gondi, C.S.; Rao, J.S.; Veeravalli, K.K. Glioma Stem Cell Invasion through Regulation of the Interconnected ERK, Integrin A6 and N-Cadherin Signaling Pathway. *Cell. Signal.* **2012**, *24*, 2076–2084. [CrossRef]
45. Camand, E.; Peglion, F.; Osmani, N.; Sanson, M.; Etienne-Manneville, S. N-Cadherin Expression Level Modulates Integrin-Mediated Polarity and Strongly Impacts on the Speed and Directionality of Glial Cell Migration. *J. Cell Sci.* **2012**, *125*, 844–857. [CrossRef] [PubMed]
46. Senbanjo, L.T.; Chellaiah, M.A. CD44: A Multifunctional Cell Surface Adhesion Receptor Is a Regulator of Progression and Metastasis of Cancer Cells. *Front. Cell Dev. Biol.* **2017**, *5*, 18. [CrossRef]
47. Ivanova, E.L.; Costa, B.; Eisemann, T.; Lohr, S.; Boskovic, P.; Eichwald, V.; Meckler, J.; Jugold, M.; Orian-Rousseau, V.; Peterziel, H.; et al. CD44 Expressed by Myeloid Cells Promotes Glioma Invasion. *Front. Oncol.* **2022**, *12*, 3957. [CrossRef]
48. Lu, R.; Wu, C.; Guo, L.; Liu, Y.; Mo, W.; Wang, H.; Ding, J.; Wong, E.T.; Yu, M. The Role of Brevican in Glioma: Promoting Tumor Cell Motility in Vitro and in Vivo. *BMC Cancer* **2012**, *12*, 607. [CrossRef] [PubMed]
49. Xia, S.; Lal, B.; Tung, B.; Wang, S.; Goodwin, C.R.; Laterra, J. Tumor Microenvironment Tenascin-C Promotes Glioblastoma Invasion and Negatively Regulates Tumor Proliferation. *Neuro-Oncology* **2016**, *18*, 507–517. [CrossRef]
50. Viapiano, M.S.; Hockfield, S.; Matthews, R.T. BEHAB/Brevican Requires ADAMTS-Mediated Proteolytic Cleavage to Promote Glioma Invasion. *J. Neurooncol.* **2008**, *88*, 261–272. [CrossRef]
51. Sarkar, S.; Zemp, F.J.; Senger, D.; Robbins, S.M.; Yong, V.W. ADAM-9 is a novel mediator of tenascin-C-stimulated invasiveness of brain tumor–initiating cells. *Neuro-Oncology* **2015**, *17*, 1095–1105. [CrossRef] [PubMed]
52. Vollmann-Zwerenz, A.; Leidgens, V.; Feliciello, G.; Klein, C.A.; Hau, P. Tumor Cell Invasion in Glioblastoma. *Int. J. Mol. Sci.* **2020**, *21*, 1932. [CrossRef]
53. Ang, L.C.; Zhang, Y.; Cao, L.; Yang, B.L.; Young, B.; Kiani, C.; Lee, V.; Allan, K.; Yang, B.B. Versican Enhances Locomotion of Astrocytoma Cells and Reduces Cell Adhesion through Its G1 Domain. *J. Neuropathol. Exp. Neurol.* **1999**, *58*, 597–605. [CrossRef]
54. Joseph, J.V.; Magaut, C.R.; Storevik, S.; Geraldo, L.H.; Mathivet, T.; Latif, A.; Rudewicz, J.; Guyon, J.; Gambaretti, M.; Haukas, F.; et al. TGF-β promotes microtube formation in glioblastoma through Thrombospondin 1. *Neuro-Oncology* **2022**, *24*, 541–553. [CrossRef] [PubMed]
55. Yu, Q.; Xue, Y.; Liu, J.; Xi, Z.; Li, Z.; Liu, Y.; Gregory, B.; Oliver, G. Fibronectin Promotes the Malignancy of Glioma Stem-Like Cells Via Modulation of Cell Adhesion, Differentiation, Proliferation and Chemoresistance. *Front. Mol. Neurosci.* **2018**, *11*, 130. [CrossRef] [PubMed]
56. Mohiuddin, E.; Wakimoto, H. Extracellular Matrix in Glioblastoma: Opportunities for Emerging Therapeutic Approaches. *Am. J. Cancer Res.* **2021**, *11*, 3742–3754. [PubMed]
57. Bellier, J.; Nokin, M.; Caprasse, M.; Peulen, O.; Bellier, J.; Nokin, M.; Caprasse, M.; Tiamiou, A.; Blomme, A.; Scheijen, J.L.; et al. Methylglyoxal Scavengers Resensitize KRAS-Mutated Colorectal Tumors to Cetuximab. *Cell Rep.* **2020**, *30*, 1400–1416. [CrossRef]

Selbstständigkeitserklärung

Hiermit erkläre ich an Eides statt, dass ich die hier vorliegende Habilitationsschrift selbständig verfasst und keine anderen als die angegebenen Quellen und Hilfsmittel benutzt habe.

Halle, den 10.12.2023 Dr. med. Maximilian Scheer

Erklärung über frühere Habilitationsversuche

Ich erkläre, dass frühere Habilitationsversuche nicht stattfanden, und dass an keiner anderen Fakultät oder Universität ein Habilitationsverfahren im Gange ist.

Halle, den 10.12.2023 Dr. med. Maximilian Scheer

Tabellarischer Lebenslauf

Angaben zur Person:

Name:	Dr. Maximilian Scheer

Beruflicher Werdegang:

seit 09/2017	Assistenzarzt, Klinik für Neurochirurgie, Universitätsklinikum Halle, Medizinische Fakultät der Martin-Luther-Universität Halle-Wittenberg
03/2017 - 09/2017	Assistenzarzt, Klinik für Neurologie, Martin-Gropius-Krankenhaus, Gesellschaft für Leben und Gesundheit, Eberswalde

Akademische Ausbildung:

10/2010 - 03/2017	Studium der Humanmedizin, Martin-Luther-Universität Halle-Wittenberg, Gesamtnote: Sehr gut
11/2013 - 02/2017	Doktorarbeit im Institut für Physiologische Chemie (Prof. Dr. Horstkorte): "Einfluss von Glykierung auf Neuroblastom-Zellen" (Verteidigung 20.02.2017), Note: Cum laude

Förderungen und Preise:

01/2024	Reisestipendium für den Deutschen Krebskongress
07/2023	Bewilligung der Drittmittel „Intraoperative Neuronavigation und serverbasierte Eingriffsplanung" – Großgeräte der Länder (DFG; Antragsverantwortlich) – 844.000€
05/2023	Bewilligung der Förderung „Thrombembolie-Risiko nach Operationen an intrakraniellen Tumoren unter intraoperativer Anwendung einer intermittierenden pneumatischen Kompression der Beine: Eine prospektive, randomisierte, einfach verblindete Multicenter-Studie" durch die DFG (Mitantragsteller), Fördersumme 1.100.000€
04/2023	Wilhelm- Roux-Förderung: Anschubfinanzierung in Höhe von 5.000€ aufgrund der Einreichung eines DFG-Einzelantrages
10/2022	Posterpreis der Gesellschaft für Schädelbasischirurige: „Rezidiv und Progress nach mikrochirurgischer Versorgung von Vestibularisschwannomen", 500€

seit 04/2021	Clinician Scientist Programm der Universitätsmedizin Halle; umgerechnet ca. 120.000€
06/2018 – 06/2021	Wilhelm-Roux-Förderung: Posttranslationale Modifikationen in Meningeomen; Kooperation mit dem Institut für Physiologische Chemie (Prof. Dr. Horstkorte), Fördersumme 150.000 €
10/2010 – 02/2017	Stipendium der Gesellschaft für Leben und Gesundheit, ca. 36.000€

Zusätzliche Qualifikationen:

- Kurs als Prüfers / Hauptprüfer (Basis sowie Aufbaukurs gemäß AMG; KKS-Netzwerk)
- Fachkunde Strahlenschutz
- *Eurospine Basic Diploma*
- Kurs als Projektleiter / Beauftragter für biologische Sicherheit
- Hochschuldidaktik-Kurs
- Versuchstierkunde

Mitgliedschaften:

- DGNC – Deutsche Gesellschaft für Neurochirurgie
- NOA – Neuroonkologische Arbeitsgemeinschaft inkl. YoungNOA
- EANS – European Association of Neurosurgical Societies
- AANS – American Association of Neurological Surgeons
- ClinSciNet – Clinician Scientist Network (Gründungsmitglied, Vorstand)

Reviewer-Tätigkeit

- Interdisciplinary Neurosurgery
- Military Medical Research
- Frontiers in Neurology
- Brain Sciences
- Cancers
- Journal of Clinical Medicine

Danksagung

In erster Linie möchte bei Professor Rüdiger Horstkorte bedanken, welcher mich seit meiner Doktorarbeit auf meinem Weg als Mentor und als Freund begleitet. So gelang es sehr früh eine intramurale Förderung zu erhalten, welche entscheidend für alle Folgeprojekte war. Ohne sein Wissen und seine Unterstützung wäre dieser Weg so nicht möglich gewesen.

Ich möchte mich bei meinem Chef, Professor Christian Strauss, für die Initiative zur Bewerbung für das Clinician Scientist Programm und seine Unterstützung bei der Umsetzung herzlich bedanken. Ohne diese Förderung wäre die bisherige wissenschaftliche Karriere nicht erreichbar gewesen.

Auf diesem Weg möchte ich mich nochmals für die exzellente Arbeit der ehemaligen Doktoranden Paola Schildhauer sowie Philipp Selke bedanken. Ohne die herausragende Leistung und die daraus hervorgegangenen Publikationen wäre dieses Projekt nicht so weit fortgeschritten.

Weiterhin möchte ich mich bei der Leitung unseren Labors, Frau Doktor Sandra Leisz, bedanken. Durch die gute und produktive Zusammenarbeit war es möglich, einige wissenschaftliche Projekte zu etablieren. Dabei habe ich die gute Ergänzung klinischer Ideen mit dem *Know-how* der Grundlagenforschung sehr geschätzt.

Ein besonderer Dank gilt meiner Freundin sowie meiner Familie, welche mir immer zur Seite gestanden haben und mich verständnisvoll auf diesem Weg begleitet haben.